

A high priority shipment

**How nuclease delivery by SLX4 mediates DNA
interstrand crosslink repair**

Wouter Hoogenboom

ISBN	978-90-393-7218-0
Copyright	© 2019 W.S. Hoogenboom
Cover	Bike chain DNA, by W.S. Hoogenboom
Layout and design	W.S. Hoogenboom
Printed by	Ridderprint BV
	Printed on recycled paper

The research described in the thesis was performed at the Hubrecht Institute of The Royal Netherlands School of Arts and Sciences (KNAW), Utrecht, The Netherlands

A high priority shipment

**How nuclease delivery by SLX4 mediates DNA
interstrand crosslink repair**

Een verzending met hoge prioriteit

**Hoe nuclease-afgifte door SLX4 de reparatie van DNA interstrand
crosslinks bemiddelt**

(met een samenvatting in het Nederlands)

Proefschrift

ter verkrijging van de graad van doctor aan de
Universiteit Utrecht
op gezag van de
rector magnificus, prof.dr. H.R.B.M. Kummeling,
ingevolge het besluit van het college voor promoties
in het openbaar te verdedigen op

dinsdag 17 december 2019 des middags te 4.15 uur

door

Wouter Simon Hoogenboom

geboren op 3 maart 1987
te Lutong, Maleisië

Promotor: Prof. dr. W.L. de Laat

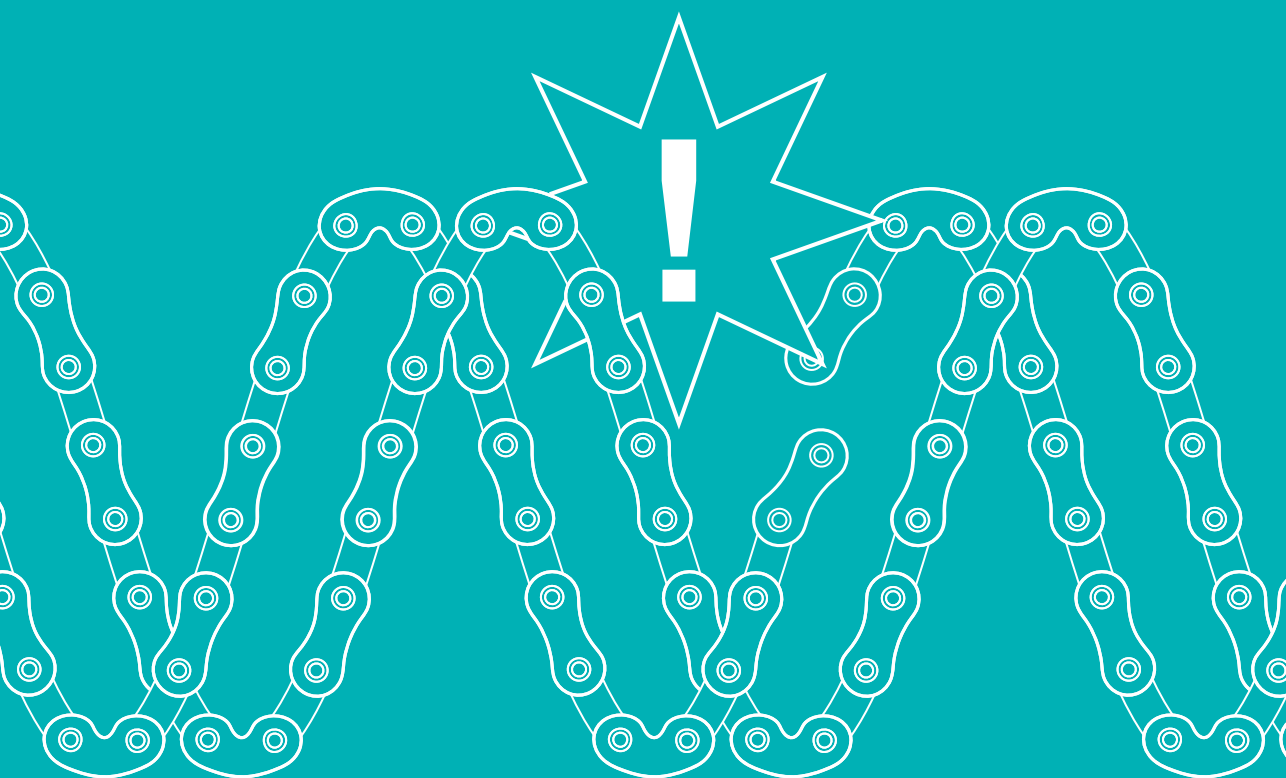
Co-promotor: Dr. P. Knipscheer

voor Marit



Table of contents

Chapter 1	_____	9
	General introduction _____	10
	Thesis outline _____	33
Chapter 2	_____ <i>Xenopus</i> egg extract: A powerful tool to study genome maintenance mechanisms _____	45
Chapter 3	_____ Recruitment and positioning determine the specific role of XPF-ERCC1 in ICL repair _____	67
Chapter 4	_____ The role of SLX4 and its associated nucleases in DNA interstrand crosslink repair _____	99
Chapter 5	_____ Two domains mediate SLX4/FANCP recruitment to DNA interstrand crosslinks _____	127
Chapter 6	_____ General discussion _____	151
Addendum	_____	161
	Nederlandstalige samenvatting _____	162
	Curriculum Vitae _____	167
	Publications _____	169
	Dankwoord / Acknowledgements _____	170

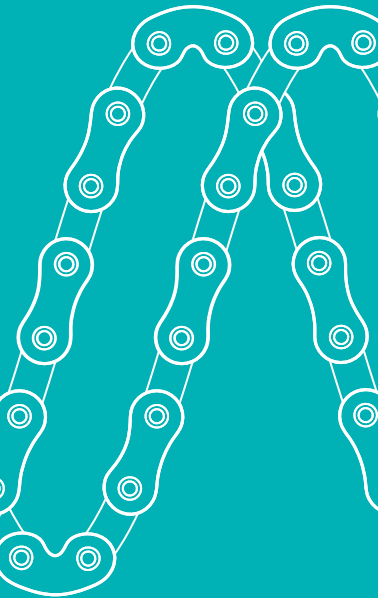


Chapter 1

General introduction

Wouter S. Hoogenboom and Puck Knipscheer

Oncode Institute, Hubrecht Institute–KNAW and University Medical Center
Utrecht, Utrecht, The Netherlands



The DNA damage response

Much like our immune system that fights a continuous battle against all kinds of pathogens entering our bodies, our cells are endlessly working to keep our genomic information safe. External sources, products of cellular metabolism and spontaneous events are estimated to inflict 70 thousand DNA lesions per day in each of our 37 trillion cells (Bianconi *et al.*, 2013, Lindahl & Barnes, 2000, Tubbs & Nussenzweig, 2017). For our own survival and for genetic information to be faithfully transmitted to offspring, the presence of a strong DNA damage response (DDR) is vital. The DDR is initiated when a lesion in the DNA is recognized by sensor proteins. These sensors initiate signaling pathways that influence a variety of cellular processes, such as transcription, cell-cycle arrest, DNA repair, damage tolerance, and apoptosis (Figure 1) (Jackson & Bartek, 2009). When defects in DDR factors induce erroneous responses, DNA damage is a major source of mutations, which can have drastic consequences including developmental defects, premature aging, and severe cancer susceptibility (Giglia-Mari *et al.*, 2011, Hoeijmakers, 2001, Hoeijmakers, 2007). DNA repair is a vital aspect of the DDR by preventing the formation of mutations. Detailed knowledge of DNA repair systems helps to understand the onset of genetic diseases and develop therapies. In this chapter I will discuss DNA damage and repair in general before moving on to the repair of DNA interstrand crosslinks, which is the subject of this thesis.

DNA damage, causes and consequences

DNA damage comes in various shapes and sizes; the exact type of lesion dictates how it is recognized and repaired. Here, I describe several types of DNA damage and other sources

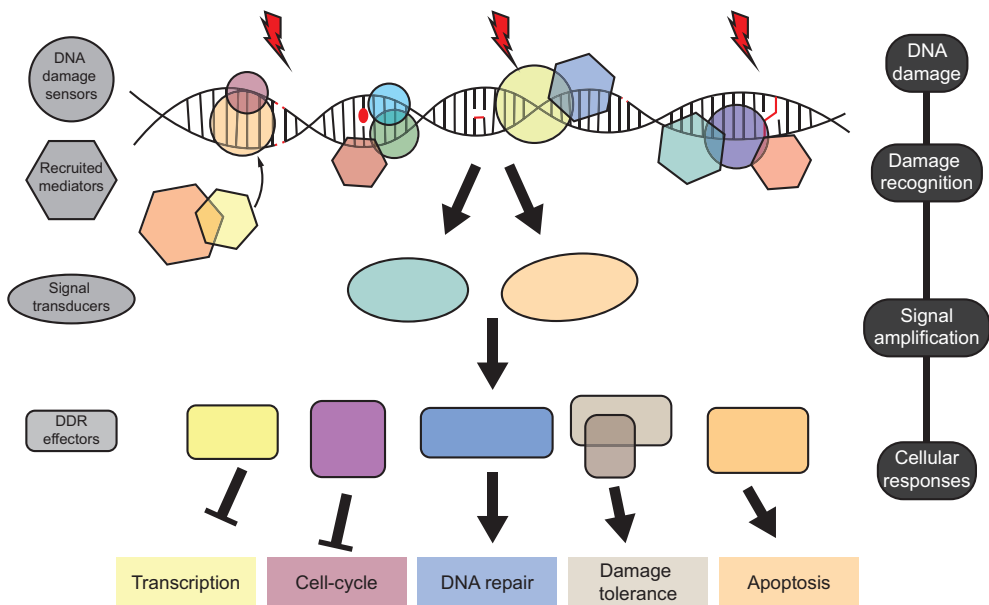


Figure 1: Model for the DNA damage response (DDR). DNA damage, which can be a variety of lesions, is detected by specialized sensor proteins. These sensors initiate signaling pathways that are amplified and converted to cellular responses via mediators, transducers, and effector proteins. Adapted from: Jackson & Bartek, 2009.

of mutagenicity categorized into two main classes based on its origin: endogenous and exogenous.

Endogenous DNA damage occurs when reactive molecules that are naturally present within cells engage with DNA. Reactive oxygen species (ROS) such as radicals and hydrogen peroxide are a major cause of mutations in all aerobic organisms (Bjelland & Seeberg, 2003). They are formed as byproducts of respiration in mitochondria and other catabolic and anabolic processes. ROS species can react with DNA directly, causing a wide variety of oxidative base lesions and a high incidence of single strand breaks (SSBs), but they can also indirectly contribute to DNA damage by oxidation of lipid molecules, generating aldehyde products that in turn react with bases to form adducts (Marnett, 2000). Methylation of DNA bases occurs frequently in healthy cells but is enhanced by external factors such as tobacco smoke. If left unrepaired, methylated DNA bases are a major source of spontaneous mutations (Chatterjee & Walker, 2017). A major mutagenic and cytotoxic lesion produced by various methylating agents is *O*⁶-methylguanine (*O*⁶-meG) (Xu *et al.*, 2016). In addition, spontaneous events such as base deamination or hydrolysis of nucleotide residues result in non-coding bases or abasic sites. Other sources of endogenously formed mutations include cellular processes such as DNA replication, that can induce base mismatches, insertions, and deletions (Chatterjee & Walker, 2017).

Exogenous sources of DNA damage include all environmental threats to the integrity of a DNA molecule. Ionizing radiation (IR), such as gamma or X-rays, can damage DNA directly or indirectly by creating radicals. Ultraviolet (UV) radiation can cause intrastrand crosslinks between two adjacent pyrimidines, DNA-protein crosslinks (DPCs), and single strand breaks (SSBs). Genotoxic chemicals often originate from food, tobacco smoke, industrial dyes, high temperature cooking, fuels and pesticides. Examples of such reactive molecules are alkylating agents and aromatic compounds that form adducts and other persistent lesions on the DNA. Some compounds carry two reactive groups enabling them to crosslink two molecules together, which can result in the formation of DPCs and DNA-DNA interstrand crosslinks (ICLs) or intrastrand crosslinks (Chatterjee & Walker, 2017).

When the DDR is triggered by the detection of a DNA lesion this often leads to a cell-cycle arrest, inhibition of transcription and replication, and activation of DNA repair pathways. Successful removal of the damage inactivates the DDR and normal functioning of the cell is resumed. If the damage is not removed, persistent DDR signaling can trigger permanent cell-cycle withdrawal or cell death by apoptosis, with the intention to prevent tumor formation (Campisi & d'Adda di Fagagna, 2007). In the event that this fails, the surviving cells could try to replicate the damaged DNA, generating mutations. These mutations, that are now permanent, might give rise to altered proteins and drive genetic diseases such as cancer (Basu, 2018). Ironically, treatment of cancer often involves compounds that chemically react with DNA, such as DNA crosslinkers (Cheung-Ong *et al.*, 2013). When this is effective, the DDR in fast-dividing cancer cells arrests cell-cycle progression and induces apoptosis, causing tumors to stop growing and even decrease in size. However, this also applies to healthy cells, which is why chemotherapy causes side-effects such as hair loss. To prevent all this from happening, our cells have various DNA repair mechanisms at their disposal that are capable of neutralizing most of the injuries that our DNA endures. How these mechanisms work to restore DNA damage is the subject of the next section.

DNA repair pathways

Once the DDR is activated by the presence of a DNA lesion, it will initiate action to restore the DNA to an undamaged state. Various systems are in place that execute the DNA repair, in some cases a complex interplay that involves many factors and several consecutive steps. Here, I describe the most well-known DNA repair mechanisms.

Direct DNA repair

Replication of damaged bases can cause mutations. Direct DNA repair is the simplest form of DNA repair since the damage is directly reversed. Direct repair mechanisms do not require a template, since the types of damage that they neutralize are base-specific. In human cells, two major mechanisms are active: reversal of O-alkylated DNA damage by O⁶-alkylguanine-DNA alkyltransferases (AGTs) and reversal of N-alkylated DNA damage by AlkB family dioxygenases (Yi & He, 2013).

Base excision repair (BER)

BER restores bases containing small chemical alterations. DNA glycosylases recognize a specific base damage, such as specific types of oxidative base lesions, methylations, or deaminations. Glycosylases flip out the damaged base from the DNA double helix into their active site where the base is cleaved from the sugar-phosphate backbone, resulting in an abasic (apurinic/apyrimidinic, AP) site. The AP endonuclease 1 (APE1) recognizes AP sites and incises the backbone, effectively creating a single strand break. In the 'short-patch' branch of BER the DNA polymerase β (Pol β) places a nucleotide at the AP site and removes the 5'-terminal baseless sugar via its lyase activity (Robertson *et al.*, 2009). The remaining nick is sealed by a complex consisting of X-ray repair cross-complementation gene 1 (XRCC1) and DNA ligase III (LIG3). The 'long-patch' BER mechanism involves the DNA polymerases Pol β , Pol δ or Pol ϵ , and proliferating nuclear antigen (PCNA) for the synthesis of a larger patch past the excised base. The resulting flap is removed by flap endonuclease 1 (FEN1) and the backbone is sealed by DNA ligase I (LIG1) (Hakem, 2008, Hoeijmakers, 2001, Sawant *et al.*, 2017).

Single strand break repair (SSBR)

Single strand breaks (SSB) occur frequently in our genome and can result in a double strand break (DSB) when encountered by a replication fork. 'Direct' SSBs can arise from ROS-induced sugar damage while 'indirect' SSBs are generated during BER. In addition, SSBs can arise by abortive topoisomerase 1 (TOP1) activity, for instance following collision with RNA polymerase (RNAP) creating a TOP1-linked SSB (TOP1-SSB). Direct SSBs are detected by poly(ADP-ribose) polymerase 1 (PARP1) binding and activation, whereas indirect and TOP1-SSBs might not require such detection because they are created in a scheduled fashion by cellular enzymes or 'detected' by the collision of RNAP and TOP1. Once an SSB is detected the ends undergo processing by specialized enzymes. Subsequent gap filling and ligation steps are identical to the short- and long-patch branches of BER (Caldecott, 2008).

Nucleotide excision repair (NER); Figure 2

NER repairs various single strand lesions that are unsuitable for repair by BER, such as lesions that are helix-distorting, bulky or affect multiple bases. An important example is UV damage. NER encompasses two subpathways: global genome NER (GG-NER), that functions throughout the genome, and transcription-coupled NER (TC-NER), that is triggered by a block in transcription and therefore is only active in transcribed regions. Both subpathways follow the same basic repair steps: damage recognition, unwinding of the DNA helix flanking the damage, dual incisions and eviction of the damage-containing oligonucleotide, DNA synthesis, and ligation of the backbone. The difference between the two subpathways lies in their mechanism of damage recognition.

GG-NER recognizes lesions that slightly distort the normal Watson-Crick double helix, which is detected either by the heterotrimeric XPC-RAD23B-centrin2 complex (Sugasawa, 2010, Sugasawa *et al.*, 1998) or by the UV-damaged DNA-binding protein (UV-DDB, or XPE) (Scrima *et al.*, 2008). UV-DDB specifically binds subtly distorting UV lesions and facilitates loading of XPC. Highly distorting lesions are more easily detected and repaired compared to mildly distorting lesions (Marteijn *et al.*, 2014). XPC promotes recruitment of the large transcription factor IIH (TFIIH) complex (Araujo *et al.*, 2001, Yokoi *et al.*, 2000). TFIIH locally unwinds the duplex DNA and performs a first round of 'damage verification' with the use of the helicase activity of two subunits, XPB and XPD (Figure 2) (Coin *et al.*, 1998, Li *et al.*, 2015). Replication protein A (RPA) then stabilizes the structure by binding undamaged single-stranded DNA (ssDNA), while xeroderma pigmentosum protein A (XPA) binds the damaged DNA. XPA-RPA is also implicated in damage verification by probing for abnormal backbone structure (Hoeijmakers, 2001), at which point the NER apparatus could still be dismantled (Li *et al.*, 2015, Thoma & Vasquez, 2003). XPA next recruits the structure-specific endonuclease (SSE) xeroderma pigmentosum protein F-excision repair cross-complementation group 1 (XPF-ERCC1) through its interaction with ERCC1 (Faridounnia *et al.*, 2018). In a tightly coordinated process, XPF-ERCC1 makes an incision at the 5' side of the damage, after which repair synthesis is initiated. XPG, an SSE with an opposite polarity of substrate specificity, next incises the DNA on the 3' side allowing completion of repair synthesis (Staresinic *et al.*, 2009). Repair synthesis is mediated by the DNA polymerases δ , ϵ and κ (Pol δ , ϵ and κ) and the backbone is ligated by LIG1 or LIG3 (Moser *et al.*, 2007).

TC-NER is initiated when progression of RNA polymerase II (RNA pol II) is blocked by a damage, including types that are not easily recognized by GG-NER such as oxidative lesions (Goode *et al.*, 2002, Hoeijmakers, 2001, Marteijn *et al.*, 2014, Schwertman *et al.*, 2013). Several factors are recruited to these transcription-blocking DNA lesions including the Spt16 subunit of the histone chaperone FACT, UV-stimulated scaffold protein A (UVSSA), ubiquitin-specific-processing protease 7 (USP7), and Cockayne syndrome group A (CSA) and B (CSB) (Marteijn *et al.*, 2014, Schwertman *et al.*, 2012, Wienholz *et al.*, 2019). The stalled RNA pol II prevents NER machinery from accessing the lesion, which is proposed to be solved by RNA pol II dissociation from the template DNA, backtracking, or degradation (Marteijn *et al.*, 2014). CSB may be involved in this, while UVSSA and USP7 counteract ubiquitin-mediated degradation of CSB until remodeling of RNA pol II is completed (Schwertman *et al.*, 2013). Core-NER factors are subsequently recruited and repair follows the same mechanism as for GG-NER (Figure 2).

Deficiency in NER is associated with several genetic diseases. Patients that have

1 xeroderma pigmentosum (XP), Cockayne syndrome (CS), trichothiodystrophy (TTD), cerebro-oculo-facio-skeletal syndrome (COFS) or UV-sensitive syndrome (UV^sS) are all hypersensitive to UV radiation but display also various other phenotypes (Moses, 2001, Natale & Raquer, 2017, Vermeulen & Fouteri, 2013). Mutations in one gene, such as XPD or XPF, are in some cases associated with different diseases, which is indicative of distinct roles in the subpathways of NER.

Mismatch repair (MMR)

MMR corrects mismatched nucleotides that are incorporated during DNA replication, preventing them from developing into permanent mutations. MMR leads to an ~100-fold increase in DNA replication fidelity (Cortez, 2019). Two major components of this repair pathway are MutS and MutL, that in humans exist as heterodimers in several forms. MutS protein homolog 2 (MSH2) and 6 (MSH6) form MutSa which recognizes single base-base mismatches, while short insertions or deletions (indels) are detected by MutSβ that is made up of MSH2 and MSH3. MutL protein homolog 1 (MLH1) is found in three different heterodimers with PMS2 (MutLa), MLH3 (MutLβ), and PMS1 (MutLy), of which MutLa is the major MutL homolog for MMR. Since both bases in a mismatch are undamaged it is crucial for the MMR system to identify the newly synthesized strand to remove the misincorporated base. How this is achieved is not fully understood and this 'strand discrimination signal' has been the subject of intensive research (Ghodgaonkar *et al.*, 2013, Hombauer *et al.*, 2011, Kadyrov *et al.*, 2009, Kleczkowska *et al.*, 2001, Pena-Diaz & Jiricny, 2010, Pluciennik *et al.*, 2010, St Charles *et al.*, 2015, Wei *et al.*, 2003). Nicks in the daughter strand, which are actively made by MutLa during replication but also formed between adjacent Okazaki fragments, strongly contribute to the detection of strand specificity in MMR. In addition, incorporated ribonucleotides during DNA replication are also exploited for strand discrimination. Subsequently, nicks are used to excise a stretch of nucleotides from the newly synthesized strand that includes the mismatch. The missing nucleotides in the gap are resynthesized by DNA Pol δ and the nick is sealed by LIG1 (Cortez, 2019, Fishel, 2015, Iyama & Wilson, 2013, Larrea *et al.*, 2010, Liu *et al.*, 2017, Yuan *et al.*, 2004). **Chapter 2** contains an overview of studies performed in *Xenopus* egg extracts on the mechanism of MMR.

Ribonucleotide excision repair (RER)

Ribonucleotides are appropriately incorporated in the genome by the RNA primase component of DNA polymerase α (Pol α) to initiate lagging strand replication at each Okazaki fragment, but in some cases also incorrectly by replicative DNA polymerases (Williams *et al.*, 2016). The presence of ribonucleotides in DNA may result in the generation of single- and double-strand breaks, thus contributing to genome instability. Maturation of Okazaki fragments is promoted by Pol δ that displaces the RNA primer, generating a flap that is removed by FEN1. Incorrectly incorporated ribonucleotides are recognized by RNaseH2 that cuts the backbone immediately 5' to the ribonucleotide. Pol δ then uses the nick and entry point to displace the ribonucleotide and a ssDNA flap, which is excised by FEN1. In both cases the nick is sealed by LIG1 (Sparks *et al.*, 2012).

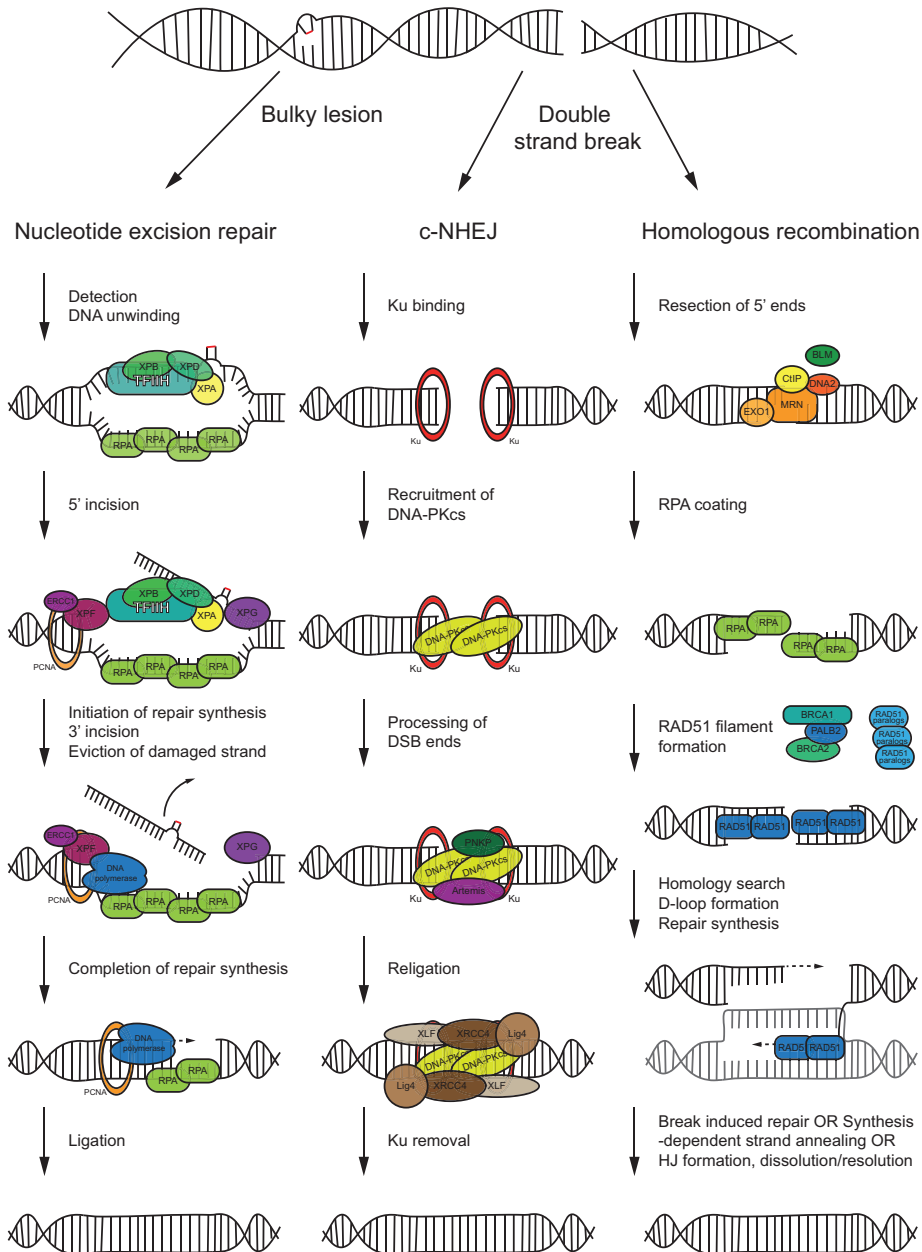


Figure 2: Schematic representation of three important repair pathways. Simplified mechanisms of the DNA repair pathways nucleotide excisions repair (NER), canonical non-homologous end joining (c-NHEJ), and homologous recombination (HR). Bulky lesions, that could be caused by UV radiation, are detected by one of two subpathways: global genome NER (GG-NER) or transcription-coupled NER (TC-NER). After detection (not indicated in this figure) these pathways converge and core-NER factors are recruited which remove a stretch of DNA containing the damaged base(s) and fill the gap with undamaged DNA. Double strand DNA breaks (DSBs) are repaired by various pathways including c-NHEJ and HR. c-NHEJ enables efficient joining of the ends but is error-prone. HR requires resection of the DSB ends, and an intact sister chromatid, but is generally error-free. See text for details. Adapted from: Marteijn *et al.*, 2014 and Panier & Boulton, 2014.

Double strand break repair

Double strand breaks (DSBs) are toxic lesions that, if left unrepaired, can result in cell death, while if misrepaired can cause chromosomal translocations. DSBs could in principle be induced directly by simultaneous and opposite SSBs, however they are far more likely to arise from the repair of other lesions or when a replication fork collapses (Jeggo & Lobrich, 2006). There are at least four different mechanisms by which DSBs can be repaired, each with its own advantages and disadvantages. The choice of repair mechanism is at least in part dictated by the extent of active replication and whether the DSB ends have been subject to DNA end resection (Ceccaldi *et al.*, 2016a, Karanam *et al.*, 2012).

Canonical non-homologous end-joining (c-NHEJ); Figure 2. c-NHEJ is the dominant pathway for the repair of DSBs in the G1 and G2 phases of the cell cycle (Karanam *et al.*, 2012). The mechanism is promoted by p53-binding protein 1 (53BP1) which suppresses DNA end resection (Panier & Boulton, 2014). c-NHEJ could potentially join ends from different chromosomes, but it is believed that restricted movement due to chromatin organization in the nucleus contributes to proper rejoining of previously linked DNA ends (Sallmyr & Tomkinson, 2018). c-NHEJ works independently of sequence homology and therefore functions in absence of a sister template and is relatively error-prone. The Ku heterodimer, consisting of Ku70 and Ku80 subunits, detects and binds DSB ends and recruits other components of the c-NHEJ machinery (Figure 2). Ku forms the DNA-dependent protein kinase (DNA-PK) complex together with DNA-PK catalytic subunit (DNA-PKcs); activated DNA-PKcs extensively phosphorylates itself and other c-NHEJ factors. The c-NHEJ pathway supports simple religation when overhangs are fully compatible, however many DSBs bear distinct structures such as varying ssDNA overhangs and chemical modifications of nearby nucleotides. Several enzymes are involved in processing of the DSB ends. These include c-NHEJ polymerases Pol λ and Pol μ and possibly other polymerases for gap filling, the structure-specific endonuclease Artemis that has a role in a subset of IR-induced DSBs, and removal of non-ligatable groups at the end of a strand by polynucleotide kinase 3' phosphatase (PNKP). A consequence of such end processing can be the insertion or deletion of several nucleotides, thereby generating mutations (Rodgers & McVey, 2016). The c-NHEJ specific ligase DNA ligase IV (LIG4) in complex with XRCC4 is essential for resealing of the break. XRCC4 forms long filaments with XRCC4-like factor (XLF), which are likely to have an importance for DNA binding. It is unclear whether the two strands are ligated in a coordinated or sequential fashion during c-NHEJ. After ligation the Ku heterodimer needs to be removed from the DNA, this may involve proteolytic degradation or nuclease activity of meiotic recombination 11 homolog 1 (MRE11) (Chiruvella *et al.*, 2013, Radhakrishnan *et al.*, 2014). The mechanism of c-NHEJ is extensively studied using *Xenopus* egg extracts, which is reviewed in **chapter 2**.

Homologous recombination (HR); Figure 2. The HR pathway for repair of DSBs requires a homology donor, usually in the form of a sister chromatid. Therefore, the HR pathway is most active during S-phase and G2-phase of the cell cycle when sister chromatids are available (Karanam *et al.*, 2012). At the start of the pathway the 5' ends of the DSB are resected to form an extended region of 3' ssDNA, which involves the nucleases MRE11-RAD50-NBS1 (MRN), EXO1, DNA2, and CtIP, and the helicase complex BLM-TOP3-RMI1 (Figure 2) (Symington, 2014). Replication protein A (RPA) proteins rapidly bind the ssDNA to protect it from degradation and eliminate secondary structures. Subsequently, RPA is replaced by ssDNA binding protein RAD51. Several factors, called mediators, promote

the nucleation of this RAD51 nucleoprotein filament. Known mediators are the five different RAD51 paralogs (RAD51B, RAD51C, RAD51D, XRCC2, and XRCC3), RAD52 that destabilizes RPA-ssDNA binding, and breast cancer type 2 susceptibility protein (BRCA2). BRCA2 contains domains for binding single stranded DNA (ssDNA), double stranded DNA (dsDNA) and several RAD51 proteins to target filament nucleation to the dsDNA junction at the resected end (Suwaki *et al.*, 2011, Wright *et al.*, 2018). BRCA1 promotes HR by antagonizing the 53BP1 resection-suppressing function, but also promotes recruitment of BRCA2 to DSBs through the bridging protein PALB2 (Oliver *et al.*, 2009, Prakash *et al.*, 2015). Once the RAD51 filament is active it must find a homology donor from which to initiate DNA synthesis, a process that is not fully understood. One strand of duplex DNA is destabilized to open the helix and to allow bases to be sampled for complementarity with those within the filament. When this is found it allows the formation of the synaptic complex. The 3' end of the invading strand forms a primer-template junction for DNA synthesis, forming a structure known as the displacement loop (D-loop). RAD54 is an ATPase that acts as a motor protein for enhancing D-loop formation and the transition to DNA synthesis to fill in the gaps. Three subpathways are distinguished for the next step, the choice of which has consequences for the accuracy of repair. Break-induced repair (BIR) functions in absence of a second 3' overhang and can lead to loss-of-heterozygosity (LOH). During synthesis-dependent strand annealing (SDSA), which is dominant in somatic cells, the extended D-loop is abandoned and re-annealed with the overhang of the second end. This avoids LOH and crossover between chromosomes. In contrast, a double Holliday junction (HJ) can lead to crossovers. A double HJ is formed when the extended D-loop captures the resected second end. HJs are dissolved by a mechanism involving BLM and topoisomerase 3 (dissolution), which results in noncrossover products, or resolved by endonucleases (resolution). HJ resolution is catalysed by flap endonuclease GEN homolog 1 (GEN1), leading to crossover products, or by the MUS81 structure specific endonuclease subunit-essential meiotic structure-specific endonuclease 1 (MUS81-EME1) and synthetic lethal of unknown function 4 and 1 (SLX4-SLX1) nucleases complexes, the products of which are noncrossover (Heyer *et al.*, 2010, Wright *et al.*, 2018, Wyatt & West, 2014). Although HR is generally seen as an error-free repair mechanism, DNA synthesis during elongation of the invading strand is relatively mutagenic (Guirouilh-Barbat *et al.*, 2014).

Alternative end joining (alt-EJ) pathways. The microhomology mediated end joining (MMEJ) and single strand annealing (SSA) pathways for DSB repair also involve resection of DSB ends and are believed to be active in S-phase before the chromosome or locus where the DSB occurred has been replicated (Bhargava *et al.*, 2016, Ceccaldi *et al.*, 2016a). Similar to HR, end resection involves MRN and CtIP, although exact mechanisms and additional factors can be dissimilar. In the MMEJ pathway resection is mediated by poly(APD-ribose) polymerase 1 (PARP1), which is also involved in DNA synapsis via a short (2 to 20 nucleotides) sequence complementarity. Nonhomologous 3' ssDNA tails are removed although the identity of the involved nuclease(s) is not established, indicating functional redundancy. Any gap-filling is mediated by the error-prone DNA polymerase θ (Pol θ), which could also generate insertions, and strands are ligated by Ligase III in complex with XRCC1 (LIG3-XRCC1). MMEJ generates deletions in the rejoined duplex DNA (Chiruvella *et al.*, 2013, Sallmyr & Tomkinson, 2018). SSA involves end joining between scattered sequence repeats of >25 nucleotides, which is mediated by RAD52 (Sallmyr & Tomkinson, 2018). Removal of the 3' ssDNA tails, which are usually longer than in MMEJ,

1 is dependent on XPF-ERCC1 and enhanced by RAD52. The gap-filling polymerase(s) and DNA ligase(s) for SSA are currently not identified. SSA leads to the deletion of one of the repeats and the intermediate genetic information (Bhargava *et al.*, 2016, Heyer *et al.*, 2010, Sallmyr & Tomkinson, 2018).

DNA interstrand crosslink (ICL) repair.

ICLs are damages that covalently attach both strand of the DNA duplex and are very toxic to cells. Although the chemotherapeutic potential has been exploited for more than 70 years, much of the knowledge about the occurrence of endogenously formed ICLs and repair systems that restore ICL damage stems from the last few decades. The major mechanism for the repair of ICLs, the Fanconi anemia pathway, requires pathway-specific steps as well as the contribution of other repair mechanisms, including HR and NER. Since this pathway is the subject of this thesis, I will describe ICL damage, the disease Fanconi anemia, and the repair of ICLs in more detail below.

DNA interstrand crosslinks

DNA interstrand crosslinks (ICLs) are formed when two bases from complementary strands are covalently linked by a crosslinking agent. When the first crosslinking agents were discovered it was not known whether and how they affected DNA. The potential of crosslinking agents for the treatment of cancer was discovered by accident, when victims of a large contamination of sulphur mustard in 1943 presented at the clinic with very specific reductions in white blood cell count (Deans & West, 2011). Later, a stable form mustard gas, mechlorethamine, was successful in clinical trials and various derivatives were developed, some of which are still used today. After the double helical structure of DNA was elucidated it was established that nitrogen mustards are bifunctional alkylating agents that form an ICL by reacting with the N^7 -positions of two guanine residues on complementary strands (Guainazzi & Scharer, 2010). The first publication of 'Nitrogen Mustard Therapy' in 1946 (Goodman *et al.*, 1946) was followed by the development of other crosslinking agents for the treatment of cancer (Figure 3). Mitomycin C (MMC), which is produced by the microorganism *Streptomyces caespitosus*, was discovered in the 1950s as an antitumor crosslinker (Tomasz, 1995). Cisplatin was first synthesized in 1845 before the antiproliferative potential of platinum compounds was published in 1969 (Rosenberg *et al.*, 1969). This led to the approval of cisplatin for clinical usage in 1978 (Gomez-Ruiz *et al.*, 2012) followed by the derivatives carboplatin (1989) and oxaliplatin (1994) (Monneret, 2011). To this day, crosslinking agents are widely used for the treatment of cancer and many new crosslinkers are currently in clinical trials (Brulikova *et al.*, 2012, Deans & West, 2011).

It has been estimated that each human cell has to repair approximately 10 ICLs per day, and that 20-40 unresolved ICL lesions can lead to cell death (Clouston *et al.*, 2013, Grillari *et al.*, 2007). Fast-dividing cells, such as tumor cells, are particularly sensitive to ICL damage. ICLs prevent strand separation, which is essential for cellular processes such as DNA replication and transcription. Some ICLs also significantly distort the structure of duplex DNA, locally affecting access of DNA-binding proteins. Rapidly dividing cells such as tumor cells strongly rely on DNA replication and are therefore particularly sensitive to ICL damage. Tumor cells that are confronted with a high incidence of ICLs react to this by

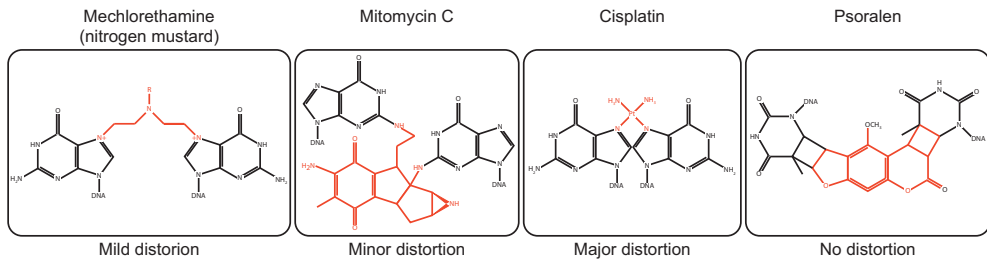


Figure 3: Schematic representation of the chemical structure of ICLs formed by different crosslinking agents. Different DNA crosslinking agents form structurally distinct interstrand crosslinks (ICLs), and cause different distortions in the DNA double helix. Indicated crosslinking agents attached to nucleobases from opposite strands are shown in red. Nucleobases are shown in black. Adapted from: Lopez-Martinez *et al.*, 2016.

entering cell-cycle arrest or inducing apoptosis, or they could choose to continue to cell division with damaged chromosomes, leading to mitotic catastrophe which could also kill the cell (Deans & West, 2011, Jo & Kim, 2015).

It is important to note that ICL inducing agents frequently induce several other types of DNA damage in addition to ICL damage. The efficacy of ICL induction can be as low as 5% of all adducts formed for nitrogen mustards, implying that 95% is non-ICL damage including monoadducts and covalent links between bases in the same strand called intrastrand crosslinks (Dronkert & Kanaar, 2001, Rink & Hopkins, 1995). Similarly, MMC and platinum compounds are inefficient crosslinkers with 15% and 5-8% ICLs, respectively (Malinge *et al.*, 1999, Warren *et al.*, 1998). Combined treatment with psoralen and UV-A induces ICLs remarkably efficient, generating up to 90% ICLs (Huang *et al.*, 2013, Lai *et al.*, 2008). Different crosslinking agents also induce distinct ICLs with respect to their chemical and structural conformation. For instance, crystallographic and NMR studies have shown that a cisplatin ICL distorts the DNA duplex much more than a psoralen ICL (Figure 3) (Huang *et al.*, 2013, Lopez-Martinez *et al.*, 2016, Spielmann *et al.*, 1995). Together, these aspects may have far-reaching consequences for the toxicity, detection, and repair of various crosslinks, and could affect the outcomes of studies that use crosslinking agents.

The above-mentioned ICL inducing agents are predominantly man-made. Our cells possess sophisticated mechanisms for the removal of ICLs (described below), which suggests that there are intracellular sources of ICL damage. However, it is currently unclear how ICLs are formed within cells, as they cannot be visualized, are formed infrequently and in some cases are inherently unstable (Scharer, 2005). Research has indicated reactive aldehydes, that are produced by various cellular mechanisms, as important endogenous crosslinking agents. Oxidative stress, which is promoted by a fat-rich diet, causes lipid peroxidation which leads to the production malondialdehyde, crotonaldehyde, and acrolein (Grillari *et al.*, 2007, Niedernhofer *et al.*, 2003, Pang & Andreassen, 2009, Scharer, 2005, Stone *et al.*, 2008). Recent studies have shown that formaldehyde, a natural occurring compound in our tissues, and acetaldehyde, which is produced by the metabolism of alcohol, are also likely to induce ICL damage when they are not sufficiently catalyzed by the ADH5 and ALDH2 enzymes, respectively (Garaycochea *et al.*, 2012, Hira *et al.*, 2013, Langevin *et al.*, 2011, Ridpath *et al.*, 2007, Rosado *et al.*, 2011, Sakai & Sugawara, 2019). Another endogenous compound that likely contributes to the formation of ICLs is

1 nitric oxide, of which low levels are present in our cells (Caulfield *et al.*, 2003). However, endogenous ICL-inducing compounds crosslink other types of molecules in addition to DNA, making it difficult to determine which lesion drives toxicity (Bagby, 2018, Duxin & Walter, 2015).

Fanconi anemia

The first indication that our cells possess a mechanism specific for the repair of ICLs came from the discovery of the disease Fanconi anemia. In 1927 the Swiss pediatrician Guido Fanconi described a family in which three boys, aged 5 – 7, all suffered from a severe condition that resembled pernicious anemia, a special kind of anemia characterized by macrocytic red blood cells, increased haemolysis and low levels of vitamin B12 (although the latter was not known at the time). In all three children the disease had manifested between the ages five and seven and was associated with birth defects, microcephaly (small head), brown skin pigmentation, cutaneous haemorrhage and hypoplasia of the testes, and a fatal outcome. In contrast to classical pernicious anemia no increased haemolysis was observed. Fanconi recognized this strange selection of symptoms as a disease on its own which he named ‘familial infantile pernicious anemia.’ After more cases were reported in the following years the syndrome was renamed as ‘Fanconi anemia’ (FA) in 1931 (Auerbach, 2009, Lobitz & Velleuer, 2006). With the identification of more cases in the decades that followed it became clear that the syndrome was remarkably variable between patients. Currently, Fanconi anemia is regarded a rare disease with an estimated incidence of 1 in 350,000 births (Mohanty, 2016).

The phenotypes that are associated with Fanconi anemia are remarkably widespread and can even differ between monozygotic twins. Two-third of the patients have major congenital malformations including: skin, growth, eyes, skeletal, kidney/urinary tract, ears, genital, cardio-pulmonary, gastrointestinal, central nervous system. Anomalies can be unilateral, which indicates that the underlying cellular defect is not sufficient to cause developmental defects but dramatically increases the odds that a defect will occur. Patients that have no major malformations are usually later diagnosed, when hematologic dysfunction develops. Bone marrow failure (BMF) is very common among FA patients, as well as myelodysplastic syndrome (MDS) and acute myeloid leukemia (AML). In addition to AML, FA patients have a high susceptibility for developing solid tumors at relatively early age. Many FA patients are infertile: approximately 50% of female and almost all of male FA patients (Auerbach, 2009).

Fanconi’s observations formed the basis for the diagnosis of FA for many years, but the concept of the FA phenotype differed between clinicians (Auerbach, 2009). Research groups in the 60’s were able to show that FA patients suffered from chromosomal instability, which was further induced by DNA-crosslinking substances such as MMC and diepoxybutane (DEB). Schroeder and colleagues were the first to suggest spontaneous chromosomal breakage as cellular marker for FA, but this was too inconsistent (Schroeder, 1964). In contrast, cellular hypersensitivity to chromosome-breaking effects of crosslinking agents did show to be a reliable marker. Nowadays, MMC or DEB chromosomal breakage responses of patient derived cells is considered the gold standard for the diagnosis of FA (Bagby, 2018, Oostra *et al.*, 2012). Other diagnostic tools include next generation sequencing (NGS) and complementation analysis to identify the affected gene and the specific genetic mutation (Dufour, 2017, Ghemlas *et al.*, 2015).

At present, no cure is available for FA patients. Patients with BMF benefit from stem cell transplantation (SCT), which is the most important component for treatment of FA patients and currently the only option capable of prolonging the survival of patients. Other than several decades ago, SCT is now combined with strict preparative diets that prevent cytotoxicity from DNA alkylating agents and irradiation. This has dramatically improved the SCT outcome and life expectancy of patients. An adverse consequence of this is that more patients develop solid tumors (Dufour, 2017).

Guido Fanconi was occupied with the underlying genetic defects and patterns of inheritance of FA. He suspected that the disease could not be caused by mutations in a single gene. In addition, based on observed inheritance patterns he did not believe the widely held view that it was an autosomal recessive disorder (Lobitz & Velleuer, 2006). For the identification of an FA gene, an inactivating mutation must be associated with aberrant chromosomal breakage responses of patient derived cells to MMC or DEB, while complementation with the wild type version of the mutant alleles must correct this phenotype (Bagby, 2018). To date, 22 different genes have been identified, associated with Fanconi anemia or an FA-like syndrome, and designated as complementation groups FANCA-FANCW (Knies *et al.*, 2017). These genes encode proteins that are essential for the coordinated repair of DNA interstrand crosslinks.

FA proteins cooperate with non-FA proteins and proteins from other DNA repair pathways to activate cell cycle checkpoints in response to ICL damage and repair the ICL lesion. The mechanism of the FA pathway is described in more detail below. Briefly, ICLs are thought to be detected by FANCM when replication forks stall at the lesion, recruiting the FA core complex that consists of 8 FA proteins (FANCA, -B, -C, -E, -F, -G, and -L) and three FA-associated proteins (FAAPs). Together with FANCT, the FA core complex carries out the monoubiquitylation of FANCI and FANCD2, which marks the activation of the FA pathway. Downstream processes result in ICL unhooking mediated by SLX4 (FANCP) and XPF (FANCP), which induces a double strand break (DSB) and allows bypass of the unhooked lesion on one of the strands by TLS polymerases, including FANCV (subunit of Pol ζ). The DSB is restored via homologous recombination which involves several FA proteins: RAD51 (FANCR), RAD51 paralogs RAD51C (FANCO) and XRCC2 (FANCU), BRIP1 (FANCJ), BRCA2 (FANCD1), PALB2 (FANCN), BRCA1 (FANCS), and RFW3 (FANCW). The deubiquitinase (DUB) USP1-UAF1 heterodimer ensures deubiquitylation of the ID2 complex and the adducted base is removed by NER.

FA is an autosomal recessive disorder, with the exception of FANCB that is located on the X chromosome (Meetei *et al.*, 2004) and heterozygous dominant-negative mutations in RAD51 (FANCR) that cause an FA-like syndrome (Ameziane *et al.*, 2015, Wang *et al.*, 2015). Heterozygous mutations in several other FA genes are associated with an increased risk for developing cancers (Lobitz & Velleuer, 2006, Niraj *et al.*, 2019). The translocase FANCM, which was reported to cause FA in 2005 (Meetei *et al.*, 2005), was recently disqualified as a true FA protein (Bogliolo *et al.*, 2018, Catucci *et al.*, 2018). The phenotype could not be complemented with cDNA of wild-type FANCM and the patient was later shown to have biallelic mutations in FANCA (Singh *et al.*, 2009). Biallelic truncating mutations in FANCM are shown to cause a cancer predisposition syndrome that is distinct from FA (Bogliolo *et al.*, 2018, Catucci *et al.*, 2018). Despite this, FANCM is strongly associated with the FA pathway.

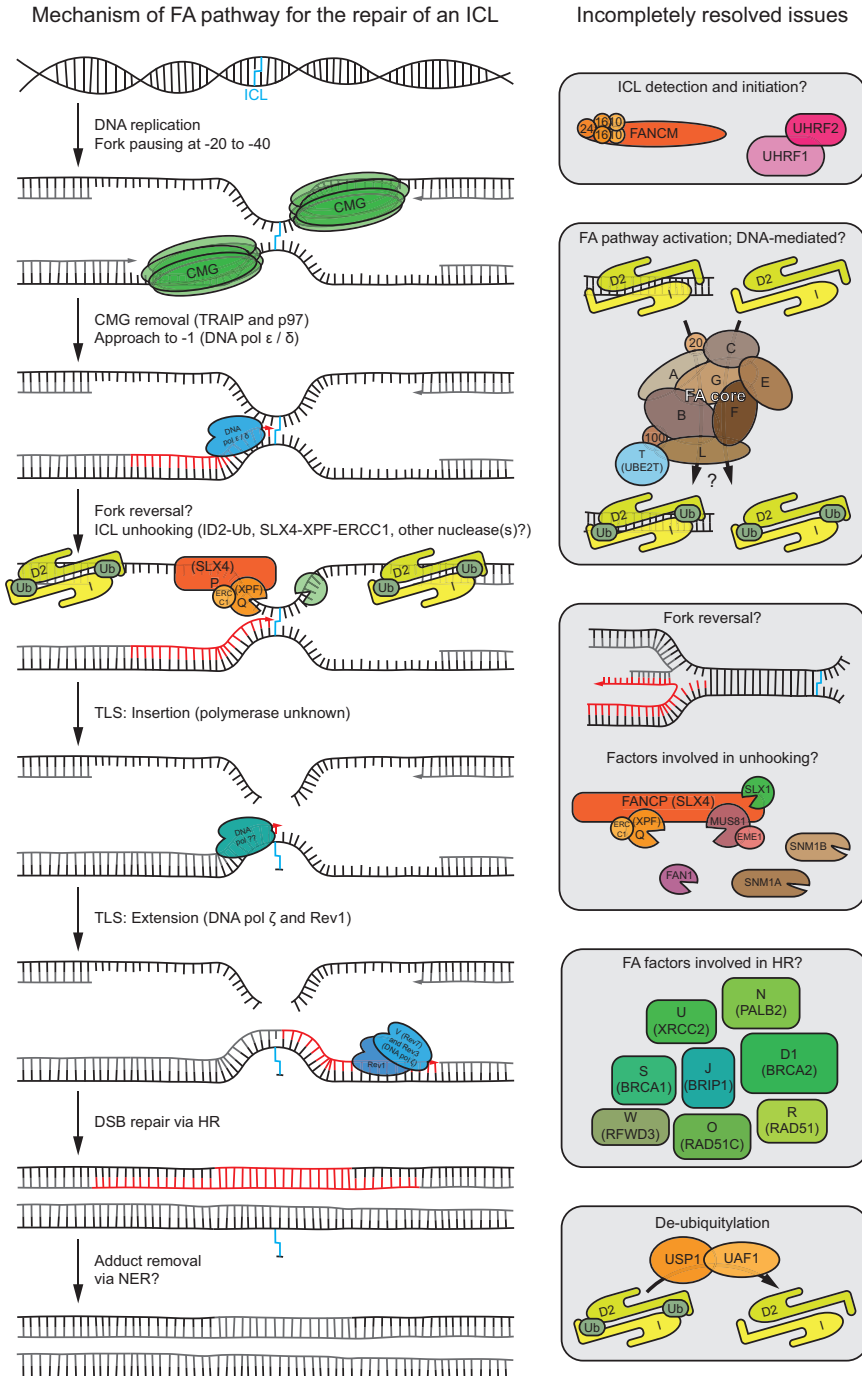


Figure 4: Schematic representation of the FA pathway for ICL repair and several unresolved issues. The Fanconi anemia pathway is a replication-dependent pathway that leads to the repair of an ICL after replication forks have stalled at the crosslink. Repair involves several signaling and DNA-processing steps. Many mechanistic details are currently elusive; several are shown schematically on the right in grey boxes. See text for details.

ICL repair by the Fanconi anemia pathway

ICLs can be repaired throughout the cell cycle and there is evidence for a number of different repair mechanisms, both replication-dependent and replication-independent. However, it is believed that ICLs are predominantly repaired in S phase (Akkari *et al.*, 2001, Akkari *et al.*, 2000, De Silva *et al.*, 2000, Rothfuss & Grompe, 2004, Sobbeck *et al.*, 2006, Taniguchi *et al.*, 2002). The products of the Fanconi anemia genes cooperate in the Fanconi anemia (FA) pathway, which requires DNA replication (Räschle *et al.*, 2008, Zhang & Walter, 2014). How the FA proteins restore ICL damage has long been elusive. With the help of genetic studies that showed the involvement of various classes of proteins, including structure-specific nucleases, TLS polymerases, and proteins involved in HR, a hypothetical model for ICL repair in S phase was developed (McHugh *et al.*, 2001, Niedernhofer *et al.*, 2005). With the use of a soluble extract system based on *Xenopus* eggs, which supports efficient, regulated and physiological vertebrate DNA replication (Walter *et al.*, 1998), a more detailed model for the repair of ICLs by the FA pathway could be developed (Räschle *et al.*, 2008). In this *Xenopus* egg extract system, plasmids harboring a single, site-specific ICL are repaired in a replication-dependent fashion. The use of *Xenopus* egg extracts for the biochemical dissection of DNA repair mechanisms is further discussed in **chapter 2**. This system plays a central role in the studies that were conducted for the completion of this thesis, which are presented in **chapters 3, 4, and 5**.

Here, I will provide an overview of our current understanding of the mechanism by which the FA pathway restores ICL damage, which includes several steps (Figure 4). In addition to the FA pathway, other pathways have been implicated in the repair of ICLs. These will be briefly discussed at the end of this chapter.

ICL detection and initiation

Replication forks that encounter an ICL are unable to separate the DNA strands due to the covalent nature of the crosslinked DNA, causing them to stall. An early role in activating repair is attributed to FANCM that binds to the ICL with the help of several FAAPs (FAAP24, FAAP16/MHF1, FAAP10/MHF2) (Figure 4) (Ciccia *et al.*, 2007, Huang *et al.*, 2010, Singh *et al.*, 2010, Yang *et al.*, 2013). This FANCM-FAAP24-MHF complex is thought to play a major role early in the FA pathway by recruiting replication protein A (RPA), ataxia telangiectasia and Rad3-related (ATR), and ATR interacting protein (ATRIP) to these sites, which helps triggering checkpoint activation and FA pathway activation in response to ICL damage (Collins *et al.*, 2009, Huang *et al.*, 2010). In addition, it plays a role in targeting the FA core complex to ICLs with the help of FANCI (Castella *et al.*, 2015, Ciccia *et al.*, 2007).

The function of the FA core complex in response to ICLs is the addition of a single ubiquitin to both FANCI and FANCD2 in response to ICL damage (Ishiai *et al.*, 2008). The FA core complex is made up of 9 subunits, 7 of which are *bona fide* FA gene products (FANCA, -B, -C, -E, -F, -G, and -L), in addition to 2 FAAPs (FAAP20 and FAAP100) for which disease-associated mutations have not (yet) been found (Walden & Deans, 2014). The FA core complex is extensively studied, as >98% of FA patients have lost the ability to perform the monoubiquitylation of FANCI and FANCD2 (Tan & Deans, 2017). Several autonomous modules can be distinguished in the structure of the FA core complex that have different and partially unknown functions (Huang *et al.*, 2014, Medhurst *et al.*, 2006, Rajendra *et al.*, 2014). Crucial components for FANCD2 monoubiquitylation are at least

1

FANCL, the E3 ubiquitin-protein ligase subunit of the core complex, and UBE2T (FANCT), the E2 conjugating enzyme, which combined with an E1 enzyme are sufficient to perform the reaction *in vitro* (Alpi *et al.*, 2008, Meetei *et al.*, 2003, Rickman *et al.*, 2015). Recent biochemical studies have demonstrated that higher order structures of the subcomplexes ensure symmetric monoubiquitylation of FANCI and FANCD2 together (Swuec *et al.*, 2017, van Twest *et al.*, 2017).

Despite this seemingly dependence of FA-mediated ICL repair on the FANCM-FAAP24-MHF complex, it is shown that cells depleted of components of this complex exhibit incomplete loss of monoubiquitylation of FANCI and FANCD2 (Wang *et al.*, 2013, Yan *et al.*, 2010). This indicates that FANCM function is not essential to initiate the FA pathway in response to ICL damage, which could be explained by the existence of alternative mechanisms to activate downstream processes. Indeed, recent studies have demonstrated that ubiquitin-like with PHD RING finger domain 1 (UHRF1), with the help of its paralog UHRF2, is able to recognize ICL damage and promote repair (Figure 4) (Liang *et al.*, 2015, Motnenko *et al.*, 2018, Tian *et al.*, 2015). However, these studies also present conflicting results, as one study involves UHRF1 in the FA pathway by promoting recruitment of FANCD2 (Liang *et al.*, 2015), while the other study demonstrates an FA-independent role for UHRF1 (Tian *et al.*, 2015). Collectively, this shows that ICL recognition and initiation of the FA pathway are poorly understood and require further investigation.

Monoubiquitylation and deubiquitylation of FANCI and FANCD2

FANCI and FANCD2 form a heterodimer (ID2) that binds the DNA around the ICL and activates downstream processes in the FA pathway upon its monoubiquitylation by the FA core complex (Alpi *et al.*, 2008, Garcia-Higuera *et al.*, 2001, Knipscheer *et al.*, 2009, Smogorzewska *et al.*, 2007). The proteins are structurally very similar (Joo *et al.*, 2011) and a monoubiquitin is ligated onto the residues Lys523 of FANCI and Lys561 of FANCD2 (Garcia-Higuera *et al.*, 2001, Sims *et al.*, 2007, Smogorzewska *et al.*, 2007). These studies furthermore demonstrated that monoubiquitylation of FANCI and FANCD2 are interdependent and that mutation of the lysine residues to arginines abrogated their function in ICL repair. *In vitro* reconstitution of the monoubiquitylation reaction has suggested that FANCI enhances monoubiquitylation of FANCD2 and ensures that monoubiquitylation is restricted to the physiological Lys561 residue (Alpi *et al.*, 2008, Longerich *et al.*, 2014). However, ubiquitylation of FANCI appears to be less crucial to conferring ICL resistance (Ishiai *et al.*, 2008, Smogorzewska *et al.*, 2007).

The monoubiquitylated ID2 complex associates with chromatin to promote ICL repair processes, although it is not completely understood whether the monoubiquitylation reaction occurs prior to recruitment to ICLs or on chromatin (Figure 4) (Lopez-Martinez *et al.*, 2016). The K561R mutation of FANCD2 is reported to abrogate recruitment of ID2 to chromatin (Knipscheer *et al.*, 2009, Lopez-Martinez *et al.*, 2016). However, other evidence points towards a model in which the ID2 complex binds to DNA before it is monoubiquitylated. Crystal structures of the ID2 complex demonstrate that the target sites for ubiquitylation are embedded in the heterodimer interface (Joo *et al.*, 2011), yet the monoubiquitylation reaction on FANCD2 is enhanced by heterodimerization with FANCI (Longerich *et al.*, 2014, Sato *et al.*, 2012). The reaction is also stimulated by the presence of duplex or branched DNA, suggesting that monoubiquitylation occurs while the ID2 complex is localized at a stalled replication fork (Liang *et al.*, 2016, Longerich *et al.*, 2014,

Sobeck *et al.*, 2007). It is possible that monoubiquitylation of ID2 induces retention at the crosslink rather than recruitment (Lopez-Martinez *et al.*, 2016). A recent study has suggested that phosphorylation of FANCD2 inhibits ID2 binding to DNA, allowing for regulation of DNA recruitment and monoubiquitylation (Lopez-Martinez *et al.*, 2019).

Completion of the FA pathway is not only dependent on ubiquitylation but also seems to rely on de-ubiquitylation of monoubiquitylated ID2 complex, probably to ensure recycling and prevent deregulated recruitment of FANCD2 (Ishiai *et al.*, 2008). The deubiquitylating (DUB) enzyme responsible for this is the ubiquitin carboxyl-terminal hydrolase 1-USP1-associated factor 1 (USP1-UAF1) heterodimer (Figure 4) (Cohn *et al.*, 2009, Cohn *et al.*, 2007, Nijman *et al.*, 2005). Recent work has shown that de-ubiquitylation *in vitro* only occurs when DNA is removed from the monoubiquitylated ID2 complex (van Twest *et al.*, 2017). Consistent with an essential role in FA-mediated ICL repair, USP1 deficient mice develop an FA-like phenotype (Kim *et al.*, 2009). Interestingly, USP1-UAF1 is also responsible for the de-ubiquitylation of Lys164-ubiquitylated proliferating cell nuclear antigen (PCNA), a modification that is associated with recruitment of TLS polymerases (Hoege *et al.*, 2002, Kannouche *et al.*, 2004). However, this PCNA modification is poorly elicited by cellular treatment with MMC, suggesting this may not be important for ICL repair (Hicks *et al.* 2010). Together, the dynamics of ID2 monoubiquitylation and its reversibility are incompletely understood.

Fork convergence, CMG unloading, approach, and fork reversal

Replication-dependent ICL repair in *Xenopus* egg extracts requires the convergence of two replication forks to the ICL (Zhang *et al.*, 2015). This was shown by blocking the progression of one replication fork before it reached the ICL on a plasmid, which inhibited unloading of the replicative CMG helicase (comprised of CDC45, MCM2-7, GINS) and ICL repair. Instead, when both replication forks are converged, transient stalling of replication is observed 20-40 nucleotides from the ICL, consistent with the footprint of CMG that unwinds the DNA ahead of the replicative polymerase (Fu *et al.*, 2011, Räschle *et al.*, 2008). The convergence of two forks triggers unloading of CMG, allowing one fork to approach the ICL (Figure 4) (Fu *et al.*, 2011).

CMG unloading was reported to be promoted by BRCA1, resulting from the observation that immunodepletion of BRCA1 from extracts prevented unloading (Long *et al.*, 2014). However, these conclusions were recently attenuated with the finding that the use of BRCA1 antiserum resulted in a co-depletion of TRAF-interacting protein (TRAIIP) which was concurrently shown to be the actual mediator of CMG unloading (Wu *et al.*, 2019). TRAIIP is a ubiquitin E3 ligase that is essential for both FA-mediated repair and NEIL3-dependent repair of ICLs, an alternative replication-dependent pathway for the repair of ICLs that is described below and in **chapter 2**. TRAIIP acts by ubiquitylating stalled CMGs at a converged fork, initially recruiting NEIL3 through a direct interaction with a short ubiquitin chain. However, when NEIL3 cannot process the ICL and CMGs remain stalled, the ubiquitin chains become longer and CMG is susceptible to unloading, which is mediated by the p97 ATPase (Fullbright *et al.*, 2016).

'Approach' is triggered by unloading of CMG and is restricted to one fork, which stops 1 nucleotide from the lesion (Figure 4) (Fu *et al.*, 2011, Long *et al.*, 2014). Which fork will approach the ICL appears to be random and not influenced by the order of arrival at the ICL (Räschle *et al.*, 2008, Zhang *et al.*, 2015). Indirect data suggests that approach is carried

1
out by pol ϵ or pol δ , both high-fidelity polymerases (Budzowska *et al.*, 2015). Blocking approach with aphidicolin, a drug that inhibits polymerases α , ϵ , δ , and ζ , prevents further downstream processes for the repair of the ICL (Long *et al.*, 2014). However, FANCD2 recruitment to ICLs is not affected when fork convergence or approach is blocked (Long *et al.*, 2014, Zhang *et al.*, 2015), suggesting that extension of the leading strand contributes in one way or another to downstream repair processes, such as the formation of structure that is cleavable by associated structure specific endonucleases (SSEs).

A recent study demonstrated with the use of electron microscopy (EM) that repair intermediates of ICL-containing plasmids in *Xenopus* egg extracts undergo fork reversal (Figure 4) (Amunugama *et al.*, 2018). Replication fork reversal can be used as a protective measure when a fork encounters a DNA lesion, preventing fork collapse and chromosomal breakage (Neelsen & Lopes, 2015). Fork reversal during ICL repair is dependent on CMG unloading and this finding is complemented with *in vitro* experiments demonstrating how fork reversal could contribute to the combined action of XPF-ERCC1 and an unknown exonuclease in the unhooking of the ICL (Amunugama *et al.*, 2018), which is further discussed below. However, the proposed model is currently speculative since only a subset of plasmids undergo fork reversal and evidence that it is essential for ICL repair is lacking. In addition, fork reversal does not depend on leading strand approach (Amunugama *et al.*, 2018). Collectively, it remains to be determined what the functions of approach and fork reversal are during ICL repair and how they contribute to the next step in the pathway, the unhooking incisions.

Unhooking incisions

A functional 'consequence' of ID2 monoubiquitylation during ICL repair is the nucleolytic unhooking of the crosslink, which requires at least the structure-specific endonuclease (SSE) XPF-ERCC1 and the scaffold protein SLX4 (Figure 4) (Klein Douwel *et al.*, 2014, Knipscheer *et al.*, 2009). This key step in the FA pathway for ICL repair is the subject of this thesis.

When the importance of monoubiquitylation of the ID2 complex was identified, it was not known how ubiquitylated FANCD2 contributed to ICL repair (Garcia-Higuera *et al.*, 2001, Sims *et al.*, 2007, Smogorzewska *et al.*, 2007). Later, with the use of *Xenopus* egg extracts it was demonstrated that unhooking incisions are dependent on FANCD2 and its monoubiquitylation (Knipscheer *et al.*, 2009). It was shown that in absence of monoubiquitylated ID2, the leading strand persisted 1 nucleotide from the ICL and further repair was inhibited. This was also the first evidence that the FA pathway was directly required for replication-coupled ICL repair. However, FANCI and FANCD2 lack any nuclease domains, and the mechanism by which monoubiquitylated ID2 promotes unhooking incisions was unclear.

Several nucleases were implicated in the FA pathway based on cellular sensitivity to ICL-inducing agents (Figure 4) (Zhang & Walter, 2014). It was suggested that ICL unhooking involved incisions on both sides of the crosslink, suggesting that two SSEs with opposing structure preference could be required (Klein Douwel *et al.*, 2014). Work in our laboratory has demonstrated that XPF(FANCD2)-ERCC1 is essential for ICL repair and unhooking incisions, whereas two other SSEs, MUS81-EME1 and FAN1, are not (Klein Douwel *et al.*, 2014). In addition, this study showed that SLX4 (FANCP) is required for recruitment of XPF-ERCC1 to ICL sites, while in turn monoubiquitylated FANCD2

promotes efficient recruitment of both SLX4 and XPF-ERCC1 (Klein Douwel *et al.*, 2014). In absence of XPF-ERCC1, no incisions occur, indicating that a first incision by XPF allows subsequent nucleolytic steps required for ICL unhooking, or the presence or activity of XPF is required for the first incision by another endonuclease. Alternatively, XPF-ERCC1 could be responsible for both incisions. Despite having a structural preference, XPF-ERCC1 has the ability to do this based on *in vitro* experiments with fork-like DNA templates (Fisher *et al.*, 2008, Hodskinson *et al.*, 2014, Kuraoka *et al.*, 2000).

The heterodimer **XPF-ERCC1** is a member of the MUS81/XPF family of endonucleases and consists of a catalytically active subunit, xeroderma pigmentosum complementation group F (XPF), and a structural subunit that provides substrate specificity, excision repair cross complementation group 1 (ERCC1) (Ciccia *et al.*, 2008). In complex, XPF-ERCC1 is a 3'-flap endonuclease that cuts in the double stranded DNA near the double to single stranded DNA junction of several DNA structures (Bowles *et al.*, 2012). XPF-ERCC1 has essential roles in nucleotide excision repair (NER) and in the single strand annealing (SSA) pathway for double strand break repair, as discussed earlier in this chapter. Interestingly, no other NER factors are similarly associated with ICL repair (De Silva *et al.*, 2000). In accordance, XPF is a *bona fide* FA factor since mutations in the gene encoding XPF are associated with Fanconi anemia (Bogliolo *et al.*, 2013). Disease-specific mutations are reported for XPF (Kashiyama *et al.*, 2013); how these mutations affect the specific role in ICL repair is the subject of **chapter 3** of this thesis.

The role of XPF-ERCC1 in ICL repair is linked to an interaction with SLX4 (Crossan *et al.*, 2011, Fekairi *et al.*, 2009, Kim *et al.*, 2013, Munoz *et al.*, 2009, Stoepker *et al.*, 2011, Svendsen *et al.*, 2009), and this interaction could enhance the nuclease activity (Hodskinson *et al.*, 2014). How SLX4 facilitates XPF-ERCC1-mediated incisions is examined in **chapter 4**.

SLX4 (synthetic lethal of unknown function 4) is a scaffold protein for three SSEs: XPF-ERCC1, MUS81-EME1, and SLX1. Interactions with these nucleases are mediated by the MEI9^{XPF} interaction like region (MLR), SAF-A/B, Acinus and PIAS (SAP), and SLX1 binding domain (SBD) domains, respectively (Fekairi *et al.*, 2009). SLX4 itself harbors no nuclease activity, but the association with these SSEs allows the full complex to cleave a wide array of branched DNA structures (Wyatt *et al.*, 2017). SLX4 is associated with several genome maintenance processes (Guervilly & Gaillard, 2018). As discussed earlier in this chapter, SLX4 is required for the noncrossover branch of Holliday junction (HJ) resolution, which is one of the subpathways of homologous recombination (HR) (Wyatt & West, 2014). This function of SLX4 requires association with SLX1 and MUS81-EME1, but not XPF-ERCC1. SLX4 also employs its interaction with MUS81-EME1, and to lesser extent SLX1, for responses to replication stress (Guervilly *et al.*, 2015, Malacaria *et al.*, 2017, Sarbajna *et al.*, 2014). SLX4 has furthermore functions in telomere maintenance and common fragile site (CFS) replication, for which it uses its ability to cut various branched structures (Guervilly *et al.*, 2015, Minocherhomji *et al.*, 2015, Ouyang *et al.*, 2015, Sarkar *et al.*, 2015, Svendsen *et al.*, 2009, Wilson *et al.*, 2013). The nuclease activity of MUS81-EME1 does not depend on SLX4, although its association with SLX4 relaxes its substrate specificity (Wyatt *et al.*, 2017). In contrast, the 5'-flap endonuclease **SLX1** (synthetic lethal of unknown function 1) is reported to exist as an inactive homodimer that becomes an active heterodimer upon interaction with SLX4 (Gaur *et al.*, 2015). As a purified heterodimer, SLX4-SLX1 cleaves many different DNA substrates with a preference for nicking the 3' side

of a branched structure within 2-4 nucleotides from the double to single stranded DNA junction (Fricke & Brill, 2003, Gaur *et al.*, 2015, Wyatt *et al.*, 2013).

1
SLX4 is essential for ICL repair, as SLX4-deficient cells are hypersensitive to crosslinking agents and mutations in the gene encoding for SLX4 are associated with Fanconi anemia (Fekairi *et al.*, 2009, Kim *et al.*, 2011, Munoz *et al.*, 2009, Stoepker *et al.*, 2011, Svendsen *et al.*, 2009). SLX1 has been proposed to function in ICL unhooking, where it could be essential or act redundantly with Fanconi-associated nuclease 1 (FAN1) or a possible other endonuclease for performing the 5' nick, unhooking the ICL after the initial incision by XPF-ERCC1 (Klein Douwel *et al.*, 2014, Zhang & Walter, 2014). However, mouse embryonic fibroblasts (MEFs) that are SLX1-deficient or expressing a nuclease-dead mutant display mild sensitivity to ICL-inducing agents, in contrast to SLX4-deficient cells that are much more sensitive (Castor *et al.*, 2013). In another study, expression of a truncated SLX4 protein that lacks the SBD in SLX4-deficient MEFs partially rescues sensitivity to MMC (Hodskinson *et al.*, 2014). These results suggest that SLX1 could contribute to, but is not essential for, ICL repair. The function of SLX1 in the FA pathway is explored in **chapter 4**, where we show that ICL repair is not dependent on SLX1. SLX4 contains a Broad-Complex, Tramtrack and Bric-a-brac (BTB) domain that is known for mediating protein-protein complex formation and homodimerization (Chen *et al.*, 1995). Indeed, the BTB domain is shown to facilitate SLX4 dimerization, while dimerization-disrupting mutations mildly sensitize cells to crosslinking agents (Guervilly *et al.*, 2015, Yin *et al.*, 2016). In **chapter 4** we show that the BTB domain is dispensable for ICL repair. Work by our laboratory has shown that monoubiquitylated FANCD2 promotes recruitment of SLX4 to ICLs (Klein Douwel *et al.*, 2014), but the mechanism by which SLX4 recruitment is achieved is elusive. Two N-terminal ubiquitin-binding zinc finger (UBZ) domains are associated with SLX4 recruitment and ICL repair, and are also affected in an FA-causing patient mutation, but the roles of these domains is poorly understood. These issues are addressed in **chapter 5**, where we show that UBZ domains are important for SLX4 recruitment and ICL repair, although the molecular details of a link with monoubiquitylated FANCD2 is not elucidated.

The lack of any incisions in absence of XPF-ERCC1 could also be explained by the involvement of an exonuclease during ICL unhooking (Klein Douwel *et al.* 2014). The 5' to 3' exonucleases sensitivity to nitrogen mustard protein 1A (SNM1A) and 1B (SNM1B) have been suggested to act in ICL unhooking (Allerston *et al.*, 2015, Cattell *et al.*, 2010, Sengerova *et al.*, 2012, Zhang & Walter, 2014), and cells deficient of **SNM1A** or **SNM1B** display sensitivity to ICL-inducing agents (Ishiai *et al.*, 2004). SNM1A, and to lesser extent SNM1B, could load from a nick induced by XPF-ERCC1 and digest ssDNA past an ICL, essentially eliminating the need for a second incision (Sengerova *et al.*, 2012, Wang *et al.*, 2011). Other data is in accordance with this model and includes the requirement for RPA in neutralizing the inhibiting effect of a nascent leading strand (Abdullah *et al.*, 2017). Consistent with a role for fork reversal on unhooking incisions is the observation that XPF cannot incise X-shaped DNA structures whereas a leading strand template was readily processed (Amunugama *et al.*, 2018). However, these experiments were not performed in the context of SLX4 which could enhance XPF activity (Hodskinson *et al.*, 2014). Alternatively, SNM1A could employ its recently identified endonuclease activity for ICL unhooking (Buzon *et al.*, 2018). **FAN1** also harbors 5' to 3' exonuclease activity in addition to its activity as an endonuclease (Kratz *et al.*, 2010, Liu *et al.*, 2010, MacKay *et al.*, 2010, Smogorzewska *et al.*, 2010). FAN1 forms a direct interaction with FANCD2 for recruitment to stalled replication forks and is associated with ICL repair (Lachaud *et*

al., 2016), although work by our laboratory has shown that ICL repair is not dependent on FAN1 (Klein Douwel *et al.*, 2014). Indeed, patients with deficiencies in FAN1 did not develop Fanconi anemia but suffered from karyomegalic interstitial nephritis (KIN), which is characterized by renal failure. However, FAN1 could have a redundant role in ICL repair. Together, the exact mechanism of unhooking incisions during ICL repair are poorly understood, and future studies are needed to determine which nucleases are involved and how monoubiquitylation of FANCD2 results in ICL unhooking.

Translesion synthesis (TLS)

After unhooking incisions, the unhooked nucleotide including the ICL is still attached to one of the parental DNA strands. This adduct needs to be bypassed to continue replication, which is performed by specialized polymerases that allow more tolerant base-pairing at the cost of replication fidelity (Hoeijmakers, 2001). Indeed, cells from FA patients show a reduction in point mutations compared to healthy cells (Niedernhofer *et al.*, 2005, Niedzwiedz *et al.*, 2004). This process is called translesion synthesis (TLS) and often involves multiple polymerases performing the reaction in two steps: insertion of a nucleotide across the adducted base and extension past the inserted nucleotide (Figure 4) (Shachar *et al.*, 2009).

The involvement of the TLS polymerases Pol ζ and Rev1 was suggested from cellular hypersensitivities to ICL-inducing agents (Gan *et al.*, 2008, Hara *et al.*, 2010, Niedzwiedz *et al.*, 2004). Consistently, depletion of Rev7, a subunit of Pol ζ , inhibited repair in *Xenopus* egg extracts and resulted in accumulation of products containing the inserted nucleotide, indicating that Pol ζ is required for extension past the ICL (Räschle *et al.*, 2008). Rev1 was long believed to be responsible for the insertion step, however immunodepletion of Rev1 from *Xenopus* egg extracts had the same effect on the process of TLS as Rev7 depletion, suggesting a coordinated role for Rev1 and Pol ζ in extension (Budzowska *et al.*, 2015). Rev1 could have a role in recruiting TLS complex components to ICLs and is itself recruited by the FA core complex but not by monoubiquitylated FANCD2 (Budzowska *et al.*, 2015, Kim *et al.*, 2012, Mirchandani *et al.*, 2008, Niedzwiedz *et al.*, 2004). Consistent with this, Rev1 appears to be responsible for the error-prone replication during ICL repair, as mutation rates in cells deficient of FA core components are reduced whereas FANCD2-deficient cells display increased mutation rates (Budzowska *et al.*, 2015).

It is currently unclear which polymerase is responsible for the insertion step during ICL repair, which will be challenging to determine since there is a lot of variability in the possible structure of the unhooked ICL and the candidate TLS polymerases that could act on them (Roy & Scharer, 2016). Moreover, the choice of TLS polymerase appears to be determined by the type of ICL, which is apparent from the observation that Pol ζ is required for TLS of cisplatin ICLs but not for nitrogen mustard ICLs (Räschle *et al.*, 2008).

DSB repair through HR

Unhooking incisions during repair of ICLs produce a double strand break (DSBs) that needs to be repaired. The contribution of c-NHEJ, alt-EJ, and SSA to FA-associated genomic instability is poorly understood (Kottemann & Smogorzewska, 2013). However, the occurrence of FA patients that harbor mutations in many genes related to homologous recombination (HR) indicate a preference for this repair pathway. The mechanism of HR is

described earlier in this chapter.

1 Interestingly, not all these patients acquire an FA syndrome but rather an FA-like syndrome, which lacks the development of bone marrow failure (BMF). Homozygous mutations in BRCA1, BRCA2, and PALB2 are often hypomorphic, indicating their diminished activity of HR allows survival at the cost of developing an FA-like syndrome (Niraj *et al.*, 2019). In another case, a dominant-negative mutation in RAD51 abrogated ICL repair but not general HR, indicating a differential function in HR during the repair of ICLs (Wang *et al.*, 2015). Mutations of several other FA gene products that appear to have a function downstream of FANCD2-dependent pathway activation are associated with HR but their pathogenesis is currently poorly understood (Niraj *et al.*, 2019).

Adduct removal through NER

After the DSB is restored, the adducted nucleotide is still present and needs to be removed for completion of ICL repair. It is generally thought that the NER pathway is involved in the process, although the precise molecular mechanism remains elusive (Mouw & D'Andrea, 2014). Accordingly, several NER-deficient cell lines display hypersensitivity to ICL-inducing agents, although this is mild compared to ERCC1- and XPF-deficient cells (De Silva *et al.*, 2000, Wood, 2010), indicating that ICL repair does not depend on other NER factors as much as it does on XPF-ERCC1. It is possible that the adduct is removed in the next cell cycle, which would explain why this is inefficient in *Xenopus* egg extracts (Räschle *et al.*, 2008). Future studies are needed to elucidate this issue.

Alternative ICL repair pathways

Although ICL repair via the FA pathway is considered the major repair pathway adopted by cells, the existence of alternative repair mechanisms has been demonstrated. Accumulating evidence suggests that structurally distinct ICLs could be repaired via different repair mechanisms, adding an additional layer of complexity to how cells can respond to ICL damage.

ICL traverse

ICLs were considered definitive blocks to DNA replication until a study demonstrated that ICLs induced by treatment with 4,5',8-trimethyl psoralen (TMP) and UV were efficiently 'traversed' in Chinese hamster ovary (CHO) cells, which was partially mediated by the translocase activity of FANCM (Huang *et al.*, 2013). This traverse reaction does not directly lead to ICL repair, instead it generates X-shaped structures that are similar to the structure of a dual converged fork, which has been suggested to be important for subsequent repair by the FA pathway (Amunugama *et al.*, 2018, Zhang *et al.*, 2015, Zhang & Walter, 2014). However, ICL traverse is not observed in *Xenopus* egg extracts. The functional relevance of traverse is unclear but probably not crucial for ICL repair considering that FANCM-deficient cells display modest sensitivity to ICL inducing agents (Huang *et al.*, 2014, Mosedale *et al.*, 2005).

Much is unclear about the mechanism by which a replication fork could traverse an ICL. Initially only the translocase activity of FANCM was shown to contribute to ICL traverse, although traverse is also observed in absence of FANCM, suggesting an additional mechanism (Huang *et al.*, 2013). Subsequent studies have demonstrated the involvement

of the Bloom syndrome RecQ like helicase-DNA topoisomerase III alpha-RecQ mediated genome instability protein 1 and 2 (BLM-Top3 α -RMI) helicase complex, PCNA, ATR, and the ID2 complex, but not its monoubiquitylation, to the process (Ling *et al.*, 2016, Mutreja *et al.*, 2018, Rohleder *et al.*, 2016). These factors could promote traverse by remodeling of the replisome (Huang *et al.*, 2019). Future work is needed to unravel the mechanism and functional relevance of ICL traverse. ICLs induced by TMP cause minimal distortion of the DNA, which could be a prerequisite for efficient traverse.

NEIL3-dependent ICL repair

Although ICL traverse is not observed in *Xenopus* egg extracts, the incubation of a plasmid carrying a psoralen/UV- or abasic site-derived ICL did recently lead to the characterization of a previously unidentified ICL repair pathway (Semlow *et al.*, 2016). In contrast to cisplatin- or nitrogen mustard-derived ICLs, these crosslinks were repaired in a replication-dependent manner without the need for FANCD2-induced incisions. Instead, the DNA glycosylase NEIL3 was shown to resolve psoralen and abasic site ICLs by cleaving the *N*-glycosyl bond between the sugar and the base of either one of the crosslinked nucleotides. When this bond cannot be cleaved, for example in absence of NEIL3, repair is channelled through the FA pathway. Further details about this mechanism are discussed in **chapter 2**.

Recent work has elucidated the mechanism by which the pathway choice is made (Wu *et al.*, 2019). Converged replication forks at an ICL are recognized by TRAF-interacting protein (TRAIP), a ubiquitin E3 ligase that ubiquitylates components of the CMG helicase. This serves initially to recruit NEIL3, which forms a direct interaction with CMG via short ubiquitin chains. When the ICL is not resolved, for instance in absence of NEIL3 or when the forks are stalled at a cisplatin ICL that cannot be processed by NEIL3, the ubiquitin chains elongate and the long chains are a signal for the unloading and degradation of CMG that is mediated by the p97 ATPase (Fullbright *et al.*, 2016). This allows one of the leading strands to approach the ICL and the subsequent repair steps required for FA-mediated ICL repair (Wu *et al.*, 2019).

Replication-independent repair

Although ICLs are predominantly repaired by replication-dependent mechanisms, repair is also observed to occur in a replication-independent manner, which could be crucial for maintaining genome integrity in non-cycling cells such as neurons (Lopez-Martinez *et al.*, 2016).

The mechanism of replication-independent repair (RIR) is elusive and highly dependent on the type of crosslink (Hlavin *et al.*, 2010). The NER factor XPC is associated with the recognition of bulky ICLs, which subsequently recruits other NER factors including XPF and XPG (Wang *et al.*, 2001). Similar to NER, XPF and XPG incise the DNA to unhook the ICL, creating a gap that is filled by a TLS polymerase (Muniandy *et al.*, 2009, Sarkar *et al.*, 2006, Wang *et al.*, 2001). However, the involvement of XPC is debated and CSB is also involved in recruiting repair machinery to ICLs (Enoiu *et al.*, 2012, Wang *et al.*, 2001). Furthermore, studies have generated conflicting results about the use of TLS polymerases by RIR, indicating that this is at least in part determined by the type of ICL (Enoiu *et al.*, 2012, Roy & Scharer, 2016, Shen *et al.*, 2009, Williams *et al.*, 2012). In addition, a recent

1 study indicated the existence of a replication-independent repair mechanism based on the mismatch repair (MMR) machinery, which is particularly active at distorting ICLs (Kato *et al.*, 2017).

Additional functions of the FA pathway

Several FA proteins have functions outside the FA pathway for the repair of ICLs. The FA pathway plays an important role in preventing genomic instability resulting from destabilization or collapse of a stalled replication fork (Ceccaldi *et al.*, 2016b, Sumpter & Levine, 2017). The ID2 complex, BRCA1, and BRCA2 localize to and stabilize stalled replication forks, protecting nascent DNA from degradation by nucleases (Lossaint *et al.*, 2013, Schlacher *et al.*, 2012). New origin firing and entry into mitosis is suppressed by FANCD2 (Chaudhury *et al.*, 2014), while FANCI also has an FA core-independent role in promoting firing of dormant origins (Chen *et al.*, 2015). FANCD2, FANCI, and BRCA2, but also BLM and FAN1, cooperate to promote the recovery of stalled forks (Raghunandan *et al.*, 2015). Genome stability is also protected by FANCD2 and FANCI that are thought to contribute to the resolution of ultrafine bridges, which arise from the replication of common fragile sites (CFS) (Chan *et al.*, 2009, Howlett *et al.*, 2005, Naim & Rosselli, 2009). The FA pathway is associated with the removal of R-loops, transcription-associated DNA:RNA hybrids that can be a threat to genome stability (Garcia-Rubio *et al.*, 2015, Schwab *et al.*, 2015). In addition, a number of FA core proteins as well as FANCD2, BRCA1, and BRCA2, are required for autophagy of mitochondria, while FANCC also functions in autophagy for viruses (Sumpter *et al.*, 2016).

Concluding remarks

Despite the fact that individual aspects of the Fanconi anemia pathway have been extensively studied, important details regarding the mechanism are still unclear. Recent identifications of a previously uncharacterized ICL repair pathway and advances in our understanding of the endogenous metabolites underlying FA are amongst many exciting developments that are seen in this field of research. Although these developments could contribute to better treatment of FA patients and advancements of chemotherapy in the future, more work is needed to exploit the full potential of understanding how ICLs are formed, repaired, and how they achieve their cytotoxicity. It sure has been fascinating to see how our knowledge of the subject has evolved over the course of one thesis (which has to be said is by no means a reliable measure of time).

Thesis outline

DNA interstrand crosslinks (ICLs) are toxic DNA lesions that prevent strand separation by covalently attaching the DNA strands. While cancers are often treated with ICL inducing drugs such as cisplatin, some cancers build resistance to chemotherapeutics by upregulation of DNA repair factors. A detailed understanding of how repair proteins restore ICL damage is therefore favorable to help improve therapies and to fight resistance. This thesis aims to elucidate the mechanism of ICL unhooking, a crucial step in the repair of cisplatin ICLs, using extracts derived from eggs of the frog species *Xenopus laevis*. The *Xenopus* egg extract system is a unique tool that enables to recapitulate eukaryotic DNA replication and other genome maintenance pathways outside the cell. **Chapter 2** contains a comprehensive description of how *Xenopus* egg extracts have been used to study several genome maintenance mechanisms.

Cisplatin-ICLs are repaired by the replication-dependent Fanconi anemia pathway, a complex mechanism that is defective in patients that have the genetic cancer-predisposition disorder Fanconi anemia (FA). This pathway involves nucleolytic incisions to unhook the ICL from one of the strands, which requires monoubiquitylated FANCD2 (FANCD2-Ub), the scaffold protein SLX4, and the structure specific endonuclease XPF-ERCC1. XPF-ERCC1 also has an essential role nucleotide excision repair (NER), a pathway for the removal of bulky lesions on DNA. Upregulation of XPF-ERCC1 is associated with chemotherapeutic resistance, which is why targeting ICL repair-specific functions has potential clinical applications. In **chapter 3** we examine how mutations in XPF specifically affect its function in ICL repair. We identify such mutations in the nuclease domain as well as in the binding interface with the ICL repair-specific binding partner SLX4. Interaction with SLX4 is crucial for recruitment, and possibly also for correct positioning, of XPF-ERCC1 to ICL-containing DNA substrates. These data help to explain why certain mutations in XPF-ERCC1 cause Fanconi anemia while others do not. In **chapter 4** we consider the role of SLX4 in the FA pathway. We identify residues that are crucial for binding and recruiting XPF-ERCC1 to ICLs, which is essential for ICL repair. In contrast, a large portion of SLX4 appears not to be important for ICL repair, which rules out potential roles for binding partners interacting with this region. We also report a novel link of the XPF-binding domain with recruitment of SLX4 to ICLs, a theme that is further explored in the next chapter. In **chapter 5** we show that SLX4 recruitment is mediated by two domains. Recruitment likely involves interaction with a protein containing a polyubiquitin chain, but the identity of this factor remains elusive. Although FANCD2-Ub promotes recruitment of SLX4, we demonstrate that this is not mediated by a direct interaction. SLX4 recruitment is complex and involves at least one unknown factor. In **chapter 6** we discuss the various findings of the previous chapters and place them in a larger context while providing future directions.

References

- 1
- Abdullah UB, McGouran JF, Brolihs S, Ptchelkine D, El-Sagheer AH, Brown T & McHugh PJ (2017) RPA activates the XPF-ERCC1 endonuclease to initiate processing of DNA interstrand crosslinks. *The EMBO journal* 36: 2047-2060
- Akkari YM, Bateman RL, Reifsteck CA, D'Andrea AD, Olson SB & Grompe M (2001) The 4N cell cycle delay in Fanconi anemia reflects growth arrest in late S phase. *Mol Genet Metab* 74: 403-12
- Akkari YM, Bateman RL, Reifsteck CA, Olson SB & Grompe M (2000) DNA replication is required to elicit cellular responses to psoralen-induced DNA interstrand cross-links. *Molecular and cellular biology* 20: 8283-9
- Allerston CK, Lee SY, Newman JA, Schofield CJ, McHugh PJ & Gileadi O (2015) The structures of the SNM1A and SNM1B/Apollo nuclease domains reveal a potential basis for their distinct DNA processing activities. *Nucleic acids research* 43: 11047-60
- Alpi AF, Pace PE, Babu MM & Patel KJ (2008) Mechanistic insight into site-restricted monoubiquitination of FANCD2 by Ube2t, FANCL, and FANCI. *Molecular cell* 32: 767-77
- Ameziane N, May P, Haitjema A, van de Vrugt HJ, van Rossum-Fikkert SE, Ristic D, Williams GJ, Balk J, Rockx D, Li H, Rooimans MA, Oostra AB, Velleuer E, Dietrich R, Bleijerveld OB, Maarten Altelaar AF, Meijers-Heijboer H, Joenje H, Glusman G, Roach J *et al.* (2015) A novel Fanconi anaemia subtype associated with a dominant-negative mutation in RAD51. *Nature communications* 6: 8829
- Amunugama R, Willcox S, Wu RA, Abdullah UB, El-Sagheer AH, Brown T, McHugh PJ, Griffith JD & Walter JC (2018) Replication Fork Reversal during DNA Interstrand Crosslink Repair Requires CMG Unloading. *Cell reports* 23: 3419-3428
- Araujo SJ, Nigg EA & Wood RD (2001) Strong functional interactions of TFIIH with XPC and XPG in human DNA nucleotide excision repair, without a preassembled repairosome. *Molecular and cellular biology* 21: 2281-91
- Auerbach AD (2009) Fanconi anemia and its diagnosis. *Mutation research* 668: 4-10
- Bagby G (2018) Recent advances in understanding hematopoiesis in Fanconi Anemia. *F1000Research* 7: 105
- Basu AK (2018) DNA Damage, Mutagenesis and Cancer. *Int J Mol Sci* 19
- Bhargava R, Onyango DO & Stark JM (2016) Regulation of Single-Strand Annealing and its Role in Genome Maintenance. *Trends Genet* 32: 566-575
- Bianconi E, Piovesan A, Facchin F, Beraudi A, Casadei R, Frabetti F, Vitale L, Pelleri MC, Tassani S, Piva F, Perez-Amodio S, Strippoli P & Canaider S (2013) An estimation of the number of cells in the human body. *Ann Hum Biol* 40: 463-71
- Bjelland S & Seeberg E (2003) Mutagenicity, toxicity and repair of DNA base damage induced by oxidation. *Mutation research* 531: 37-80
- Bogliolo M, Bluteau D, Lespinasse J, Pujol R, Vasquez N, d'Enghien CD, Stoppa-Lyonnet D, Leblanc T, Soulier J & Surrallès J (2018) Biallelic truncating FANCM mutations cause early-onset cancer but not Fanconi anemia. *Genet Med* 20: 458-463
- Bogliolo M, Schuster B, Stoecker C, Derkunt B, Su Y, Raams A, Trujillo JP, Minguillon J, Ramirez MJ, Pujol R, Casado JA, Banos R, Rio P, Knies K, Zuniga S, Benitez J, Bueren JA, Jaspers NG, Scharer OD, de Winter JP *et al.* (2013) Mutations in ERCC4, encoding the DNA-repair endonuclease XPF, cause Fanconi anemia. *American journal of human genetics* 92: 800-6
- Bowles M, Lally J, Fadden AJ, Mouilleron S, Hammonds T & McDonald NQ (2012) Fluorescence-based incision assay for human XPF-ERCC1 activity identifies important elements of DNA junction recognition. *Nucleic acids research* 40: e101
- Brulikova L, Hlavac J & Hradil P (2012) DNA interstrand cross-linking agents and their chemotherapeutic potential. *Curr Med Chem* 19: 364-85
- Budzowska M, Graham TG, Sobock A, Waga S & Walter JC (2015) Regulation of the Rev1-pol zeta complex during bypass of a DNA interstrand crosslink. *The EMBO journal* 34: 1971-85
- Buzon B, Grainger R, Huang S, Rzadki C & Junop MS (2018) Structure-specific endonuclease activity of SNM1A enables processing of a DNA interstrand crosslink. *Nucleic acids research*
- Caldecott KW (2008) Single-strand break repair and genetic disease. *Nature reviews Genetics* 9: 619-31
- Campisi J & d'Adda di Fagagna F (2007) Cellular senescence: when bad things happen to good cells. *Nat Rev Mol Cell Biol* 8: 729-40
- Castella M, Jacquemont C, Thompson EL, Yeo JE, Cheung RS, Huang JW, Sobock A, Hendrickson EA & Taniguchi T (2015) FANCI Regulates Recruitment of the FA Core Complex at Sites of DNA Damage Independently of FANCD2. *PLoS genetics* 11: e1005563
- Castor D, Nair N, Declais AC, Lachaud C, Toth R, Macartney TJ, Lilley DM, Arthur JS & Rouse J (2013) Cooperative control of holliday junction resolution and DNA repair by the SLX1 and MUS81-EME1 nucleases. *Molecular cell* 52: 221-33
- Cattell E, Sengerova B & McHugh PJ (2010) The SNM1/Pso2 family of ICL repair nucleases: from yeast to man. *Environmental and molecular mutagenesis* 51: 635-45
- Catucci I, Osorio A, Arver B, Neidhardt G, Bogliolo M, Zanardi F, Riboni M, Minardi S, Pujol R, Azzollini J, Peissel B, Manoukian S, De Vecchi G, Casola S, Hauke J, Richters L, Rhiem K, Schmutzler RK, Wallander K, Torngren T *et al.* (2018) Individuals with FANCM biallelic mutations do not develop Fanconi anemia, but show risk for breast cancer, chemotherapy

- toxicity and may display chromosome fragility. *Genet Med* 20: 452-457
- Caulfield JL, Wishnok JS & Tannenbaum SR (2003) Nitric oxide-induced interstrand cross-links in DNA. *Chem Res Toxicol* 16: 571-4
- Ceccaldi R, Rondinelli B & D'Andrea AD (2016a) Repair Pathway Choices and Consequences at the Double-Strand Break. *Trends Cell Biol* 26: 52-64
- Ceccaldi R, Sarangi P & D'Andrea AD (2016b) The Fanconi anaemia pathway: new players and new functions. *Nat Rev Mol Cell Biol* 17: 337-49
- Chan KL, Palmai-Pallag T, Ying S & Hickson ID (2009) Replication stress induces sister-chromatid bridging at fragile site loci in mitosis. *Nat Cell Biol* 11: 753-60
- Chatterjee N & Walker GC (2017) Mechanisms of DNA damage, repair, and mutagenesis. *Environmental and molecular mutagenesis* 58: 235-263
- Chaudhury I, Stroik DR & Sobock A (2014) FANCD2-controlled chromatin access of the Fanconi-associated nuclease FAN1 is crucial for the recovery of stalled replication forks. *Molecular and cellular biology* 34: 3939-54
- Chen W, Zollman S, Couderc JL & Laski FA (1995) The Btb Domain of Bric a Brac Mediates Dimerization in-Vitro (Retracted Article. See Vol 17, Pg 6772, 1997). *Molecular and cellular biology* 15: 3424-3429
- Chen YH, Jones MJ, Yin Y, Crist SB, Colnaghi L, Sims RJ, 3rd, Rothenberg E, Jallepalli PV & Huang TT (2015) ATR-mediated phosphorylation of FANCI regulates dormant origin firing in response to replication stress. *Molecular cell* 58: 323-38
- Cheung-Ong K, Giaever G & Nislow C (2013) DNA-damaging agents in cancer chemotherapy: serendipity and chemical biology. *Chem Biol* 20: 648-59
- Chiruvella KK, Liang Z & Wilson TE (2013) Repair of double-strand breaks by end joining. *Cold Spring Harb Perspect Biol* 5: a012757
- Ciccia A, Ling C, Coulthard R, Yan Z, Xue Y, Meetei AR, Laghmani el H, Joenje H, McDonald N, de Winter JP, Wang W & West SC (2007) Identification of FAAP24, a Fanconi anemia core complex protein that interacts with FANCM. *Molecular cell* 25: 331-43
- Ciccia A, McDonald N & West SC (2008) Structural and functional relationships of the XPF/MUS81 family of proteins. *Annu Rev Biochem* 77: 259-87
- Clauson C, Schärer OD & Niedernhofer L (2013) Advances in understanding the complex mechanisms of DNA interstrand cross-link repair. *Cold Spring Harb Perspect Biol* 5: a012732
- Cohn MA, Kee Y, Haas W, Gygi SP & D'Andrea AD (2009) UAF1 is a subunit of multiple deubiquitinating enzyme complexes. *The Journal of biological chemistry* 284: 5343-51
- Cohn MA, Kowal P, Yang K, Haas W, Huang TT, Gygi SP & D'Andrea AD (2007) A UAF1-containing multisubunit protein complex regulates the Fanconi anemia pathway. *Molecular cell* 28: 786-97
- Coin F, Marinoni JC, Rodolfo C, Fribourg S, Pedrini AM & Egly JM (1998) Mutations in the XPD helicase gene result in XP and TTD phenotypes, preventing interaction between XPD and the p44 subunit of TFIIH. *Nature genetics* 20: 184-8
- Collins NB, Wilson JB, Bush T, Thomashevski A, Roberts KJ, Jones NJ & Kupfer GM (2009) ATR-dependent phosphorylation of FANCA on serine 1449 after DNA damage is important for FA pathway function. *Blood* 113: 2181-90
- Cortez D (2019) Replication-Coupled DNA Repair. *Molecular cell* 74: 866-876
- Crosby GP, van der Weyden L, Rosado IV, Langevin F, Gaillard PH, McIntyre RE, Sanger Mouse Genetics P, Gallagher F, Kettunen MI, Lewis DY, Brindle K, Arends MJ, Adams DJ & Patel KJ (2011) Disruption of mouse Slx4, a regulator of structure-specific nucleases, phenocopies Fanconi anemia. *Nature genetics* 43: 147-52
- De Silva IU, McHugh PJ, Clingen PH & Hartley JA (2000) Defining the roles of nucleotide excision repair and recombination in the repair of DNA interstrand cross-links in mammalian cells. *Molecular and cellular biology* 20: 7980-90
- Deans AJ & West SC (2011) DNA interstrand crosslink repair and cancer. *Nat Rev Cancer* 11: 467-80
- Dronkert ML & Kanaar R (2001) Repair of DNA interstrand cross-links. *Mutation research* 486: 217-47
- Dufour C (2017) How I manage patients with Fanconi anaemia. *Br J Haematol* 178: 32-47
- Duxin JP & Walter JC (2015) What is the DNA repair defect underlying Fanconi anemia? *Current opinion in cell biology* 37: 49-60
- Enoiu M, Jiricny J & Schärer OD (2012) Repair of cisplatin-induced DNA interstrand crosslinks by a replication-independent pathway involving transcription-coupled repair and translesion synthesis. *Nucleic acids research* 40: 8953-64
- Faridounnia M, Folkers GE & Boelens R (2018) Function and Interactions of ERCC1-XPF in DNA Damage Response. *Molecules* 23
- Fekairi S, Scaglione S, Chahwan C, Taylor ER, Tissier A, Coulon S, Dong MQ, Ruse C, Yates JR, 3rd, Russell P, Fuchs RP, McGowan CH & Gaillard PH (2009) Human SLX4 is a Holliday junction resolvase subunit that binds multiple DNA repair/recombination endonucleases. *Cell* 138: 78-89
- Fishel R (2015) Mismatch repair. *The Journal of biological chemistry* 290: 26395-403
- Fisher LA, Bessho M & Bessho T (2008) Processing of a psoralen DNA interstrand cross-link by XPF-ERCC1 complex in vitro. *The Journal of biological chemistry* 283: 1275-81
- Fricke WM & Brill SJ (2003) Slx1-Slx4 is a second structure-specific endonuclease functionally redundant with Sgs1-Top3. *Genes & development* 17: 1768-78
- Fu YV, Yardimci H, Long DT, Ho TV, Guainazzi A,

- Bermudez VP, Hurwitz J, van Oijen A, Scharer OD & Walter JC (2011) Selective bypass of a lagging strand roadblock by the eukaryotic replicative DNA helicase. *Cell* 146: 931-41
- Fullbright G, Rycenga HB, Gruber JD & Long DT (2016) p97 Promotes a Conserved Mechanism of Helicase Unloading during DNA Cross-Link Repair. *Molecular and cellular biology* 36: 2983-2994
- Gan GN, Wittschieben JP, Wittschieben BO & Wood RD (2008) DNA polymerase zeta (pol zeta) in higher eukaryotes. *Cell Res* 18: 174-83
- Garaycochea JI, Crossan GP, Langevin F, Daly M, Arends MJ & Patel KJ (2012) Genotoxic consequences of endogenous aldehydes on mouse haematopoietic stem cell function. *Nature* 489: 571-5
- Garcia-Higuera I, Taniguchi T, Ganesan S, Meyn MS, Timmers C, Hejna J, Grompe M & D'Andrea AD (2001) Interaction of the Fanconi anemia proteins and BRCA1 in a common pathway. *Molecular cell* 7: 249-62
- Garcia-Rubio ML, Perez-Calero C, Barroso SI, Tumini E, Herrera-Moyano E, Rosado IV & Aguilera A (2015) The Fanconi Anemia Pathway Protects Genome Integrity from R-loops. *PLoS genetics* 11: e1005674
- Gaur V, Wyatt HD, Komorowska W, Szczepanowski RH, de Sanctis D, Gorecka KM, West SC & Nowotny M (2015) Structural and Mechanistic Analysis of the Slx1-Slx4 Endonuclease. *Cell reports* 10: 1467-1476
- Ghemlas I, Li H, Zlateska B, Klaassen R, Fernandez CV, Yanofsky RA, Wu J, Pastore Y, Silva M, Lipton JH, Brossard J, Michon B, Abish S, Steele M, Sinha R, Belletrutti M, Breakey VR, Jardine L, Goodyear L, Sung L *et al.* (2015) Improving diagnostic precision, care and syndrome definitions using comprehensive next-generation sequencing of the inherited bone marrow failure syndromes. *J Med Genet* 52: 575-84
- Ghodgaonkar MM, Lazzaro F, Olivera-Pimentel M, Artola-Boran M, Cejka P, Reijns MA, Jackson AP, Plevani P, Muzi-Falconi M & Jiricny J (2013) Ribonucleotides misincorporated into DNA act as strand-discrimination signals in eukaryotic mismatch repair. *Molecular cell* 50: 323-32
- Giglia-Mari G, Zotter A & Vermeulen W (2011) DNA damage response. *Cold Spring Harb Perspect Biol* 3: a000745
- Gomez-Ruiz S, Maksimovic-Ivanic D, Mijatovic S & Kaluderovic GN (2012) On the discovery, biological effects, and use of Cisplatin and metalocenes in anticancer chemotherapy. *Bioinorg Chem Appl* 2012: 140284
- Goode EL, Ulrich CM & Potter JD (2002) Polymorphisms in DNA repair genes and associations with cancer risk. *Cancer Epidemiol Biomarkers Prev* 11: 1513-30
- Goodman LS, Wintrobe MM & *et al.* (1946) Nitrogen mustard therapy; use of methyl-bis (beta-chloroethyl) amine hydrochloride and tris (beta-chloroethyl) amine hydrochloride for Hodgkin's disease, lymphosarcoma, leukemia and certain allied and miscellaneous disorders. *J Am Med Assoc* 132: 126-32
- Grillari J, Katinger H & Voglauer R (2007) Contributions of DNA interstrand cross-links to aging of cells and organisms. *Nucleic acids research* 35: 7566-76
- Guainazzi A & Scharer OD (2010) Using synthetic DNA interstrand crosslinks to elucidate repair pathways and identify new therapeutic targets for cancer chemotherapy. *Cell Mol Life Sci* 67: 3683-97
- Guervilly JH & Gaillard PH (2018) SLX4: multitasking to maintain genome stability. *Crit Rev Biochem Mol Biol* 53: 475-514
- Guervilly JH, Takedachi A, Naim V, Scaglione S, Chawhan C, Lovera Y, Despras E, Kuraoka I, Kannouche P, Rosselli F & Gaillard PH (2015) The SLX4 complex is a SUMO E3 ligase that impacts on replication stress outcome and genome stability. *Molecular cell* 57: 123-37
- Guirouilh-Barbat J, Lambert S, Bertrand P & Lopez BS (2014) Is homologous recombination really an error-free process? *Frontiers in genetics* 5: 175
- Hakem R (2008) DNA-damage repair; the good, the bad, and the ugly. *The EMBO journal* 27: 589-605
- Hara K, Hashimoto H, Murakumo Y, Kobayashi S, Kogame T, Unzai S, Akashi S, Takeda S, Shimizu T & Sato M (2010) Crystal structure of human REV7 in complex with a human REV3 fragment and structural implication of the interaction between DNA polymerase zeta and REV1. *The Journal of biological chemistry* 285: 12299-307
- Heyer WD, Ehmsen KT & Liu J (2010) Regulation of homologous recombination in eukaryotes. *Annual review of genetics* 44: 113-39
- Hira A, Yabe H, Yoshida K, Okuno Y, Shiraishi Y, Chiba K, Tanaka H, Miyano S, Nakamura J, Kojima S, Ogawa S, Matsuo K, Takata M & Yabe M (2013) Variant ALDH2 is associated with accelerated progression of bone marrow failure in Japanese Fanconi anemia patients. *Blood* 122: 3206-9
- Hlavin EM, Smeaton MB, Noronha AM, Wilds CJ & Miller PS (2010) Cross-link structure affects replication-independent DNA interstrand cross-link repair in mammalian cells. *Biochemistry* 49: 3977-88
- Hodskinson MR, Silhan J, Crossan GP, Garaycochea JI, Mukherjee S, Johnson CM, Scharer OD & Patel KJ (2014) Mouse SLX4 is a tumor suppressor that stimulates the activity of the nuclease XPF-ERCC1 in DNA crosslink repair. *Molecular cell* 54: 472-84
- Hoeghe C, Pfander B, Moldovan GL, Pyrowolakis G & Jentsch S (2002) RAD6-dependent DNA repair is linked to modification of PCNA by ubiquitin and SUMO. *Nature* 419: 135-41
- Hoeijmakers JH (2001) Genome maintenance mechanisms for preventing cancer. *Nature* 411: 366-74
- Hoeijmakers JH (2007) Genome maintenance mechanisms are critical for preventing cancer as

- well as other aging-associated diseases. *Mech Ageing Dev* 128: 460-2
- Hombauer H, Campbell CS, Smith CE, Desai A & Kolodner RD (2011) Visualization of eukaryotic DNA mismatch repair reveals distinct recognition and repair intermediates. *Cell* 147: 1040-53
- Howlett NG, Taniguchi T, Durkin SG, D'Andrea AD & Glover TW (2005) The Fanconi anemia pathway is required for the DNA replication stress response and for the regulation of common fragile site stability. *Human molecular genetics* 14: 693-701
- Huang J, Liu S, Bellani MA, Thazhathveetil AK, Ling C, de Winter JP, Wang Y, Wang W & Seidman MM (2013) The DNA translocase FANCM/MHF promotes replication traverse of DNA interstrand crosslinks. *Molecular cell* 52: 434-46
- Huang J, Zhang J, Bellani MA, Pokharel D, Gichimu J, James RC, Gali H, Ling C, Yan Z, Xu D, Chen J, Meetei AR, Li L, Wang W & Seidman MM (2019) Remodeling of Interstrand Crosslink Proximal Replisomes Is Dependent on ATR, FANCM, and FANCD2. *Cell reports* 27: 1794-1808 e5
- Huang M, Kim JM, Shiotani B, Yang K, Zou L & D'Andrea AD (2010) The FANCM/FAAP24 complex is required for the DNA interstrand crosslink-induced checkpoint response. *Molecular cell* 39: 259-68
- Huang Y, Leung JW, Lowery M, Matsushita N, Wang Y, Shen X, Huang D, Takata M, Chen J & Li L (2014) Modularized functions of the Fanconi anemia core complex. *Cell reports* 7: 1849-57
- Ishiai M, Kimura M, Namikoshi K, Yamazoe M, Yamamoto K, Arakawa H, Agematsu K, Matsushita N, Takeda S, Buerstedde JM & Takata M (2004) DNA cross-link repair protein SNM1A interacts with PIAS1 in nuclear focus formation. *Molecular and cellular biology* 24: 10733-41
- Ishiai M, Kitao H, Smogorzewska A, Tomida J, Kinomura A, Uchida E, Saberi A, Kinoshita E, Kinoshita-Kikuta E, Koike T, Tashiro S, Elledge SJ & Takata M (2008) FANCI phosphorylation functions as a molecular switch to turn on the Fanconi anemia pathway. *Nature structural & molecular biology* 15: 1138-46
- Iyama T & Wilson DM, 3rd (2013) DNA repair mechanisms in dividing and non-dividing cells. *DNA repair* 12: 620-36
- Jackson SP & Bartek J (2009) The DNA-damage response in human biology and disease. *Nature* 461: 1071-8
- Jeggio P & Lohrich M (2006) Radiation-induced DNA damage responses. *Radiat Prot Dosimetry* 122: 124-7
- Jo U & Kim H (2015) Exploiting the Fanconi Anemia Pathway for Targeted Anti-Cancer Therapy. *Molecules and cells* 38: 669-76
- Joo W, Xu G, Persky NS, Smogorzewska A, Rudge DG, Buzovetsky O, Elledge SJ & Pavletich NP (2011) Structure of the FANCI-FANCD2 complex: insights into the Fanconi anemia DNA repair pathway. *Science* 333: 312-6
- Kadyrov FA, Genschel J, Fang Y, Penland E, Edelman W & Modrich P (2009) A possible mechanism for exonuclease 1-independent eukaryotic mismatch repair. *Proceedings of the National Academy of Sciences of the United States of America* 106: 8495-500
- Kannouche PL, Wing J & Lehmann AR (2004) Interaction of human DNA polymerase eta with monoubiquitinated PCNA: a possible mechanism for the polymerase switch in response to DNA damage. *Molecular cell* 14: 491-500
- Karanam K, Kafri R, Loewer A & Lahav G (2012) Quantitative live cell imaging reveals a gradual shift between DNA repair mechanisms and a maximal use of HR in mid S phase. *Molecular cell* 47: 320-9
- Kashiyama K, Nakazawa Y, Pilz DT, Guo C, Shimada M, Sasaki K, Fawcett H, Wing JF, Lewin SO, Carr L, Li TS, Yoshiura K, Utani A, Hirano A, Yamashita S, Greenblatt D, Nardo T, Stefanini M, McGibbon D, Sarkany R *et al.* (2013) Malfunction of nuclease ERCC1-XPF results in diverse clinical manifestations and causes Cockayne syndrome, xeroderma pigmentosum, and Fanconi anemia. *American journal of human genetics* 92: 807-19
- Kato N, Kawasoe Y, Williams H, Coates E, Roy U, Shi Y, Beese LS, Scharer OD, Yan H, Gottesman ME, Takahashi TS & Gautier J (2017) Sensing and Processing of DNA Interstrand Crosslinks by the Mismatch Repair Pathway. *Cell reports* 21: 1375-1385
- Kim H, Yang K, Dejsuphong D & D'Andrea AD (2012) Regulation of Rev1 by the Fanconi anemia core complex. *Nature structural & molecular biology* 19: 164-70
- Kim JM, Parmar K, Huang M, Weinstock DM, Ruit CA, Kutok JL & D'Andrea AD (2009) Inactivation of murine Usp1 results in genomic instability and a Fanconi anemia phenotype. *Dev Cell* 16: 314-20
- Kim Y, Lach FP, Desetty R, Hanenberg H, Auerbach AD & Smogorzewska A (2011) Mutations of the SLX4 gene in Fanconi anemia. *Nature genetics* 43: 142-6
- Kim Y, Spitz GS, Veturi U, Lach FP, Auerbach AD & Smogorzewska A (2013) Regulation of multiple DNA repair pathways by the Fanconi anemia protein SLX4. *Blood* 121: 54-63
- Kleczkowska HE, Marra G, Lettieri T & Jiricny J (2001) hMSH3 and hMSH6 interact with PCNA and colocalize with it to replication foci. *Genes & development* 15: 724-36
- Klein Douwel D, Boonen RA, Long DT, Szypowska AA, Räschle M, Walter JC & Knipscheer P (2014) XPF-ERCC1 acts in Unhooking DNA interstrand crosslinks in cooperation with FANCD2 and FANCP/SLX4. *Molecular cell* 54: 460-71
- Knies K, Inano S, Ramirez MJ, Ishiai M, Surrallés J, Takata M & Schindler D (2017) Biallelic mutations in the ubiquitin ligase RFD3 cause Fanconi

- anemia. *J Clin Invest* 127: 3013-3027
- Knipscheer P, Räschle M, Smogorzewska A, Enoiu M, Ho TV, Scharer OD, Elledge SJ & Walter JC (2009) The Fanconi anemia pathway promotes replication-dependent DNA interstrand cross-link repair. *Science* 326: 1698-701
- Kottemann MC & Smogorzewska A (2013) Fanconi anaemia and the repair of Watson and Crick DNA crosslinks. *Nature* 493: 356-63
- Kratz K, Schopf B, Kaden S, Sendoel A, Eberhard R, Lademann C, Cannavo E, Sartori AA, Hengartner MO & Jiricny J (2010) Deficiency of FANCD2-associated nuclease KIAA1018/FAN1 sensitizes cells to interstrand crosslinking agents. *Cell* 142: 77-88
- Kuraoka I, Kobertz WR, Ariza RR, Biggerstaff M, Essigmann JM & Wood RD (2000) Repair of an interstrand DNA cross-link initiated by ERCC1-XPF repair/recombination nuclease. *The Journal of biological chemistry* 275: 26632-6
- Lachaud C, Slean M, Marchesi F, Lock C, Odell E, Castor D, Toth R & Rouse J (2016) Karyomegalic interstitial nephritis and DNA damage-induced polyploidy in Fan1 nuclease-defective knock-in mice. *Genes & development* 30: 639-44
- Lai C, Cao H, Hearst JE, Corash L, Luo H & Wang Y (2008) Quantitative analysis of DNA interstrand cross-links and monoadducts formed in human cells induced by psoralens and UVA irradiation. *Anal Chem* 80: 8790-8
- Langevin F, Crossan GP, Rosado IV, Arends MJ & Patel KJ (2011) Fancd2 counteracts the toxic effects of naturally produced aldehydes in mice. *Nature* 475: 53-8
- Larrea AA, Lujan SA & Kunkel TA (2010) SnapShot: DNA mismatch repair. *Cell* 141: 730 e1
- Li CL, Golebiowski FM, Onishi Y, Samara NL, Sugasawa K & Yang W (2015) Tripartite DNA Lesion Recognition and Verification by XPC, TFIIH, and XPA in Nucleotide Excision Repair. *Molecular cell* 59: 1025-34
- Liang CC, Li Z, Lopez-Martinez D, Nicholson WV, Venien-Bryan C & Cohn MA (2016) The FANCD2-FANCI complex is recruited to DNA interstrand crosslinks before monoubiquitination of FANCD2. *Nature communications* 7: 12124
- Liang CC, Zhan B, Yoshikawa Y, Haas W, Gygi SP & Cohn MA (2015) UHRF1 is a sensor for DNA interstrand crosslinks and recruits FANCD2 to initiate the Fanconi anemia pathway. *Cell reports* 10: 1947-56
- Lindahl T & Barnes DE (2000) Repair of endogenous DNA damage. *Cold Spring Harbor symposia on quantitative biology* 65: 127-33
- Ling C, Huang J, Yan Z, Li Y, Ohzeki M, Ishiai M, Xu D, Takata M, Seidman M & Wang W (2016) Bloom syndrome complex promotes FANCM recruitment to stalled replication forks and facilitates both repair and traverse of DNA interstrand crosslinks. *Cell Discov* 2: 16047
- Liu D, Keijzers G & Rasmussen LJ (2017) DNA mismatch repair and its many roles in eukaryotic cells. *Mutation research* 773: 174-187
- Liu T, Ghosal G, Yuan J, Chen J & Huang J (2010) FAN1 acts with FANCI-FANCD2 to promote DNA interstrand cross-link repair. *Science* 329: 693-6
- Lobitz S & Velleuer E (2006) Guido Fanconi (1892-1979): a jack of all trades. *Nat Rev Cancer* 6: 893-8
- Long DT, Joukov V, Budzowska M & Walter JC (2014) BRCA1 promotes unloading of the CMG helicase from a stalled DNA replication fork. *Molecular cell* 56: 174-85
- Longerich S, Kwon Y, Tsai MS, Hlaing AS, Kupfer GM & Sung P (2014) Regulation of FANCD2 and FANCI monoubiquitination by their interaction and by DNA. *Nucleic acids research* 42: 5657-70
- Lopez-Martinez D, Kupculak M, Yang D, Yoshikawa Y, Liang CC, Wu R, Gygi SP & Cohn MA (2019) Phosphorylation of FANCD2 Inhibits the FANCD2/FANCI Complex and Suppresses the Fanconi Anemia Pathway in the Absence of DNA Damage. *Cell reports* 27: 2990-3005 e5
- Lopez-Martinez D, Liang CC & Cohn MA (2016) Cellular response to DNA interstrand crosslinks: the Fanconi anemia pathway. *Cell Mol Life Sci* 73: 3097-114
- Lossaint G, Larroque M, Ribeyre C, Bec N, Larroque C, Decaillet C, Gari K & Constantinou A (2013) FANCD2 binds MCM proteins and controls replisome function upon activation of s phase checkpoint signaling. *Molecular cell* 51: 678-90
- MacKay C, Declais AC, Lundin C, Agostinho A, Deans AJ, MacArtney TJ, Hofmann K, Gartner A, West SC, Helleday T, Lilley DM & Rouse J (2010) Identification of KIAA1018/FAN1, a DNA repair nuclease recruited to DNA damage by monoubiquitinated FANCD2. *Cell* 142: 65-76
- Malacaria E, Franchitto A & Pichierrri P (2017) SLX4 Prevents GEN1-Dependent DSBs During DNA Replication Arrest Under Pathological Conditions in Human Cells. *Scientific reports* 7: 44464
- Malinge JM, Giraud-Panis MJ & Leng M (1999) Interstrand cross-links of cisplatin induce striking distortions in DNA. *J Inorg Biochem* 77: 23-9
- Marnett LJ (2000) Oxyradicals and DNA damage. *Carcinogenesis* 21: 361-70
- Marteijn JA, Lans H, Vermeulen W & Hoeijmakers JH (2014) Understanding nucleotide excision repair and its roles in cancer and ageing. *Nat Rev Mol Cell Biol* 15: 465-81
- McHugh PJ, Spanswick VJ & Hartley JA (2001) Repair of DNA interstrand crosslinks: molecular mechanisms and clinical relevance. *The Lancet Oncology* 2: 483-490
- Medhurst AL, Laghmani el H, Steltenpool J, Ferrer M, Fontaine C, de Groot J, Roomans MA, Scheper RJ, Meetei AR, Wang W, Joenje H & de Winter JP (2006) Evidence for subcomplexes in the Fanconi

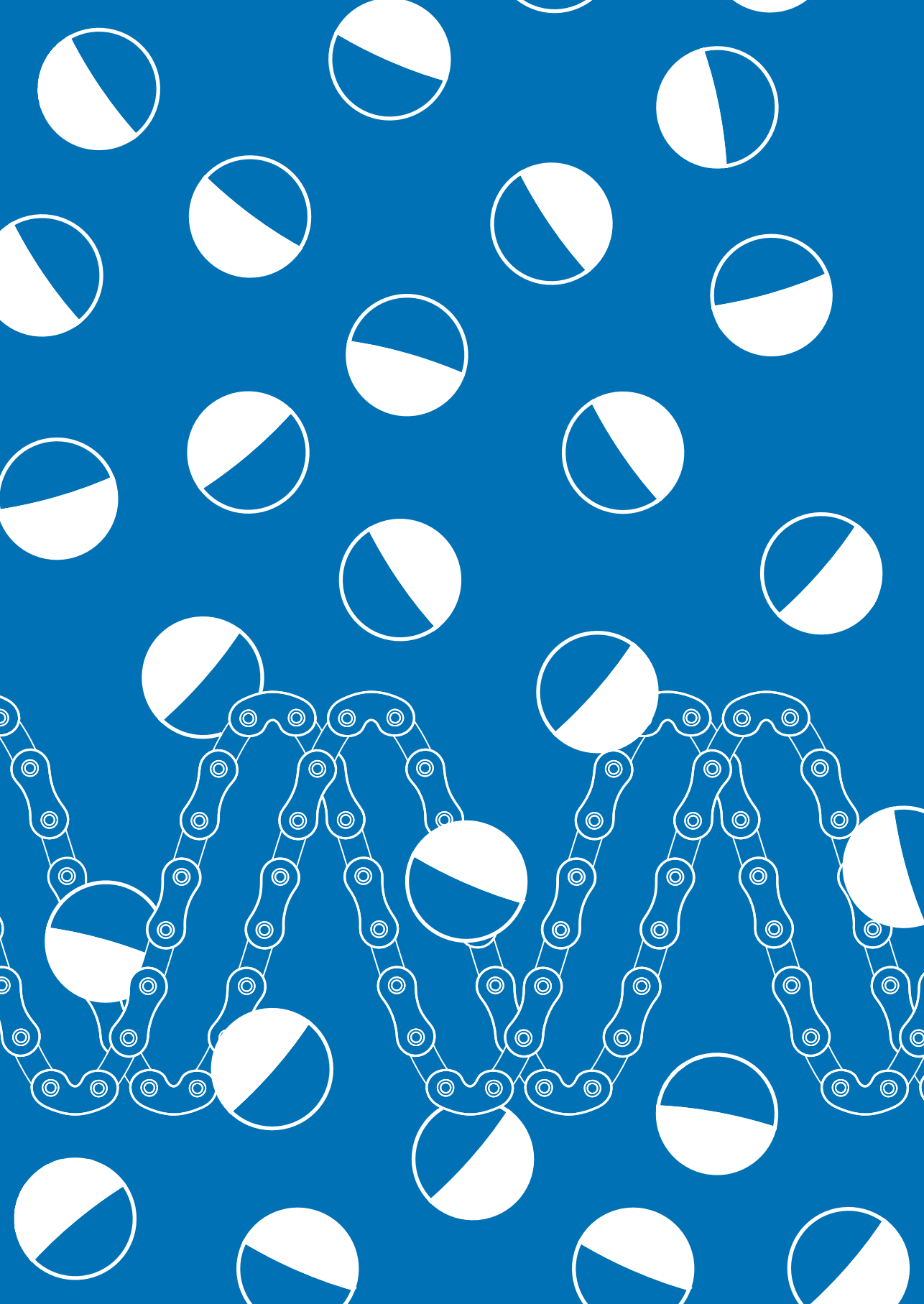
- anemia pathway. *Blood* 108: 2072-80
- Meetei AR, de Winter JP, Medhurst AL, Wallisch M, Waisfisz Q, van de Vrugt HJ, Oostra AB, Yan Z, Ling C, Bishop CE, Hoatlin ME, Joenje H & Wang W (2003) A novel ubiquitin ligase is deficient in Fanconi anemia. *Nature genetics* 35: 165-70
- Meetei AR, Levitus M, Xue Y, Medhurst AL, Zwaan M, Ling C, Roomans MA, Bier P, Hoatlin M, Pals G, de Winter JP, Wang W & Joenje H (2004) X-linked inheritance of Fanconi anemia complementation group B. *Nature genetics* 36: 1219-24
- Meetei AR, Medhurst AL, Ling C, Xue Y, Singh TR, Bier P, Steltenpool J, Stone S, Dokal I, Mathew CG, Hoatlin M, Joenje H, de Winter JP & Wang W (2005) A human ortholog of archaeal DNA repair protein Hef is defective in Fanconi anemia complementation group M. *Nature genetics* 37: 958-63
- Minocherhomji S, Ying S, Bjerregaard VA, Bursomanno S, Aleliunaite A, Wu W, Mankouri HW, Shen H, Liu Y & Hickson ID (2015) Replication stress activates DNA repair synthesis in mitosis. *Nature* 528: 286-90
- Mirchandani KD, McCaffrey RM & D'Andrea AD (2008) The Fanconi anemia core complex is required for efficient point mutagenesis and Rev1 foci assembly. *DNA repair* 7: 902-11
- Mohanty D (2016) Understanding complexity of Fanconi anaemia. *Indian J Med Res* 143: 132-4
- Monneret C (2011) Platinum anticancer drugs. From serendipity to rational design. *Ann Pharm Fr* 69: 286-95
- Mosedale G, Niedzwiedz W, Alpi A, Perrina F, Pereira-Leal JB, Johnson M, Langevin F, Pace P & Patel KJ (2005) The vertebrate Hef ortholog is a component of the Fanconi anemia tumor-suppressor pathway. *Nature structural & molecular biology* 12: 763-71
- Moser J, Kool H, Giakzidis I, Caldecott K, Mullenders LH & Foustier MI (2007) Sealing of chromosomal DNA nicks during nucleotide excision repair requires XRCC1 and DNA ligase III alpha in a cell-cycle-specific manner. *Molecular cell* 27: 311-23
- Moses RE (2001) DNA damage processing defects and disease. *Annu Rev Genomics Hum Genet* 2: 41-68
- Motnenko A, Liang CC, Yang D, Lopez-Martinez D, Yoshikawa Y, Zhan B, Ward KE, Tian J, Haas W, Spingardi P, Kessler BM, Kriacounis S, Gygi SP & Cohn MA (2018) Identification of UHRF2 as a novel DNA interstrand crosslink sensor protein. *PLoS genetics* 14: e1007643
- Mouw KW & D'Andrea AD (2014) Crosstalk between the nucleotide excision repair and Fanconi anemia/BRCA pathways. *DNA repair* 19: 130-4
- Muniandy PA, Thapa D, Thazhathveetil AK, Liu ST & Seidman MM (2009) Repair of laser-localized DNA interstrand cross-links in G1 phase mammalian cells. *The Journal of biological chemistry* 284: 27908-17
- Munoz IM, Hain K, Declais AC, Gardiner M, Toh GW, Sanchez-Pulido L, Heuckmann JM, Toth R, Macartney T, Eppink B, Kanaar R, Ponting CP, Lilley DM & Rouse J (2009) Coordination of structure-specific nucleases by human SLX4/BTBD12 is required for DNA repair. *Molecular cell* 35: 116-27
- Mutreja K, Krietsch J, Hess J, Ursich S, Berti M, Roessler FK, Zellweger R, Patra M, Gasser G & Lopes M (2018) ATR-Mediated Global Fork Slowing and Reversal Assist Fork Traverse and Prevent Chromosomal Breakage at DNA Interstrand Cross-Links. *Cell reports* 24: 2629-2642 e5
- Naim V & Rosselli F (2009) The FANCC pathway and mitosis: a replication legacy. *Cell Cycle* 8: 2907-11
- Natale V & Raquer H (2017) Xeroderma pigmentosum-Cockayne syndrome complex. *Orphanet J Rare Dis* 12: 65
- Neelsen KJ & Lopes M (2015) Replication fork reversal in eukaryotes: from dead end to dynamic response. *Nat Rev Mol Cell Biol* 16: 207-20
- Niedernhofer LJ, Daniels JS, Rouzer CA, Greene RE & Marnett LJ (2003) Malondialdehyde, a product of lipid peroxidation, is mutagenic in human cells. *The Journal of biological chemistry* 278: 31426-33
- Niedernhofer LJ, Lalai AS & Hoeijmakers JH (2005) Fanconi anemia (cross)linked to DNA repair. *Cell* 123: 1191-8
- Niedzwiedz W, Mosedale G, Johnson M, Ong CY, Pace P & Patel KJ (2004) The Fanconi anaemia gene FANCC promotes homologous recombination and error-prone DNA repair. *Molecular cell* 15: 607-20
- Nijman SM, Huang TT, Dirac AM, Brummelkamp TR, Kerkhoven RM, D'Andrea AD & Bernards R (2005) The deubiquitinating enzyme USP1 regulates the Fanconi anemia pathway. *Molecular cell* 17: 331-9
- Niraj J, Farkkila A & D'Andrea AD (2019) The Fanconi Anemia Pathway in Cancer. *Annual review of cancer biology* 3: 457-478
- Oliver AW, Swift S, Lord CJ, Ashworth A & Pearl LH (2009) Structural basis for recruitment of BRCA2 by PALB2. *EMBO reports* 10: 990-6
- Oostra AB, Nieuwint AW, Joenje H & de Winter JP (2012) Diagnosis of fanconi anemia: chromosomal breakage analysis. *Anemia* 2012: 238731
- Ouyang J, Garner E, Hallet A, Nguyen HD, Rickman KA, Gill G, Smogorzewska A & Zou L (2015) Noncovalent interactions with SUMO and ubiquitin orchestrate distinct functions of the SLX4 complex in genome maintenance. *Molecular cell* 57: 108-22
- Pang Q & Andreassen PR (2009) Fanconi anemia proteins and endogenous stresses. *Mutation research* 668: 42-53
- Panier S & Boulton SJ (2014) Double-strand break repair: 53BP1 comes into focus. *Nat Rev Mol Cell Biol* 15: 7-18
- Pena-Diaz J & Jiricny J (2010) PCNA and MutLalpha: partners in crime in triplet repeat expansion? *Proceedings of the National Academy of Sciences of the United States of America* 107: 16409-10
- Pluciennik A, Dzantiev L, Iyer RR, Constantin N,

- Kadyrov FA & Modrich P (2010) PCNA function in the activation and strand direction of MutLalpha endonuclease in mismatch repair. *Proceedings of the National Academy of Sciences of the United States of America* 107: 16066-71
- Prakash R, Zhang Y, Feng W & Jasin M (2015) Homologous recombination and human health: the roles of BRCA1, BRCA2, and associated proteins. *Cold Spring Harb Perspect Biol* 7: a016600
- Radhakrishnan SK, Jette N & Lees-Miller SP (2014) Non-homologous end joining: emerging themes and unanswered questions. *DNA repair* 17: 2-8
- Raghunandan M, Chaudhury I, Kelich SL, Nananberg H & Sobeck A (2015) FANCD2, FANCI and BRCA2 cooperate to promote replication fork recovery independently of the Fanconi Anemia core complex. *Cell Cycle* 14: 342-53
- Rajendra E, Oestergaard VH, Langevin F, Wang M, Dornan GL, Patel KJ & Passmore LA (2014) The genetic and biochemical basis of FANCD2 monoubiquitination. *Molecular cell* 54: 858-69
- Räschle M, Knipscheer P, Enouï M, Angelov T, Sun J, Griffith JD, Ellenberger TE, Scharer OD & Walter JC (2008) Mechanism of replication-coupled DNA interstrand crosslink repair. *Cell* 134: 969-80
- Rickman KA, Lach FP, Abhyankar A, Donovan FX, Sanborn EM, Kennedy JA, Sougnez C, Gabriel SB, Elemento O, Chandrasekharappa SC, Schindler D, Auerbach AD & Smogorzewska A (2015) Deficiency of UBE2T, the E2 Ubiquitin Ligase Necessary for FANCD2 and FANCI Ubiquitination, Causes FA-T Subtype of Fanconi Anemia. *Cell reports* 12: 35-41
- Ridpath JR, Nakamura A, Tano K, Luke AM, Sonoda E, Arakawa H, Buerstedde JM, Gillespie DA, Sale JE, Yamazoe M, Bishop DK, Takata M, Takeda S, Watanabe M, Swenberg JA & Nakamura J (2007) Cells deficient in the FANCI/BRCA pathway are hypersensitive to plasma levels of formaldehyde. *Cancer Res* 67: 11117-22
- Rink SM & Hopkins PB (1995) A mechlorethamine-induced DNA interstrand cross-link bends duplex DNA. *Biochemistry* 34: 1439-45
- Robertson AB, Klungland A, Rognes T & Leiros I (2009) DNA repair in mammalian cells: Base excision repair: the long and short of it. *Cell Mol Life Sci* 66: 981-93
- Rodgers K & McVey M (2016) Error-Prone Repair of DNA Double-Strand Breaks. *J Cell Physiol* 231: 15-24
- Rohleder F, Huang J, Xue Y, Kuper J, Round A, Seidman M, Wang W & Kisker C (2016) FANCM interacts with PCNA to promote replication traverse of DNA interstrand crosslinks. *Nucleic acids research* 44: 3219-32
- Rosado IV, Langevin F, Crossan GP, Takata M & Patel KJ (2011) Formaldehyde catabolism is essential in cells deficient for the Fanconi anemia DNA-repair pathway. *Nature structural & molecular biology* 18: 1432-4
- Rosenberg B, VanCamp L, Trosko JE & Mansour VH (1969) Platinum compounds: a new class of potent antitumour agents. *Nature* 222: 385-6
- Rothfuss A & Grompe M (2004) Repair kinetics of genomic interstrand DNA cross-links: evidence for DNA double-strand break-dependent activation of the Fanconi anemia/BRCA pathway. *Molecular and cellular biology* 24: 123-34
- Roy U & Scharer OD (2016) Involvement of translesion synthesis DNA polymerases in DNA interstrand crosslink repair. *DNA repair* 44: 33-41
- Sakai W & Sugasawa K (2019) Importance of finding the bona fide target of the Fanconi anemia pathway. *Genes Environ* 41: 6
- Sallmyr A & Tomkinson AE (2018) Repair of DNA double-strand breaks by mammalian alternative end-joining pathways. *The Journal of biological chemistry* 293: 10536-10546
- Sarbajna S, Davies D & West SC (2014) Roles of SLX1-SLX4, MUS81-EME1, and GEN1 in avoiding genome instability and mitotic catastrophe. *Genes & development* 28: 1124-36
- Sarkar J, Wan B, Yin J, Vallabhaneni H, Horvath K, Kulikowicz T, Bohr VA, Zhang Y, Lei M & Liu Y (2015) SLX4 contributes to telomere preservation and regulated processing of telomeric joint molecule intermediates. *Nucleic acids research* 43: 5912-23
- Sarkar S, Davies AA, Ulrich HD & McHugh PJ (2006) DNA interstrand crosslink repair during G1 involves nucleotide excision repair and DNA polymerase zeta. *The EMBO journal* 25: 1285-94
- Sato Y, Yamagata A, Goto-Ito S, Kubota K, Miyamoto R, Nakada S & Fukai S (2012) Molecular basis of Lys-63-linked polyubiquitination inhibition by the interaction between human deubiquitinating enzyme OTUB1 and ubiquitin-conjugating enzyme UBC13. *The Journal of biological chemistry* 287: 25860-8
- Sawant A, Floyd AM, Dangeti M, Lei W, Sobol RW & Patrick SM (2017) Differential role of base excision repair proteins in mediating cisplatin cytotoxicity. *DNA repair* 51: 46-59
- Scharer OD (2005) DNA interstrand crosslinks: natural and drug-induced DNA adducts that induce unique cellular responses. *ChemBiochem* 6: 27-32
- Schlacher K, Wu H & Jasin M (2012) A distinct replication fork protection pathway connects Fanconi anemia tumor suppressors to RAD51-BRCA1/2. *Cancer Cell* 22: 106-16
- Schroeder TM, Anshütz, F. & Knopp, A. (1964) Spontane Chromosomenaberrationen bei familiärer Panmyelopathie. *Hum Genet* 1
- Schwab RA, Nieminuszczy J, Shah F, Langton J, Lopez Martinez D, Liang CC, Cohn MA, Gibbons RJ, Deans AJ & Niedzwiedz W (2015) The Fanconi Anemia Pathway Maintains Genome Stability by Coordinating Replication and Transcription. *Molecular cell* 60: 351-61
- Schwertman P, Lagarou A, Dekkers DH, Raams A, van

- der Hoek AC, Laffeber C, Hoeijmakers JH, Demmers JA, Fousteri M, Vermeulen W & Marteijn JA (2012) UV-sensitive syndrome protein UVSSA recruits USP7 to regulate transcription-coupled repair. *Nature genetics* 44: 598-602
- Schwertman P, Vermeulen W & Marteijn JA (2013) UVSSA and USP7, a new couple in transcription-coupled DNA repair. *Chromosoma* 122: 275-84
- Scrima A, Konickova R, Czyzewski BK, Kawasaki Y, Jeffrey PD, Groisman R, Nakatani Y, Iwai S, Pavletich NP & Thoma NH (2008) Structural basis of UV DNA-damage recognition by the DDB1-DDB2 complex. *Cell* 135: 1213-23
- Semlow DR, Zhang J, Budzowska M, Drohat AC & Walter JC (2016) Replication-Dependent Unhooking of DNA Interstrand Cross-Links by the NEIL3 Glycosylase. *Cell* 167: 498-511 e14
- Sengerova B, Allerston CK, Abu M, Lee SY, Hartley J, Kiakos K, Schofield CJ, Hartley JA, Gileadi O & McHugh PJ (2012) Characterization of the human SNM1A and SNM1B/Apollo DNA repair exonucleases. *The Journal of biological chemistry* 287: 26254-67
- Shachar S, Ziv O, Avkin S, Adar S, Wittschieben J, Reissner T, Chaney S, Friedberg EC, Wang Z, Carell T, Geacintov N & Livneh Z (2009) Two-polymerase mechanisms dictate error-free and error-prone translesion DNA synthesis in mammals. *The EMBO journal* 28: 383-93
- Shen X, Do H, Li Y, Chung WH, Tomasz M, de Winter JP, Xia B, Elledge SJ, Wang W & Li L (2009) Recruitment of fanconi anemia and breast cancer proteins to DNA damage sites is differentially governed by replication. *Molecular cell* 35: 716-23
- Sims AE, Spiteri E, Sims RJ, 3rd, Arita AG, Lach FP, Landers T, Wurm M, Freund M, Neveling K, Hanenberg H, Auerbach AD & Huang TT (2007) FANCI is a second monoubiquitinated member of the Fanconi anemia pathway. *Nature structural & molecular biology* 14: 564-7
- Singh TR, Bakker ST, Agarwal S, Jansen M, Grassman E, Godthelp BC, Ali AM, Du CH, Rooimans MA, Fan Q, Wahengbam K, Steltenpool J, Andreassen PR, Williams DA, Joenje H, de Winter JP & Meetei AR (2009) Impaired FANCD2 monoubiquitination and hypersensitivity to camptothecin uniquely characterize Fanconi anemia complementation group M. *Blood* 114: 174-80
- Singh TR, Saro D, Ali AM, Zheng XF, Du CH, Killen MW, Sachpatzidis A, Wahengbam K, Pierce AJ, Xiong Y, Sung P & Meetei AR (2010) MHF1-MHF2, a histone-fold-containing protein complex, participates in the Fanconi anemia pathway via FANCM. *Molecular cell* 37: 879-86
- Smogorzewska A, Desetty R, Saito TT, Schlabach M, Lach FP, Sowa ME, Clark AB, Kunkel TA, Harper JW, Colaiacovo MP & Elledge SJ (2010) A genetic screen identifies FAN1, a Fanconi anemia-associated nuclease necessary for DNA interstrand crosslink repair. *Molecular cell* 39: 36-47
- Smogorzewska A, Matsuoka S, Vinciguerra P, McDonald ER, 3rd, Hurov KE, Luo J, Ballif BA, Gygi SP, Hofmann K, D'Andrea AD & Elledge SJ (2007) Identification of the FANCI protein, a monoubiquitinated FANCD2 paralog required for DNA repair. *Cell* 129: 289-301
- Sobeck A, Stone S, Costanzo V, de Graaf B, Reuter T, de Winter J, Wallisch M, Akkari Y, Olson S, Wang W, Joenje H, Christian JL, Lupardus PJ, Cimprich KA, Gautier J & Hoatlin ME (2006) Fanconi anemia proteins are required to prevent accumulation of replication-associated DNA double-strand breaks. *Molecular and cellular biology* 26: 425-37
- Sobeck A, Stone S & Hoatlin ME (2007) DNA structure-induced recruitment and activation of the Fanconi anemia pathway protein FANCD2. *Molecular and cellular biology* 27: 4283-92
- Sparks JL, Chon H, Cerritelli SM, Kunkel TA, Johansson E, Crouch RJ & Burgers PM (2012) RNase H2-initiated ribonucleotide excision repair. *Molecular cell* 47: 980-6
- Spielmann HP, Dwyer TJ, Sastry SS, Hearst JE & Wemmer DE (1995) DNA structural reorganization upon conversion of a psoralen furan-side monoadduct to an interstrand cross-link: implications for DNA repair. *Proceedings of the National Academy of Sciences of the United States of America* 92: 2345-9
- St Charles JA, Liberti SE, Williams JS, Lujan SA & Kunkel TA (2015) Quantifying the contributions of base selectivity, proofreading and mismatch repair to nuclear DNA replication in *Saccharomyces cerevisiae*. *DNA repair* 31: 41-51
- Staresinic L, Fagbemi AF, Enzlin JH, Gourdin AM, Wijgers N, Dunand-Sauthier I, Giglia-Mari G, Clarkson SG, Vermeulen W & Scharer OD (2009) Coordination of dual incision and repair synthesis in human nucleotide excision repair. *The EMBO journal* 28: 1111-20
- Stoepker C, Hain K, Schuster B, Hilhorst-Hofstee Y, Rooimans MA, Steltenpool J, Oostra AB, Eirich K, Korthof ET, Nieuwint AW, Jaspers NG, Bettecken T, Joenje H, Schindler D, Rouse J & de Winter JP (2011) SLX4, a coordinator of structure-specific endonucleases, is mutated in a new Fanconi anemia subtype. *Nature genetics* 43: 138-41
- Stone MP, Cho YJ, Huang H, Kim HY, Kozekov ID, Kozekova A, Wang H, Minko IG, Lloyd RS, Harris TM & Rizzo CJ (2008) Interstrand DNA cross-links induced by alpha,beta-unsaturated aldehydes derived from lipid peroxidation and environmental sources. *Acc Chem Res* 41: 793-804
- Sugasawa K (2010) Regulation of damage recognition in mammalian global genomic nucleotide excision repair. *Mutation research* 685: 29-37
- Sugasawa K, Ng JM, Masutani C, Iwai S, van der Spek PJ, Eker AP, Hanaoka F, Bootsma D & Hoeijmakers JH (1998) Xeroderma pigmentosum group C protein complex is the initiator of global genome

- nucleotide excision repair. *Molecular cell* 2: 223-32
- Sumpter R, Jr. & Levine B (2017) Emerging functions of the Fanconi anemia pathway at a glance. *Journal of cell science* 130: 2657-2662
- Sumpter R, Jr., Sirasanagandla S, Fernandez AF, Wei Y, Dong X, Franco L, Zou Z, Marchal C, Lee MY, Clapp DW, Hanenberg H & Levine B (2016) Fanconi Anemia Proteins Function in Mitophagy and Immunity. *Cell* 165: 867-81
- Suwaki N, Klare K & Tarsounas M (2011) RAD51 paralogs: roles in DNA damage signalling, recombinational repair and tumorigenesis. *Semin Cell Dev Biol* 22: 898-905
- Svendsen JM, Smogorzewska A, Sowa ME, O'Connell BC, Gygi SP, Elledge SJ & Harper JW (2009) Mammalian BTBD12/SLX4 assembles a Holliday junction resolvase and is required for DNA repair. *Cell* 138: 63-77
- Swuec P, Renault L, Borg A, Shah F, Murphy VJ, van Twest S, Snijders AP, Deans AJ & Costa A (2017) The FA Core Complex Contains a Homo-dimeric Catalytic Module for the Symmetric Mono-ubiquitination of FANCI-FANCD2. *Cell reports* 18: 611-623
- Symington LS (2014) End resection at double-strand breaks: mechanism and regulation. *Cold Spring Harb Perspect Biol* 6
- Tan W & Deans AJ (2017) A defined role for multiple Fanconi anemia gene products in DNA-damage-associated ubiquitination. *Experimental hematology* 50: 27-32
- Taniguchi T, Garcia-Higuera I, Andreassen PR, Gregory RC, Grompe M & D'Andrea AD (2002) S-phase-specific interaction of the Fanconi anemia protein, FANCD2, with BRCA1 and RAD51. *Blood* 100: 2414-20
- Thoma BS & Vasquez KM (2003) Critical DNA damage recognition functions of XPC-hHR23B and XPA-RPA in nucleotide excision repair. *Mol Carcinog* 38: 1-13
- Tian Y, Paramasivam M, Ghosal G, Chen D, Shen X, Huang Y, Akhter S, Legerski R, Chen J, Seidman MM, Qin J & Li L (2015) UHRF1 contributes to DNA damage repair as a lesion recognition factor and nuclease scaffold. *Cell reports* 10: 1957-66
- Tomasz M (1995) Mitomycin C: small, fast and deadly (but very selective). *Chem Biol* 2: 575-9
- Tubbs A & Nussenzweig A (2017) Endogenous DNA Damage as a Source of Genomic Instability in Cancer. *Cell* 168: 644-656
- van Twest S, Murphy VJ, Hodson C, Tan W, Swuec P, O'Rourke JJ, Heierhorst J, Crismani W & Deans AJ (2017) Mechanism of Ubiquitination and Deubiquitination in the Fanconi Anemia Pathway. *Molecular cell* 65: 247-259
- Vermeulen W & Foustier M (2013) Mammalian transcription-coupled excision repair. *Cold Spring Harb Perspect Biol* 5: a012625
- Walden H & Deans AJ (2014) The Fanconi anemia DNA repair pathway: structural and functional insights into a complex disorder. *Annual review of biophysics* 43: 257-78
- Walter J, Sun L & Newport J (1998) Regulated chromosomal DNA replication in the absence of a nucleus. *Molecular cell* 1: 519-29
- Wang AT, Kim T, Wagner JE, Conti BA, Lach FP, Huang AL, Molina H, Sanborn EM, Zierhut H, Cornes BK, Abhyankar A, Sougnez C, Gabriel SB, Auerbach AD, Kowalczykowski SC & Smogorzewska A (2015) A Dominant Mutation in Human RAD51 Reveals Its Function in DNA Interstrand Crosslink Repair Independent of Homologous Recombination. *Molecular cell* 59: 478-90
- Wang AT, Sengerova B, Cattell E, Inagawa T, Hartley JM, Kiakos K, Burgess-Brown NA, Swift LP, Enzlin JH, Schofield CJ, Gileadi O, Hartley JA & McHugh PJ (2011) Human SNM1A and XPF-ERCC1 collaborate to initiate DNA interstrand cross-link repair. *Genes & development* 25: 1859-70
- Wang X, Peterson CA, Zheng H, Nairn RS, Legerski RJ & Li L (2001) Involvement of nucleotide excision repair in a recombination-independent and error-prone pathway of DNA interstrand cross-link repair. *Molecular and cellular biology* 21: 713-20
- Wang Y, Leung JW, Jiang Y, Lowery MG, Do H, Vasquez KM, Chen J, Wang W & Li L (2013) FANCM and FAAP24 maintain genome stability via cooperative as well as unique functions. *Molecular cell* 49: 997-1009
- Warren AJ, Ihnat MA, Ogdon SE, Rowell EE & Hamilton JW (1998) Binding of nuclear proteins associated with mammalian DNA repair to the mitomycin C-DNA interstrand crosslink. *Environmental and molecular mutagenesis* 31: 70-81
- Wei K, Clark AB, Wong E, Kane MF, Mazur DJ, Parris T, Kolas NK, Russell R, Hou H, Jr., Kneitz B, Yang G, Kunkel TA, Kolodner RD, Cohen PE & Edelman W (2003) Inactivation of Exonuclease 1 in mice results in DNA mismatch repair defects, increased cancer susceptibility, and male and female sterility. *Genes & development* 17: 603-14
- Wienholz F, Zhou D, Turkyilmaz Y, Schwertman P, Tresini M, Pines A, van Toorn M, Bezstarosti K, Demmers JAA & Marteijn JA (2019) FACT subunit Spt16 controls UVSSA recruitment to lesion-stalled RNA Pol II and stimulates TC-NER. *Nucleic acids research* 47: 4011-4025
- Williams HL, Gottesman ME & Gautier J (2012) Replication-independent repair of DNA interstrand crosslinks. *Molecular cell* 47: 140-7
- Williams JS, Lujan SA & Kunkel TA (2016) Processing ribonucleotides incorporated during eukaryotic DNA replication. *Nat Rev Mol Cell Biol* 17: 350-63
- Wilson JS, Tejera AM, Castor D, Toth R, Blasco MA & Rouse J (2013) Localization-dependent and -independent roles of SLX4 in regulating telomeres. *Cell reports* 4: 853-60
- Wood RD (2010) Mammalian nucleotide excision repair proteins and interstrand crosslink repair.

- Environmental and molecular mutagenesis* 51: 520-6
- Wright WD, Shah SS & Heyer WD (2018) Homologous recombination and the repair of DNA double-strand breaks. *The Journal of biological chemistry* 293: 10524-10535
- Wu RA, Semlow DR, Kamimae-Lanning AN, Kochenova OV, Chistol G, Hodskinson MR, Amunugama R, Sparks JL, Wang M, Deng L, Mimoso CA, Low E, Patel KJ & Walter JC (2019) TRAP is a master regulator of DNA interstrand crosslink repair. *Nature*
- Wyatt HD, Laister RC, Martin SR, Arrowsmith CH & West SC (2017) The SMX DNA Repair Tri-nuclease. *Molecular cell* 65: 848-860 e11
- Wyatt HD, Sarbajna S, Matos J & West SC (2013) Coordinated actions of SLX1-SLX4 and MUS81-EME1 for Holliday junction resolution in human cells. *Molecular cell* 52: 234-47
- Wyatt HD & West SC (2014) Holliday junction resolvases. *Cold Spring Harb Perspect Biol* 6: a023192
- Xu W, Kool D, O'Flaherty DK, Keating AM, Sacre L, Egli M, Noronha A, Wilds CJ & Zhao L (2016) O(6)-2'-Deoxyguanosine-butylene-O(6)-2'-deoxyguanosine DNA Interstrand Cross-Links Are Replication-Blocking and Mutagenic DNA Lesions. *Chem Res Toxicol* 29: 1872-1882
- Yan Z, Delannoy M, Ling C, Daece D, Osman F, Muniandy PA, Shen X, Oostra AB, Du H, Steltenpool J, Lin T, Schuster B, Decaillet C, Stasiak A, Stasiak AZ, Stone S, Hoatlin ME, Schindler D, Woodcock CL, Joenje H *et al.* (2010) A histone-fold complex and FANCM form a conserved DNA-remodeling complex to maintain genome stability. *Molecular cell* 37: 865-78
- Yang H, Zhang T, Tao Y, Wang F, Tong L & Ding J (2013) Structural insights into the functions of the FANCM-FAAP24 complex in DNA repair. *Nucleic acids research* 41: 10573-83
- Yi C & He C (2013) DNA repair by reversal of DNA damage. *Cold Spring Harb Perspect Biol* 5: a012575
- Yin J, Wan B, Sarkar J, Horvath K, Wu J, Chen Y, Cheng G, Wan K, Chin P, Lei M & Liu Y (2016) Dimerization of SLX4 contributes to functioning of the SLX4-nuclease complex. *Nucleic acids research* 44: 4871-80
- Yokoi M, Masutani C, Maekawa T, Sugawara K, Ohkuma Y & Hanaoka F (2000) The xeroderma pigmentosum group C protein complex XPC-HR23B plays an important role in the recruitment of transcription factor IIH to damaged DNA. *The Journal of biological chemistry* 275: 9870-5
- Yuan F, Gu L, Guo S, Wang C & Li GM (2004) Evidence for involvement of HMGB1 protein in human DNA mismatch repair. *The Journal of biological chemistry* 279: 20935-40
- Zhang J, Dewar JM, Budzowska M, Motnenko A, Cohn MA & Walter JC (2015) DNA interstrand cross-link repair requires replication-fork convergence. *Nature structural & molecular biology* 22: 242-7
- Zhang J & Walter JC (2014) Mechanism and regulation of incisions during DNA interstrand cross-link repair. *DNA repair* 19: 135-42



Chapter 2

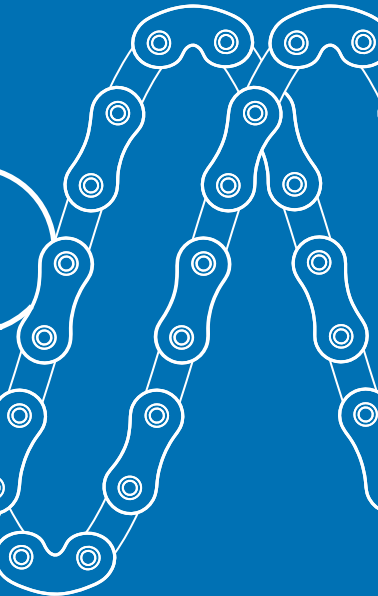
Xenopus egg extract: A powerful tool to study genome maintenance mechanisms

Wouter S. Hoogenboom[#], Daisy Klein Douwel[#], and Puck Knipscheer^{*}

Hubrecht Institute - KNAW, University Medical Center Utrecht & Cancer Genomics Netherlands, The Netherlands

[#]) These authors contributed equally to this work

^{*}Corresponding author. Email: p.knipscheer@hubrecht.eu



Abstract

DNA repair pathways are crucial to maintain the integrity of our genome and prevent genetic diseases such as cancer. There are many different types of DNA damage and specific DNA repair mechanisms have evolved to deal with these lesions. In addition to these repair pathways there is an extensive signaling network that regulates processes important for repair, such as cell cycle control and transcription. Despite extensive research, DNA damage repair and signaling are not fully understood. In vitro systems such as the *Xenopus* egg extract system, have played, and still play, an important role in deciphering the molecular details of these processes. *Xenopus laevis* egg extracts contain all factors required to efficiently perform DNA repair outside a cell, using mechanisms conserved in humans. These extracts have been used to study several genome maintenance pathways, including mismatch repair, non-homologous end joining, ICL repair, DNA damage checkpoint activation, and replication fork stability. Here we describe how the *Xenopus* egg extract system, in combination with specifically designed DNA templates, contributed to our detailed understanding of these pathways.

1. Introduction

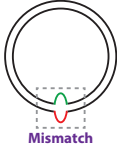
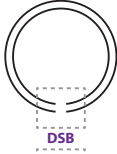
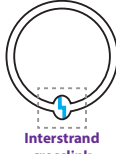
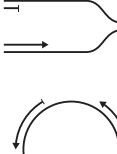
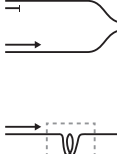
The integrity of our genome is protected by a large variety of DNA repair mechanisms that counteract the continuous DNA damage resulting from both endogenous and exogenous sources. Malfunctioning of any of these mechanisms can lead to DNA mutations and is often associated with an increased risk of developing cancer (Hoeijmakers, 2009). In addition, defects in specific DNA repair pathways can lead to a large variety of diseases, that are in many cases characterized by developmental defects, premature ageing and cancer predisposition (O'Driscoll, 2012, Ribezzo *et al.*, 2016). At the same time, deficiencies in DNA repair pathways have emerged as a powerful characteristic to enhance cancer therapy based on synthetic lethality (Pearl *et al.*, 2015, Rehman *et al.*, 2010). Understanding the molecular mechanisms of DNA repair pathways is important to develop such therapies, but also to further understand DNA repair deficiency diseases and the mechanisms that keep our genome stable.

Genetics and cell biology have provided many important insights into DNA repair pathways on a cellular and organismal level. However, to understand the biochemistry underlying these pathways, *in vitro* systems have proven to be very effective. *Xenopus* egg extracts have been used to study a variety of complex cellular processes, such as mitosis, actin metabolism, nuclear transport, apoptosis, DNA replication, and DNA repair (Hardwick & Philpott, 2015). *Xenopus* egg extracts contain a high concentration of proteins required to drive the rapid cell divisions after fertilization of the egg. DNA replication and repair are highly conserved between *Xenopus laevis* and mammals, making this system well-suited to study these processes in detail. In addition, despite the major advances that have recently been made in the reconstitution of budding yeast DNA replication from purified components, the *Xenopus* egg extract system is currently the only system that enables efficient vertebrate DNA replication to take place outside the cell. This system has also been extensively used to study replication-linked processes, such as checkpoint activation, responses to replication fork stalling and DNA interstrand crosslink repair. Many genome maintenance mechanisms have been studied using *Xenopus* egg extracts, and in this review we will focus on mismatch repair, non-homologous end joining, interstrand crosslink repair, checkpoint activation, and replication fork stability. In particular, we will discuss how the use of specific DNA templates has enabled the recapitulation of these pathways and contributed to the understanding of their molecular mechanisms (Table 1).

2. *Xenopus* egg extract

The conventional *Xenopus* egg extract is made by crushing mature *Xenopus laevis* eggs at a moderate speed to produce an unfractionated egg cytoplasm extract, called low speed supernatant or LSS (Lohka & Masui, 1983) (Fig. 1). Addition of this extract to demembrated sperm chromatin results in the formation of a nucleus around the DNA and a single, complete round of DNA replication (Blow & Laskey, 1986, Newport, 1987). DNA replication in this system depends on the formation of nuclei, and when membranes are removed by centrifuging the extract at higher speed, the resulting 'high speed supernatant' or HSS (Fig. 1) does not support DNA replication. However, also in the absence of active DNA replication, both LSS and HSS support efficient DNA repair, most likely due to the high concentration of repair factors in the extract. Although the LSS extract provided many insights into biological processes, the requirement for nuclei formation to allow DNA replication presents some limitations. Factors that affect nuclei formation, or

Table 1: Summary of repair pathways studied in *Xenopus* egg extracts and the DNA templates that are used for this.

Pathway	MMR	NHEJ	ICL repair	Damage checkpoint activation		Fork stalling
				ATR	ATM	
Substrate schematic						
Substrate detail	- DNA plasmid containing mismatch	- Linearized plasmid DNA - Linear fragments Containing: - 3' overhang - 5' overhang - blunt ends	- DNA plasmid containing ICL ICL type: - cisplatin - nitrogen mustard - abasic site - psoralen	- Chromatin DNA, polymerase-helicase uncoupling by aphidicolin - M13 ssDNA circular DNA with annealed primers	- linear dsDNA fragments - Digested dsDNA plasmid	- Chromatin DNA, polymerase-helicase uncoupling by aphidicolin - ssDNA plasmid containing G-quadruplex
Extract	- HSS - NPE	- LSS - HSS	- HSS+NPE - HSS	- LSS - NPE	- LSS - HSS	- LSS - HSS
Refs	(Brooks <i>et al.</i> , 1989; Kawasoe <i>et al.</i> , 2016; Varlet <i>et al.</i> , 1990, Varlet <i>et al.</i> , 1996; Ghodgaonkar <i>et al.</i> , 2013)	(Davis & Chen, 2013; Pfeiffer & Vielmetter, 1988; Di Virgilio & Gautier, 2005; Beyert <i>et al.</i> , 1994; Zhu & Peng, 2016; Daza <i>et al.</i> , 1996; Thode <i>et al.</i> , 1990)	(Deans & West, 2011; Niedernhofer <i>et al.</i> , 2005; Räschele <i>et al.</i> , 2008; Angelov <i>et al.</i> , 2009; Enoiu <i>et al.</i> , 2012; Zhang <i>et al.</i> , 2015; Le Breton <i>et al.</i> , 2011; Fu <i>et al.</i> , 2011; Knipscheer <i>et al.</i> , 2009; Bluteau <i>et al.</i> , 2016)	(Willis <i>et al.</i> , 2012; Cupello <i>et al.</i> , 2016; Yazinski & Zou, 2016; Dasso & Newport, 1990; Kumagai <i>et al.</i> , 1998; Byun, 2005; Michael <i>et al.</i> , 2000; Van <i>et al.</i> , 2010; Lupardus, 2002; MacDougall <i>et al.</i> , 2007; Kumagai <i>et al.</i> , 2006; Hashimoto <i>et al.</i> , 2006; Kumagai & Dunphy, 2000; Kumagai & Duhphy, 2003; Jones <i>et al.</i> , 2003; Lee & Dunphy, 2010; Lee <i>et al.</i> , 2007; Lee & Dunphy, 2013; Duursma <i>et al.</i> , 2013)	(Yan & Michael, 2009; Bétous <i>et al.</i> , 2013; Costanzo <i>et al.</i> , 2000; You <i>et al.</i> , 2005; Dupré <i>et al.</i> , 2006; You <i>et al.</i> , 2007)	(Ramírez-Lugo <i>et al.</i> , 2011; Couch <i>et al.</i> , 2013)

that are not imported into the nuclei, cannot be investigated, and small DNA molecules such as plasmids do not replicate efficiently (Blow & Laskey, 1986). To circumvent these issues, a nucleus-free DNA replication system was developed that involves two extracts that are added sequentially to the DNA (Walter *et al.*, 1998). Incubation of the DNA in the membrane-free HSS leads to the assembly of pre-replication complexes (pre-RCs) by loading of ORC, Cdc6, Cdt1, and MCM2-7. Addition of a highly concentrated nucleoplasmic egg extract (NPE) triggers replication initiation and allows a single, complete round of DNA replication (Lebofsky *et al.*, 2009, Tutter & Walter, 2006). To make NPE, nuclei formed in LSS are harvested and the nucleoplasm is isolated by high-speed centrifugation (Fig. 1). This two-extract system promotes efficient replication of defined DNA substrates such as (modified) DNA plasmids, and has the added advantage that replication initiation is relatively synchronous. Therefore, this is a unique system to study replication-coupled DNA repair processes.

3. Mismatch repair

The mismatch repair (MMR) pathway deals with base misinsertions and small inserts or deletions that are introduced during DNA replication. The repair process occurs in roughly

four phases: mismatch recognition, identification of the error-containing nascent strand, removal of the mismatched strand, and finally resynthesis and ligation to restore the double helix. Deficiencies in MMR genes increase mutation rates by several orders of magnitude and leads to a predisposition to cancer, most frequently colon cancer (Jiricny, 2013, Li & Martin, 2016).

The mechanism of mismatch repair has been studied in *Xenopus* egg extracts since the late 1980s, initiated by a study by Brooks et al. in 1989. This study showed that a mismatch induces local DNA synthesis spanning up to a few hundred nucleotides around the mismatched site (Brooks *et al.*, 1989). While this study used an HSS egg extract to support mismatch repair, a more recent study demonstrated that a nuclear extract (NPE) is more efficient in MMR (Kawasoe *et al.*, 2016). Mismatch-containing plasmid DNA templates are commonly generated using single stranded phagemids that are converted to double stranded plasmids by annealing a mismatched second strand, or by extension from a mismatched primer. Repair of these mismatches is highly efficient in egg extract and occurs independently of replicative DNA synthesis.

The mismatch-containing sequences are often designed in such a way that repair can be monitored by the generation or loss of recognition sites for specific restriction enzymes. Using this method, Varlet et al. found that mismatch repair in *Xenopus* egg extracts is not equally efficient for all possible mismatches and seems to be most efficient for GT and AC mismatched pairs (Varlet *et al.*, 1990). This has also been observed in mammalian in vitro systems, indicating that the MMR mechanism is highly conserved (Holmes *et al.*, 1990, Thomas *et al.*, 1991).

A major unresolved issue in the mismatch repair field is the identity of the strand discrimination signal. The repair machinery must determine which of the two DNA strands is the newly synthesized strand and therefore contains the mismatched nucleotide. Early experiments in egg extract showed that the presence of a nick on one of the two strands increased the efficiency of repair of this nicked strand, indicating that a nick can serve as such a strand discrimination signal (Varlet *et al.*, 1996). It is tempting to reason that this nick can be used as a starting point for repair synthesis, however, this study showed that

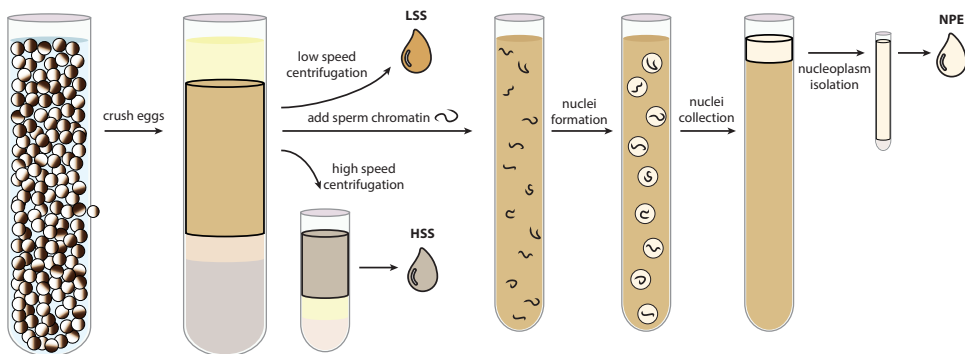


Figure 1: Schematic representation of *Xenopus* egg extract preparation. Unfertilized *Xenopus laevis* eggs are crushed and the crude cytoplasmic fraction is collected. A low speed centrifugation ($100.000 \times g$) step produces cytoplasmic extract including the membranes (LSS). A high speed ($260.000 \times g$) centrifugation step produces cytoplasmic extract without membranes (HSS). Incubation of the crude cytoplasmic extract with sperm chromatin, in the presence of ATP, induces nuclei formation. Nucleoplasm (NPE) is isolated by centrifugation after collection of the nuclei.

2

this is not the case. Repair synthesis occurred close to, and on either side of, the mismatch regardless of where the nick was positioned. This indicates that the nick has a signaling role rather than serving as a starting point for strand removal, as was also more recently observed (Kawasoe *et al.*, 2016). Consistent with this, it was found in human cell extracts that the nick that serves as strand discrimination signal is not necessarily the starting point of strand removal and repair synthesis. The MMR factor MutL α is an endonuclease that makes several additional nicks, on either side of the mismatch, after recognition of the mismatch containing strand (Kadyrov *et al.*, 2006). This is specifically important if the strand discrimination nick is 3' of the mismatch, since the exonuclease that removes the mismatched strand only acts from 5' to 3' end.

While a nick has been shown to serve as a strand discrimination signal in several eukaryotic *in vitro* systems (Holmes *et al.*, 1990, Thomas *et al.*, 1991), there are other mechanisms that can serve this purpose. It has been demonstrated that ribonucleotides that are erroneously built into the DNA during replication can help to identify the nascent strand (Ghodgaonkar *et al.*, 2013, Lujan *et al.*, 2013), likely by producing a nick as an intermediate of repair. The base excision repair (BER) pathway also creates nicks during repair that could potentially serve to discriminate between DNA strands. A recent study used human cell and *Xenopus* egg extracts to show that processing of oxidized guanines that are mismatched to an adenine, can also facilitate MMR (Repmann *et al.*, 2015). This study used a plasmid template containing an oxidized guanine (G $^{\circ}$) opposite to a C or an A, in addition to a GT mismatch in the vicinity. Processing of the mismatched A opposite the G $^{\circ}$ by the MutY-homologue (MYH) resulted in enhanced MMR of the GT mismatch. However, the presence of a C opposite the G $^{\circ}$ did not enhance MMR, indicating that G $^{\circ}$ processing by the glycosylase OGG1 is inhibited and no strand discrimination signal is generated. This suggests an elegant mechanism to ensure MMR takes place on the nascent strand that contained the mismatched A and not on the parental strand containing the G $^{\circ}$ (Repmann *et al.*, 2015).

In addition to these mechanisms based on the presence or regeneration of nicks, it has also been suggested that the directional loading of PCNA can provide strand discrimination information (Pluciennik *et al.*, 2010, Umar *et al.*, 1996). Using NPE extract and a mismatched plasmid template loaded with PCNA in an orientation-specific manner, Kawasoe *et al.* recently showed that PCNA can serve as such a strand discrimination signal even in the absence of nicks on the template DNA (Kawasoe *et al.*, 2016). In addition, this study showed that the mismatch repair factor MutS α , which directly interacts with PCNA, helps to retain PCNA on the DNA until repair is finished.

4. Non-homologous end joining

Double-strand breaks (DSBs) are repaired by two main mechanisms: homologous recombination (HR) and non-homologous end joining (NHEJ). HR promotes error-free repair by using sequence information from a sister chromatid, while NHEJ simply ligates the two ends of the DNA together, which often leads to deletions or insertions. Some aspects of HR have been studied in *Xenopus* egg extracts, but NHEJ has been more extensively studied using this system. During non-homologous end joining, the two ends of the DSB are first bound by the Ku70-Ku80 (Ku70/80) heterodimer, which is followed by the recruitment of the DNA-dependent protein kinase catalytic subunit (DNA-PKcs). DNA end ligation, if necessary preceded by DNA end-processing, is mediated by DNA ligase

4, its essential cofactor XRCC4, and the XRCC4 paralogs XLF and PAXX (Chiruvella *et al.*, 2013, Radhakrishnan *et al.*, 2014). Defects in NHEJ have been linked to immunodeficiency syndromes and cancer development (Davis & Chen, 2013, O'Driscoll, 2012).

Non-homologous DNA ends are readily joined in *Xenopus* egg extract, as was first demonstrated in the late nineteen eighties by Pfeiffer and Vielmetter (Pfeiffer & Vielmetter, 1988). This study, and most of the following studies, used linearized plasmid DNA containing 3' or 5' single-stranded overhangs or blunt ends. Both LSS and HSS egg extracts support efficient NHEJ (Di Virgilio & Gautier, 2005). End joining in *Xenopus* egg extract is mostly error-free, and the process involves end-alignment or overlap and filling in of the gaps (Beyert *et al.*, 1994, Zhu & Peng, 2016). While NHEJ in human cell extracts seems to follow the same mechanisms (Daza *et al.*, 1996), the efficiency is much higher in *Xenopus* egg extracts, possibly due to the high concentration of Ku proteins (Labhart, 1999).

Xenopus egg extracts have proven to be extremely useful to examine the roles of specific proteins in NHEJ. In 1990, even before any of the currently known alignment factors were identified, an important study provided evidence that there must be a protein that keeps the DNA ends perfectly aligned during end joining (Thode *et al.*, 1990). This model was based on the observation that the filling in of a DSB end containing a 3' overhang can precede ligation, suggesting that DNA synthesis starts from the other 3' DSB end and passes the nick. This can only occur when the ends are perfectly aligned. Soon after Ku70/80 was identified, it was confirmed that it also plays a role in the end joining observed in *Xenopus* egg extracts (Labhart, 1999). However, this study did not rescue the NHEJ defect after Ku70 depletion with recombinant protein, a necessary control to rule out unspecific effects. In follow up work it was shown that a Ku-dependent mechanism ligates ends with non-compatible 3' overhangs by forming a 2 nt overlap by non-canonical base pairing, from which the fill-in of the remaining gaps is initiated (Sandoval & Labhart, 2002). A role for Ku70 was later confirmed by several other reports (Di Virgilio & Gautier, 2005, Graham *et al.*, 2016, Zhu & Peng, 2016), and DNA-PK was also shown to be required for NHEJ in egg extract (Di Virgilio & Gautier, 2005, Gu *et al.*, 1996, Gu *et al.*, 1998). Finally, a very recent report used *Xenopus* egg extracts to show that p97 and Ku80 ubiquitylation are required for unloading of Ku from DSBs after repair has finished (van den Boom *et al.*, 2016).

MRE11 is a subunit of the MRE11-Rad50-Nbs1 (MRN) complex, and while this protein has an important role in NHEJ in *Saccharomyces cerevisiae*, in vertebrates this was controversial. Di Virgilio and Gautier reported that depletion of MRE11 from cytosolic egg extract does not affect the efficiency or kinetics of NHEJ, nor does it affect its fidelity (Di Virgilio & Gautier, 2005). However, this study used immunodepletion to remove MRE11 from extract, and it is difficult to fully exclude the possibility that the small amount of MRE11 remaining is sufficient to support NHEJ. In addition, these experiments were performed on clean DNA ends produced by restriction enzymes, while *in vivo* substrates could be more complex. In support of this, recent studies in *Xenopus* egg extract showed that MRE11 is required for joining of ends with 5' bulky adducts (Liao *et al.*, 2016) and during an alternative pathway of NHEJ (alt-NHEJ) where resection is required (Taylor *et al.*, 2010). In mammalian systems, it has now been shown that MRE11 contributes to alt-NHEJ and also to some extent to canonical-NHEJ (Rass *et al.*, 2009, Xie *et al.*, 2009).

A single-molecule study using *Xenopus* egg extract recently elucidated a 2-step

2

mechanism for synapsis of the DNA ends during NHEJ (Graham *et al.*, 2016). First, a thorough analysis using immunodepletions and rescue experiments, showed a requirement for Ku70/80, DNA-PKcs, XLF, XRCC4 and Lig4, for the end joining of blunt ended linear DNA substrate. This further validates the *Xenopus* egg extract system as a physiologically relevant *in vitro* system to study NHEJ. Single-molecule experiments were performed in egg extract to monitor the interaction between Cy3-labeled blunt ended DNA molecules tethered to a glass surface and Cy5-labeled DNA molecules in solution. This revealed two types of interaction between the DNA ends: a long-range interaction in which the Cy5-labeled DNA was tethered to the Cy3-labeled DNA on the surface, at a distance too large for FRET to occur, and a short-range interaction in which a FRET signal could be detected between the dyes present on each end. The long range interaction was short lived and dependent on Ku70/80 and DNA-PK but not its catalytic activity, while the short range interaction, in addition to these factors, required the catalytic activity of DNA-PK, as well as Lig4, XLF and XRCC4. These results show that the DNA ends are brought together for ligation in a multi-step process that requires different NHEJ factors at each stage (Thode *et al.*, 1990). How each factor contributes to these different interaction modes, and how the transition between the two modes is facilitated remains to be further investigated. In addition, it will be of great interest to study the ligation of DNA ends that are modified, or carry 3' or 5' extensions, using this system.

5. Interstrand crosslink repair

DNA interstrand crosslinks (ICLs) are toxic DNA lesions that covalently connect the two strands of the DNA. ICLs can be formed endogenously by byproducts of cellular metabolism such as aldehydes, but can also be induced by ICL inducing chemicals, such as Mitomycin C, nitrogen mustards and cisplatin. Because ICLs prevent strand separation and inhibit DNA replication and transcription, they are extremely toxic to rapidly dividing cells, which is why ICL inducing agents are often used in cancer chemotherapy (Deans & West, 2011). In cells, most ICLs are repaired in S-phase, while a minor pathway acts in G1. Until less than a decade ago, little was known about the molecular mechanism of ICL repair. Genetics had implicated structure-specific endonucleases, translesion polymerases, and HR factors in this repair process and a model was postulated that involved replication fork collision, ICL unhooking by dual incisions, TLS past the unhooked ICL and HR to restart the replication fork (Niedernhofer *et al.*, 2005). However, this model was not experimentally confirmed and it did not explain a role for the Fanconi anemia proteins in ICL repair. Fanconi anemia (FA) is a cancer predisposition disorder caused by a defect in any of the 21 currently known FA genes. Cells of FA patients are extremely sensitive to ICL inducing agents, suggesting that the FA pathway plays a role in ICL repair.

Understanding the molecular mechanism of ICL repair was hampered by the lack of a system to study it biochemically, but this changed in 2008 when replication-coupled ICL repair was recapitulated in *Xenopus* egg extract (Ben-Yehoyada *et al.*, 2009, Räschle *et al.*, 2008). Since then, this system has made extensive contributions to our understanding of the molecular mechanism of ICL repair. The system makes use of plasmid DNA templates that contain a site-specific ICL in combination with HSS and NPE egg extracts, that allow replication to start simultaneously on each plasmid (Knipscheer *et al.*, 2012). This enables the dissection of the different stages of ICL repair. Importantly, a direct readout for ICL repair is possible by the regeneration of a restriction site that is blocked by the ICL

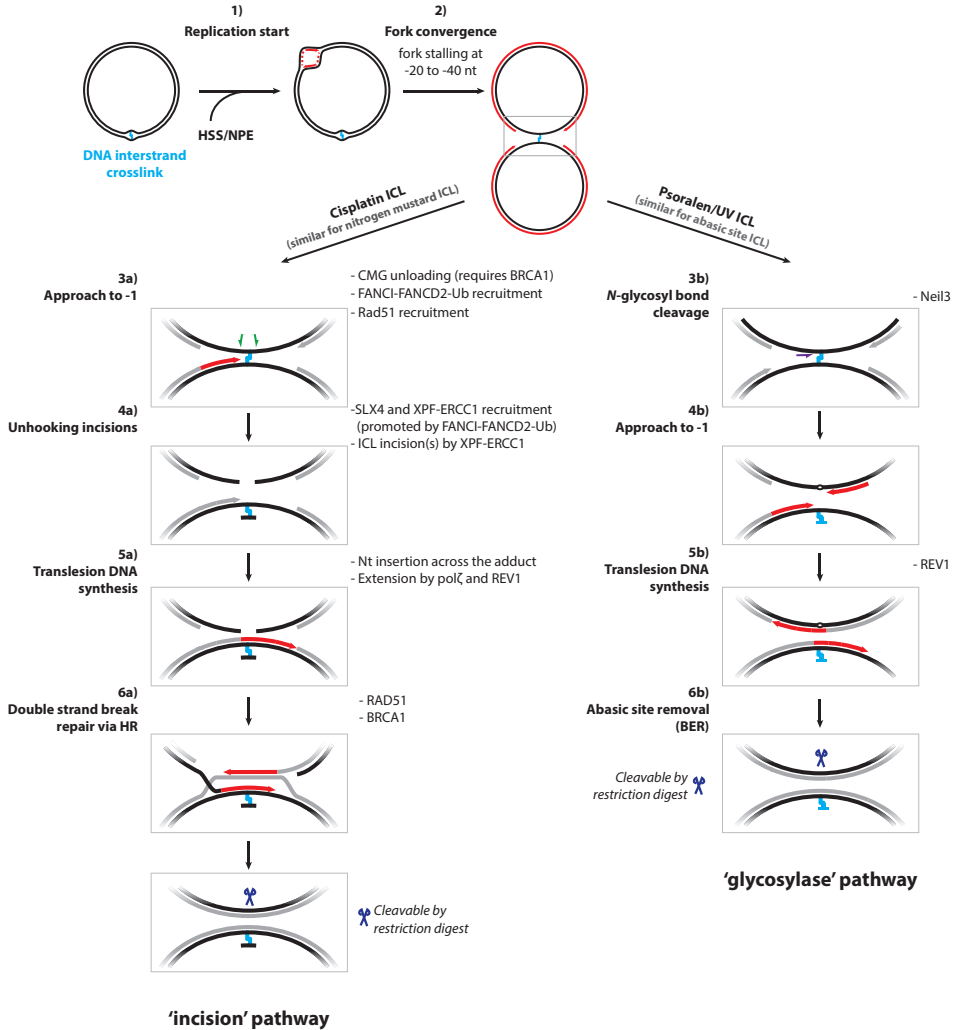


Figure 2: Model for DNA replication-dependent ICL repair in *Xenopus* egg extract. ICL unhooking can occur via nucleolytic incisions on the parental strand ('incisions' pathway, left), or via cleavage of the N-glycosyl bond of one of the crosslinked nucleotides ('glycosylase' pathway, right). Both pathways require replication fork convergence to initiate repair. Repair steps are indicated on the left of each pathway, proteins involved on the right. See text for detailed explanation of repair steps.

(Räschle *et al.*, 2008). Several different types of crosslinks can be induced in plasmids such as nitrogen mustard-like, MMC-like, psoralen/UV, abasic-site or cisplatin ICLs (Angelov *et al.*, 2009, Ben-Yehoyada *et al.*, 2009, Enoiu *et al.*, 2012, Semlow *et al.*, 2016, Zhang *et al.*, 2015).

Replication-dependent ICL repair in *Xenopus* egg extracts is most intensively studied using cisplatin and nitrogen mustard-like crosslinks and is initiated when replication forks from either side converge at the ICL (Räschle *et al.*, 2008) (Fig. 2, step 1 and 2). Although one study indicated that some ICL processing can take place upon fork arrival from one side, it was not clear whether this leads to ICL repair (Le Breton *et al.*, 2011). A more recent

2

study showed that dual fork collision is a prerequisite for ICL repair in *Xenopus* egg extract (Zhang *et al.*, 2015). After fork convergence and stalling of the forks 20 to 40 nucleotides from the ICL, one of the replication forks resumes DNA synthesis and stalls again when it is only one or a few nucleotides from the crosslink (Räschle *et al.*, 2008) (Fig. 2, step 3a). This 'approach' step can only occur once the CMG helicase is unloaded from the DNA, a step that depends on fork convergence (Fu *et al.*, 2011, Zhang *et al.*, 2015). In addition, another study showed that the HR factor BRCA1 (FANCS) has an unexpected early function in ICL repair in promoting this CMG unloading step (Long *et al.*, 2014). Although it remains to be seen whether fork convergence is required for the repair of all ICLs in mammalian cells, this mechanism does have the important advantage that ICL repair only starts once DNA replication is completed. This avoids unreplicated regions or replication fork collapse due to the inability of CMG reloading during S-phase.

CMG unloading and approach of one of the replication forks to the ICL is followed by endonucleolytic incisions on the parental strand on either side of the ICL that effectively 'unhook' the ICL from one of the DNA strands (Fig. 2, step 4a). This repair step requires the activation of the Fanconi anemia pathway by ubiquitylation of the FANCI-FANCD2 complex (Knipscheer *et al.*, 2009). Work in other systems has shown that this is mediated by a ubiquitin E3 ligase complex consisting of 8 FA proteins and the UBE2T(FANCT) ubiquitin conjugating enzyme (Kottemann & Smogorzewska, 2013). In follow-up studies using *Xenopus* egg extract, it was shown that ubiquitylated FANCI-FANCD2 is recruited to the site of the ICL, where it promotes the recruitment of an 'incision complex', consisting of the structure specific endonuclease XPF(FANCD1)-ERCC1 and the nuclease scaffold protein SLX4(FANCP) (Klein Douwel *et al.*, 2014). XPF-ERCC1 is responsible for making at least one of the unhooking incisions, and possibly both (Klein Douwel *et al.*, 2014).

Once the ICL is unhooked from one of the strands, lesion bypass across the adduct on the opposite strand restores the integrity of one of the sister molecules (Fig. 2, step 5a). Lesion bypass most likely takes place in two steps: first a nucleotide is inserted across from the unhooked ICL by an unknown polymerase, then the strand is extended by polymerase ζ in collaboration with REV1. This is based on the finding that depletion of REV7, the regulatory subunit of polymerase ζ , as well as depletion of REV1, both cause an arrest of lesion bypass after a nucleotide has been inserted across from a cisplatin ICL (Budzowska *et al.*, 2015, Räschle *et al.*, 2008). Interestingly, in contrast to cisplatin ICLs, a nitrogen mustard ICL did not require REV7 for lesion bypass (Räschle *et al.*, 2008). Nonetheless, REV7 was recently identified as an FA gene (FANCV) confirming the importance of this protein in ICL repair (Bluteau *et al.*, 2016).

The molecule containing the DSB is regenerated by homologous recombination using the restored sister molecule (Long *et al.*, 2011) (Fig. 2, step 6a). Rad51 is a critical component of HR during ICL repair but may also have a function in early stages of the repair process (Long *et al.*, 2011). This has been suggested because Rad51 (FANCR) is recruited to the ICL even before unhooking incisions have taken place. This would be analogous to the dual role of BRCA1(FANCS) that functions in CMG unloading and presumably also in HR during ICL repair (Long *et al.*, 2014). The sister molecule that contains the adduct is not efficiently repaired in *Xenopus* egg extract and will not become available for restriction digest (Deans & West, 2011).

For years it was thought that the FA pathway-dependent ICL repair mechanism was the only replication-dependent ICL repair mechanism, however, very recently

a second mechanism was identified using *Xenopus* egg extracts (Semlow *et al.*, 2016). This study showed that plasmids carrying psoralen/UV- and abasic site-derived ICLs are repaired independently of the FA pathway. However, this pathway is dependent on DNA replication and requires two replication forks to converge at the ICL. Interestingly, in this repair mechanism, the ICL is not unhooked by dual incisions on the parental strand and thereby avoids formation of a DSB. Instead, the glycosylase Neil3 unhooks the two DNA strands by breaking the *N*-glycosyl bond between the sugar and the base of one of the crosslinked nucleotides (Fig. 2, step 3b). This generates one sister molecules that contains an abasic site, and another sister molecule that contains a normal nucleotide or an adduct depending on the chemical nature of the ICL. TLS is required to bypass the abasic site and the adducted nucleotide (Fig. 2, step 5b). Because no DSB is formed during this process, it does not require homologous recombination. While this mechanism is faster and less complex compared to the incision-dependent mechanism, it is also likely to be more mutagenic because it involves bypass of an abasic site (Semlow *et al.*, 2016). These findings also raised some important questions. Neil3 is a bifunctional glycosylase that breaks *N*-glycosyl bonds but also contains lyase activity, which promotes cleavage of the phosphodiester backbone. Semlow *et al.* suggest that the lyase activity of Neil3 is inhibited during replication-dependent ICL repair because this would lead to a double-strand break and these are not observed during ICL unhooking. A possible alternative explanation could be that lyase activity of Neil3 acts after the bypass of the AP site by TLS. To settle this issue, it would be interesting to make a separation of function mutant of Neil3 that is an inactive lyase, but active glycosylase. Another important question that arises from this work is how these two mechanisms act on ICLs in cells. Importantly, FA pathway deficiency causes the serious disorder Fanconi anemia, indicating that not all ICLs can be repaired by the Neil3 pathway. This is consistent with the initial work in *Xenopus* egg extracts showing that replication-dependent repair of a cisplatin ICL is fully dependent on the FA pathway (Knipscheer *et al.*, 2009). It is tempting to speculate that the preferred pathway choice is predominantly determined by the chemical nature of the ICL and the degree of DNA distortion it induces. However, it is still unclear what the main source of ICLs in cells is. Abasic site ICLs have been suggested to form *in vivo*, but there are also strong indications that aldehydes may produce the majority of endogenous ICLs (Langevin *et al.*, 2011). How aldehyde-induced ICLs are repaired is currently unclear, but based on genetic experiments it seems very likely that these are, at least in part, repaired by the FA pathway. Future experiments are required to identify the nature of endogenous ICLs and the mechanism(s) used to repair them.

In addition to these replication-coupled ICL repair mechanisms, there is also a replication-independent ICL repair mechanism that has been studied in HSS *Xenopus* egg extracts (Ben-Yehoyada *et al.*, 2009, Williams *et al.*, 2012). These studies use an MMC-like ICL-containing plasmid as a template and repair is quantified by a quantitative PCR on the reaction products. Replication-independent repair does not depend on the FA pathway, REV7, or Rad51 but does require polymerase κ and PCNA (Ben-Yehoyada *et al.*, 2009, Williams *et al.*, 2012). Other methods have indicated the requirement of REV1, polymerase ζ and polymerase η in this repair pathway, as well as several factors involved in nucleotide excision repair (Enoiu *et al.*, 2012, Shen *et al.*, 2009, Shen *et al.*, 2006). Although the study by Ben-Yehoyada *et al.* showed that the FA pathway is not directly involved in replication-independent ICL repair in HSS/NPE, it also shows that the FA core complex does play a role in activation of an ATR-dependent checkpoint response after ICL damage. This is

consistent with work in mammalian cells that show that certain FA factors are recruited to ICLs independent of DNA replication (Shen *et al.*, 2009). In contrast, experiments in *Xenopus* egg extract previously indicated that the recruitment of FA factors requires DNA replication (Sobeck *et al.*, 2009). While the upstream role of the FA proteins in checkpoint activation requires further investigation, ATR signaling has been shown to be important for activation of the FA pathway (Andreassen *et al.*, 2004, Ho *et al.*, 2006, Ishiai *et al.*, 2008).

Also, the repair of DNA-protein crosslinks (DPCs) has been studied in egg extract (Duxin *et al.*, 2014). In this study, a substrate for DPC repair was created by covalently attaching the methyltransferase HpaII to a plasmid DNA template site-specifically. DPC repair in *Xenopus* egg extract is dependent on DNA replication and is initiated by replication fork stalling at the DPC. Then, partial degradation of the DPC allows bypass of the remaining adduct by the translesion polymerase ζ . There are strong indications that the protease that degrades the crosslinked protein is the metalloprotease SPRTN/DVC1 (Stingele *et al.*, 2016, Vaz *et al.*, 2016), but this has not yet been shown in the *Xenopus* egg extract system. If immunodepletion of SPRTN from *Xenopus* egg extracts inhibits DPC repair, this system would be well-suited to study the biochemical details and regulation of this pathway.

6. Damage checkpoint activation

DNA damage triggers a cellular response referred to as the DNA damage response (DDR). The DDR coordinates cell cycle checkpoints and DNA repair, and can induce cell senescence or apoptosis. Defects in this pathway often lead to genomic instability and cancer predisposition (Hanahan & Weinberg, 2011). The two key kinases in the DDR are the ataxia telangiectasia mutated (ATM) and the ATM and Rad3-related (ATR). ATM primarily responds to double-strand breaks (DSBs), while ATR responds to primed single stranded DNA (ssDNA) (Marechal & Zou, 2013). Both ATM and ATR signaling pathways have been studied in *Xenopus* egg extract and we will give a brief overview of a subset of these studies. More elaborate reviews and protocols have been published elsewhere (Costanzo *et al.*, 2004, Cupello *et al.*, 2016, Garner & Costanzo, 2009, Srinivasan & Gautier, 2011, Willis *et al.*, 2012).

6.1. ATR

ATR is recruited to RPA bound ssDNA via its interaction partner ATRIP. In addition, the Rad9-Hus1-Rad1 (9-1-1) complex is recruited to ssDNA-dsDNA junctions and binding of Topoisomerase II β -binding protein 1 (TopBP1) to both ATR and the 9-1-1 complex is important to activate ATR. Many additional factors can influence ATR activation and, once activated, ATR phosphorylates numerous downstream effector proteins that play a role in genome maintenance, including Chk1 and RPA (Yazinski & Zou, 2016).

The ATR signaling pathway can be activated in *Xenopus* egg extract using a variety of DNA substrates. Already in the early nineties, aphidicolin, an inhibitor of polymerase α , ϵ , δ , and ζ , was used to prevent the completion of DNA replication in LSS. This study showed that the presence of unreplicated DNA induces a cell cycle checkpoint that inhibits the entry into mitosis (Dasso & Newport, 1990). Later, similar experiments showed that this checkpoint is mediated by Chk1 phosphorylation (Kumagai *et al.*, 1998). Using the nuclear egg extract NPE and plasmid DNA it was demonstrated that aphidicolin induces

the ATR signaling pathway by uncoupling the replicative helicase from the polymerases, thereby generating single-stranded DNA (Byun *et al.*, 2005). In addition to DNA unwinding, polymerase α is also required for the activation of ATR (Byun *et al.*, 2005, Michael *et al.*, 2000), most likely by generating primers on ssDNA and thereby creating additional ssDNA-dsDNA junctions (Van *et al.*, 2010). Other DNA lesions, such as UV and MMS, can also induce ATR signaling in egg extract, likely by uncoupling the replicative helicases from the polymerases (Lupardus *et al.*, 2002). Interestingly, DNA interstrand crosslinks also induce Chk1 phosphorylation, even though this helicase-polymerase uncoupling is not possible (Ben-Yehoyada *et al.*, 2009, Räschle *et al.*, 2008). The DNA structures that are required for ATR activation are further characterized by using M13-based circular ssDNA templates with primers annealed to it. These studies showed that ssDNA-dsDNA junctions with a free 5' end activate ATR, and that ATR activation can be enhanced by larger ssDNA regions or additional 5' ends (MacDougall *et al.*, 2007, Van *et al.*, 2010).

The activation of ATR by interaction with TopBP1 has been studied in detail using LSS extract in combination with aphidicolin. TopBP1 uses its ATR activation domain (AAD) to interact with and activate ATR (Hashimoto *et al.*, 2006, Kumagai *et al.*, 2006). The interaction is further enhanced by ATR-dependent phosphorylation of the AAD domain (Hashimoto *et al.*, 2006). An additional regulator of the ATR signaling pathway, Claspin, was also identified in *Xenopus* egg extract and mediates the phosphorylation of Chk1 (Kumagai & Dunphy, 2000, Kumagai & Dunphy, 2003).

The 9-1-1 complex is recruited to ssDNA-dsDNA junctions by the Rad17-dependent RFC (replication factor-C)-like complex (Jones *et al.*, 2003) and Rad17 may directly mediate the interaction between the 9-1-1 complex and TopBP1 (Lee & Dunphy, 2010). Furthermore, direct interaction between the Rad9 component of the 9-1-1 complex and TopBP1 is required for ATR activation, although this interaction does not seem to be required for TopBP1 recruitment to ssDNA (Duursma *et al.*, 2013, Lee & Dunphy, 2013, Lee *et al.*, 2007). It has been suggested that TopBP1 loading precedes 9-1-1 recruitment to ssDNA/dsDNA junctions and is mediated by polymerase α (Yan & Michael, 2009). In addition, a recent study using M13-based ATR activating DNA structures, showed that the MRN complex is important for the recruitment of TopBP1 and ATR signaling (Duursma *et al.*, 2013). This was later also demonstrated using aphidicolin treated chromatin in egg extract (Lee & Dunphy, 2013). This was a surprising finding as the MRN complex had previously only been implicated in ATM signaling.

Finally, translesion synthesis (TLS) polymerases have also been shown to play a role in ATR signaling in *Xenopus* egg extract. Upon generation of long stretches of ssDNA after addition of aphidicolin, polymerase α was implicated, together with polymerase β , in generating small stretches of dsDNA that are required to load the 9-1-1 complex (Betous *et al.*, 2013). In addition, REV1 does not seem to be involved in loading of the core activating complex RPA-ATR/ATRIP-TopBP1-9-1-1 but seems to function downstream in activation of Chk1 (DeStephanis *et al.*, 2015).

6.2. ATM

At the site of a double-strand break (DSB), ATM is recruited and activated by interaction with the MRN complex, which also localizes to these lesions. Activated ATM then phosphorylates histone H2AX that subsequently recruits MDC1. This initiates a ubiquitylation cascade at the site of damage, mediated by the ubiquitin ligases RNF8 and RNF168, leading to the

recruitment of other DSB regulators such as 53BP1 and BRCA1. When a sister chromatid is present, in late S or G2 phases, DSBs are repaired via homologous recombination (HR). This is initiated by activation of DNA end resection, leading to the removal of the Ku70/80 heterodimer from the DNA ends. In the absence of a sister chromatid, DNA end resection is inhibited and the DSB is repaired via non-homologous end joining (NHEJ). Importantly, the activation of ATM by DSBs leads to the phosphorylation of many downstream effectors, such as Chk2 and p53, which not only mediate DNA repair but also cell cycle arrest and apoptosis (Marechal & Zou, 2013).

ATM signaling can be activated in *Xenopus* egg extracts with DNA substrates that mimic double-strand breaks, such as DNA plasmids cut with restriction enzymes (Costanzo *et al.*, 2000, You *et al.*, 2005) or annealed oligos (Yoo *et al.*, 2004). Double stranded linear DNA fragments were also used to study the role of MRN in ATM activation. MRN was reported to activate ATM by a direct interaction between its NBS1 subunit and ATM (Dupre *et al.*, 2006, You *et al.*, 2005) but also by tethering DNA and thereby increasing the local DNA concentration (Dupre *et al.*, 2006). Consistent with this, it was demonstrated that ATM activation depends on the concentration of DNA ends and the DNA length (You *et al.*, 2007). It was suggested that the exonuclease activity of the MRN complex is required for ATM activation (Dupre *et al.*, 2008) and that oligonucleotides generated at DSBs further activate ATM (Jazayeri *et al.*, 2008).

Xenopus egg extracts have also been used to screen chemicals for ATM activation. The readout was the phosphorylation of histone H2AX in response to linearized plasmids and this screen identified the small molecule mirin as an inhibitor of ATM activation (Dupre *et al.*, 2008). Mirin directly inhibits the endonuclease activity of the MRN complex required for homologous recombination but also MRN-dependent ATM activation.

In addition to activation of ATM, DSBs can also activate ATR. Using annealed oligos and sperm DNA digested by EcoRI, Yoo *et al.* demonstrated that ATM phosphorylates TopBP1 leading to enhanced ATR interaction and activation (Yoo *et al.*, 2009). The interaction between ATM and TopBP1 also seems to require CtIP and the MRN complex (Ramirez-Lugo *et al.*, 2011, Yoo *et al.*, 2009).

7. Replication fork stalling

Stalling of DNA replication can occur when the replication fork encounters a physical impediment, such as unrepaired DNA lesions or stable secondary DNA structures. Extensive fork stalling can induce ATR checkpoint activation, which can promote fork stabilization and recovery. This process is not fully understood but involves many ATR target proteins, including homologous recombination factors, nucleases and helicases, and may involve a regressed replication fork as an intermediate (Cortez, 2015, Yeeles *et al.*, 2013). Malfunctioning of the ATR checkpoint response, or failure to resolve the blocked replication fork, results in replication fork collapse. This causes a double-strand break and can lead to chromosomal rearrangements and genome instability.

In human cells, stalled replication forks are most often induced by addition of hydroxyurea, which depletes dNTP pools. In *Xenopus* egg extract, fork stalling can be accomplished by the addition of aphidicolin. Using LSS egg extract in combination with aphidicolin-treated sperm chromatin, it was established that ATR and ATM signaling, as well as the proteins Tipin and MRE11, are required for the recovery after fork stalling

(Errico *et al.*, 2007, Trenz *et al.*, 2006). Furthermore, it was shown that phosphorylation of the DNA translocase SMARCAL1 by ATR plays an important role in limiting fork processing to ensure stabilization of a stalled fork (Couch *et al.*, 2013). In addition to fork stalling, fork collapse was mimicked in egg extract by adding a nicking enzyme to the reaction, resulting in a DSB once the replication fork encountered the nick. This work indicated that some of the replisome components, such as GINS and polymerase ϵ , unload after fork collapse, and their reloading is mediated by Rad51 and MRE11 (Hashimoto *et al.*, 2011).

Repetitive DNA sequences, or sequences that contain secondary structures, can also induce replication fork stalling. *Xenopus* egg extract (LSS) was recently used to study replication of human chromosomal segments containing repetitive sequences (Aze *et al.*, 2016). While the repetitive sequences caused mild reduction in replication fork progression, indicative of fork stalling, surprisingly, this was not accompanied by ATR activation. Electron microscopy showed dense DNA structures that likely prevent RPA loading and ATR activation at these repetitive centromeric sequences to facilitate their replication (Aze *et al.*, 2016). Another study used single stranded DNA templates to investigate how the DNA replication machinery bypasses stable secondary DNA structures, called G-quadruplexes, formed in G-rich sequences (Castillo Bosch *et al.*, 2014). In this study, DNA replication starts from a primer on the G-quadruplex containing ssDNA templates in HSS. Replication stalls transiently at the site of the G-quadruplex structure and resumes quickly after the secondary structure has been resolved. Unwinding of the G-quadruplex structure is in part mediated by the FANCI helicase. This study suggests that there are several different mechanisms present in egg extract that can unwind these secondary structures. Consistent with this, several helicases have been shown to be able to unwind G-quadruplexes in reconstitution systems (Mendoza *et al.*, 2016). In the future, the *Xenopus* egg extract system can be used to gain insight into the relative roles of these helicases in G-quadruplex unwinding, and to study how these unwinding mechanisms are regulated.

8. Discussion and future directions

The *Xenopus* egg extract system has made major contributions to our knowledge of several important genome maintenance pathways. The ability of these extracts to support DNA replication and repair, and the use of cleverly designed DNA templates (see Table 1), has provided unique opportunities to determine important mechanistic details of DNA repair pathways. Immunodepletion of specific proteins, in combination with rescue experiments using wildtype and mutant proteins, has proven to be a valuable method to determine biochemical function of the proteins acting in these pathways. However, the dependence on immunodepletions to remove specific proteins can also be a limitation. It is time consuming and expensive to generate antibodies capable of depletion, and co-depletion of interacting factors can complicate the results of the experiments. Yet, the latter can also be used as an advantage to gain insights into the composition of protein complexes in a physiological setting.

In the future, the development of additional sequence specific chemical modifications to DNA templates, such as various different DNA interstrand crosslinks, can create many additional opportunities to examine poorly understood DNA repair pathways. In addition, *Xenopus* egg extracts are efficient in nucleosome assembly, which enables the examination of chromatin remodeling during DNA repair in addition to damage dependent histone

2

modifications. Furthermore, several recent studies have shown the great potential of combining the *Xenopus* egg extract system with mass spectrometry. This approach has been used to identify novel factors in checkpoint signaling and DSB repair (Duursma *et al.*, 2013, Räschle *et al.*, 2015). DNA templates, with repair factors bound to them, are isolated during these processes and the proteins are identified by mass spectrometry. The recent sequencing of the *Xenopus laevis* genome will further facilitate such approaches (Session *et al.*, 2016). A similar technique that allows the isolation and identification of proteins on nascent DNA (iPond) from cells has recently been developed by the Cortez laboratory (Sirbu *et al.*, 2011). While this is a very effective technique it depends on active DNA replication and it does not allow the use of exogenous modified DNA templates. Another promising development is the combination of *Xenopus* egg extract with single-molecule techniques that was recently established to study NHEJ. If this approach is expanded to study additional DNA repair pathways it could make major contributions in our knowledge of the biochemistry and kinetics of these pathways.

Recently, the Diffley laboratory succeeded in the *in vitro* reconstruction of budding yeast DNA replication initiation and elongation from purified components (Yeeles *et al.*, 2015, Yeeles *et al.*, 2017). This is a major accomplishment and will be invaluable in our biochemical understanding of DNA replication. Further development of this system will likely allow the study of several replication-linked processes such as DNA repair, chromatin remodeling and histone modifications. However, this system depends on the knowledge of all components required for these processes and this is not always available. In addition, there is no active signaling or cell cycle context in this system, which also limits the questions that can be addressed. Nonetheless, a combination of reconstitution, extract, and cellular systems will be required to start fully understanding the biochemical details of DNA repair mechanisms. This is of great importance for understanding how our genome is kept stable and can help the development of novel anti-cancer drugs.

Acknowledgements

We apologize to our colleagues whose work we did not cite because of space constraints. This work was supported by the Netherlands organization for Scientific Research (VIDI 700.10.421 to P.K.) and a project grant from the Dutch Cancer Society (KWF HUBR 2015-7736 to P.K.). We thank Tatsuro Takahashi, Thomas Graham and Anja Duursma for suggestions on parts of the manuscript.

References

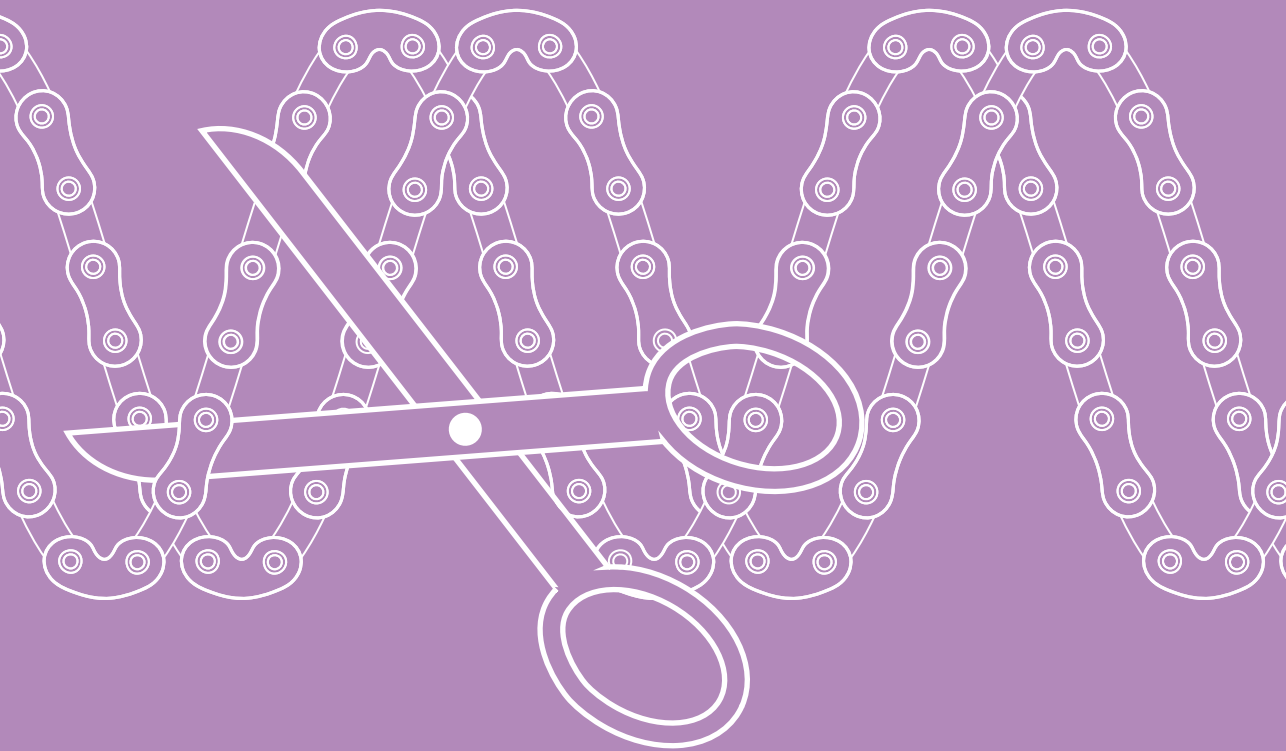
- Andreassen PR, D'Andrea AD & Taniguchi T (2004) ATR couples FANCD2 monoubiquitination to the DNA-damage response. *Genes & development* 18: 1958-63
- Angelov T, Guainazzi A & Scharer OD (2009) Generation of DNA interstrand cross-links by post-synthetic reductive amination. *Organic letters* 11: 661-4
- Aze A, Sannino V, Soffientini P, Bachi A & Costanzo V (2016) Centromeric DNA replication reconstitution reveals DNA loops and ATR checkpoint suppression. *Nat Cell Biol* 18: 684-91
- Ben-Yehoyada M, Wang LC, Kozekov ID, Rizzo CJ, Gottesman ME & Gautier J (2009) Checkpoint signaling from a single DNA interstrand crosslink. *Molecular cell* 35: 704-15
- Betous R, Pillaire MJ, Pierini L, van der Laan S, Recolin B, Ohl-Seguy E, Guo C, Niimi N, Gruz P, Nohmi T, Friedberg E, Cazaux C, Maiorano D & Hoffmann JS (2013) DNA polymerase kappa-dependent DNA synthesis at stalled replication forks is important for CHK1 activation. *The EMBO journal* 32: 2172-85
- Beyert N, Reichenberger S, Peters M, Hartung M, Gottlich B, Goedecke W, Vielmetter W & Pfeiffer P (1994) Nonhomologous DNA end joining of synthetic hairpin substrates in *Xenopus laevis* egg extracts. *Nucleic acids research* 22: 1643-50
- Blow JJ & Laskey RA (1986) Initiation of DNA replication in nuclei and purified DNA by a cell-free extract of *Xenopus* eggs. *Cell* 47: 577-87
- Bluteau D, Masliah-Planchon J, Clairmont C, Rousseau A, Ceccaldi R, Dubois d'Enghien C, Bluteau O, Cuccuini W, Gachet S, Peffault de Latour R, Leblanc T, Socie G, Baruchel A, Stoppa-Lyonnet D, D'Andrea AD & Soulier J (2016) Biallelic inactivation of REV7 is associated with Fanconi anemia. *J Clin Invest* 126: 3580-4
- Brooks P, Dohet C, Almouzni G, Mechali M & Radman M (1989) Mismatch repair involving localized DNA synthesis in extracts of *Xenopus* eggs. *Proceedings of the National Academy of Sciences of the United States of America* 86: 4425-9
- Budzowska M, Graham TG, Sobeck A, Waga S & Walter JC (2015) Regulation of the Rev1-pol zeta complex during bypass of a DNA interstrand crosslink. *The EMBO journal* 34: 1971-85
- Byun TS, Pacek M, Yee MC, Walter JC & Cimprich KA (2005) Functional uncoupling of MCM helicase and DNA polymerase activities activates the ATR-dependent checkpoint. *Genes & development* 19: 1040-52
- Castillo Bosch P, Segura-Bayona S, Koole W, van Heteren JT, Dewar JM, Tijsterman M & Knipscheer P (2014) FANCI promotes DNA synthesis through G-quadruplex structures. *The EMBO journal* 33: 2521-33
- Chiruvella KK, Liang Z & Wilson TE (2013) Repair of double-strand breaks by end joining. *Cold Spring Harb Perspect Biol* 5: a012757
- Cortez D (2015) Preventing replication fork collapse to maintain genome integrity. *DNA repair* 32: 149-157
- Costanzo V, Robertson K & Gautier J (2004) *Xenopus* cell-free extracts to study the DNA damage response. *Methods Mol Biol* 280: 213-27
- Costanzo V, Robertson K, Ying CY, Kim E, Avvedimento E, Gottesman M, Grieco D & Gautier J (2000) Reconstitution of an ATM-dependent checkpoint that inhibits chromosomal DNA replication following DNA damage. *Molecular cell* 6: 649-59
- Couch FB, Bansbach CE, Driscoll R, Luzwick JW, Glick GG, Betous R, Carroll CM, Jung SY, Qin J, Cimprich KA & Cortez D (2013) ATR phosphorylates SMARCAL1 to prevent replication fork collapse. *Genes & development* 27: 1610-23
- Cupello S, Richardson C & Yan S (2016) Cell-free *Xenopus* egg extracts for studying DNA damage response pathways. *Int J Dev Biol* 60: 229-236
- Dasso M & Newport JW (1990) Completion of DNA replication is monitored by a feedback system that controls the initiation of mitosis in vitro: studies in *Xenopus*. *Cell* 61: 811-23
- Davis AJ & Chen DJ (2013) DNA double strand break repair via non-homologous end-joining. *Transl Cancer Res* 2: 130-143
- Daza P, Reichenberger S, Gottlich B, Hagmann M, Feldmann E & Pfeiffer P (1996) Mechanisms of nonhomologous DNA end-joining in frogs, mice and men. *Biological chemistry* 377: 775-86
- Deans AJ & West SC (2011) DNA interstrand crosslink repair and cancer. *Nat Rev Cancer* 11: 467-80
- DeStephanis D, McLeod M & Yan S (2015) REV1 is important for the ATR-Chk1 DNA damage response pathway in *Xenopus* egg extracts. *Biochemical and biophysical research communications* 460: 609-15
- Di Virgilio M & Gautier J (2005) Repair of double-strand breaks by nonhomologous end joining in the absence of Mre11. *The Journal of cell biology* 171: 765-71
- Dupre A, Boyer-Chatenet L & Gautier J (2006) Two-step activation of ATM by DNA and the Mre11-Rad50-Nbs1 complex. *Nature structural & molecular biology* 13: 451-7
- Dupre A, Boyer-Chatenet L, Sattler RM, Modi AP, Lee JH, Nicolette ML, Kopelovich L, Jasin M, Baer R, Paull TT & Gautier J (2008) A forward chemical genetic screen reveals an inhibitor of the Mre11-Rad50-Nbs1 complex. *Nature chemical biology* 4: 119-25
- Duursma AM, Driscoll R, Elias JE & Cimprich KA (2013) A role for the MRN complex in ATR activation via TOPBP1 recruitment. *Molecular cell* 50: 116-22
- Duxin JP, Dewar JM, Yardimci H & Walter JC (2014) Repair of a DNA-protein crosslink by replication-coupled proteolysis. *Cell* 159: 346-57

- Enoiu M, Jiricny J & Schärer OD (2012) Repair of cisplatin-induced DNA interstrand crosslinks by a replication-independent pathway involving transcription-coupled repair and translesion synthesis. *Nucleic acids research* 40: 8953-64
- Errico A, Costanzo V & Hunt T (2007) Tipin is required for stalled replication forks to resume DNA replication after removal of aphidicolin in *Xenopus* egg extracts. *Proceedings of the National Academy of Sciences of the United States of America* 104: 14929-34
- Fu YV, Yardimci H, Long DT, Ho TV, Guainazzi A, Bermudez VP, Hurwitz J, van Oijen A, Schärer OD & Walter JC (2011) Selective bypass of a lagging strand roadblock by the eukaryotic replicative DNA helicase. *Cell* 146: 931-41
- Garner E & Costanzo V (2009) Studying the DNA damage response using in vitro model systems. *DNA repair* 8: 1025-37
- Ghodgaonkar MM, Lazzaro F, Olivera-Pimentel M, Artola-Boran M, Cejka P, Reijns MA, Jackson AP, Plevani P, Muzi-Falconi M & Jiricny J (2013) Ribonucleotides misincorporated into DNA act as strand-discrimination signals in eukaryotic mismatch repair. *Molecular cell* 50: 323-32
- Graham TG, Walter JC & Loparo JJ (2016) Two-Stage Synapsis of DNA Ends during Non-homologous End Joining. *Molecular cell* 61: 850-8
- Gu XY, Bennett RA & Povirk LF (1996) End-joining of free radical-mediated DNA double-strand breaks in vitro is blocked by the kinase inhibitor wortmannin at a step preceding removal of damaged 3' termini. *The Journal of biological chemistry* 271: 19660-3
- Gu XY, Weinfeld MA & Povirk LF (1998) Implication of DNA-dependent protein kinase in an early, essential, local phosphorylation event during end-joining of DNA double-strand breaks in vitro. *Biochemistry* 37: 9827-35
- Hanahan D & Weinberg RA (2011) Hallmarks of cancer: the next generation. *Cell* 144: 646-74
- Hardwick LJ & Philpott A (2015) An oncologists friend: How *Xenopus* contributes to cancer research. *Dev Biol* 408: 180-7
- Hashimoto Y, Puddu F & Costanzo V (2011) RAD51- and MRE11-dependent reassembly of uncoupled CMG helicase complex at collapsed replication forks. *Nature structural & molecular biology* 19: 17-24
- Hashimoto Y, Tsujimura T, Sugino A & Takisawa H (2006) The phosphorylated C-terminal domain of *Xenopus* Cut5 directly mediates ATR-dependent activation of Chk1. *Genes Cells* 11: 993-1007
- Ho GP, Margossian S, Taniguchi T & D'Andrea AD (2006) Phosphorylation of FANCD2 on two novel sites is required for mitomycin C resistance. *Molecular and cellular biology* 26: 7005-15
- Hoeijmakers JH (2009) DNA damage, aging, and cancer. *The New England journal of medicine* 361: 1475-85
- Holmes J, Jr., Clark S & Modrich P (1990) Strand-specific mismatch correction in nuclear extracts of human and *Drosophila melanogaster* cell lines. *Proceedings of the National Academy of Sciences of the United States of America* 87: 5837-41
- Ishiai M, Kitao H, Smogorzewska A, Tomida J, Kinomura A, Uchida E, Saberi A, Kinoshita E, Kinoshita-Kikuta E, Koike T, Tashiro S, Elledge SJ & Takata M (2008) FANCI phosphorylation functions as a molecular switch to turn on the Fanconi anemia pathway. *Nature structural & molecular biology* 15: 1138-46
- Jazayeri A, Balestrini A, Garner E, Haber JE & Costanzo V (2008) Mre11-Rad50-Nbs1-dependent processing of DNA breaks generates oligonucleotides that stimulate ATM activity. *The EMBO journal* 27: 1953-62
- Jiricny J (2013) Postreplicative mismatch repair. *Cold Spring Harb Perspect Biol* 5: a012633
- Jones RE, Chapman JR, Puligilla C, Murray JM, Car AM, Ford CC & Lindsay HD (2003) XRad17 is required for the activation of XChk1 but not XCds1 during checkpoint signaling in *Xenopus*. *Mol Biol Cell* 14: 3898-910
- Kadyrov FA, Dzantiev L, Constantin N & Modrich P (2006) Endonucleolytic function of MutLalpha in human mismatch repair. *Cell* 126: 297-308
- Kawase Y, Tsurimoto T, Nakagawa T, Masukata H & Takahashi TS (2016) MutSalpha maintains the mismatch repair capability by inhibiting PCNA unloading. *Elife* 5
- Klein Douwel D, Boonen RA, Long DT, Szypowska AA, Räschle M, Walter JC & Knipscheer P (2014) XPF-ERCC1 acts in Unhooking DNA interstrand crosslinks in cooperation with FANCD2 and FANCP/SLX4. *Molecular cell* 54: 460-71
- Knipscheer P, Räschle M, Schärer OD & Walter JC (2012) Replication-coupled DNA interstrand cross-link repair in *Xenopus* egg extracts. *Methods Mol Biol* 920: 221-43
- Knipscheer P, Räschle M, Smogorzewska A, Enoi M, Ho TV, Schärer OD, Elledge SJ & Walter JC (2009) The Fanconi anemia pathway promotes replication-dependent DNA interstrand cross-link repair. *Science* 326: 1698-701
- Kottemann MC & Smogorzewska A (2013) Fanconi anaemia and the repair of Watson and Crick DNA crosslinks. *Nature* 493: 356-63
- Kumagai A & Dunphy WG (2000) Claspin, a novel protein required for the activation of Chk1 during a DNA replication checkpoint response in *Xenopus* egg extracts. *Molecular cell* 6: 839-49
- Kumagai A & Dunphy WG (2003) Repeated phosphopeptide motifs in Claspin mediate the regulated binding of Chk1. *Nat Cell Biol* 5: 161-5
- Kumagai A, Guo Z, Emami KH, Wang SX & Dunphy WG (1998) The *Xenopus* Chk1 protein kinase mediates a caffeine-sensitive pathway of checkpoint control in cell-free extracts. *The Journal of cell biology*

- 142: 1559-69
- Kumagai A, Lee J, Yoo HY & Dunphy WG (2006) TopBP1 activates the ATR-ATRIP complex. *Cell* 124: 943-55
- Labhart P (1999) Ku-dependent nonhomologous DNA end joining in *Xenopus* egg extracts. *Molecular and cellular biology* 19: 2585-93
- Langevin F, Crossan GP, Rosado IV, Arends MJ & Patel KJ (2011) Fancd2 counteracts the toxic effects of naturally produced aldehydes in mice. *Nature* 475: 53-8
- Le Breton C, Hennion M, Arimondo PB & Hyrien O (2011) Replication-fork stalling and processing at a single psoralen interstrand crosslink in *Xenopus* egg extracts. *PLoS one* 6: e18554
- Lebofsky R, Takahashi T & Walter JC (2009) DNA replication in nucleus-free *Xenopus* egg extracts. *Methods Mol Biol* 521: 229-52
- Lee J & Dunphy WG (2010) Rad17 plays a central role in establishment of the interaction between TopBP1 and the Rad9-Hus1-Rad1 complex at stalled replication forks. *Mol Biol Cell* 21: 926-35
- Lee J & Dunphy WG (2013) The Mre11-Rad50-Nbs1 (MRN) complex has a specific role in the activation of Chk1 in response to stalled replication forks. *Mol Biol Cell* 24: 1343-53
- Lee J, Kumagai A & Dunphy WG (2007) The Rad9-Hus1-Rad1 checkpoint clamp regulates interaction of TopBP1 with ATR. *The Journal of biological chemistry* 282: 28036-44
- Li SKH & Martin A (2016) Mismatch Repair and Colon Cancer: Mechanisms and Therapies Explored. *Trends Mol Med* 22: 274-289
- Liao S, Tammaro M & Yan H (2016) The structure of ends determines the pathway choice and Mre11 nuclease dependency of DNA double-strand break repair. *Nucleic acids research* 44: 5689-701
- Lohka MJ & Masui Y (1983) Formation in vitro of sperm pronuclei and mitotic chromosomes induced by amphibian ooplasmic components. *Science* 220: 719-21
- Long DT, Joukov V, Budzowska M & Walter JC (2014) BRCA1 promotes unloading of the CMG helicase from a stalled DNA replication fork. *Molecular cell* 56: 174-85
- Long DT, Räschle M, Joukov V & Walter JC (2011) Mechanism of RAD51-dependent DNA interstrand cross-link repair. *Science* 333: 84-7
- Lujan SA, Williams JS, Clausen AR, Clark AB & Kunkel TA (2013) Ribonucleotides are signals for mismatch repair of leading-strand replication errors. *Molecular cell* 50: 437-43
- Lupardus PJ, Byun T, Yee MC, Hekmat-Nejad M & Cimprich KA (2002) A requirement for replication in activation of the ATR-dependent DNA damage checkpoint. *Genes & development* 16: 2327-32
- MacDougall CA, Byun TS, Van C, Yee MC & Cimprich KA (2007) The structural determinants of checkpoint activation. *Genes & development* 21: 898-903
- Marechal A & Zou L (2013) DNA damage sensing by the ATM and ATR kinases. *Cold Spring Harb Perspect Biol* 5
- Mendoza O, Bourdoncle A, Boule JB, Brosh RM, Jr. & Mergny JL (2016) G-quadruplexes and helicases. *Nucleic acids research* 44: 1989-2006
- Michael WM, Ott R, Fanning E & Newport J (2000) Activation of the DNA replication checkpoint through RNA synthesis by primase. *Science* 289: 2133-7
- Newport J (1987) Nuclear reconstitution in vitro: stages of assembly around protein-free DNA. *Cell* 48: 205-17
- Niedernhofer LJ, Lalai AS & Hoeijmakers JH (2005) Fanconi anemia (cross)linked to DNA repair. *Cell* 123: 1191-8
- O'Driscoll M (2012) Diseases associated with defective responses to DNA damage. *Cold Spring Harb Perspect Biol* 4
- Pearl LH, Schierz AC, Ward SE, Al-Lazikani B & Pearl FM (2015) Therapeutic opportunities within the DNA damage response. *Nat Rev Cancer* 15: 166-80
- Pfeiffer P & Vielmetter W (1988) Joining of nonhomologous DNA double strand breaks in vitro. *Nucleic acids research* 16: 907-24
- Pluciennik A, Dzantiev L, Iyer RR, Constantin N, Kadyrov FA & Modrich P (2010) PCNA function in the activation and strand direction of MutLalpha endonuclease in mismatch repair. *Proceedings of the National Academy of Sciences of the United States of America* 107: 16066-71
- Radhakrishnan SK, Jette N & Lees-Miller SP (2014) Non-homologous end joining: emerging themes and unanswered questions. *DNA repair* 17: 2-8
- Ramirez-Lugo JS, Yoo HY, Yoon SJ & Dunphy WG (2011) CtIP interacts with TopBP1 and Nbs1 in the response to double-stranded DNA breaks (DSBs) in *Xenopus* egg extracts. *Cell Cycle* 10: 469-80
- Räschle M, Knipscheer P, Enoiu M, Angelov T, Sun J, Griffith JD, Ellenberger TE, Schärer OD & Walter JC (2008) Mechanism of replication-coupled DNA interstrand crosslink repair. *Cell* 134: 969-80
- Räschle M, Smeenk G, Hansen RK, Temu T, Oka Y, Hein MY, Nagaraj N, Long DT, Walter JC, Hofmann K, Storchova Z, Cox J, Bekker-Jensen S, Mailand N & Mann M (2015) DNA repair. Proteomics reveals dynamic assembly of repair complexes during bypass of DNA cross-links. *Science* 348: 1253671
- Rass E, Grabarz A, Plo I, Gautier J, Bertrand P & Lopez BS (2009) Role of Mre11 in chromosomal nonhomologous end joining in mammalian cells. *Nature structural & molecular biology* 16: 819-24
- Rehman FL, Lord CJ & Ashworth A (2010) Synthetic lethal approaches to breast cancer therapy. *Nat Rev Clin Oncol* 7: 718-24
- Repmann S, Olivera-Harris M & Jiricny J (2015) Influence of oxidized purine processing on strand directionality of mismatch repair. *The Journal of*

- biological chemistry* 290: 9986-99
- Ribizzo F, Shiloh Y & Schumacher B (2016) Systemic DNA damage responses in aging and diseases. *Semin Cancer Biol* 37-38: 26-35
- Sandoval A & Labhart P (2002) Joining of DNA ends bearing non-matching 3'-overhangs. *DNA repair* 1: 397-410
- Semlow DR, Zhang J, Budzowska M, Drohat AC & Walter JC (2016) Replication-Dependent Unhooking of DNA Interstrand Cross-Links by the NEIL3 Glycosylase. *Cell* 167: 498-511 e14
- Session AM, Uno Y, Kwon T, Chapman JA, Toyoda A, Takahashi S, Fukui A, Hikosaka A, Suzuki A, Kondo M, van Heeringen SJ, Quigley I, Heinz S, Ogino H, Ochi H, Hellsten U, Lyons JB, Simakov O, Putnam N, Stites J *et al.* (2016) Genome evolution in the allotetraploid frog *Xenopus laevis*. *Nature* 538: 336-343
- Shen X, Do H, Li Y, Chung WH, Tomasz M, de Winter JP, Xia B, Elledge SJ, Wang W & Li L (2009) Recruitment of fanconi anemia and breast cancer proteins to DNA damage sites is differentially governed by replication. *Molecular cell* 35: 716-23
- Shen X, Jun S, O'Neal LE, Sonoda E, Bemark M, Sale JE & Li L (2006) REV3 and REV1 play major roles in recombination-independent repair of DNA interstrand cross-links mediated by monoubiquitinated proliferating cell nuclear antigen (PCNA). *The Journal of biological chemistry* 281: 13869-72
- Sirbu BM, Couch FB, Feigerle JT, Bhaskara S, Hiebert SW & Cortez D (2011) Analysis of protein dynamics at active, stalled, and collapsed replication forks. *Genes & development* 25: 1320-7
- Sobeck A, Stone S, Landais I, de Graaf B & Hoatlin ME (2009) The Fanconi anemia protein FANCM is controlled by FANCD2 and the ATR/ATM pathways. *The Journal of biological chemistry* 284: 25560-8
- Srinivasan SV & Gautier J (2011) Study of cell cycle checkpoints using *Xenopus* cell-free extracts. *Methods Mol Biol* 782: 119-58
- Stingle J, Bellelli R, Alte F, Hewitt G, Sarek G, Maslen SL, Tsutakawa SE, Borg A, Kjaer S, Tainer JA, Shekel JM, Groll M & Boulton SJ (2016) Mechanism and Regulation of DNA-Protein Crosslink Repair by the DNA-Dependent Metalloprotease SPRTN. *Molecular cell* 64: 688-703
- Taylor EM, Cecillon SM, Bonis A, Chapman JR, Povirk LF & Lindsay HD (2010) The Mre11/Rad50/Nbs1 complex functions in resection-based DNA end joining in *Xenopus laevis*. *Nucleic acids research* 38: 441-54
- Thode S, Schafer A, Pfeiffer P & Vielmetter W (1990) A novel pathway of DNA end-to-end joining. *Cell* 60: 921-8
- Thomas DC, Roberts JD & Kunkel TA (1991) Heteroduplex repair in extracts of human HeLa cells. *The Journal of biological chemistry* 266: 3744-51
- Trenz K, Smith E, Smith S & Costanzo V (2006) ATM and ATR promote Mre11 dependent restart of collapsed replication forks and prevent accumulation of DNA breaks. *The EMBO journal* 25: 1764-74
- Tutter AV & Walter JC (2006) Chromosomal DNA replication in a soluble cell-free system derived from *Xenopus* eggs. *Methods Mol Biol* 322: 121-37
- Umar A, Buermeier AB, Simon JA, Thomas DC, Clark AB, Liskay RM & Kunkel TA (1996) Requirement for PCNA in DNA mismatch repair at a step preceding DNA resynthesis. *Cell* 87: 65-73
- Van C, Yan S, Michael WM, Waga S & Cimprich KA (2010) Continued primer synthesis at stalled replication forks contributes to checkpoint activation. *The Journal of cell biology* 189: 233-46
- van den Boom J, Wolf M, Weimann L, Schulze N, Li F, Kaschani F, Riemer A, Zierhut C, Kaiser M, Iliakis G, Funabiki H & Meyer H (2016) VCP/p97 Extracts Sterically Trapped Ku70/80 Rings from DNA in Double-Strand Break Repair. *Molecular cell* 64: 189-198
- Varlet I, Canard B, Brooks P, Cerovic G & Radman M (1996) Mismatch repair in *Xenopus* egg extracts: DNA strand breaks act as signals rather than excision points. *Proceedings of the National Academy of Sciences of the United States of America* 93: 10156-61
- Varlet I, Radman M & Brooks P (1990) DNA mismatch repair in *Xenopus* egg extracts: repair efficiency and DNA repair synthesis for all single base-pair mismatches. *Proceedings of the National Academy of Sciences of the United States of America* 87: 7883-7
- Vaz B, Popovic M, Newman JA, Fielden J, Aitkenhead H, Halder S, Singh AN, Vendrell I, Fischer R, Torrecilla I, Drobnitzky N, Freire R, Amor DJ, Lockhart PJ, Kessler BM, McKenna GW, Gileadi O & Ramadan K (2016) Metalloprotease SPRTN/DVC1 Orchestrates Replication-Coupled DNA-Protein Crosslink Repair. *Molecular cell* 64: 704-719
- Walter J, Sun L & Newport J (1998) Regulated chromosomal DNA replication in the absence of a nucleus. *Molecular cell* 1: 519-29
- Williams HL, Gottesman ME & Gautier J (2012) Replication-independent repair of DNA interstrand crosslinks. *Molecular cell* 47: 140-7
- Willis J, DeStephanis D, Patel Y, Gowda V & Yan S (2012) Study of the DNA damage checkpoint using *Xenopus* egg extracts. *J Vis Exp*: e4449
- Xie A, Kwok A & Scully R (2009) Role of mammalian Mre11 in classical and alternative nonhomologous end joining. *Nature structural & molecular biology* 16: 814-8
- Yan S & Michael WM (2009) TopBP1 and DNA polymerase-alpha directly recruit the 9-1-1 complex to stalled DNA replication forks. *The Journal of cell biology* 184: 793-804
- Yazinski SA & Zou L (2016) Functions, Regulation, and Therapeutic Implications of the ATR Checkpoint Pathway. *Annual review of genetics* 50: 155-173
- Yeeles JT, Deegan TD, Janska A, Early A & Diffley JF

- (2015) Regulated eukaryotic DNA replication origin firing with purified proteins. *Nature* 519: 431-5
- Yeeles JT, Poli J, Mariani KJ & Pasero P (2013) Rescuing stalled or damaged replication forks. *Cold Spring Harb Perspect Biol* 5: a012815
- Yeeles JTP, Janska A, Early A & Diffley JFX (2017) How the Eukaryotic Replisome Achieves Rapid and Efficient DNA Replication. *Molecular cell* 65: 105-116
- Yoo HY, Kumagai A, Shevchenko A, Shevchenko A & Dunphy WG (2009) The Mre11-Rad50-Nbs1 complex mediates activation of TopBP1 by ATM. *Mol Biol Cell* 20: 2351-60
- Yoo HY, Shevchenko A, Shevchenko A & Dunphy WG (2004) Mcm2 is a direct substrate of ATM and ATR during DNA damage and DNA replication checkpoint responses. *The Journal of biological chemistry* 279: 53353-64
- You Z, Bailis JM, Johnson SA, Dilworth SM & Hunter T (2007) Rapid activation of ATM on DNA flanking double-strand breaks. *Nat Cell Biol* 9: 1311-8
- You Z, Chahwan C, Bailis J, Hunter T & Russell P (2005) ATM activation and its recruitment to damaged DNA require binding to the C terminus of Nbs1. *Molecular and cellular biology* 25: 5363-79
- Zhang J, Dewar JM, Budzowska M, Motnenko A, Cohn MA & Walter JC (2015) DNA interstrand cross-link repair requires replication-fork convergence. *Nature structural & molecular biology* 22: 242-7
- Zhu S & Peng A (2016) Non-homologous end joining repair in Xenopus egg extract. *Scientific reports* 6: 27797



Chapter 3

Recruitment and positioning determine the specific role of XPF-ERCC1 in ICL repair

Daisy Klein Douwel, Wouter S. Hoogenboom, Rick A.C.M. Boonen[†] and Puck Knipscheer^{*}

Hubrecht Institute - KNAW, University Medical Center Utrecht & Cancer Genomics Netherlands, The Netherlands

[†]) Present address: Department of Human Genetics, Leiden University Medical Center, Leiden, The Netherlands

^{*}Corresponding author. Tel: +31 302121800; E-mail: p.knipscheer@hubrecht.eu

Abstract

XPF-ERCC1 is a structure specific endonuclease pivotal for several DNA repair pathways and, when mutated, can cause multiple diseases. Although the disease-specific mutations are thought to affect different DNA repair pathways, the molecular basis for this is unknown. Here we examine the function of XPF-ERCC1 in DNA interstrand crosslink (ICL) repair. We used *Xenopus* egg extracts to measure both ICL and nucleotide excision repair, and we identified mutations that are specifically defective in ICL repair. One of these separation of function mutations resides in the helicase-like domain of XPF and disrupts binding to SLX4 and recruitment to the ICL. A small deletion in the same domain supports recruitment of XPF to the ICL, but inhibited the unhooking incisions most likely by disrupting a second, transient interaction with SLX4. Finally, mutation of residues in the nuclease domain did not affect localization of XPF-ERCC1 to the ICL but did prevent incisions on the ICL substrate. Our data supports a model in which the ICL repair specific function of XPF-ERCC1 is dependent on recruitment, positioning and substrate recognition.

Introduction

The structure-specific endonuclease XPF-ERCC1 participates in multiple genome maintenance pathways, including nucleotide excision repair (NER), DNA interstrand crosslink (ICL) repair, certain branches of double stranded break (DSB) repair and telomere maintenance. Mutations in XPF-ERCC1 have been associated with the genetic disorders Xeroderma pigmentosum (XP), Cockayne syndrome (CS), Cerebro-Oculo-Facio-Skeletal Syndrome (COFS), Fanconi Anemia (FA) and premature aging. These phenotypes are believed to be caused by a defect in one, or several, of the genome maintenance pathways XPF-ERCC1 is involved in, but the molecular basis for this is unknown.

XPF is a 3' flap endonuclease that contains an N-terminal helicase-like domain, a central ERCC4-type nuclease domain, and a C-terminal helix-hairpin-helix (HhH) domain with which it interacts with its cofactor ERCC1 (Fig 1A). Very little is known about the role of the helicase-like domain, but it is important for nuclease activity (Bowles *et al.*, 2012). The function of XPF-ERCC1 in NER, a pathway that removes helix distorting lesions, has been extensively studied (Friedberg, 2011, Gillet & Schärer, 2006). After damage recognition by upstream NER factors, XPF-ERCC1 is recruited to the lesion by XPA and excises a short oligo containing the damage in collaboration with another nuclease XPG. (Huang *et al.*, 1992, Li *et al.*, 1995, Spivak, 2015). Defects in NER factors are associated with the genetic disease Xeroderma pigmentosum (XP), which is characterized by sun light sensitivity and skin cancer predisposition. Uniquely among NER factors, deficiency in XPF-ERCC1 not only causes UV sensitivity, but also results in hypersensitivity to ICL-inducing agents, indicating an additional role for this protein in the repair of interstrand crosslinks (De Silva *et al.*, 2000, Kuraoka *et al.*, 2000, Niedernhofer *et al.*, 2004).

ICLs are toxic DNA lesions that covalently link both strands of the DNA together, thereby blocking DNA replication and transcription. ICLs are formed endogenously by products of cellular metabolism, but are also induced at high doses by certain chemotherapeutic drugs. The major pathway of ICL repair is coupled to DNA replication and involves the coordinated action of many DNA repair proteins including the Fanconi anemia (FA) pathway proteins. Mutations in any of the 21 currently known FA genes give rise to Fanconi anemia (FA), a cancer-susceptibility disorder characterized by cellular sensitivity to ICL-inducing agents (Dong *et al.*, 2015, Kottemann & Smogorzewska, 2013). Using a *Xenopus* egg extract based assay we and others have recently elucidated a molecular mechanism of replication-coupled ICL repair (Fig EV1) (Räschle *et al.*, 2008). This mechanism requires the convergence of two replication forks at an ICL during DNA replication (Zhang *et al.*, 2015). Both forks initially stall 20 to 40 nucleotides from the crosslink followed by CMG helicase unloading allowing one fork to approach to within 1 nucleotide of the crosslink (Fu *et al.*, 2011, Long *et al.*, 2011, Räschle *et al.*, 2008). Dual incisions on either side of the ICL then unhook the lesion from one of the strands. This critical repair step requires the endonuclease XPF(FANCD1)-ERCC1, which is recruited to the ICL by the large scaffold protein SLX4(FANCD2), and depends on the activation of the Fanconi anemia pathway by ubiquitylation of the FANCI-FANCD2 complex (Klein Douwel *et al.*, 2014, Knipscheer *et al.*, 2009). After unhooking, a nucleotide is inserted across from the adducted base, followed by strand extension by REV1 and polymerase ζ , consisting of REV7/FANCV and REV3 (Budzowska *et al.*, 2015, Mamrak *et al.*, 2017, Räschle *et al.*, 2008). This strand now acts as a template for repair of the opposite strand by HR (Long *et al.*, 2011), leading to fully repaired products.

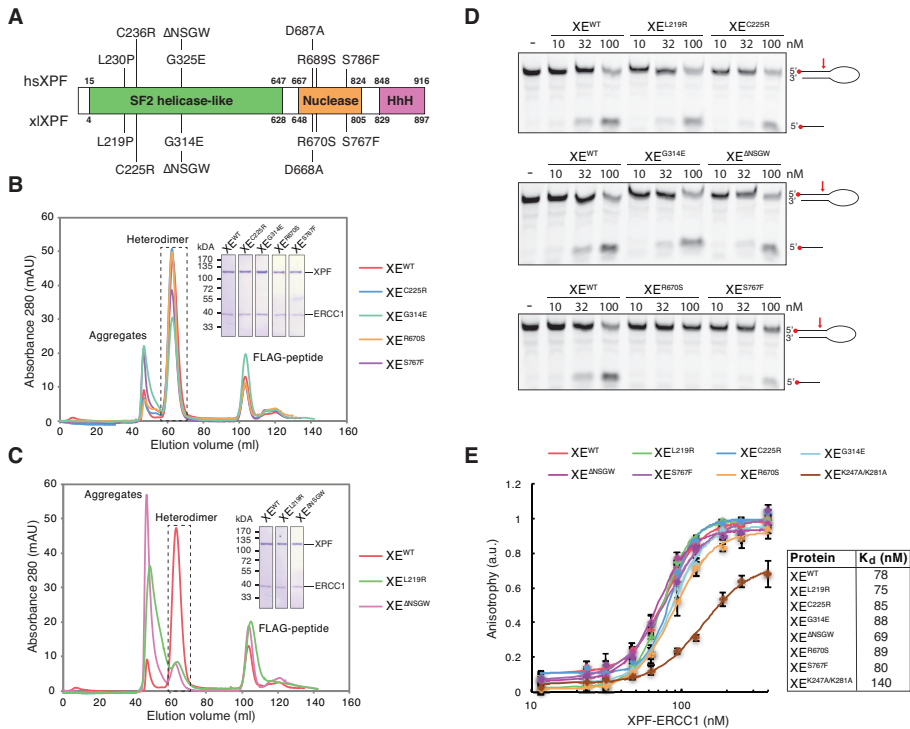


Figure 1: Characterization of mutant XPF-ERCC1 complexes. A) Schematic representation of the domain organization of the XPF protein. Domain boundaries of human and *Xenopus laevis* XPF are indicated. Relevant mutations of the human protein, and the *Xenopus laevis* equivalents, are indicated on top and bottom respectively. B) Superdex 200 gel filtration column elution profile of wild type XPF-ERCC1 and indicated mutant complexes. Aggregates eluted in the void volume of the column (~45ml) while the active XPF-ERCC1 heterodimer eluted at ~65 ml. The peak eluting at ~105 ml contains the FLAG peptide used to elute the protein from the FLAG affinity resin. The heterodimer peak was isolated, proteins were separated on SDS PAGE and stained with Coomassie blue (inset). C) As in (B) but for different mutant complexes that showed more aggregation. D) Wild type and indicated mutant XPF-ERCC1 complexes were incubated with a 5'-FAM-labeled stem-loop DNA substrate (10 nM) at room temperature for 30 minutes. Reaction products were separated on a 12% urea PAGE gel and visualized using a fluorescence imaging system. E) Wild type and mutant XPF-ERCC1 complexes at various concentrations were incubated with a 5'-FAM labeled 3' flap DNA substrate (10 nM) and fluorescent anisotropy was measured. Graphs were fitted to calculate dissociation constants (K_d's) as described in the method section. The error bars represent s.d. from three measurements. Experimental replicates are shown in Fig EV2.

Patient phenotypes linked to specific XPF mutations can be extremely valuable in determining pathway specific functions. Most patients with a mutation in XPF suffer from a mild form of XP and are deficient in NER. These patients express residual protein and are likely proficient in ICL repair, because they do not show features of FA (Ahmad *et al.*, 2010). In some cases, XPF mutations can lead to much more severe phenotypes. An extreme progeroid syndrome was caused by a mutation in the helicase-like domain of XPF (R153P). This patient suffered from neurological and hematological defects and a cellular sensitivity to UV and ICLs indicating both NER and ICL repair were defective (Niedernhofer *et al.*, 2006). Another patient, with a mutation in the same XPF domain (C236R), presented with phenotypes of XP, but also of CS, such as developmental and neurological abnormalities

(Kashiyama *et al.*, 2013). This patient also showed FA-like features and ICL sensitivity suggestive of a defect in ICL repair. In addition, some patients with specific mutations in XPF were diagnosed with Fanconi anemia and showed no signs of XP (Bogliolo *et al.*, 2013). These mutations were mapped to the helicase-like domain (L230P), and the nuclease domain (R689S) of XPF.

To examine what features of XPF-ERCC1 determine its specificity in ICL repair we employed the *Xenopus* egg extract system. We monitored both replication-coupled ICL repair and nucleotide excision repair and identified five XPF mutants that are deficient in ICL repair and proficient in NER. Although all of these mutants showed a defect in ICL unhooking, the majority was still efficiently recruited to the ICL. In contrast, mutation of xXPF leucine 219, equivalent to the human leucine 230 mutated in Fanconi anemia, abrogated this ICL localization. This was caused by a defect in interaction with SLX4. We propose there are two interaction sites between XPF and SLX4, one ensuring recruitment of XPF to the ICL, and another to promote its nuclease activity. This dual interaction site, in combination with residues in the nuclease domain ensuring substrate specificity, dictate the ICL repair specific function of XPF-ERCC1.

Results

XPF mutants form functional complexes with ERCC1.

To study the role of XPF-ERCC1 in ICL repair, we selected a set of XPF mutations that we predicted to specifically affect this process. In the helicase-like domain, two point mutations were found in patients with FA and FA-like symptoms, L230P and C236R (Bogliolo *et al.*, 2013, Kashiyama *et al.*, 2013). These mutated residues correspond to residues L219 and C225 in *Xenopus laevis* XPF, that is 75% identical to human XPF (Fig 1A). Another mutation in XPF's helicase-like domain, *hsG325E* (*x/G314E*), was reported to disrupt the interaction of XPF with the BTB domain of SLX4 (Andersen *et al.*, 2009). This interaction is likely specific to ICL repair and not NER because SLX4 deficient cells are not UV sensitive (Crossan *et al.*, 2011). With the aim to further disrupt this interaction, we generated a deletion mutant lacking G314 and three surrounding residues that were predicted to form a loop (XPF^{ΔNSGW}). Finally, in the nuclease domain, we analyzed 2 mutations, R689S and S786F (*x/R670S* and *x/S676F*). The R689S mutation was associated with Fanconi anemia (Bogliolo *et al.*, 2013) and the S786F mutation sensitizes cells to MMC, but not UV radiation (Osorio *et al.*, 2013).

We co-expressed flag-tagged xXPF wild type and mutants with His-tagged *hsERCC1* in Sf9 insect cells and purified the complex by affinity purification. We previously showed that the xXPF-*hsERCC1* complex (referred to as XPF-ERCC1 from here on) supports ICL-repair in *Xenopus* egg extracts (Klein Douwel *et al.*, 2014). Expression levels of all mutant complexes were similar to wild type levels except for the XPF^{L219P}-ERCC1 (XE^{L219P}) complex that was previously reported to be unstable (Bogliolo *et al.*, 2013, Hashimoto *et al.*, 2015). To examine the function of leucine 219, we instead mutated it to an arginine and found that XE^{L219R} was expressed at normal levels. When wild type XPF-ERCC1 was subjected to gel filtration chromatography, the majority of the protein eluted at the expected range for a heterodimer while a small fraction of inactive aggregates eluted in the void volume of the column, similar to what was previously described (Fig 1B) (Enzlin & Scharer, 2002). The XE^{C225R}, XE^{G314E}, XE^{R670S} and XE^{S767F} mutant complexes behaved similarly to the wild type on gel filtration (Fig 1B) and the peak containing the heterodimer was isolated and used

for further experiments. However, the XE^{L219R} and XE^{ΔNSGW} mutant complexes showed an increased aggregate peak and lower heterodimer peak (Fig 1C). Nevertheless, when this heterodimer peak was isolated and re-run on a gel filtration column it did not aggregate (Fig EV2A).

We next examined the endonuclease activity of the mutant XPF-ERCC1 complexes. To this end, a fluorescently labeled stem loop substrate was incubated with increasing concentrations of protein, and reaction products were separated by denaturing urea PAGE. All XPF-ERCC1 complexes with mutations in the helicase-like domain showed nuclease activity similar to wild type protein, as seen by the appearance of the incision product (Fig 1D, top two panels, and Fig EV2B). Importantly, this demonstrates that the XE^{L219R} and XE^{ΔNSGW} complexes, that showed increased aggregation upon expression, are fully active after isolation of the heterodimer peak. The XE^{S767F} complex was slightly reduced in nuclease activity while the XE^{R670S} complex showed a more dramatic reduction and was only capable of cutting the substrate at high concentrations (Fig 1D and Fig EV2D). This was not surprising as both mutations are located in the nuclease domain of XPF, and the human equivalent of the R670S mutant has decreased nuclease activity (Enzlin & Scharer, 2002, Su *et al.*, 2012). We also analyzed the endonuclease activity on a 3' flap substrate and obtained similar results (Fig EV2C). In conclusion, all mutants except R670S have nuclease activity similar to wild type protein.

Finally, we analyzed the DNA binding of the mutant XPF-ERCC1 complexes. For this, a fluorescently labeled 3' flap substrate was incubated with increasing concentrations of XPF-ERCC1 and fluorescence anisotropy was measured to assess binding. All our mutants showed very similar binding curves and the K_d values derived from these curves were comparable to each other and to wild type XPF-ERCC1 (Fig 1E and Fig EV2E). This indicates that the mutations do not affect DNA binding affinity. To validate our results we measured fluorescence anisotropy of a mutant XPF-ERCC1 carrying two point mutations in ERCC1 (K247A and K281A) that were previously shown to affect DNA binding (Su *et al.*, 2012). Consistent with this, we found that this XE^{KAKA} mutant had reduced affinity for DNA (Fig 1E and Fig EV2E).

In summary, we purified six mutant XPF-ERCC1 complexes that are predicted to affect ICL repair. All mutant complexes form stable heterodimers and interact normally with DNA. The nuclease activity of the mutants is similar to wild type, with the exception of one mutation in the nuclease domain.

Mutations in the helicase-like and the nuclease domains abrogate ICL repair.

To investigate the effect of the XPF mutations on ICL repair, we used *Xenopus* egg extract. This system recapitulates DNA replication-coupled repair of a sequence-specific cisplatin ICL situated on a plasmid template (pICL) (Räschle *et al.*, 2008). Moreover, it enables the quantification of repair by the regeneration of a Sapl restriction site that is blocked by the crosslink (Fig 2A). We immuno-depleted ERCC1 from egg extract and complemented the repair reaction with wild type or mutant XPF-ERCC1. Since depletion of ERCC1 leads to equal depletion of XPF (Klein Douwel *et al.*, 2014), we refer to this depletion as an XPF-ERCC1 depletion. Because depletion of XPF-ERCC1 leads to co-depletion of SLX4, we also complemented all the depleted reactions with purified xSLX4 protein unless stated otherwise (Fig EV3A) (Klein Douwel *et al.*, 2014). Reactions were stopped at various time points, DNA repair intermediates were isolated, and digested with Sapl to quantify ICL

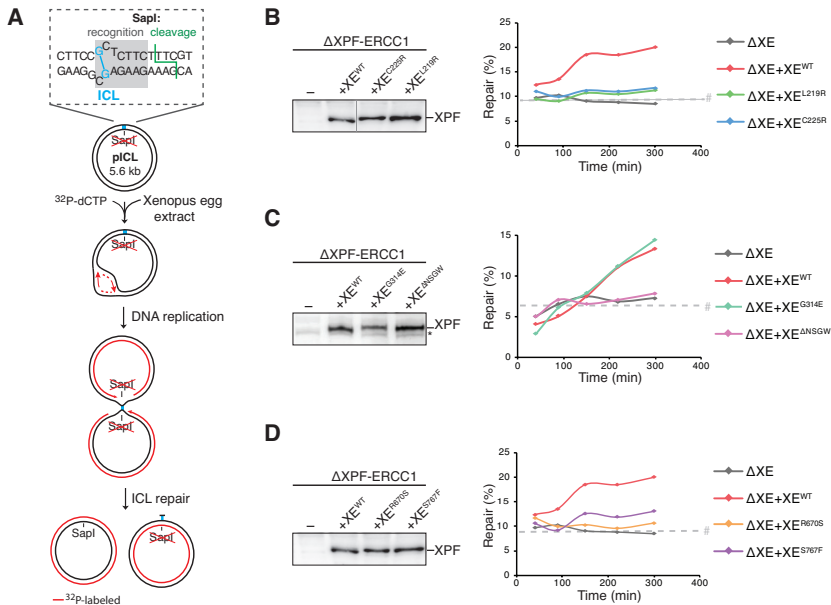


Figure 2: Effect of mutations in XPF-ERCC1 on ICL repair in *Xenopus* egg extract. A) Schematic representation of repair of a plasmid containing a site-specific cisplatin ICL (pICL) in *Xenopus* egg extract. The SapI site that is blocked by the ICL becomes available on one of the replicated molecules after full repair via HR using the sister molecule (Fig EV1). The sister molecule is repaired by lesion bypass, but retains the unhooked ICL that is not removed efficiently in *Xenopus* egg extract (Räschle *et al.*, 2008). B) XPF-ERCC1-depleted (ΔXE) and XPF-ERCC1-depleted extracts complemented with wild type (XE^{WT}) or indicated mutant XPF-ERCC1 (XE^{MUT}) were analyzed by western blot using α-XPF antibodies (left panel). Line within blot indicates position where irrelevant lanes were removed. These extracts were used to replicate pICL. Replication intermediates were isolated and digested with HincII, or HincII and SapI, and separated on agarose gel. Repair efficiency, represented by SapI regeneration, was calculated as described (Räschle *et al.*, 2008) and plotted (right panel). C) and D) As in (B) but analyzing different XPF-ERCC1 mutant complexes. Experimental replicates are shown in Fig EV3. Note: repair levels can differ per batch of individually prepared extract or per depletion experiment and can only be compared within an experiment. #, SapI fragments from contaminating uncrosslinked plasmid present in varying degrees in pICL preparations. *, background band.

repair. A small fraction of non-crosslinked plasmids is present in pICL preparations leading to a constant background of SapI digestible replication products. XPF-ERCC1 depleted extracts did not support ICL repair above this background while addition of recombinant wild type XPF-ERCC1 (XE^{WT}) restored ICL repair (Fig 2B, C and D) (Klein Douwel *et al.*, 2014). XE^{L219R} and XE^{C225R}, which carry mutations in the helicase-like domain of XPF, did not efficiently rescue ICL repair (Fig 2B and Fig EV3B). We then tested the other two helicase-like domain mutants, that were expected to affect the interaction with the BTB domain of SLX4. While addition of XE^{G314E} to XPF-ERCC1 depleted extract supported ICL repair, the deletion mutant XE^{ΔNSGW} was defective in ICL repair (Fig 2C and Fig EV3C). This suggests that this region is important for ICL repair, likely through mediating interaction with SLX4. Finally, XPF-ERCC1 depleted extracts were supplemented with the nuclease domain mutants XE^{R670S} and XE^{S767F}. Both mutants were unable to restore ICL-repair (Fig 2D and Fig EV3B). These results show that specific residues in the helicase-like domain and the nuclease domain of XPF-ERCC1 are required for ICL repair.

ICL repair deficient XPF mutants are proficient in NER.

To determine whether the XPF mutations specifically affect ICL repair, we investigated their activity in nucleotide excision repair (NER). During NER, the endonucleases XPF-ERCC1 and XPG make incisions on either side of a lesion, creating a gap that is subsequently filled in. This gap-filling DNA synthesis is called unscheduled DNA synthesis (UDS) to differentiate it from the semi-conservative DNA synthesis that takes place during replication. UDS can be measured on UV-damaged plasmids incubated in a high speed supernatant *Xenopus* egg extract and used as a readout for NER activity (Fig 3A) (Gaillard *et al.*, 1996, Shivji *et al.*, 1994). To this end, we incubated non-damaged or UV-damaged plasmid in a non-replicating *Xenopus* egg extract in the presence of ^{32}P -dCTP. The DNA was subsequently isolated, linearized, and the products were separated on an agarose gel (Fig 3B). While a UV damaged plasmid showed clear incorporation of ^{32}P -dCTP indicative of UDS, a non-damaged plasmid only showed some background incorporation, probably due to nicks created during plasmid preparation (Fig 3B, lane 1 and 2). To confirm that the UDS on the UV damaged template is a result of the repair, we directly monitored cyclobutane pyrimidine dimers and showed that *Xenopus* egg extract is capable of removing these lesions (Fig EV4C). To further validate that the unscheduled DNA synthesis is caused by NER, we showed that UDS is strongly reduced after depletion of NER factors PCNA as well as XPA (Fig EV4D and E). In addition, we found that immunodepletion of XPF (Fig EV4A) strongly reduced UV-dependent UDS (Fig 3B, compare lane 2 and 4, and Fig 3C). The slight increase in UDS compared to the non-damaged plasmid is likely caused by an incomplete depletion of XPF-ERCC1 or other repair mechanisms present in the extract. Addition of wild type XPF-ERCC1 (XE^{WT}) to XPF-depleted extracts fully rescued UDS, while addition of a catalytically inactive XE^{D668A} mutant did not support UDS (Fig 3B, compare lane 5

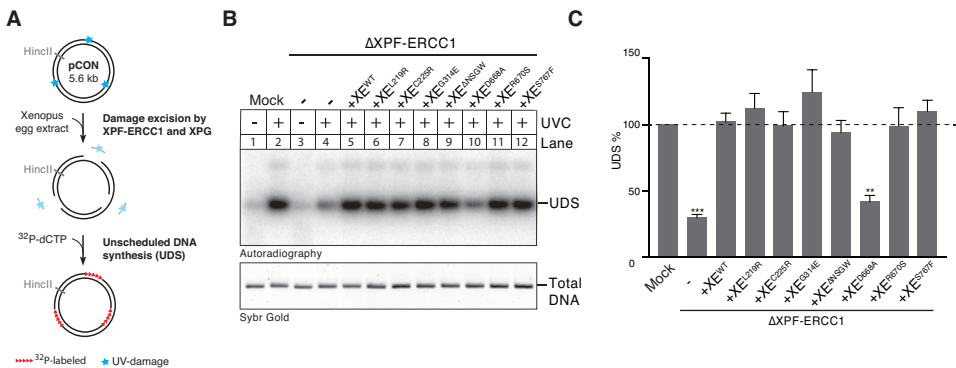


Figure 3: XPF-ERCC1 mutant complexes are active in nucleotide excision repair (NER). A) Schematic representation of unscheduled DNA synthesis (UDS) during NER on a UV treated template in high speed supernatant (HSS) egg extract. B) Mock depleted, XPF-ERCC1-depleted (ΔXE), and XPF-ERCC1-depleted extracts complemented with wild type (XE^{WT}) or mutant XPF-ERCC1 (XE^{MUT}) were incubated with untreated or UV-treated plasmids for 2 hours at room temperature in presence of ^{32}P - α -dCTP. Reaction products were isolated, linearized with *Hinc*II and separated on a 0.8% agarose gel. The DNA was visualized by autoradiography to show incorporation of ^{32}P - α -dCTP during UDS (upper panel) and stained with SYBR gold for total DNA (lower panel). C) The incorporation of ^{32}P - α -dCTP was quantified, the background signal from non-damaged plasmid was subtracted and the signal for the mock depletion condition was set to 100% to normalize the data. Error bars represent s.e.m of three independent experiments. **, $p=0.003$ ***, $p=0.0004$, paired *t*-test comparing all condition to the mock. All non-marked conditions did not show a statistical difference from the mock condition.

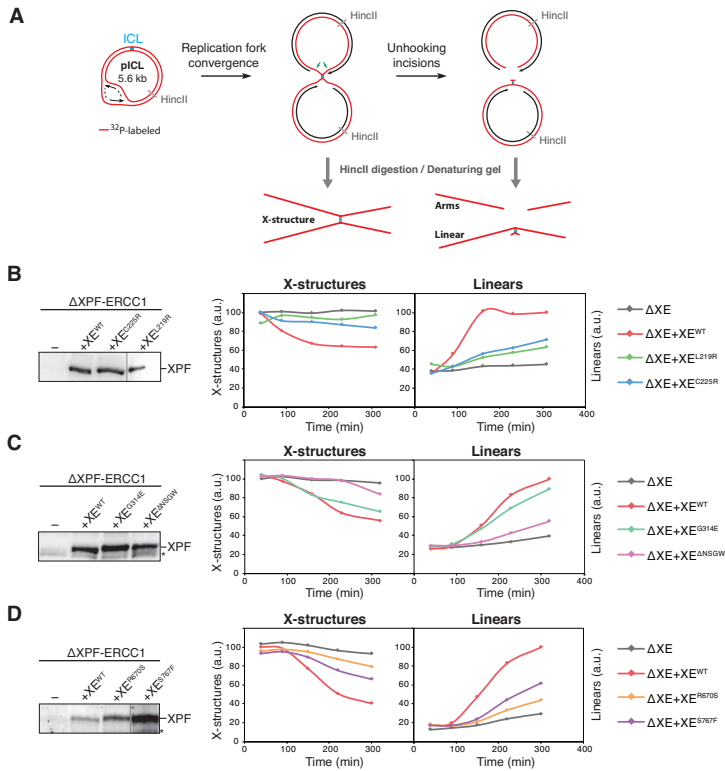


Figure 4: XPF-ERCC1 separation of function mutants are all defective in ICL unhooking. A) Schematic representation of the assay used to directly measure unhooking incisions. ³²P-labeled parental stands are indicated in red. Products before and after ICL unhooking during repair are indicated. HincII digestion of repair intermediates yield X-structures, arms and linears under denaturing conditions. B) XPF-ERCC1-depleted (Δ XE) or XPF-ERCC1-depleted egg extract complemented with wild type (XE^{WT}) or mutant XPF-ERCC1 (XE^{MUT}) were incubated with pre-labeled pICL. Repair products were isolated at indicated times, linearized with HincII, separated on a denaturing agarose gel, and visualized by autoradiography. The X-structures and linear products were quantified and plotted (right panel). The extracts used were analyzed by western blot using α -XPF antibodies to verify depletion and the levels of added recombinant protein (left panel). C) and D) As in (B) but using different XPF-ERCC1 mutant complexes. Experimental replicates are shown in Appendix Fig S1. Line within blot indicates position where irrelevant lanes were removed. *, background band.

and 10, Fig 3C and EV4B). This shows that XPF-ERCC1 is required for UDS in *Xenopus* egg extract. We then complemented an XPF-ERCC1 depleted extract with the XPF-ERCC1 mutants and found that all mutants were able to rescue the NER defect (Fig 3B and C). This observation was especially striking for the XE^{R670S} mutant whose nuclease activity on model DNA templates was strongly reduced (Figure 1D). This finding is consistent with a previous report in which the human equivalent of this mutant was able to make NER incisions, although there was a difference in the position of the incisions compared to the wild type protein (Su *et al.*, 2012).

In summary, we identified 3 mutations in the helicase-like domain (XE^{L219R}, XE^{C225R} and XE^{ANS5GW}) and two in the nuclease domain (XE^{R670S} and XE^{S767F}) that are defective in ICL repair, while supporting functional NER. Strikingly, this separation of function is achieved by mutations in two different domains of XPF-ERCC1.

Separation of function mutations in XPF specifically affect ICL incisions

To determine the mechanism underlying the specific inhibition of ICL repair in these mutants, we examined which step in ICL repair was affected. We previously showed that XPF is required for ICL unhooking (Klein Douwel *et al.*, 2014). However, XPF could also have additional roles downstream, for example in HR, that might be affected by our mutations (Bergstrahl & Sekelsky, 2008). To directly monitor unhooking incisions that take place on the parental strand, we pre-labeled pICL with ^{32}P -dCTP using nick translation and replicated it in *Xenopus* egg extract. Replication intermediates were linearized and separated on a denaturing agarose gel. At early times, the parental strand migrates as a large X-structure, while after crosslink unhooking during repair, it is converted to a linear molecule and arms (Fig 4A; and Knipscheer *et al.*, 2009). The decline of the X-shaped structures and the accumulation of the linears are a direct readout of unhooking incisions. In XPF-ERCC1 depleted extract, the X-structures persists (Fig 4B-D, left panel, and Appendix Fig S1), and the appearance of linear structures is greatly reduced (Fig 4B-D, right panel, and Appendix Fig S1), indicating the unhooking incisions are blocked (see also Klein Douwel *et al.*, 2014). Addition of wild type XPF-ERCC1 (XE^{WT}) rescues this incision defect (Fig 4B, C and D, left panel and Appendix Fig S1) whereas the helicase-like domain mutants XE^{L219R} or XE^{C225R} did not (Fig 4B and Appendix Fig S1). The XE^{G314E} mutant did not inhibit incisions, while the $\text{XE}^{\text{ANS5GW}}$ mutant caused a strong reduction in ICL unhooking (Fig 4C and Appendix Fig S1). This is consistent with our earlier observation that the point mutant is functional in ICL repair while the deletion mutant is not. Finally, we found that the nuclease domain mutants XE^{R670S} and XE^{S767F} were unable to support efficient incisions (Fig 4D and Appendix Fig S1). These results show that all our separation of function mutants are defective in ICL unhooking, which explains their inability to support ICL repair.

The $\text{XPF}^{\text{L219R}}$ -ERCC1 mutant complex is not recruited to the ICL

A possible explanation for why our mutants were not able to support ICL unhooking is that they are not recruited to the site of damage. To test this, we examined XPF recruitment by chromatin immunoprecipitation (ChIP). We replicated pICL in extract depleted of XPF-ERCC1 and supplemented with wild type or mutant XPF-ERCC1 (Appendix Fig S2A), and performed chromatin immunoprecipitation with XPF antibodies at various time points. An unrelated plasmid (pQuant) was added to the reaction to determine background protein recruitment to undamaged DNA. The co-precipitated DNA was recovered and amplified by quantitative PCR with primers specific to the ICL region or to pQuant (Fig 5A). Using this assay, we recently showed that XPF is specifically recruited to the ICL at the time of unhooking incisions (Klein Douwel *et al.*, 2014). The exact timing of recruitment can vary as a result of the immunodepletion procedure. We first examined the most N-terminal mutant XE^{L219R} and found that, in contrast to the wild type protein, recruitment of this mutant to the ICL was completely blocked (Fig 5B). In contrast, the XE^{C225R} complex, containing a mutation just six residues further downstream, was recruited to the ICL as efficiently as the wild type protein (Fig 5C and Appendix Fig S2B). We then examined the $\text{XE}^{\text{ANS5GW}}$ mutant and found that it was recruited normally to the ICL (Fig 5D and Appendix Fig S2C). This is striking, because this region was shown to be important for the interaction between XPF and SLX4 (Andersen *et al.*, 2009) and we have previously shown that SLX4 is important for the recruitment of XPF to the ICL. Lastly, we examined the recruitment of the nuclease domain mutants XE^{R670S} and XE^{S767F} . Both mutants were recruited to the ICL as

efficiently as the wild type protein (Fig 5E and F and Fig S6D).

We conclude that all mutants, except for XE^{L219R}, are recruited normally to the site of damage, suggesting the defect in incisions observed for these mutants is due to a defect in proper positioning of the nuclease within the repair complex.

XPF lysine 219 is part of the major binding site between XPF and SLX4

To determine why XE^{L219R} is not recruited to the ICL we examined recruitment of both SLX4 and XPF to the ICL by ChIP. When we supplemented an XPF-ERCC1 depleted reaction with XPF-ERCC1 only, and not SLX4, XPF was not recruited to the ICL (Fig 6A and Fig EVA-C; and (Klein Douwel *et al.*, 2014)). Supplemented SLX4 bound to the ICL and rescued the recruitment of wild type XPF-ERCC1 (Fig 6A and Fig EV5A-C), but not of the XE^{L219R} mutant complex (Fig 6A and Fig EV5A-C). These results show that a single point mutations can abrogate XPF recruitment and strongly suggest that this is caused by a defect in the direct interaction with SLX4.

To confirm this, we co-expressed FLAG-tagged XE^{WT} and XE^{L219R} with His-tagged SLX4 in Sf9 insect cells, immunoprecipitated XPF, and examined co-precipitation of SLX4. His-SLX4 was enriched after immunoprecipitation of wild type XPF-ERCC1, but not XPF^{L219R}-ERCC1, indicating this mutant does not bind SLX4 (Fig 6B and Fig EV5D). These findings indicate that XPF's leucine 219 is essential for the interaction between XPF and SLX4 and therefore required for the recruitment of XPF to the site of damage.

Two domains in SLX4 have been implicated in the interaction between SLX4 and

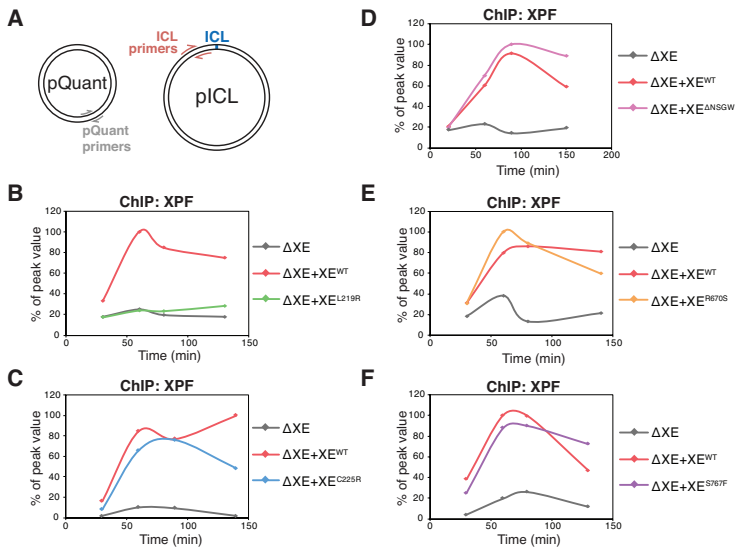


Figure 5: Recruitment of XPF-ERCC1 mutants to the ICL during repair. A) Schematic representation showing the primer locations on pICL and pQuant. B) pICL was replicated in XPF-ERCC1 depleted (Δ XE) or XPF-ERCC1-depleted egg extract supplemented with wild type (XE^{WT}) or mutant XPF-ERCC1 (XE^{MUT}) (See Appendix Fig S2). Samples were taken at various times and immunoprecipitated with α -XPF antibodies. Co-precipitated DNA was isolated and analyzed by quantitative PCR using the primers depicted in (A). The qPCR data was plotted as the percentage of peak value with the highest value within one experiment set to 100%. C)- F) As in (B) but using the indicated XPF-ERCC1 mutant complexes. Experimental replicates are shown in Appendix Fig S2.

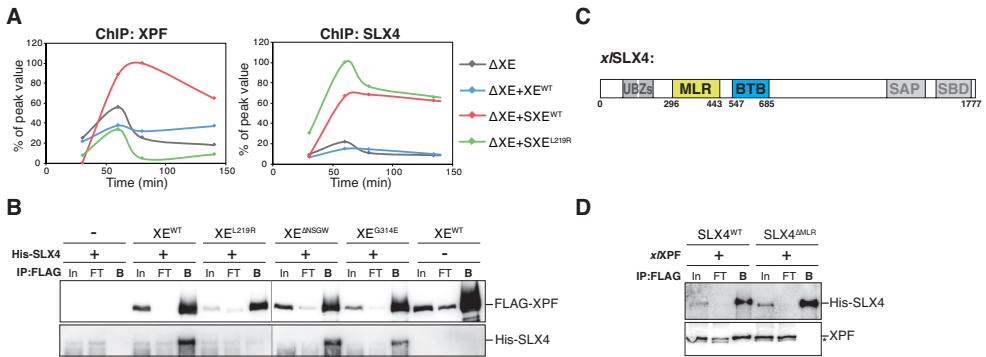


Figure 6: XPF leucine 219 is part of the major interaction site between XPF and SLX4. A) pICL was replicated in XPF-ERCC1 depleted (Δ XE) extract or in XPF-ERCC1 depleted extract supplemented with wild type XPF-ERCC1 only (+X^{WT}), wild type XPF-ERCC1 and SLX4 (+SX^{WT}), or XPF^{L219R}-ERCC1 and SLX4 (+SX^{E^{L219R}}) (See Fig EV5A). Samples were taken at the indicated times and immunoprecipitated with α -XPF (left panel) or α -SLX4 antibodies (right panel). Co-precipitated DNA was isolated and analyzed by quantitative PCR using ICL or pQuant primers. The qPCR data was plotted as the percentage of peak value with the highest value set to 100%. B) Wild type and mutant FLAG-XPF-ERCC1 were co-expressed with His-SLX4 in Sf9 insect cells. Cells were lysed and XPF was immunoprecipitated via the FLAG-tag. Samples were analyzed by western blot using α -FLAG and α -His antibodies. In is input, FT is flow through fraction, B is fraction bound to beads. C) Schematic representation of x/SLX4 proteins, with the MLR and BTB domains indicated. Experimental replicates are shown in Appendix Fig EV5. D) Purified wild type FLAG-SLX4 and FLAG-SLX4^{ΔMLR} were added to *Xenopus* egg extract. SLX4 was immunoprecipitated via the FLAG-tag. Samples were analyzed by western blot using α -FLAG and α -XPF antibodies. Line within blot indicates position where irrelevant lanes were removed. *, background band.

XPF. The previously mentioned BTB domain and the MUS312/MEI9 interaction-like, or MLR, domain (Fig 6C) (Fekairi *et al.*, 2009, Kim *et al.*, 2013). To further investigate the importance of the MLR domain for the interaction with XPF we purified x/SLX^{WT} and x/SLX4^{ΔMLR}. In contrast to wild type SLX4, the Δ MLR mutant was not able to bind XPF from *Xenopus* egg extract (Figure 6D). This shows that the MLR domain of SLX4 acts as the major interaction site with XPF, which is in line with previous reports in human cells (Kim *et al.*, 2013). Based on our data this domain most likely interacts with leucine 219 of XPF.

Finally, we set out to examine the role of the interaction between the SLX4 BTB domain and XPF. The *hs*G325E mutation in XPF abrogates the interaction between XPF and the BTB domain of SLX4 (Andersen *et al.*, 2009). We found that the XE^{G314E} and XE^{ΔNSGW} mutants were both able to interact normally with full length SLX4 (Fig 6B and Fig EV5D). This is consistent with previous reports showing that the BTB domain is not essential for SLX4 and XPF interaction (Guervilly *et al.*, 2015, Kim *et al.*, 2013). One explanation for these observations is that this interaction is transient and can only be observed in absence of the major interaction site involving the MLR domain. To be able to study this we cloned and purified the SLX4 BTB domain alone and examined the interaction with XPF using size exclusion chromatography. However, even using an excess of BTB domain protein we did not observe an interaction with XPF-ERCC1 (Fig EV5E). This indicates that this is not a high affinity interaction site.

These findings, together with previous reports, support a model in which XPF and SLX4 interact through two binding sites (Figure 7). The first consists of the MLR domain of SLX4 and XPF leucine 219, and possibly a region around this residue. This is a high

affinity binding site that is responsible for the recruitment of XPF via SLX4 to ICLs. The second comprises the BTB domain of SLX4 and residues 312 to 315 of XPF. This interaction is transient, but important to promote nuclease activity of XPF possibly by orienting it properly.

Discussion

Mutations in XPF-ERCC1 affect several DNA repair pathways and can cause multiple diseases likely due to differential inhibition of these pathways. Using *Xenopus* egg extracts we have examined how certain mutations in XPF inhibit ICL repair, while maintaining proficient nucleotide excision repair. We have characterized five separation of function mutations that reside in the helicase-like and nuclease domains of XPF. While all these mutants are defective in ICL unhooking, this is caused by different mechanisms. The nuclease domain mutants are normally recruited to the ICL and most likely affect interactions with the DNA template or specific protein-protein interactions important for substrate recognition (Fig 7). The helicase-like domain mutants are part of a dual interaction site with SLX4. XPF's leucine 219 is part of a high affinity interaction site that interacts with the MLR domain of SLX4, while deletion of residue 312 to 315 of XPF disrupts a transient second interaction site with the BTB domain of SLX4 (Fig 7 and Table 1).

We have previously shown that XPF-ERCC1 is recruited to the site of damage by SLX4 (Klein Douwel *et al.*, 2014). A specific residue in the helicase-like domain of XPF has been implicated in the interaction with SLX4 (Andersen *et al.*, 2009, Yildiz *et al.*, 2002). A glycine to glutamic acid mutation at residue 325 of human XPF abrogated the interaction with SLX4 in a yeast two-hybrid assay (Andersen *et al.*, 2009). This yeast two-hybrid assay was performed with C-terminal deletion mutants of SLX4 and the interaction with XPF was pinpointed to the BTB domain. However, these mutants lacked the MLR domain which has also been implicated in the interaction with XPF (Kim *et al.*, 2013). In our hands, the equivalent mutation in *x*XPF, G314E, did not abrogate ICL repair or recruitment. Moreover, a deletion mutant in which this glycine and three additional residues around it were removed (XPF^{ΔNSGW}) interacted normally with SLX4. Based on these observations we suggest that the interaction site between the BTB domain of SLX4 and residues 312 to 315 of XPF is a minor interaction site. This is consistent with our data showing that the isolated BTB domain does not interact strongly with XPF and with results reported by Guervilly *et al.* that show only a slight decrease in XPF binding after mutation of the SLX4 BTB domain (Guervilly *et al.*, 2015). However, this interaction is important because the XPF^{ΔNSGW}-ERCC1 mutant is deficient in ICL unhooking and repair (Fig 2 and 4). Therefore we propose that this transient interaction site is important for activation

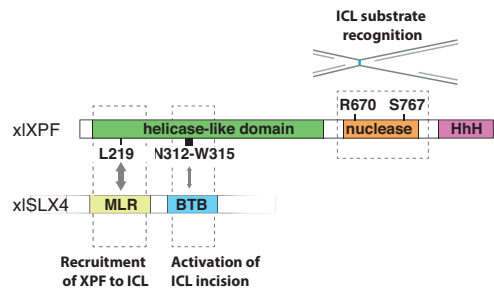


Figure 7: Model for ICL repair specific features of XPF. Lysine 219 in the helicase-like domain of XPF is essential for the interaction of XPF with the MLR domain of SLX4. This interaction mediates the recruitment of XPF to an ICL. Residues 312-315 transiently interact with the BTB domain of SLX4 and are required for the incisions of an ICL by XPF. Arginine 670 and Serine 767 in the nuclease domain of XPF are crucial for the recognition of the ICL substrate.

Table 1: Summary of features of XPF mutations.

<i>xI</i>	<i>hs</i>	Patient mutation	Clinical features	Nuclease activity	DNA binding	NER	ICL repair	Unhooking	Recruitment to ICL	SLX4 binding
XPF ^{L219R}	XPF ^{L230R}	L230P	FA	+	+	+	-	-	-	-
XPF ^{C225R}	XPF ^{C236R}	C236R	CS v CS/XP/FA	+	+	+	-	-	+	N.D.
XPF ^{G314E}	XPF ^{G325E}	N.A.	N.A.	+	+	+	+	+	N.D.	N.D.
XPF ^{ΔNSGW}	XPF ^{ΔNSGW}	N.A.	N.A.	+	+	+	-	-	+	+
XPF ^{R670S}	XPF ^{R689S}	R689S	FA	-	+	+	-	-	+	N.D.
XPF ^{S767F}	XPF ^{S786F}	N.A.	N.A.	+	+	+	-	-	+	N.D.

Abbreviations are as follows: +, normal; -, absent or defective; N.A., not applicable; N.D., not determined.

of XPF-ERCC1 by ensuring correct positioning onto its substrate. Interestingly, SLX4 has been shown to stimulate XPF-ERCC1 activity on model substrates (Hodskinson *et al.*, 2014) which could be mediated through this interaction. Although we can not exclude that this ICL repair defect of the XPF^{ΔNSGW}-ERCC1 mutant is caused by a different mechanism, the fact that this mutant completely overlaps with a previously identified interaction site strongly supports this explanation.

We and others have shown that the MLR domain of SLX4 is essential for the interaction with XPF (Fig 6 and (Kim *et al.*, 2013)), but it was not known which site on XPF was involved in this interaction. We now show that the XPF lysine 219 to arginine mutant is defective in binding to SLX4 indicating this is the site that interacts with the MLR domain. Further examination of the residues surrounding lysine 219 is required to better characterize this interaction site. Notably, our ChIP results indicate that the cysteine at position 225 is not required for the interaction. We further show that the XPF^{L219R}-ERCC1 mutant complex is defective in ICL repair but not in NER. This shows that the interaction with SLX4 is specific to the role of XPF-ERCC1 in ICL repair. This is consistent with the fact that patients with an L230P mutation suffer from FA and not XP. While previously it was assumed that poor stability of the XE^{L230P} protein was causing the FA phenotype, this data suggests that a functional defect, namely impaired interaction with SLX4, may cause, or contribute to, the disease.

Interestingly, the XPF^{C225R}-ERCC1 mutant does affect ICL recruitment but is still defective in ICL repair. Possibly this mutant does not prevent binding to SLX4, but does affect the interaction site in a way that it cannot properly position XPF for incisions. Two patients have been identified carrying the C236R (*xI*C225R) mutation, both show Cockayne syndrome (CS) phenotypes, while only one patient additionally shows a Fanconi anemia phenotype. The Cockayne syndrome phenotype is thought to be caused by a specific defect in transcription-coupled nucleotide excision repair (TC-NER). While mutations in XPF are not expected to specifically affect TC-NER, because it acts downstream in the NER pathway where the transcription-coupled and global NER pathways have come together, a CS phenotype has been observed previously in patients with mutations in XPF (Kashiyama *et al.*, 2013). Our data shows that the *xI*C225R mutation prevents ICL repair, but does not affect NER. However, *Xenopus* egg extracts are transcription incompetent and we may therefore not identify a defect in TC-NER. Why only one of the patients carrying the C236R mutation presents with a clear FA phenotype is currently unclear. Possibly the other patient has an additional mutation or specific genetic background that neutralizes the ICL repair defect.

In addition to the helicase-like domain mutants, we found two separation of function mutants in the nuclease domain of XPF. Arginine 670 is located within the active site of xXPF and mutating it to a serine severely reduces nuclease activity as was shown by us and others (Bogliolo *et al.*, 2013). Nevertheless, our data indicates that the XE^{R670S} mutant can still support NER to wild type levels. This is in line with previous data showing the human equivalent, hsXE^{R689A}, can incise an NER substrate (Enzlin & Scharer, 2002, Staresinic *et al.*, 2009, Su *et al.*, 2012). Interestingly, the human mutant protein did show a shift in incision position, suggesting the residue is not directly involved in catalysis, but contributes to the proper orientation of the active site onto the DNA substrate (Su *et al.*, 2012). This aberrant positioning is apparently not detrimental for NER but does prevent ICL repair in our assays. This is a likely explanation as the DNA template for incision differs in both repair pathways. Moreover, it is supported by the identification of a patient with the hsR689S mutation that suffers from FA, but not XP (Bogliolo *et al.*, 2013).

The S767F mutation is also located in the nuclease domain and structure predictions based on the crystal structure of the nuclease domain of archaeal XPF in complex with DNA, indicate it could be involved in protein-DNA interaction (Newman *et al.*, 2005). In our experiments this mutant shows a mild reduction in nuclease activity, is proficient in NER but largely deficient in ICL repair. We propose that, like the arginine 670, this residue is important in positioning the active site specifically on an ICL template likely by direct contact with the DNA. We did not observe reduced DNA binding affinity for these mutants most likely because XPF-ERCC1 contains multiple DNA interacting domains and it was shown that mutation of at least two of those is required to reduce this affinity (Su *et al.*, 2012).

XPF-ERCC1 is essential for the repair of ICLs induced by chemotherapy agents, such as derivatives of cisplatin and nitrogen mustards (Kirschner & Melton, 2010). Moreover, high expression of ERCC1 has been associated with poor response to chemotherapy in many cancers and could be a potential target to overcome resistance (McNeil & Melton, 2012). A better understanding of the ICL repair function of XPF-ERCC1 could potentially lead to the design of ICL-specific inhibitors that could be beneficial in cancer treatment.

Materials and Methods

Protein expression and purification

His-tagged hsERCC1 was cloned into pDONR201 (Life technologies). FLAG-tagged xXPF was cloned into pFastBac1 (Life technologies) and in pDONR201. The XPF mutations (L219R, C225R, G314E, ΔNSGW, R670S, D668A and S767F) and ERCC1 mutation (K247A/K281A) were introduced in pDONR-XPF using Quickchange site-directed mutagenesis protocol. Baculoviruses were produced using the BAC-to-BAC system (xXPF^{WT}), or the BaculoDirect system (hsERCC1 and xXPF^{MUTs}) following manufacturers protocol (Life Technologies). Proteins were expressed in suspension cultures of Sf9 insect cells by co-infection with His-hsERCC1 (or His-hsERCC1^{K247A/K281A}) and FLAG-xXPF (or FLAG-xXPF mutants) viruses for 72 hours. Cells from 750 ml culture were collected by centrifugation, resuspended in 30 ml lysis buffer (50mM K₂HPO₄ pH 8.0, 500mM NaCl, 0.1% NP-40, 10% glycerol, 0.4mM PMSF, 1 tablet/50ml Complete Mini EDTA-free Protease Inhibitor Cocktail (Roche), 10mM Imidazole) and lysed by sonication. The soluble fraction obtained after centrifugation (40.000 × g for 40 minutes at 4°C) was incubated for 1 hour at 4°C with 1 ml of Ni-NTA-agarose (Qiagen) that was pre-washed with lysis buffer. After incubation

the beads were washed using 50 ml of wash buffer (50mM K_2HPO_4 pH 8.0, 300mM NaCl, 0.1% NP-40, 10% glycerol, 0.1mM PMSF, 10 μ g/ml aproptin/leupeptin, 20mM Imidazole). The xXPF-hsERCC1 complex was eluted in elution buffer (50mM K_2HPO_4 pH 8.0, 300mM NaCl, 0.1% NP-40, 10% glycerol, 0.1mM PMSF, 10 μ g/ml aproptin/leupeptin, 250 mM Imidazole). The eluate was diluted with FLAG-wash buffer I (20mM K_2HPO_4 pH 8.0, 200mM NaCl, 0.1% NP-40, 10% glycerol, 0.4mM PMSF) and incubated for 1h at 4°C with 500 μ l of anti-FLAG M2 affinity gel (Sigma) that was pre-washed with FLAG wash buffer I. After incubation the beads were washed with 30 ml of FLAG-wash buffer I, and subsequently with 30 ml of GF buffer (25mM Hepes pH 8.0, 200mM NaCl, 10% Glycerol, 5mM β -mercaptoethanol). The xXPF-hsERCC1 complex was eluted in 3 ml of GF buffer containing 100 μ g/ml 3x FLAG peptide (Sigma). The protein was then loaded onto a HiLoad 16/600 Superdex 200pg gel-filtration column (GE Healthcare) equilibrated in GF buffer. Fractions containing the xXPF-hsERCC1 heterodimer eluted between 60 and 70 ml (Enzlin & Scharer, 2002), were pooled and concentrated with an Amicon Ultra-4 centrifuge filter unit, 30 kDa (Merck Millipore). Protein was aliquoted, flash frozen and stored at -80°C. FLAG-tagged xSLX4 was purified as previously described (Klein Douwel *et al.*, 2014). His-tagged xSLX4 was cloned into pDONR201 (Life technologies) and baculo viruses were produced using the BaculoDirect system following manufacturers protocol (Life Technologies). His-tagged xSLX4 was expressed in 150 ml suspension cultures of Sf9 insect cells for 72 hours. Cells were collected by centrifugation, resuspended in lysis buffer (50mM Tris pH 8.0, 500mM NaCl, 0.1% NP-40, 10% glycerol, 0.4mM PMSF, 10mM Imidazole, 1 tablet/10ml Complete Mini EDTA-free Protease Inhibitor Cocktail (Roche)) and lysed by sonication. The soluble fraction obtained after centrifugation (40.000 \times g for 40 minutes at 4°C) was incubated for 1 hour at 4°C with 750 μ l of Ni-NTA-agarose (Qiagen) that were pre-washed with lysis buffer. After incubation the beads were washed with wash buffer (50mM Tris pH 8.0, 300mM NaCl, 0.1% NP-40, 5% glycerol, 0.1mM PMSF, 20mM Imidazole, 10 μ g/ml aproptin/leupeptin). His-tagged xSLX4 protein was eluted in wash buffer containing 250mM Imidazole. The protein was aliquoted and stored at -80°C. The pDONR201 construct for FLAG-tagged xSLX4 was used to create the xSLX4^{AMLR} mutant. PCR amplification was used to replace the MLR domain with a short linker containing a KpnI restriction site. Expression and purification of FLAG-tagged xSLX4^{AMLR} was identical to the wild type protein.

Nuclease Assay

Nuclease assay was performed as previously described (de Laat *et al.*, 1998). The following primers were obtained (Integrated DNA technologies): SL:5'-FAM-CGCCAG CGC TCGTTTTTTTTTTTTTTTTTTTTTTTTTCCGAGCGCTGGC-'3; F1: 5'-FAM- CGCGATGCGG ATCCAA-'3; F2: 5'-CCTAGACTTAAGAGGCCAGACTTGGATCCGCATCGC -'3; F3:5'-GGCCTCTTAAGTCTAGG-3'. For the stem loop structure primer SL was heated for 3 min at 95°C, followed by step-wise cooling to allow annealing (30 min at 60°C, 30 min at 37°C, 30 min at 25°C, 30 min on ice). To assemble the 3' flap substrate primer F1 was annealed to primer F2 and F3 in a 1:1:1 ratio and annealed similar to the stem-loop substrate. Nuclease reactions (15 μ l) were carried out in nuclease buffer (50 mM Tris pH 8.0, 0.2 mM MnCl₂, 0.1 mg/ml bovine serum albumin and 0.5 mM β -mercaptoethanol) containing 100 nmol of substrate DNA and 10-100nM of recombinant XPF-ERCC1 wild type or mutant protein complex. Reactions were incubated for 30 minutes at room temperature and stopped by

addition of 15 μ l denaturing PAGE Gel Loading Buffer II (Life Technologies, Inc.). Samples were heated to 72°C for 3 minutes, snap cooled, and loaded onto a 12% denaturing urea-PAGE gel. Gels were directly measured on a Typhoon phosphor imager (GE Healthcare) on the blue 488 channel.

Fluorescent Anisotropy Binding Assay

Increasing concentrations of protein were incubated with 10nM of a 3'-Flap DNA substrate containing a 5'- fluorescent FAM label (see nuclease assay). The reaction was incubated with Annealing Buffer (25mM Hepes pH8.0, 15% glycerol, 0.1mg/ml BSA, 2mM CaCl₂) in a 384-well plate (kbioscience) for 1h at room temperature and fluorescent anisotropy was measured on a Spectramax I3 (molecular devices). The data was fitted using Origin 8.5 to the equation $y = \text{START} + (\text{END} - \text{START}) * x^n / (k^n + x^n)$, where x is the protein concentration, y is the fluorescence and k is the k_d value.

Xenopus egg extracts, DNA replication and repair assay

DNA replication and preparation of *Xenopus* egg extracts (HSS and NPE) were performed as described previously (Tutter & Walter, 2006, Walter *et al.*, 1998). Preparation of plasmid with a site-specific cisplatin ICL (piCL), and ICL repair assays were performed as described (Enoiu *et al.*, 2012, Räschle *et al.*, 2008). Briefly piCL was incubated with HSS for 20 min, following addition of two volumes of NPE (t=0) containing ³²P- α -dCTP. Aliquots of replication reaction (4-10 μ l) were stopped at various times with ten volumes of Stop Solution II (0.5% SDS, 10 mM EDTA, 50 mM Tris pH 7.5). Samples were incubated with RNase (0.13 μ g/ μ l) followed by Proteinase K (0.5 μ g/ μ l) for 30 min at 37°C each. DNA was extracted using Phenol/Chloroform, ethanol precipitated in the presence of glycogen (30 mg/ml), and resuspended in 5-10 μ l of 10 mM Tris pH 7.5. ICL repair was analyzed by digesting 1 μ l of extracted DNA with HincII, or HincII and SapI, separation on a 0.8 % native agarose gel, and quantification using autoradiography. Repair efficiency was calculated as described (Knipscheer *et al.*, 2012).

Unscheduled DNA synthesis

The assay to monitor unscheduled DNA synthesis (UDS) in *Xenopus* egg extract was adapted from (Gaillard *et al.*, 1996). A 6.25 μ l reaction containing 2.5 μ l HSS and 6 ng/ μ l non-treated or UV-C irradiated (35.000 μ J/m²) pControl was supplemented with 5mM MgCl₂, 0.5mM DTT, 4mM ATP, 40mM Phosphocreatine, 0.5 μ g creatine phosphokinase and 80 μ Ci/ml ³²P- α -dCTP (3000Ci/mmol). Reactions were incubated at room temperature for 2h and stopped by addition of ten volumes of Stop Solution II (0.5% SDS, 10 mM EDTA, 50 mM Tris pH 7.5). Samples were incubated with Proteinase K (0.5 μ g/ μ l) for 30 min at 37°C. DNA was extracted using Phenol/Chloroform, ethanol precipitated in the presence of glycogen (30 mg/ml), and resuspended in 5-10 μ l of 10 mM Tris pH 7.5. Extracted DNA (2 μ l) was digested with HincII and separated on a 0.8 % native agarose gel. The gel was stained with SYBR GOLD (Fisher) and subsequently dried and quantified using autoradiography. The background signal from non-treated plasmid was subtracted. To compare the levels of UDS between experiments the signal for wild type XPF-ERCC1 add back was set to 100%. This is because the efficiency of UDS can differ between extract preparations and depletions.

Antibodies and immunodepletions

Antibodies were raised against residues 444-797 of *x*/XPF, full length *x*/ERCC1 and residues 825-1052 of *x*/SLX4. Specificity was confirmed using Western blot (Klein Douwel *et al.*, 2014). XPF-ERCC1 was removed from extract using three rounds of depletion with the α -ERCC1 serum (HSS and NPE). ERCC1 depletion was described previously (Klein Douwel *et al.*, 2014). For the unscheduled DNA synthesis assay HSS was depleted using three rounds of an ERCC1 depletion (1 volume of PAS was bound to 1 volume of anti-serum or pre-immune serum, and added to 4 volumes of HSS) followed by three rounds of depletion with the α -XPF serum (1 volume of PAS was bound to 3 volumes of anti-serum or pre-immune serum, and added to 5 volumes of HSS). Anti-FLAG M2 antibody was purchased from Sigma and His-antibody from Westburg.

Incision assay

Incision assay was performed as described (Klein Douwel *et al.*, 2014). Briefly, pICL and pQuant were labeled via nick-translation. pQuant was added as an internal control to allow accurate calculation of incision efficiency. pICL (225 ng) and pQuant (11.25 ng) were incubated in 1.5 units NB-BSR DI enzyme (NEB) and 1 \times NEBuffer 2 for 30 minutes at room temperature. Subsequently, 11 μ l DNA Polymerase I mix (5 units of DNA Polymerase I (NEB), dATP, dGTP, dTTP (0.5 mM each), dCTP (0.4 μ M), 32 P- α -dCTP (3.3 μ M) in 1 \times NEBuffer 2) was added and this was incubated for 3 min at 16 $^{\circ}$ C. The reaction was stopped with 180 μ l Stop Solution II, treated with Proteinase K, and Phenol/Chloroform extracted. Excess label was removed using a Micro Bio-Spin 6 Column (Bio-Rad). After ethanol precipitation the pellet was resuspended in 5 μ l ELB (10 mM HEPES-KOH pH 7.7, 50 mM KCl, 2.5 mM MgCl₂ and 250 mM Sucrose). The labeled plasmid (pICL*) was used in a replication reaction and samples at various times were extracted and digested with HincII. Fragments were separated on a 0.8 % alkaline denaturing agarose gel for 18 hours at 0.85 Volts/cm, after which the gel was dried and exposed to a phosphor-screen. Quantification was performed using ImageQuant software (GE healthcare). The highest value was set at 100% for the X-shape and the Linear products.

Chromatin Immunoprecipitation

Chromatin Immunoprecipitation (ChIP) was performed as described (Pacek *et al.*, 2006). Briefly, reaction samples were crosslinked with formaldehyde, sonicated to yield DNA fragments of roughly 100-500 bp, and immunoprecipitated with the indicated antibodies. Protein-DNA crosslinks were reversed and DNA was phenol/chloroform extracted for analysis by quantitative real-time PCR with the following primers: ICL (5'-AGCCAGATTTTCTCCTCTC-3' and 5'-CATGCATTGGTTCTGCACTT-3'), and pQuant (5'-TACAAATGTACGGCCAGCAA-3' and 5'-GAGTATGAGGGAAGCGGTGA-3'). The values from pQuant primers were subtracted from the values for pICL primers.

Immunoprecipitations

Proteins were expressed in adherent cultures of Sf9 insect cells in 6-well plates by co-infection with His-*hs*ERCC1, His-*x*/SLX4 and FLAG-*x*/XPF (or FLAG-*x*/XP mutants) viruses for 72 hours. Cells were resuspended in medium and collected by centrifugation, resuspended in 250 μ l lysis buffer (50mM Tris pH 8.0, 300mM NaCl, 1% Triton, 4mM EDTA, 10 μ g/

mL aproptin/leupeptin) and lysed by sonication. After centrifugation ($20.000 \times g$ for 20 minutes at 4°C), 200 μL soluble fraction was incubated for 30 minutes at 4°C with 8 μL FLAG M2 beads (Sigma-Aldrich) that were pre-washed with lysis buffer. After incubation, the beads were washed using 2 mL lysis buffer. Beads were taken up in 50 μL 2 \times SDS sample buffer and incubated for 5 minutes at 95°C . Proteins were loaded on SDS PAGE and visualized by western blot using respective antibodies.

For immunoprecipitations from *Xenopus* egg extract FLAG-tagged *x/SLX4^{WT}* or *x/SLX4^{ΔMLR}* protein was added to NPE/HSS at a concentration of 5 ng/ μL . To each 20 μL extract, 45.5 μL IP buffer (1 \times ELB salts, 0.25M sucrose, 75mM NaCl, 2mM EDTA, 10 $\mu\text{g}/\text{mL}$ aproptin/leupeptin, 0.1% NP-40) and 10 μL pre-washed FLAG M2 beads (Sigma-Aldrich) were added. Beads were incubated for 90 minutes at 4°C and subsequently washed using 2.5 mL IP buffer. Beads were taken up in 30 μL 2 \times SDS sample buffer and incubated for 5 minutes at 95°C . Proteins were loaded on SDS PAGE and visualized by western blot using respective antibodies.

Acknowledgements

This work was supported by the Netherlands organization for Scientific Research (VIDI 700.10.421 to P.K.) and a project grant from the Dutch Cancer Society (KWF HUBR 2015-7736 to P.K.). We thank N. Martin-Pintado for assistance with the anisotropy assays and suggestions on the manuscript. We also thank J.C. Walter for the *x/PCNA* antibody and K.A. Cimprich for the *x/XPA* antibody. In addition, we thank W. Hoogenboom, J.C. Walter and J.A.F. Marteiijn for suggestions on the manuscript, the Hubrecht animal caretakers for animal support, and the other members of the Knipscheer laboratory for feedback.

Conflict of Interest

The authors declare that they have no conflict of interest.

References

- Ahmad A, Enzlin JH, Bhagwat NR, Wijgers N, Raams A, Appeldoorn E, Theil AF, JH JH, Vermeulen W, NG JJ, Scharer OD & Niedernhofer LJ (2010) Mislocalization of XPF-ERCC1 nuclease contributes to reduced DNA repair in XP-F patients. *PLoS genetics* 6: e1000871
- Andersen SL, Bergstralh DT, Kohl KP, LaRocque JR, Moore CB & Sekelsky J (2009) Drosophila MUS312 and the vertebrate ortholog BTBD12 interact with DNA structure-specific endonucleases in DNA repair and recombination. *Molecular cell* 35: 128-35
- Bergstralh DT & Sekelsky J (2008) Interstrand crosslink repair: can XPF-ERCC1 be let off the hook? *Trends Genet* 24: 70-6
- Bogliolo M, Schuster B, Stoepker C, Derkunt B, Su Y, Raams A, Trujillo JP, Minguillon J, Ramirez MJ, Pujol R, Casado JA, Banos R, Rio P, Knies K, Zuniga S, Benitez J, Bueren JA, Jaspers NG, Scharer OD, de Winter JP *et al.* (2013) Mutations in ERCC4, encoding the DNA-repair endonuclease XPF, cause Fanconi anemia. *American journal of human genetics* 92: 800-6
- Bowles M, Lally J, Fadden AJ, Moulleron S, Hammonds T & McDonald NQ (2012) Fluorescence-based incision assay for human XPF-ERCC1 activity identifies important elements of DNA junction recognition. *Nucleic acids research* 40: e101
- Budzowska M, Graham TG, Sobeck A, Waga S & Walter JC (2015) Regulation of the Rev1-pol zeta complex during bypass of a DNA interstrand crosslink. *The EMBO journal* 34: 1971-85
- Crossan GP, van der Weyden L, Rosado IV, Langevin F, Gaillard PH, McIntyre RE, Sanger Mouse Genetics P, Gallagher F, Kettunen MI, Lewis DY, Brindle K, Arends MJ, Adams DJ & Patel KJ (2011) Disruption of mouse Slx4, a regulator of structure-specific nucleases, phenocopies Fanconi anemia. *Nature genetics* 43: 147-52
- de Laat WL, Appeldoorn E, Jaspers NG & Hoeijmakers JH (1998) DNA structural elements required for ERCC1-XPF endonuclease activity. *The Journal of biological chemistry* 273: 7835-42
- De Silva IU, McHugh PJ, Clingen PH & Hartley JA (2000) Defining the roles of nucleotide excision repair and recombination in the repair of DNA interstrand cross-links in mammalian cells. *Molecular and cellular biology* 20: 7980-90
- Dong H, Nebert DW, Bruford EA, Thompson DC, Joenje H & Vasiliou V (2015) Update of the human and mouse Fanconi anemia genes. *Human genomics* 9: 32
- Enoiu M, Jiricny J & Scharer OD (2012) Repair of cisplatin-induced DNA interstrand crosslinks by a replication-independent pathway involving transcription-coupled repair and translesion synthesis. *Nucleic acids research* 40: 8953-64
- Enzlin JH & Scharer OD (2002) The active site of the DNA repair endonuclease XPF-ERCC1 forms a highly conserved nuclease motif. *The EMBO journal* 21: 2045-53
- Fekairi S, Scaglione S, Chahwan C, Taylor ER, Tissier A, Coulon S, Dong MQ, Ruse C, Yates JR, 3rd, Russell P, Fuchs RP, McGowan CH & Gaillard PH (2009) Human SLX4 is a Holliday junction resolvase subunit that binds multiple DNA repair/recombination endonucleases. *Cell* 138: 78-89
- Friedberg EC (2011) Nucleotide excision repair of DNA: The very early history. *DNA repair* 10: 668-72
- Fu YV, Yardimci H, Long DT, Ho TV, Guainazzi A, Bermudez VP, Hurwitz J, van Oijen A, Scharer OD & Walter JC (2011) Selective bypass of a lagging strand roadblock by the eukaryotic replicative DNA helicase. *Cell* 146: 931-41
- Gaillard PH, Martini EM, Kaufman PD, Stillman B, Moustacchi E & Almouzni G (1996) Chromatin assembly coupled to DNA repair: a new role for chromatin assembly factor I. *Cell* 86: 887-96
- Gillet LC & Scharer OD (2006) Molecular mechanisms of mammalian global genome nucleotide excision repair. *Chem Rev* 106: 253-76
- Guervilly JH, Takedachi A, Naim V, Scaglione S, Chawhan C, Lovera Y, Despras E, Kuraoka I, Kannouche P, Rosselli F & Gaillard PH (2015) The SLX4 complex is a SUMO E3 ligase that impacts on replication stress outcome and genome stability. *Molecular cell* 57: 123-37
- Hashimoto K, Wada K, Matsumoto K & Moriya M (2015) Physical interaction between SLX4 (FANCP) and XPF (FANCI) proteins and biological consequences of interaction-defective missense mutations. *DNA repair* 35: 48-54
- Hodskinson MR, Silhan J, Crossan GP, Garaycochea JI, Mukherjee S, Johnson CM, Scharer OD & Patel KJ (2014) Mouse SLX4 is a tumor suppressor that stimulates the activity of the nuclease XPF-ERCC1 in DNA crosslink repair. *Molecular cell* 54: 472-84
- Huang JC, Svoboda DL, Reardon JT & Sancar A (1992) Human nucleotide excision nuclease removes thymine dimers from DNA by incising the 22nd phosphodiester bond 5' and the 6th phosphodiester bond 3' to the photodimer. *Proceedings of the National Academy of Sciences of the United States of America* 89: 3664-8
- Kashiyama K, Nakazawa Y, Pilz DT, Guo C, Shimada M, Sasaki K, Fawcett H, Wing JF, Lewin SO, Carr L, Li TS, Yoshiura K, Utani A, Hirano A, Yamashita S, Greenblatt D, Nardo T, Stefanini M, McGibbon D, Sarkany R *et al.* (2013) Malfunction of nuclease ERCC1-XPF results in diverse clinical manifestations and causes Cockayne syndrome, xeroderma pigmentosum, and Fanconi anemia. *American journal of human genetics* 92: 807-19
- Kim Y, Spitz GS, Veturi U, Lach FP, Auerbach AD & Smogorzewska A (2013) Regulation of multiple DNA repair pathways by the Fanconi anemia protein SLX4. *Blood* 121: 54-63

- Kirschner K & Melton DW (2010) Multiple roles of the ERCC1-XPF endonuclease in DNA repair and resistance to anticancer drugs. *Anticancer Res* 30: 3223-32
- Klein Douwel D, Boonen RA, Long DT, Szybowska AA, Räschle M, Walter JC & Knipscheer P (2014) XPF-ERCC1 acts in Unhooking DNA interstrand crosslinks in cooperation with FANCD2 and FANCP/SLX4. *Molecular cell* 54: 460-71
- Knipscheer P, Räschle M, Schärer OD & Walter JC (2012) Replication-coupled DNA interstrand cross-link repair in *Xenopus* egg extracts. *Methods Mol Biol* 920: 221-43
- Knipscheer P, Räschle M, Smogorzewska A, Enoiu M, Ho TV, Schärer OD, Elledge SJ & Walter JC (2009) The Fanconi anemia pathway promotes replication-dependent DNA interstrand cross-link repair. *Science* 326: 1698-701
- Kochaniak AB, Habuchi S, Loparo JJ, Chang DJ, Cimprich KA, Walter JC & van Oijen AM (2009) Proliferating cell nuclear antigen uses two distinct modes to move along DNA. *The Journal of biological chemistry* 284: 17700-10
- Kottemann MC & Smogorzewska A (2013) Fanconi anaemia and the repair of Watson and Crick DNA crosslinks. *Nature* 493: 356-63
- Kuraoka I, Kobertz WR, Ariza RR, Biggerstaff M, Essigmann JM & Wood RD (2000) Repair of an interstrand DNA cross-link initiated by ERCC1-XPF repair/recombination nuclease. *The Journal of biological chemistry* 275: 26632-6
- Li L, Peterson CA, Lu X & Legerski RJ (1995) Mutations in XPA that prevent association with ERCC1 are defective in nucleotide excision repair. *Molecular and cellular biology* 15: 1993-8
- Long DT, Räschle M, Joukov V & Walter JC (2011) Mechanism of RAD51-dependent DNA interstrand cross-link repair. *Science* 333: 84-7
- Mamrak NE, Shimamura A & Howlett NG (2017) Recent discoveries in the molecular pathogenesis of the inherited bone marrow failure syndrome Fanconi anemia. *Blood Rev* 31: 93-99
- McNeil EM & Melton DW (2012) DNA repair endonuclease ERCC1-XPF as a novel therapeutic target to overcome chemoresistance in cancer therapy. *Nucleic acids research* 40: 9990-10004
- Newman M, Murray-Rust J, Lally J, Rudolf J, Fadden A, Knowles PP, White MF & McDonald NQ (2005) Structure of an XPF endonuclease with and without DNA suggests a model for substrate recognition. *The EMBO journal* 24: 895-905
- Niedernhofer LJ, Garinis GA, Raams A, Lalai AS, Robinson AR, Appeldoorn E, Odijk H, Oostendorp R, Ahmad A, van Leeuwen W, Theil AF, Vermeulen W, van der Horst GT, Meinecke P, Kleijer WJ, Vijg J, Jaspers NG & Hoeijmakers JH (2006) A new progeroid syndrome reveals that genotoxic stress suppresses the somatotrophic axis. *Nature* 444: 1038-43
- Niedernhofer LJ, Odijk H, Budzowska M, van Druenen E, Maas A, Theil AF, de Wit J, Jaspers NG, Beverloo HB, Hoeijmakers JH & Kanaar R (2004) The structure-specific endonuclease Ercc1-Xpf is required to resolve DNA interstrand cross-link-induced double-strand breaks. *Molecular and cellular biology* 24: 5776-87
- Osorio A, Bogliolo M, Fernandez V, Barroso A, de la Hoya M, Caldes T, Lasa A, Ramon y Cajal T, Santamarina M, Vega A, Quiles F, Lazaro C, Diez O, Fernandez D, Gonzalez-Sarmiento R, Duran M, Piqueras JF, Marin M, Pujol R, Surrallés J et al. (2013) Evaluation of rare variants in the new fanconi anemia gene ERCC4 (FANCO) as familial breast/ovarian cancer susceptibility alleles. *Human mutation* 34: 1615-8
- Pacek M, Tutter AV, Kubota Y, Takisawa H & Walter JC (2006) Localization of MCM2-7, Cdc45, and GINS to the site of DNA unwinding during eukaryotic DNA replication. *Molecular cell* 21: 581-7
- Räschle M, Knipscheer P, Enoiu M, Angelov T, Sun J, Griffith JD, Ellenberger TE, Schärer OD & Walter JC (2008) Mechanism of replication-coupled DNA interstrand crosslink repair. *Cell* 134: 969-80
- Shivji MK, Grey SJ, Strausfeld UP, Wood RD & Blow JJ (1994) Cip1 inhibits DNA replication but not PCNA-dependent nucleotide excision-repair. *Curr Biol* 4: 1062-8
- Spivak G (2015) Nucleotide excision repair in humans. *DNA repair* 36: 13-18
- Staresincic L, Fagbemi AF, Enzlin JH, Gourdin AM, Wijgers N, Dunand-Sauthier I, Giglia-Mari G, Clarkson SG, Vermeulen W & Schärer OD (2009) Coordination of dual incision and repair synthesis in human nucleotide excision repair. *The EMBO journal* 28: 1111-20
- Su Y, Orelli B, Madireddy A, Niedernhofer LJ & Schärer OD (2012) Multiple DNA binding domains mediate the function of the ERCC1-XPF protein in nucleotide excision repair. *The Journal of biological chemistry* 287: 21846-55
- Tutter AV & Walter JC (2006) Chromosomal DNA replication in a soluble cell-free system derived from *Xenopus* eggs. *Methods Mol Biol* 322: 121-37
- Walter J, Sun L & Newport J (1998) Regulated chromosomal DNA replication in the absence of a nucleus. *Molecular cell* 1: 519-29
- Yildiz O, Majumder S, Kramer B & Sekelsky JJ (2002) *Drosophila* MUS312 interacts with the nucleotide excision repair endonuclease MEI-9 to generate meiotic crossovers. *Molecular cell* 10: 1503-9
- Zhang J, Dewar JM, Budzowska M, Motnenko A, Cohn MA & Walter JC (2015) DNA interstrand cross-link repair requires replication-fork convergence. *Nature structural & molecular biology* 22: 242-7

Extended View Figures

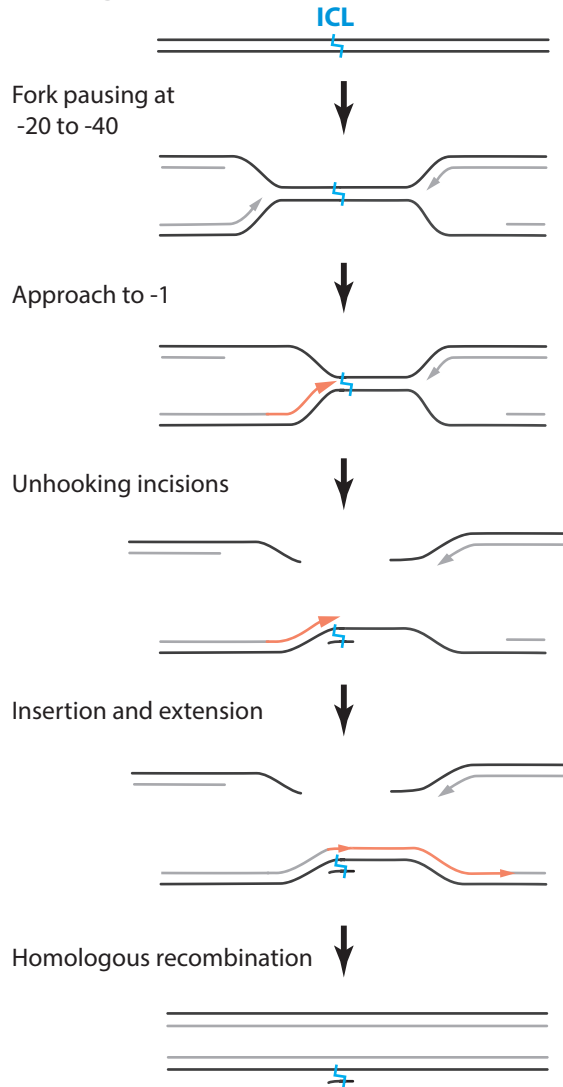


Figure EV1: Schematic representation of replication dependent ICL repair in *Xenopus* egg extract.

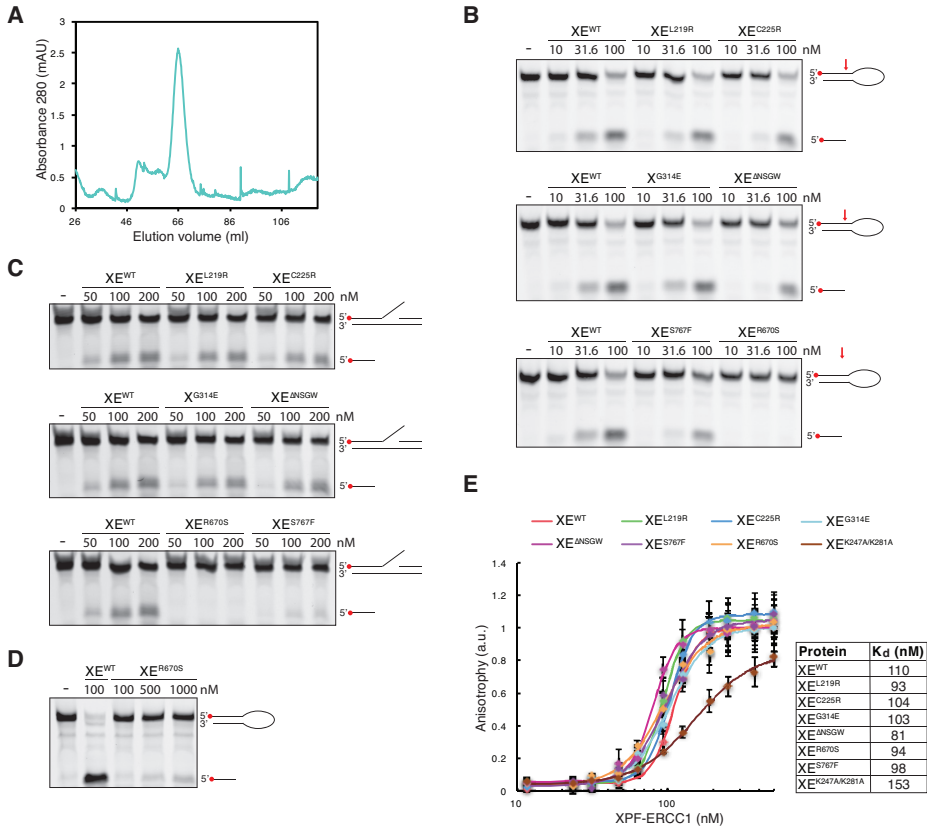


Figure EV2: Characterization of mutant XPF-ERCC1 complexes. A). Superdex 200 gel filtration column elution profile of XPF^{L219R}-ERCC1. The heterodimeric fraction depicted in Fig 1A, was collected, concentrated and re-run on the same column. The protein did not aggregate and eluted as a heterodimer at ~65 ml. B) Replicate of Fig 1D. Wild type and indicated mutant XPF-ERCC1 complexes were incubated with a 5'-FAM-labeled stem-loop DNA substrate (10 nM) at room temperature for 30 minutes. Reaction products were separated on a 12% urea PAGE gel and visualized using a fluorescence imaging system. C) as in (B) but using a 5'-FAM labeled 3' flap DNA substrate. D) As in (B) but using higher concentrations of the XE^{R670S} mutant. E) Replicate of Fig 1E. Wild type and mutant XPF-ERCC1 complexes at various concentrations were incubated with a 5'-FAM labeled 3' flap DNA substrate (10 nM) and fluorescent anisotropy was measured. Graphs were fitted to calculate dissociation constants (K_d's) as described in the method section. The error bars represent s.d. from three measurements.

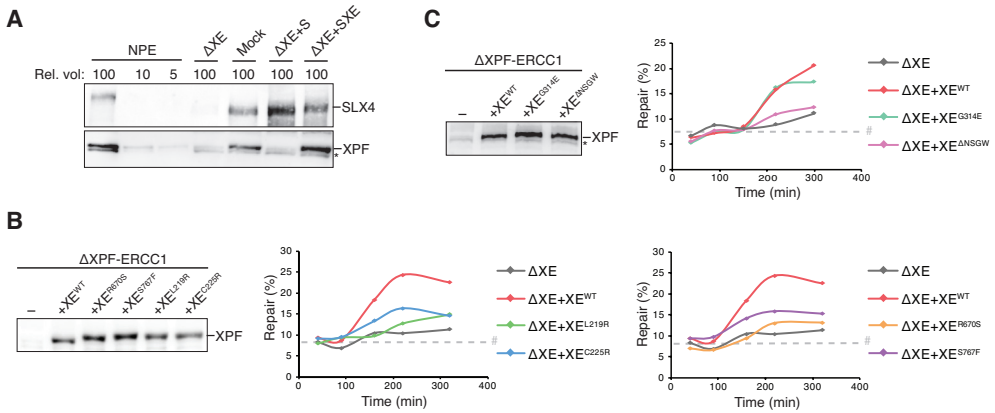


Figure EV3: Effect of mutations in XPF-ERCC1 on ICL repair in *Xenopus* egg extract. A) Mock-depleted, XPF-ERCC1 depleted (Δ XE), and XPF-ERCC1 depleted NPE complemented with SLX4 (Δ XE+S) or XPF-ERCC1 and SLX4 (Δ XE+SXE) were analyzed by western blot using α -XPF or α -SLX4 antibodies. A dilution series of undepleted NPE was loaded on the same blot to determine the degree of depletion. A relative volume of 100 corresponds to 0.2 μ l NPE. (B) Replicates of Fig 2B. XPF-ERCC1-depleted (Δ XE) and XPF-ERCC1-depleted extracts complemented with wild type (XE^{WT}) or indicated mutant XPF-ERCC1 (XE^{MUT}) were analyzed by western blot using α -XPF antibodies (left panel). These extracts were used to replicate pICL. Replication intermediates were isolated and digested with HincII, or HincII and SapI, and separated on agarose gel. Repair efficiency was calculated and plotted (right panels). (C) As in in (B) but analyzing different mutant complexes. Note: repair levels can differ per batch of individually prepared extract or per depletion experiment and can only be compared within an experiment. # SapI fragments from contaminating uncrosslinked plasmid present in varying degrees in pICL preparations. *, background band.

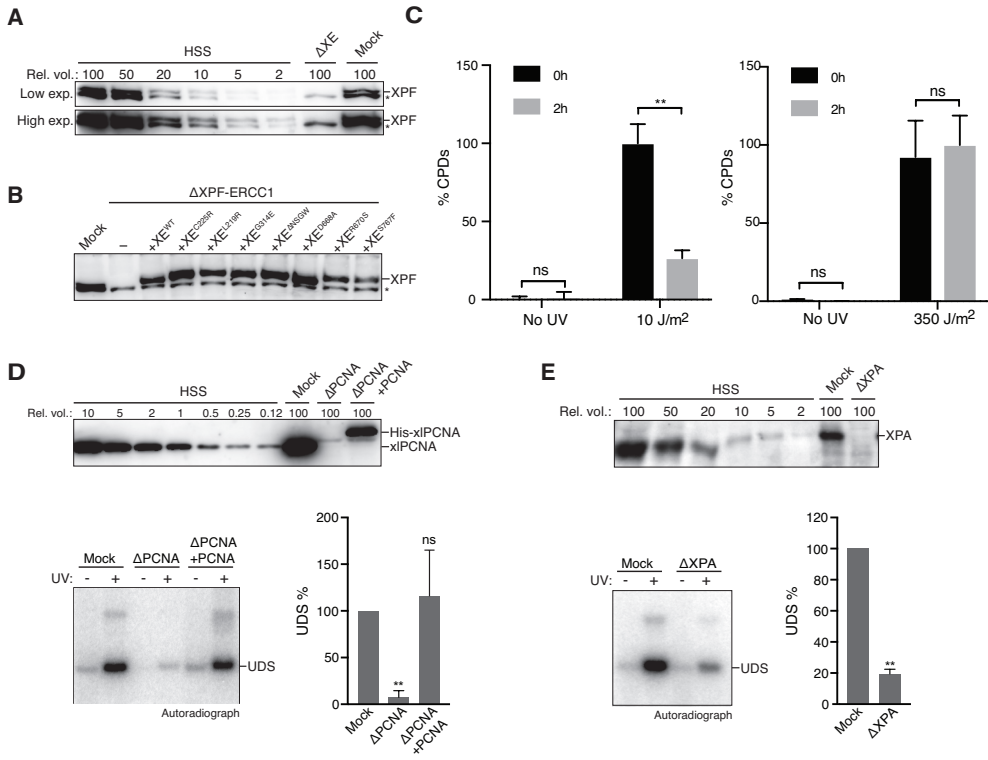


Figure EV4: XPF-ERCC1 mutant complexes are active in NER. A) Mock-depleted and XPF-ERCC1 depleted (ΔXE) High Speed Supernatant (HSS) egg extracts used in figure 3B were analyzed by western blot using α -XPF antibodies. A dilution series of undepleted NPE was loaded on the same blot to determine the degree of depletion. A relative volume of 100 corresponds to 0.2 μ l NPE. B) Mock depleted, XPF-ERCC1 depleted (ΔXE), and XPF-ERCC1 depleted HSS complemented with wild type (XE^{WT}) or mutant XPF-ERCC1 (XE^{MUT}) were analyzed by western blot using α -XPF antibodies. C) Untreated or UV-treated (10 J/m² left panel, 350 J/m² right panel) plasmid DNA was incubated in HSS for 2 hours. Samples were taken at time 0 and 2 hours, DNA was extracted and analyzed by an enzyme-linked immunosorbent assay (ELISA) for the presence of CPDs. The highest value within one experiment was set to 100%. **, $p=0.0061$. D) Mock depleted, PCNA-depleted ($\Delta PCNA$), and PCNA depleted HSS complemented with recombinant His-xIPCA ($\Delta PCNA + PCNA$) were analyzed by western blot using α -PCNA antibodies (Kochaniak *et al.*, 2009). A dilution series of undepleted NPE was loaded on the same blot to determine the degree of depletion. A relative volume of 100 corresponds to 0.2 μ l NPE (top panel). These extracts were incubated with untreated or UV-treated (350 J/m²) plasmids for 0 or 2 hours at room temperature in presence of ³²P- α -dCTP. Reaction products were isolated, linearized with HincII and separated on a 0.8 % agarose gel. The DNA was visualized by autoradiography to show incorporation of ³²P- α -dCTP during UDS (bottom left panel). The signal was quantified, the background signal from non-damaged plasmid was subtracted, and the signal for the mock depletion condition was set to 100% to normalize the data. Error bars represent s.e.m of three independent experiments. **, $p=0.0059$, paired *t*-test compared to the mock condition. E) as in (D) but using mock depleted or XPA depleted HSS. ** $p=0.0014$, ns = not significant. *, background band.

3

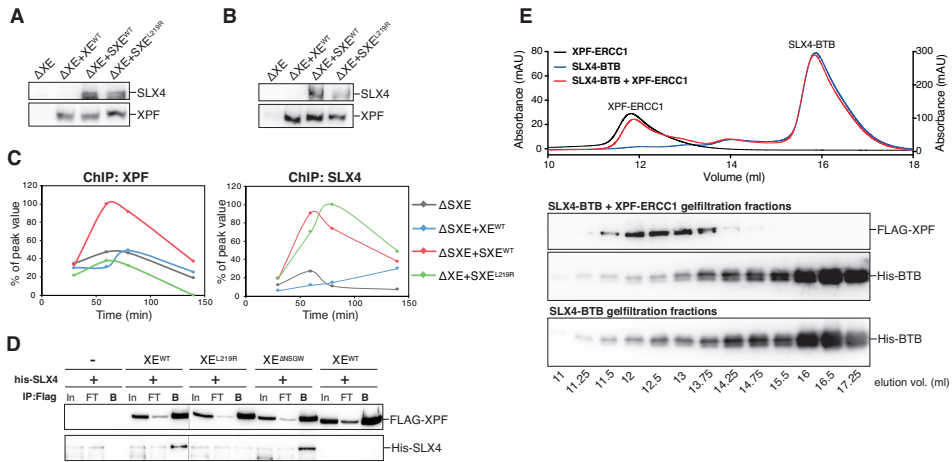
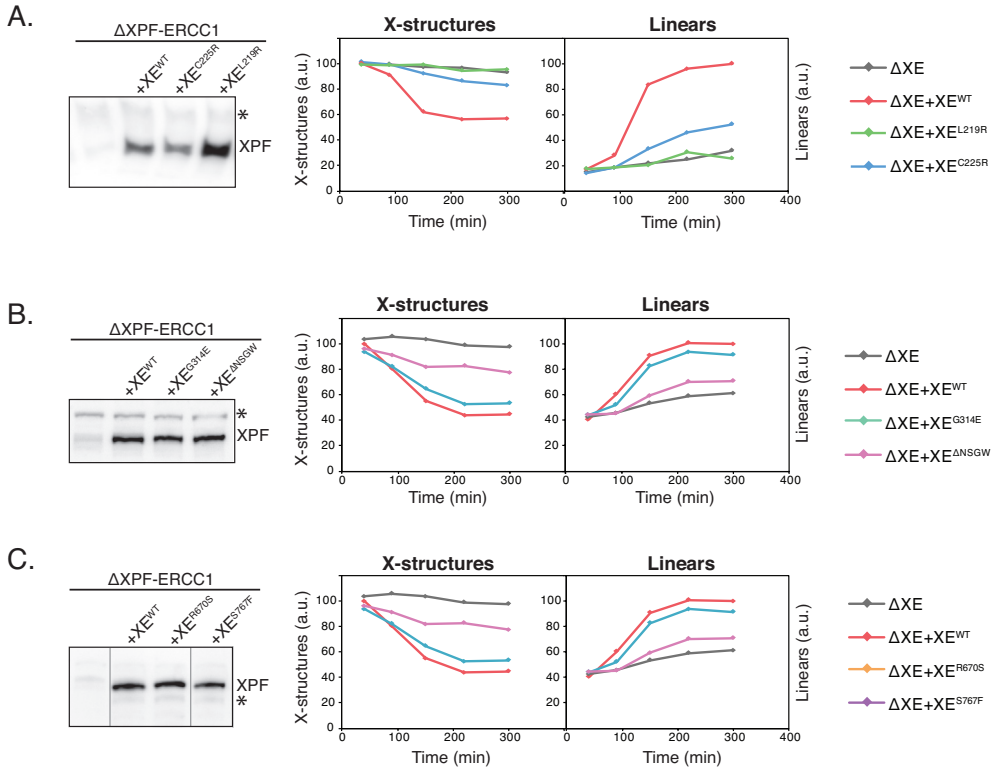
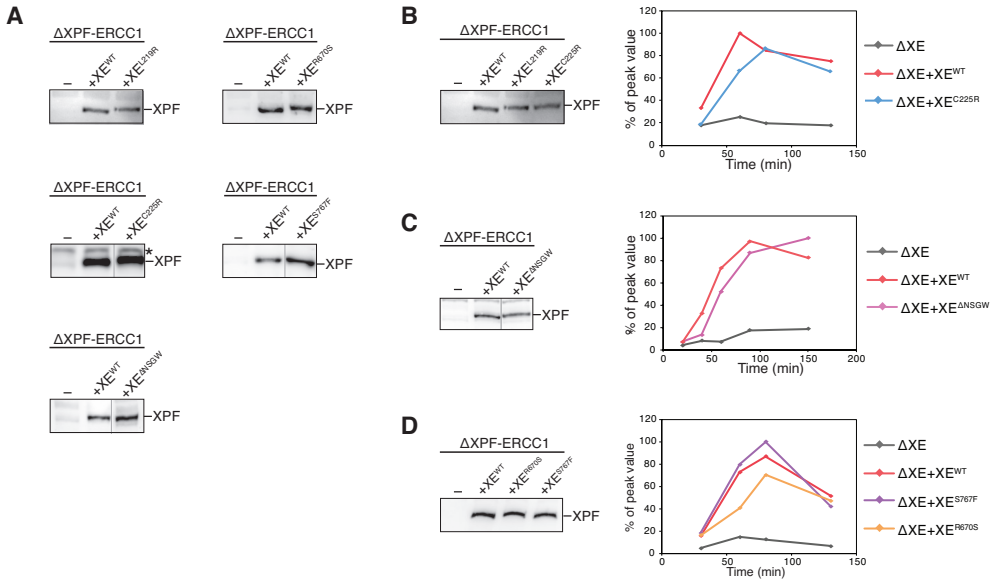


Figure EV5: XPF leucine 219 is part of the major interaction site between XPF and SLX4. A) XPF-ERCC1 depleted (Δ XE) and XPF-ERCC1 depleted NPE supplemented with XPF-ERCC1 (+XE^{WT}), XPF-ERCC1 and SLX4 (+SXE^{WT}), or XPF^{L219R}-ERCC1 and SLX4 (+SXE^{L219R}) were analyzed by western blot using α -XPF and α -SLX4 antibodies. Extracts were used for Fig 6A. B) As in (A). C) Replicate of Fig 6A. The extracts from (B), with similarly treated HSS, were used to replicate pICL. Samples were taken at the indicated times and analysed by XPF (left) and SLX4 (right) ChIP using pICL and pQuant primers. The qPCR data was plotted as the percentage of peak value with the highest value set to 100%. D) Replicate of Figure 6C. Wild type and mutant FLAG-XPF-ERCC1 were co-expressed with His-SLX4 in Sf9 insect cells. Cells were lysed and XPF was immunoprecipitated via the FLAG-tag. Samples were analyzed by western blot using α -FLAG and α -His antibodies. In is input, FT is flow through fraction, B is fraction bound to beads. E) Size exclusion chromatography of recombinant XPF-ERCC1 and BTB domain of SLX4. Superdex 200 gel filtration column elution profile of FLAG-XPF-ERCC1, His-tagged BTB domain, and both proteins combined (top panel). The XPF-ERCC1 heterodimer eluted at \sim 12 ml, while His-BTB eluted around \sim 16 ml. Collected fractions during elution were analyzed by western blot using α -XPF and α -His antibodies (bottom panel). The BTB domain protein does not shift to a higher elution volume when incubated with XPF-ERCC1 indicating the affinity is not high enough to show binding between the two proteins.

Appendix Figures



Appendix Figure S1: Separation of function mutants are all defective in ICL unhooking. A) Replicate of Fig 4B. XPF-ERCC1-depleted (Δ XE) or XPF-ERCC1-depleted egg extract complemented with wild type (XE^{WT}) or mutant XPF-ERCC1 (XE^{MUT}) were incubated with pre-labeled pICL. Repair products were isolated at indicated times, linearized with HINCII, and visualized on a denaturing agarose gel. The X-structures and linear products were quantified and plotted (right panel). The extracts used were analyzed by western blot using α -XPF antibodies to verify depletion and the levels of added recombinant protein (left panel). Line within blot indicates position where irrelevant lanes were removed. C) and D) As in (B) but using different XPF-ERCC1 mutant complexes. C) and D) As in (B) but using different XPF-ERCC1 mutant complexes. Replicates of Fig 4C and Fig 4D. Line within blot indicates position where irrelevant lanes were removed.



Appendix Figure S2: Recruitment of XPF-ERCC1 mutants to the ICL during repair. A) XPF-ERCC1 depleted (Δ XE) NPE or XPF-ERCC1 depleted NPE with wild type (XE^{WT}) or indicated mutant XPF-ERCC1 (XE^{MUT}) were analyzed by western blot using α -XPF antibodies. Extracts were used to perform CHIP in Fig 5 B, C, D and E with indicated XPF mutants. B) Replicate of Fig 5C. pICL was replicated in XPF-ERCC1 depleted (Δ XE) or XPF-ERCC1-depleted egg extract supplemented with wild type (XE^{WT}) or mutant XPF-ERCC1 (XE^{MUT}) (left panel). Samples were taken at various times and immunoprecipitated with α -XPF antibodies. Co-precipitated DNA was isolated and analyzed by quantitative PCR using the primers depicted in Fig 5A. The qPCR data was plotted as the percentage of peak value with the highest value within one experiment set to 100% (right panel). The XPF^{C225R} was analyzed in the same experiment as Fig 5A. C)- F) As in (B) but for the indicated XPF-ERCC1 mutant complexes. Replicates of Figures 5D, E and F. Line within blot indicates position where irrelevant lanes were removed. *, background band.

Appendix Supplementary Methods

Protein expression and purification

His-PCNA protein was purified as previously described (Kochaniak *et al.*, 2009). The x/SLX4 BTB domain (residues 547-685) was amplified using PCR, with an N-terminal 10xHis-tag, and cloned into pETDuet-1. The construct was transformed into Rosetta (DE3) competent cells for IPTG-induced overexpression. 150 μ L 1M IPTG was added to 400 mL culture at $OD_{600}=0.6$ and incubated for 20 hours at 20°C. Cells were collected by centrifugation, resuspended in 12 mL lysis buffer (50mM Hepes pH 8.0, 400mM NaCl, 10% glycerol, 3mM imidazole, 0.5mM PMSF, 4mM β -mercaptoethanol, 1 tablet/10mL c0mplete Mini EDTA-free Protease Inhibitor Cocktail (Roche)) and lysed by sonication. The soluble fraction obtained after centrifugation (20.000 \times g for 20 minutes at 4°C) was incubated for 90 minutes at 4°C with 250 μ L of Ni-NTA-agarose (Qiagen) that was pre-washed with lysis buffer. After incubation the beads were washed with 50 mL wash buffer (25mM Hepes pH 8.0, 300mM NaCl, 10% glycerol, 10mM imidazole, 0.2mM PMSF, 5mM β -mercaptoethanol, 10 μ g/mL aprotinin/leupeptin). The BTB domain protein was eluted in elution buffer (25mM Hepes pH 8.0, 200mM NaCl, 10% glycerol, 300mM imidazole, 5mM β -mercaptoethanol, 10 μ g/mL aprotinin/leupeptin). The elution was dialyzed using a Slide-A-Lyzer® Dialysis Cassette 3,500 MWCO 0.5 – 3 ml Capacity (Thermo Scientific) for one hour and again overnight in 500 mL dialysis buffer (25mM Hepes pH 8.0, 200mM NaCl, 10% glycerol, 5mM β -mercaptoethanol) for the removal of imidazole. The protein was aliquoted and stored at -80°C.

ELISA

To detect CPDs in UV treated plasmids before and after incubation in *Xenopus* egg extract, 6 ng/ μ L non-treated or UV-C treated plasmid DNA was incubated in a 6.25 μ L reaction containing 2.5 μ L HSS, supplemented with 5mM $MgCl_2$, 0.5mM DTT, 4mM ATP, 40mM Phosphocreatine and 0.5 μ g creatine phosphokinase. Reactions were incubated at room temperature and stopped by addition of ten volumes of Stop Solution II (0.5% SDS, 10 mM EDTA, 50 mM Tris pH 7.5) after 0 or 2 hours. Samples were incubated with Proteinase K (0.5 μ g/ μ L) for 30 min at 37°C. DNA was extracted using Phenol/Chloroform, ethanol precipitated in the presence of glycogen (30 mg/ml), and resuspended in 5-10 μ L of 10 mM Tris pH 7.5. CPDs were detected using OxiSelect UV-Induced DNA Damage ELISA Kit (Bioconnect) according to manufacturer's instructions.

Size exclusion chromatography

In order to assess the binding between XPF and SLX4-BTB, purified proteins were loaded in sodium dodecyl sulfate (SDS) sample buffer onto a Superdex 200 increase 10/300 GL gel filtration column at 4°C (GE Healthcare). The mix of XPF-ERCC1 and the SLX4 BTB domain was pre-incubated for half an hour at 4°C prior to loading. Samples were taken at different elution volumes and analyzed by western blot using respective antibodies.

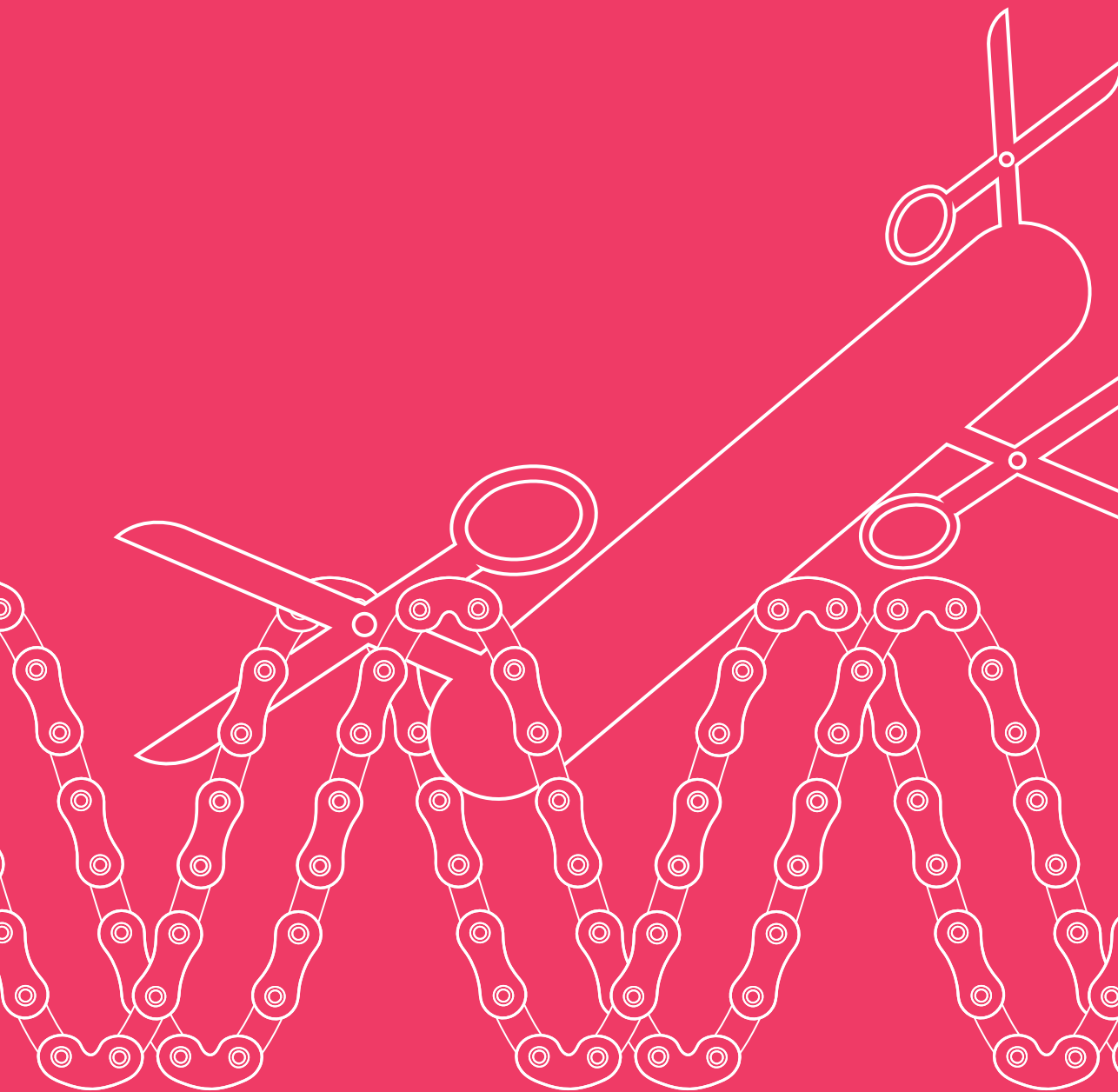
Antibodies and immunodepletions

Antibodies against x/PCNA and x/XPA were previously described (Bomgarden *et al.*, 2006, Kochaniak *et al.*, 2009). PCNA was removed from the HSS extract using 6 rounds

of depletion for 30 min or 1h at 4 °C using Protein A Sepharose Fast Flow (PAS) (GE Healthcare) bound to α /PCNA antibody (1 volume of PAS was bound to 3 volumes of anti-serum or preimmune serum, and added to 5 volumes of HSS). For the XPA depletion one volume of PAS was bound to one volume of anti-serum or pre-immune serum and added to 4 volumes of HSS for 30 min at 4°C. This was repeated 4 times.

Appendix references

- Bomgardner RD, Lupardus PJ, Soni DV, Yee MC, Ford JM & Cimprich KA (2006) Opposing effects of the UV lesion repair protein XPA and UV bypass polymerase eta on ATR checkpoint signaling. *The EMBO journal* 25: 2605-14
- Kochaniak AB, Habuchi S, Loparo JJ, Chang DJ, Cimprich KA, Walter JC & van Oijen AM (2009) Proliferating cell nuclear antigen uses two distinct modes to move along DNA. *The Journal of biological chemistry* 284: 17700-10



Chapter 4

The role of SLX4 and its associated nucleases in DNA interstrand crosslink repair

Wouter S. Hoogenboom, Rick A.C.M. Boonen[†] and Puck Knipscheer*

Oncode Institute, Hubrecht Institute–KNAW and University Medical Center
Utrecht, Utrecht, The Netherlands

[†]Present address: Department of Human Genetics, Leiden University
Medical Center, Leiden, The Netherlands

*Corresponding author. Tel: +31 30 2121875; Email: p.knipscheer@
hubrecht.eu

Adapted from: *Nucleic Acids Res.* 2019 Mar 18;47(5):2377-2388

Abstract

A key step in the Fanconi anemia pathway of DNA interstrand crosslink (ICL) repair is the ICL unhooking by dual endonucleolytic incisions. SLX4/FANCP is a large scaffold protein that plays a central role in ICL unhooking. It contains multiple domains that interact with many proteins including three different endonucleases and also acts in several other DNA repair pathways. While it is known that its interaction with the endonuclease XPF-ERCC1 is required for its function in ICL repair, which other domains act in this process is unclear. Here, we used *Xenopus* egg extracts to determine ICL repair specific features of SLX4. We show that the SLX4-interacting endonuclease SLX1 is not required for ICL repair and demonstrate that all essential SLX4 domains are located at the N-terminal half of the protein. The MLR domain is crucial for the recruitment of XPF-ERCC1 but also has an unanticipated function in recruiting SLX4 to the site of damage. Although we find the BTB is not essential for ICL repair in our system, dimerization of SLX4 could be important. Our data provide new insights into the mechanism by which SLX4 acts in ICL repair.

Introduction

DNA interstrand crosslinks (ICLs) are toxic DNA lesions that covalently attach both strands of the duplex, thereby blocking the progression of DNA and RNA polymerases. Due to their toxicity, especially for proliferating cells, DNA crosslinking agents such as cisplatin derivatives and nitrogen mustards, are widely used in cancer chemotherapies (Deans & West, 2011). However, endogenous metabolites, such as reactive aldehydes, can also induce ICLs (Voulgaridou *et al.*, 2011).

While ICLs can be repaired in the G1 phase of the cell cycle, most of the repair takes place in S-phase and is coupled to DNA replication (Akkari *et al.*, 2000, Räschle *et al.*, 2008, Williams *et al.*, 2013). In higher eukaryotes, a complex pathway has evolved to repair ICLs, which is called the Fanconi anemia (FA) pathway. This pathway is linked to the cancer predisposition syndrome Fanconi anemia (FA) that is caused by biallelic mutations in any one of the 22 currently known FA genes. Cells from FA patients are remarkably sensitive to ICL inducing agents, consistent with the FA proteins being involved in the repair of DNA interstrand crosslinks (Kottemann & Smogorzewska, 2013, Walden & Deans, 2014). Indeed, it has been shown that exogenous ICLs, for example caused by cisplatin, are repaired by the FA pathway (Knipscheer *et al.*, 2009). Although the source of the endogenous ICL that requires the FA pathway for its repair is currently not known, genetic evidence points towards reactive aldehydes (Garaycochea *et al.*, 2012, Hira *et al.*, 2013, Langevin *et al.*, 2011, Ridpath *et al.*, 2007, Rosado *et al.*, 2011). However, aldehydes induce several other types of DNA damage (Cheng *et al.*, 2003, Voulgaridou *et al.*, 2011, Wang *et al.*, 2000) and direct evidence that the aldehyde-induced ICL is repaired by the FA pathway is currently missing.

Based on experiments in *Xenopus* egg extracts, we and others have previously described a mechanism of FA pathway-dependent ICL repair in S-phase. This requires dual replication fork convergence, in some cases followed by replication fork reversal, ICL unhooking by structure-specific endonucleases, translesion synthesis (TLS), and homologous recombination (Supplemental Figure S1A, (Amunugama *et al.*, 2018, Budzowska *et al.*, 2015, Klein Douwel *et al.*, 2014, Long *et al.*, 2011, Räschle *et al.*, 2008, Zhang *et al.*, 2015)). In some cases, a single fork can bypass an ICL without unhooking, generating a similar X-shaped structure that is the substrate for ICL unhooking (Huang *et al.*, 2013). Recently, an alternative replication-dependent ICL repair pathway was identified that involves unhooking of the ICL by the glycosylase Neil3, preventing the formation of a double-strand break (Semlow *et al.*, 2016). This process is independent of FA pathway activation and specifically repairs abasic site-, and psoralen/UV-induced ICLs. This suggests that the choice for a specific ICL repair pathway is, at least in part, dependent on the type of ICL. A critical step in ICL repair by the FA pathway is the unhooking of the crosslink from one of the two DNA strands. This step requires activation of the pathway by ubiquitylation of FANCD2-FANCI that promotes the recruitment of the incision complex consisting of the endonuclease XPF(FANCD2)-ERCC1 and the scaffold protein SLX4(FANCD2) (Hodskinson *et al.*, 2014, Klein Douwel *et al.*, 2014, Knipscheer *et al.*, 2009). However, mechanistic details of this important step are currently missing.

SLX4 is a large scaffold protein that interacts with many proteins including the three endonucleases XPF-ERCC1, MUS81-EME1, and SLX1 (Figure 1A). In addition to its role in ICL repair, SLX4 acts in several other genome maintenance pathways such as homologous recombination, telomere maintenance, and the resolution of stalled replication forks (Kim,

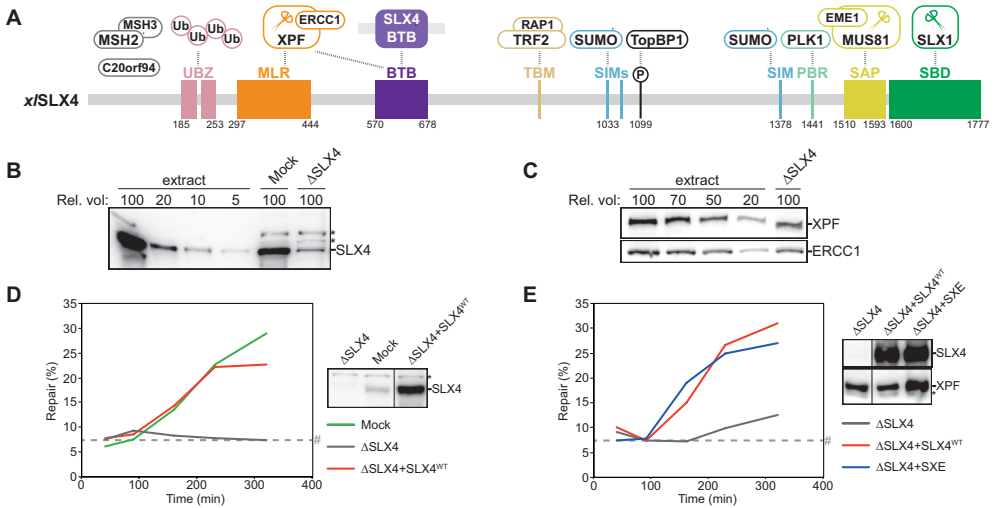


Figure 1: SLX4 depletion inhibits ICL repair in *Xenopus* egg extracts. A) Schematic illustration of the domain organization and interaction partners of SLX4 mapped on the *Xenopus laevis* SLX4 sequence. Protein interactions are represented by dashed lines. Interaction partners with unknown SLX4 interaction sites are shown in grey. Endonucleases are marked with scissors. Domain boundaries are based on previous reports (Gritenaite *et al.*, 2014, Guervilly *et al.*, 2015, Kim *et al.*, 2011, Kim *et al.*, 2013, Svendsen *et al.*, 2009). Interaction sites that do not align well with the *Xenopus laevis* sequence are not numbered and may not be conserved. Especially TRF2 interaction may be human specific (Wilson *et al.*, 2013). B) Mock- and SLX4-depleted nucleoplasmic egg extract (NPE) were analyzed by western blot using α -SLX4 antibody. A dilution series of undepleted extract was loaded on the same blot to determine the degree of depletion. A relative volume of 100 corresponds to 0.4 μ L NPE. C) As in (B) but using α -XPF (upper panel) or α -ERCC1 antibody (lower panel). D) Mock-depleted (Mock), SLX4-depleted (Δ SLX4), and SLX4-depleted NPE complemented with wild-type SLX4 (Δ SLX4+SLX4^{WT}) were analyzed by western blot using α -SLX4 antibody (right panel). These extracts, with SLX4-depleted high-speed supernatant (HSS) extract, were used to replicate pICL. Repair efficiency was calculated and plotted (left panel). A higher than endogenous concentration of recombinant SLX4 was required for complete rescue, likely due to partially loss of function of the recombinant protein during purification. E) SLX4-depleted (Δ SLX4), and SLX4-depleted NPE complemented with wild-type SLX4 (Δ SLX4+SLX4^{WT}) or wild-type SLX4 and XPF-ERCC1 (Δ SLX4+SXE) were analyzed by western blot using α -SLX4 or α -XPF antibodies (right panel). These extracts, with SLX4-depleted HSS, were used to replicate pICL. Repair efficiency was calculated and plotted (left panel). Line within blot indicates position where irrelevant lanes were removed. *, background band. #, SapI fragments from contaminating uncrosslinked plasmid present in varying degrees in different pICL preparations. See also Figure S1.

2014). These different functions are thought to be mediated by specific interactions with its binding partners. The three endonucleases bound to SLX4 affect each other's activity and substrate specificity, and together they can cleave essentially all branched DNA structures (Wyatt *et al.*, 2017). The complex of SLX4-SLX1 and MUS81-EME1 is activated in the G2/M cell cycle phase and mediates the resolution of late replication intermediates and Holliday junctions (HJs) (West *et al.*, 2015, West & Chan, 2017). The interactions of SLX4 with XPF-ERCC1, and possibly SLX1, are required for ICL repair (Castor *et al.*, 2013, Guervilly *et al.*, 2015, Kim *et al.*, 2013). In addition to the endonucleases, SLX4 interacts with the mismatch repair proteins MSH2 and MSH3, the uncharacterized open reading frame C20orf94, the telomere-binding factor TRF2, the regulator of DNA damage response TopBP1, and the mitotic kinase PLK1 (Duda *et al.*, 2016, Gritenaite *et al.*, 2014, Svendsen *et al.*, 2009, Wyatt *et al.*, 2013, Yin *et al.*, 2016). Finally, SLX4 contains several ubiquitin- and SUMO-interaction

domains (UBZs and SIMs, respectively), which are implicated in ICL repair, HJ resolution and replication stress response (Figure 1A) (Gonzalez-Prieto *et al.*, 2015, Guervilly *et al.*, 2015, Kim *et al.*, 2013, Lachaud *et al.*, 2014, Ouyang *et al.*, 2015).

We previously demonstrated that XPF-ERCC1 is required for ICL unhooking and is recruited to the site of damage by SLX4 (Klein Douwel *et al.*, 2014). The interaction of SLX4 with XPF seems to be mostly mediated by the MUS312/MEI9 interaction-like (MLR) domain of SLX4, but the Broad-Complex, Tramtrack and Bric-a-brac (BTB) domain has also been implicated (Figure 1A) (Andersen *et al.*, 2009, Guervilly *et al.*, 2015, Klein Douwel *et al.*, 2017, Yildiz *et al.*, 2002). In addition, the BTB domain plays a role in SLX4 dimerization (Guervilly *et al.*, 2015, Kim *et al.*, 2013, Yin *et al.*, 2016). So, while the recruitment of XPF-ERCC1 by SLX4 is crucial for ICL repair, the molecular basis for this recruitment is not fully understood.

Another important outstanding question concerns the identity of the second endonuclease that is likely required for ICL unhooking. Although *in vitro* reconstitution experiments have shown that XPF-ERCC1 can promote dual unhooking incisions on fork-like DNA templates (Hodskinson *et al.*, 2014, Kuraoka *et al.*, 2000), most models of ICL repair envision the involvement of a second, 5' flap, endonuclease (Crossan & Patel, 2012, Cybulski & Howlett, 2011, Kim, 2014, Zhang & Walter, 2014). Since SLX1 incises 5' flap substrates and interacts with SLX4, this is a plausible candidate. Consistent with a role for SLX1 in ICL repair it has been shown that SLX1 deficient cells are sensitive to ICL inducing agents (Andersen *et al.*, 2009, Castor *et al.*, 2013, Munoz *et al.*, 2009, Svendsen *et al.*, 2009).

The *Xenopus* egg extract system has been used by us and others to dissect biochemical details of replication-coupled DNA interstrand crosslink repair (Budzowska *et al.*, 2015, Fu *et al.*, 2011, Hoogenboom *et al.*, 2017, Knipscheer *et al.*, 2009, Long *et al.*, 2011, Räschle *et al.*, 2008, Zhang *et al.*, 2015). The use of a plasmid containing a sequence specific cisplatin ICL in this system circumvents the requirement of ICL inducing agents that generate a large fraction of non-ICL DNA lesions. Here, we used this system to examine the function of nuclease-interacting domains of SLX4 in the repair of cisplatin ICLs. We find that while SLX1 strongly associates with SLX4 in our extract, it is not required for ICL repair. Furthermore, the C-terminal half of SLX4, including the BTB domain, the SIMs, and interaction sites for MUS81, PLK1, and TopBP1 are dispensable for repair. In contrast, XPF-binding to the MLR domain of SLX4 is crucial for XPF recruitment and subsequent ICL repair. In addition to XPF-interaction, we demonstrate that the MLR domain also plays a role in efficient recruitment of SLX4 to the site of damage. Together, our findings provide novel insights into the role of SLX4 and its interaction partners in replication-dependent ICL repair.

Results

SLX4 depletion does not co-deplete essential ICL repair factors

SLX4 is a multi-domain protein that interacts with many factors and acts in several genome maintenance pathways (Figure 1A) (Kim, 2014, Svendsen *et al.*, 2009). Its role in DNA repair is mediated by the interaction with the endonucleases XPF-ERCC1, MUS81-EME1 and SLX1. Although SLX4 and its binding partners have been analyzed biochemically (Wyatt *et al.*, 2017), a clear view of which of the SLX4 domains are important for which DNA repair pathway is missing. To study the role of SLX4 in ICL repair we made use of the *Xenopus*

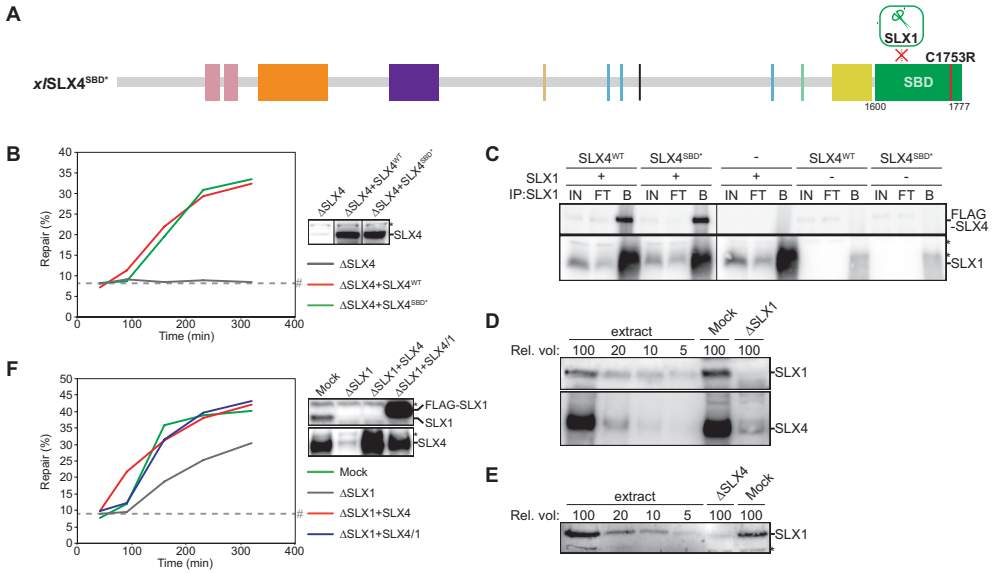


Figure 2: SLX1 is not required for ICL repair in *Xenopus* egg extracts. A) Schematic illustration of the $xSLX4^{SBD^*}$ mutant protein. The C1753R mutation, indicated by a red line, is predicted to disrupt interaction with SLX1. B) SLX4-depleted ($\Delta SLX4$), and SLX4-depleted NPE complemented with wild-type SLX4 ($\Delta SLX4 + SLX4^{WT}$) or mutant SLX4 ($\Delta SLX4 + SLX4^{SBD^*}$) were analyzed by western blot using α -SLX4 antibody (right panel). These extracts, with SLX4-depleted HSS, were used to replicate piCL. Repair efficiency was calculated and plotted (left panel). Line within blot indicates position where irrelevant lanes were removed. C) SLX1, wild-type and mutant SLX4 (SLX4^{WT} and SLX4^{SBD*} respectively) were individually expressed in Sf9 insect cells. Cells were lysed and indicated lysates were mixed and incubated. SLX1 was immunoprecipitated using PAS-conjugated α -SLX1 antibodies. The input (IN), flow-through (FT), and bound fractions (B) were analyzed by western blot using α -FLAG (upper panel) and α -SLX1 antibodies (lower panel). Line within blot indicates position where irrelevant lanes were removed. D) Mock- and SLX1-depleted NPE were analyzed by western blot using α -SLX1 (upper panel) and α -SLX4 antibodies (lower panel). A dilution series of undepleted extract was loaded on the same blots to determine the degree of depletion. A relative volume of 100 corresponds to 0.4 μ L NPE. E) Mock- and SLX4-depleted NPE were analyzed by western blot using α -SLX1 antibody. A dilution series of undepleted extract was loaded on the same blot to determine the degree of depletion. A relative volume of 100 corresponds to 0.4 μ L NPE. F) Mock-depleted (Mock), SLX1-depleted ($\Delta SLX1$), and SLX1-depleted NPE complemented with wild-type SLX4 ($\Delta SLX1 + SLX4^{WT}$) or SLX4-SLX1 complex ($\Delta SLX1 + SLX4/1$) were analyzed by western blot using α -SLX1 (upper right panel) and α -SLX4 antibodies (lower right panel). These extracts, with SLX1-depleted HSS, were used to replicate piCL. Repair efficiency was calculated and plotted (left panel). *, background band. #, SapI fragments from contaminating uncrosslinked plasmid present in varying degrees in different piCL preparations. See also Figure S2.

egg extract system that recapitulates replication-coupled ICL repair *in vitro* (Räschle *et al.*, 2008). We previously demonstrated that immunodepletion of XPF-ERCC1 co-depletes the vast majority of SLX4 from extract, and that ICL repair in XPF-ERCC1 depleted extracts is only rescued when both XPF-ERCC1 and SLX4 are supplemented (Klein Douwel *et al.*, 2014). To biochemically dissect the function of SLX4 we raised an antibody against *Xenopus laevis* SLX4 ($xSLX4$) and immunodepleted it from egg extract. Immunodepletion of SLX4 removed roughly 90% of the protein from extract and co-depleted about 50% of XPF-ERCC1 (Figure 1B and C), confirming that XPF-ERCC1 is present in excess compared to SLX4 (Klein Douwel *et al.*, 2014).

To investigate the effect of SLX4-depletion on ICL repair we replicated a plasmid containing a cisplatin interstrand crosslink (pICL) in a mock- and SLX4-depleted egg extract. Replication intermediates were isolated and repair efficiency was determined by measuring the regeneration of a Sapl recognition site that is blocked by the ICL prior to repair (Räschle *et al.*, 2008). In contrast to mock depletion, depletion of SLX4 completely abrogated ICL repair (Figure 1D, Supplemental Figure S1D). This defect was rescued upon addition of recombinant *x*/SLX4 (Figure 1D, Supplemental Figure S1B and D) indicating that no essential factors were co-depleted. To assess whether the 50% co-depletion of XPF-ERCC1 had a negative effect on the repair efficiency we added additional recombinant XPF-ERCC1 (Supplemental Figure S1C), however this did not affect the repair efficiency (Figure 1E, Supplemental Figure S1E). This indicates that the residual XPF-ERCC1 left after SLX4 depletion interacts with recombinant SLX4 to promote efficient ICL repair. Next, we used this experimental setup to study the role of the various SLX4 domains and interactors in ICL repair.

The endonuclease SLX1 is not required for ICL repair

SLX1 is a 5' flap endonuclease that is only active when in complex with SLX4 (Gaur *et al.*, 2015). Several reports have demonstrated a cellular sensitivity to ICL-inducing agents in the absence of SLX1 (Andersen *et al.*, 2009, Castor *et al.*, 2013, Munoz *et al.*, 2009). Accordingly, a model has been suggested in which SLX1 acts together with XPF-ERCC1 to perform the dual unhooking incisions during ICL repair (Zhang & Walter, 2014). However, SLX1-deficient cells are less sensitive to ICL-inducing agents compared to SLX4-deficient cells, and mouse models display a stronger phenotype when SLX4 is compromised (Wyatt & West, 2014). In addition, the stability of SLX1 seems to depend on the presence of SLX4 (Castor *et al.*, 2013, Munoz *et al.*, 2009, Wilson *et al.*, 2013), which further complicates the conclusions based on sensitivity data. To determine whether SLX1 is specifically required for ICL repair we first generated an SLX1 interaction mutant of SLX4, SLX4^{SBD*} (Figure 2A, Supplemental Figure S2A and B). This *x*/SLX4 C1753R mutation is equivalent to previously reported mutations situated in the C-terminal SLX1-binding domain (SBD) of the mouse and human proteins (Castor *et al.*, 2013, Wilson *et al.*, 2013). We immunodepleted SLX4 from egg extract, complemented the extract with SLX4^{SBD*} or wildtype SLX4 (SLX4^{WT}), and examined ICL repair efficiency (Supplemental Figure S2C). Strikingly, the SLX4^{SBD*} mutant complemented the ICL repair defect of the SLX4-depleted extract with the same efficiency as SLX4^{WT}, suggesting that the interaction with SLX1 is not required for ICL repair (Figure 2B, Supplemental Figure S2E).

To confirm that SLX4^{SBD*} disrupts the interaction with SLX1 efficiently we raised antibodies against *Xenopus laevis* SLX1 (Supplemental Figure S2F) and performed binding assays using recombinant proteins. To this end, SLX1, SLX4^{WT}, and SLX4^{SBD*} were overexpressed in insect cells, and their interaction was examined by immunoprecipitation with the SLX1 antibody. To our surprise, SLX4^{WT} and SLX4^{SBD*} co-precipitated with SLX1 with similar efficiency (Figure 2C), indicating that SLX4^{SBD*} mutant still interacts with SLX1. Although it has been shown that this mutant fails to rescue the reduced stability of SLX1 upon SLX4 depletion in mouse cells, a direct interaction assay was not reported (Castor *et al.*, 2013, Wilson *et al.*, 2013). Therefore, this mutant could affect the SLX1 affinity enough to destabilize SLX1 in SLX4 deficient cells but could still favour interaction in our overexpression setting. Nonetheless, we reasoned another method to test the function of

SLX1 in ICL repair was required. Therefore, we directly immunodepleted SLX1 from *Xenopus* egg extract. This not only depleted over 95% of SLX1, but also co-depleted ~90% SLX4 and ~50% XPF-ERCC1 (Figure 2D, Supplemental Figure S2G). Vice versa, SLX4 depletion co-depleted SLX1 to a large extent, indicating that SLX1 and SLX4 are mostly in complex in *Xenopus* egg extract (Figure 2E). We then examined ICL repair in the SLX1-depleted extract and detected a moderate repair defect compared to mock-depleted extract (Figure 2F, Supplemental Figure S2H). This defect was fully restored by addition of recombinant SLX4-SLX1 but also by SLX4 alone (Supplemental Figure S2D). This shows that the repair defect upon SLX1 depletion was caused by co-depletion of SLX4. We therefore conclude that SLX1 is not required for ICL repair in our system. Notably, these data also show that SLX1 does not play a role in the resolution of HR intermediates during ICL repair.

The C-terminal domains of SLX4 are dispensable for ICL repair

We previously demonstrated that the endonuclease MUS81-EME1 is not essential for ICL repair in *Xenopus* egg extracts (Klein Douwel *et al.*, 2014). Both MUS81-EME1 and SLX1 interact with the C-terminus of SLX4, suggesting that this region may not be required for ICL repair. Consistently, a truncated form of SLX4, lacking the C-terminal half, can partially rescue the sensitivity of SLX4 deficient cells to the ICL inducing agent mitomycin C (Hodskinson *et al.*, 2014). To assess the importance of the C-terminal domain in ICL repair directly, we generated the equivalent truncation mutant *x*/SLX4¹⁻⁸⁴⁰ (Figure 3A, Supplemental Figure S3A). In addition to the MUS81 and SLX1 interaction sites, this mutant also lacks the SUMO interaction motifs (SIMs), and the PLK1 and TopBP1 interaction sites. To verify that this mutant does not interact with SLX1 we overexpressed SLX1, SLX4^{WT}, SLX4^{SBD*} and SLX4¹⁻⁸⁴⁰ in insect cells and tested interaction by SLX4 immunoprecipitations. While wildtype SLX4 and the SBD mutant co-precipitated SLX1 efficiently, the C-terminal truncation mutant did not (Figure 3B). We then purified SLX4¹⁻⁸⁴⁰ protein and added this mutant, or SLX4^{WT}, to an SLX4-depleted extract (Supplemental Figure S3B). The truncation mutant rescued the

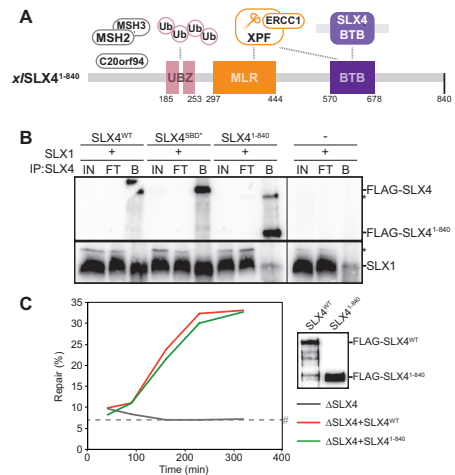


Figure 3: The N-terminal half of SLX4 is sufficient to support ICL repair.

A) Schematic illustration of the *x*/SLX4¹⁻⁸⁴⁰ mutant protein. This protein is truncated at residue 840. **B)** SLX1, wild-type SLX4 (SLX4^{WT}) and SLX4 mutants (SLX4^{MUT}) were individually expressed in Sf9 insect cells. Cells were lysed and indicated lysates were mixed and incubated. SLX4 was immunoprecipitated using PAS-conjugated α -SLX4 antibodies. The input (IN), flow-through (FT), and bound fractions (B) were analyzed by western blot using α -FLAG (upper panel) and α -SLX1 antibodies (lower panel). Line within blot indicates position where irrelevant lanes were removed. **C)** SLX4-depleted (Δ SLX4), and SLX4-depleted NPE complemented with wild-type SLX4 (Δ SLX4+SLX4^{WT}) or mutant SLX4 (Δ SLX4+SLX4¹⁻⁸⁴⁰), were used with SLX4-depleted HSS to replicate pICL. Repair efficiency was calculated and plotted (left panel). Protein dilutions of wild-type SLX4 (SLX4^{WT}) and mutant SLX4 (SLX4¹⁻⁸⁴⁰) were analyzed by western blot using α -FLAG antibody to ensure equivalent protein concentrations (right panel). *, background band. #, SapI fragments from contaminating uncrosslinked plasmid present in varying degrees in different pICL preparations. See also Figure S3.

ICL repair defect of the SLX4-depleted extract with the same efficiency as SLX4^{WT} (Figure 3C, Supplemental Figure S3C), indicating that the C-terminal half of SLX4 is dispensable for its function in ICL repair. These data show that the N-terminal half of SLX4 contains all essential domains for ICL repair, and that the SIMs, and the interactions with SLX1, MUS81, PLK1, and TopBP1 are not required.

The MLR domain is crucial for XPF-ERCC1 recruitment and important for localization of SLX4 to ICLs

During ICL repair, SLX4 recruits the endonuclease XPF-ERCC1 to the site of damage, which promotes ICL unhooking (Klein Douwel *et al.*, 2014). The major XPF interaction site on SLX4 has been mapped to the MUS312/MEI9 interaction-like (MLR) domain, while the BTB domain likely contains a secondary interaction site (Andersen *et al.*, 2009, Crossan *et al.*, 2011, Fekairi *et al.*, 2009, Guervilly *et al.*, 2015, Kim *et al.*, 2013, Klein Douwel *et al.*, 2017). Mutations in the MLR domain of SLX4 sensitize cells to ICL-inducing agents, suggesting this domain is important for ICL repair (Guervilly *et al.*, 2015, Hashimoto *et al.*, 2015, Kim *et al.*, 2013). To test this directly we purified α SLX4^{ΔMLR} (Figure 4A, Supplemental Figure S4A and D) and examined XPF interaction in *Xenopus* egg extract. We found that while SLX4^{WT} and SLX4¹⁻⁸⁴⁰ interacted with XPF, SLX4^{ΔMLR} did not (Figure 4E, Supplemental Figure S3D, and (Klein Douwel *et al.*, 2017)). Importantly, we analyzed the mutant protein by circular dichroism and showed that the spectra for the mutant and wildtype protein are highly similar, indicating that the deletion does not change the overall structure (Supplemental Figure S4F). We then tested whether the α SLX4^{ΔMLR} protein was able to rescue the ICL repair defect after SLX4 depletion. In contrast to SLX4^{WT}, SLX4^{ΔMLR} failed to rescue repair efficiency (Figure 4C, Supplemental Figure S4G). This confirms that the MLR domain of SLX4 is crucial for ICL repair, most likely by recruiting XPF-ERCC1 to the site of damage.

While XPF-ERCC1 depends on SLX4 for its localization to the ICL, the localization of SLX4 to the site of damage is independent of XPF-ERCC1 (Klein Douwel *et al.*, 2014). This leads to the prediction that SLX4^{ΔMLR} localizes to ICLs but is unable to recruit XPF-ERCC1. To test this, we employed chromatin immunoprecipitations (ChIP) of XPF and SLX4. Because our crosslinked plasmid contains a site-specific ICL we can monitor SLX4 and XPF recruitment specifically to the damage site during repair (Fu *et al.*, 2011, Klein Douwel *et al.*, 2014, Klein Douwel *et al.*, 2017, Long *et al.*, 2014, Long *et al.*, 2011). We replicated pICL in an SLX4-depleted extract supplemented with SLX4^{ΔMLR} or SLX4^{WT} and performed immunoprecipitations with XPF and SLX4 antibodies followed by quantitative PCR. As predicted, XPF was recruited to the ICL site during repair in the presence of SLX4^{WT} but not in the presence of SLX4^{ΔMLR} (Figure 4D, Supplemental Figure S4H). However, when we performed ChIP on the same samples with an SLX4 antibody we found that the SLX4^{ΔMLR} protein itself was also poorly recruited to the site of damage compared to SLX4^{WT} (Figure 4D, Supplemental Figure S4H). This suggests that the MLR domain is involved in SLX4 recruitment to the ICL. Consequently, we cannot distinguish whether the lack of recruitment of XPF-ERCC1 to the ICL, and the failure to support ICL repair, is caused by a defect in SLX4 or XPF localization to the ICL.

To clarify this, we generated an additional SLX4 mutant with point mutations in residues that were shown to be involved in XPF-binding (Guervilly *et al.*, 2015, Hashimoto *et al.*, 2015) (Figure 4B, Supplemental Figure S4B and C) and purified this α SLX4^{MLR*} mutant from insect cells (Supplemental Figure S4E). Similar to SLX4^{ΔMLR}, SLX4^{MLR*} failed

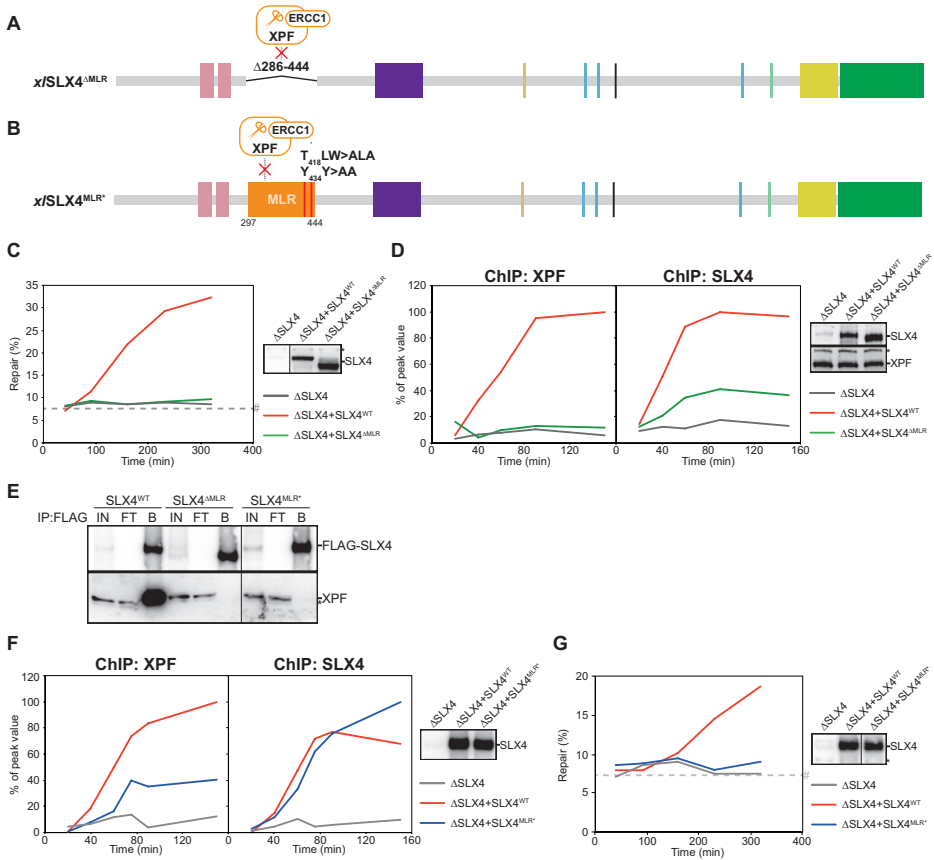


Figure 4: The MLR domain ensures XPF-binding and contributes to SLX4-recruitment to ICLs.

A) Schematic illustration of the $xSLX4^{\Delta MLR}$ mutant protein. The residues 286-444, including the MLR domain, are replaced by a short linker, indicated by a black line. This deletion is predicted to disrupt interaction with XPF-ERCC1. B) Schematic illustration of the $xSLX4^{MLR*}$ mutant protein. The four point mutations in the MLR domain, T418A, W420A, Y434A, and Y435A, are indicated by two red lines and predicted to disrupt interaction with XPF-ERCC1. C) SLX4-depleted ($\Delta SLX4$), and SLX4-depleted NPE complemented with wild-type SLX4 ($\Delta SLX4+SLX4^{WT}$) or mutant SLX4 ($\Delta SLX4+SLX4^{\Delta MLR}$) were analyzed by western blot using α -SLX4 antibody (right panel). These extracts, with SLX4-depleted HSS, were used to replicate pICL. Repair efficiency was calculated and plotted (left panel). Line within blot indicates position where irrelevant lanes were removed. D) SLX4-depleted ($\Delta SLX4$), and SLX4-depleted NPE complemented with wild-type SLX4 ($\Delta SLX4+SLX4^{WT}$) or mutant SLX4 ($\Delta SLX4+SLX4^{\Delta MLR}$) were analyzed by western blot using α -SLX4 (upper right panel) and α -XPF antibodies (lower right panel). These extracts, with SLX4-depleted HSS, were used to replicate pICL. Samples were taken at various times and immunoprecipitated with α -XPF (left panel) or α -SLX4 antibodies (middle panel). Co-precipitated DNA was isolated and analyzed by quantitative PCR using the pICL or pQuant primers. Recovery values of pQuant were subtracted from pICL recovery values. The resulting data were plotted as the percentage of peak value with the highest value within one experiment set to 100%. E) Purified wild-type SLX4 ($SLX4^{WT}$) or mutant SLX4 ($SLX4^{MUT}$) were added to HSS. After incubation, recombinant SLX4 was immunoprecipitated using anti-FLAG M2 affinity gel (Sigma). The input (IN), flow-through (FT), and bound fractions (B) were analyzed by western blot using α -FLAG (upper panel) and α -XPF antibodies (lower panel). Line within blot indicates position where irrelevant lanes were removed. F) As in (D) but using the $xSLX4^{MLR*}$ mutant protein. G) As in (C) but using the $xSLX4^{MLR*}$ mutant protein. Line within blot indicates position where irrelevant lanes were removed. *, background band. #, Sapl fragments from contaminating uncrosslinked plasmid present in varying degrees in different pICL preparations. See also Figure S4.

to co-precipitate XPF from *Xenopus* egg extract (Figure 4E), confirming that this mutant is defective in XPF interaction. We then tested the recruitment of the SLX4^{MLR*} mutant to the ICL by CHIP and found that, in contrast to SLX4^{ΔMLR}, this mutant was recruited to the ICL efficiently (Figure 4F, Supplemental Figure S4I). However, recruitment of XPF in presence of the SLX4^{MLR*} mutant was severely compromised (Figure 4F, Supplemental Figure S4I). Consistent with this, SLX4^{MLR*} did not rescue the ICL repair defect after SLX4-depletion (Figure 4G, Supplemental Figure S4J). These data show that efficient interaction of SLX4 with XPF-ERCC1 via its MLR domain is crucial for ICL repair. Moreover, it indicates that, in addition to XPF recruitment, the MLR domain harbours an additional function in localizing SLX4 to the ICL.

The BTB domain contributes to SLX4-dimerization but is not crucial for ICL repair

In addition to the MLR domain, the BTB domain of SLX4 has also been associated with XPF interaction (Andersen *et al.*, 2009, Guervilly *et al.*, 2015, Klein Douwel *et al.*, 2017), as well as with dimerization (Guervilly *et al.*, 2015, Perez-Torrado *et al.*, 2006, Yin *et al.*, 2016). BTB mutants are mildly sensitive to ICL inducing agents (Guervilly *et al.*, 2015, Kim *et al.*, 2013, Yin *et al.*, 2016) suggesting a function for this domain in ICL repair. However, whether this is mediated by dimerization or XPF interaction is not clear. To address the role of the BTB domain in ICL repair, we purified α SLX4^{BTB*}, a mutant that was reported to affect SLX4 homodimerization and XPF interaction (Guervilly *et al.*, 2015, Yin *et al.*, 2016) (Figure 5A, Supplemental Figure S4F and S5A, C, D). First, we added this mutant to egg extract and examined XPF interaction by immunoprecipitation. SLX4^{BTB*} precipitated similar levels of XPF compared to SLX4^{WT} (Figure 5C), indicating that this mutant does not affect XPF-SLX4 interaction in our extract. To assess the effect of BTB-domain mutation on ICL repair, we added purified SLX4^{BTB*} or SLX4^{WT} to SLX4-depleted extract and monitored repair efficiency. We found that mutating the BTB domain only had a minor effect on ICL repair (Figure 5D, Supplemental Figure S5F). To test whether SLX4^{BTB*} is compromised in dimerization we co-expressed His-tagged SLX4^{WT} and FLAG-tagged SLX4^{WT} or SLX4^{BTB*} in Sf9 cells and examined their co-precipitation. Surprisingly, we found no reduction in dimerization for the SLX4^{BTB*} mutant in the presence or absence of benzonase, indicating that this interaction is not mediated through DNA (Figure 5E, compare lanes 9, 12, 15, and 18).

Since the SLX4^{BTB*} mutant had no dimerization or XPF interaction defect, and no major defect in ICL repair we decided to generate another SLX4 truncation mutant, containing residues 1-558, lacking the C-terminus including the entire BTB domain (Figure 5B, Supplemental Figure S5B and E). This truncation was based on a mutation found in a Fanconi anemia patient (Kim *et al.*, 2011). SLX4¹⁻⁵⁵⁸ interacted normally with XPF (Supplemental Figure S5G) and surprisingly, it fully rescued ICL repair efficiency after SLX4 depletion (Figure 5F, Supplemental Figure S5H). This indicates that ICL repair can occur in the absence of the BTB domain. When testing dimerization we observed that SLX4¹⁻⁵⁵⁸ was still able to dimerize, although this was reduced compared to SLX4^{WT} (Figure 5G, Supplemental Figure S5I, compare lanes 6 and 9). This suggests that the BTB domain is involved in dimerization but other sites on α SLX4 also play a role in this. Collectively, this suggests that although the BTB domain of SLX4 is not crucial for ICL repair, dimerization of SLX4 could still have a role.

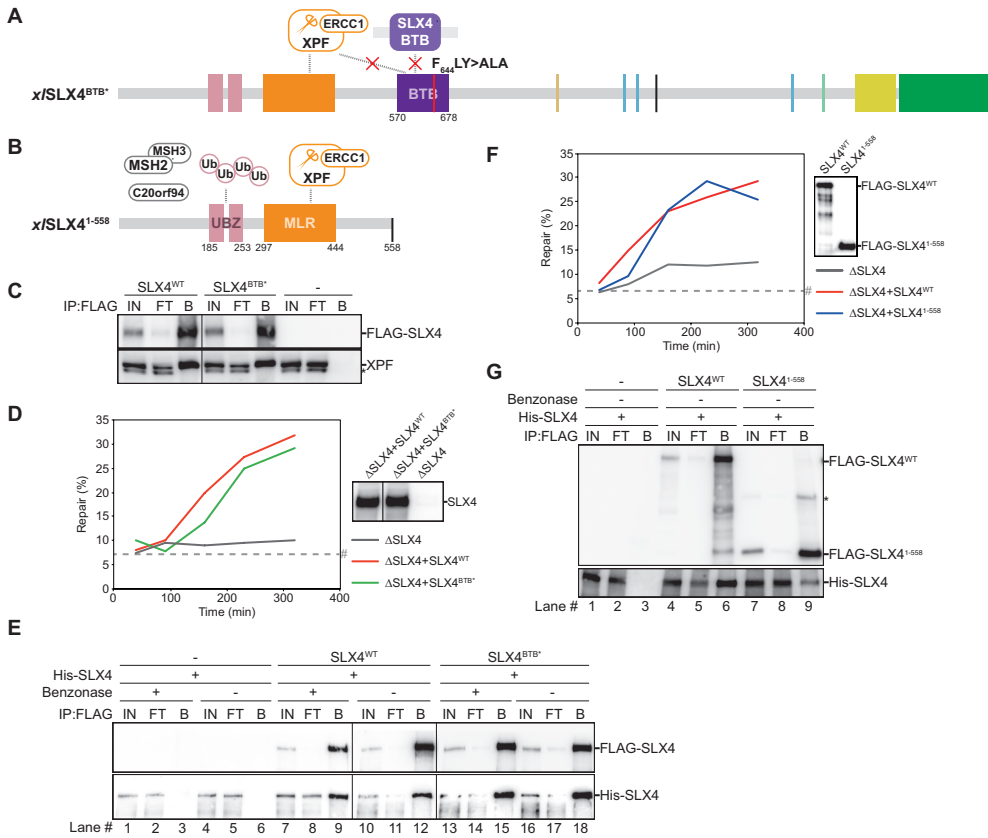


Figure 5: The BTB domain is not absolutely required for ICL repair but contributes to SLX4 dimerization. A) Schematic illustration of the $xSLX4^{BTB}$ mutant protein. The two point mutations in the BTB domain, F644A and Y646A, are indicated by a red line and predicted to affect SLX4 dimerization and XPF positioning. B) Schematic illustration of the $xSLX4^{1-558}$ mutant protein. This protein is truncated at residue 558. C) Purified wild-type SLX4 ($SLX4^{WT}$), mutant SLX4 ($SLX4^{BTB}$) or buffer (-) were added to HSS. After incubation, recombinant SLX4 was immunoprecipitated using anti-FLAG M2 affinity gel (Sigma). The input (IN), flow-through (FT), and bound fractions (B) were analyzed by western blot using α -FLAG (upper panel) and α -XPF antibodies (lower panel). Line within blot indicates position where irrelevant lanes were removed. D) SLX4-depleted ($\Delta SLX4$), and SLX4-depleted NPE complemented with wild-type SLX4 ($\Delta SLX4+SLX4^{WT}$) or mutant SLX4 ($\Delta SLX4+SLX4^{BTB}$) were analyzed by western blot using α -SLX4 antibody (right panel). These extracts, with SLX4-depleted HSS, were used to replicate pICL. Repair efficiency was calculated and plotted (left panel). Line within blot indicates position where irrelevant lanes were removed. E) Wild-type ($SLX4^{WT}$) or mutant SLX4 ($SLX4^{BTB}$) containing an N-terminal FLAG-tag and a C-terminal Strep-tag, were co-expressed with wild-type SLX4 containing an N-terminal His-tag and a C-terminal Strep-tag (His-SLX4) in Sf9 insect cells. Cells were lysed and FLAG-tagged SLX4 was immunoprecipitated using anti-FLAG M2 affinity gel (Sigma). To examine the contribution of DNA to SLX4-dimerization the cell lysates were split during the immunoprecipitation step and treated with benzonase (Sigma) (+) or buffer (-). The input (IN), flow-through (FT), and bound fractions (B) were analyzed by western blot using α -FLAG and α -His antibodies. Line within blot indicates position where irrelevant lanes were removed. F) SLX4-depleted ($\Delta SLX4$), and SLX4-depleted NPE complemented with wild-type SLX4 ($\Delta SLX4+SLX4^{WT}$) or mutant SLX4 ($\Delta SLX4+SLX4^{1-558}$), were used with SLX4-depleted HSS to replicate pICL. Repair efficiency was calculated and plotted (left panel). Protein dilutions of wild-type SLX4 ($SLX4^{WT}$) and mutant SLX4 ($SLX4^{1-558}$) were analyzed by western blot using α -FLAG antibody to ensure equivalent protein concentrations (right panel). G) As in (E) but using the $xSLX4^{1-558}$ mutant protein and without benzonase treatment. *, background band. #, SapI fragments from contaminating uncrosslinked plasmid present in varying degrees in different pICL preparations. See also Figure S5.

Discussion

A key step in the Fanconi anemia pathway for ICL repair is the ICL unhooking by backbone incisions on either side of the crosslink. SLX4(FANCP) exerts a central role in this step; upon its localization to the ICL, which is facilitated by ubiquitylation of FANCI-FANCD2, it directly recruits XPF-ERCC1 to promote unhooking incisions. It has been suggested that SLX4 has additional roles during ICL repair but this has not been shown directly. Here, we use *Xenopus* egg extracts to define ICL repair specific functions of SLX4. Our data indicate that the SLX4 interacting endonuclease SLX1 is not required for ICL repair, and therefore that SLX4 does not position two different endonucleases around the crosslink for unhooking. In addition, we find that the BTB domain of SLX4 does not play a major role in ICL repair. Finally, an essential domain for ICL repair is the MLR domain located on the N-terminal half of SLX4. We show that the MLR domain provides the major interaction site for XPF but it is also involved in the localization of SLX4 to the site of damage.

While it has been reported that SLX1 knockdown causes cellular sensitivity to crosslinking agents we demonstrated that efficient ICL repair can take place in the absence of SLX1 in *Xenopus* egg extracts (Figure 2) (Andersen *et al.*, 2009, Castor *et al.*, 2013, Munoz *et al.*, 2009, Svendsen *et al.*, 2009). This can be explained by the fact that SLX1 is required to repair other types of DNA damage that are induced by crosslinking agents. In support of this view, it has been shown that SLX1-SLX4 interaction is required for resistance to camptothecin and PARP inhibitors, and SLX1, together with SLX4 and MUS81, can process Holliday junction intermediates (Castor *et al.*, 2013, Kim *et al.*, 2013, Wyatt *et al.*, 2017). It is also consistent with the reports showing that cells deficient in SLX4, a known player in ICL repair, are much more sensitive to, and show more chromosomal instability upon treatment with ICL-inducing agents, compared to SLX1 deficient cells (Andersen *et al.*, 2009, Castor *et al.*, 2013, Fekairi *et al.*, 2009, Sarbajna *et al.*, 2014, Svendsen *et al.*, 2009). Although we show that interstrand crosslinks can be repaired without SLX1, we do not exclude that SLX1 plays a role in the repair of a subset of ICLs, or in specific cell types or conditions. In addition, another nuclease could act redundantly with SLX1 in *Xenopus* egg extract while this backup mechanism is less active in cells.

An important outstanding question is which nucleases play a role in ICL unhooking in the FA pathway. To date, the only nuclease found crucial for this step is XPF-ERCC1, further supported by the identification of XPF/FANCP as a FA complementation group (Bogliolo *et al.*, 2013, Kashiya *et al.*, 2013, Klein Douwel *et al.*, 2014). A model in which two different nucleases act in ICL unhooking has been mostly envisioned (Crossan & Patel, 2012, Sengerova *et al.*, 2011, Zhang & Walter, 2014). This second nuclease is not likely to be SLX1, MUS81, or FAN1 (Figure 2 and (Klein Douwel *et al.*, 2014)), although it is still possible that some of these could act redundantly. In addition, models have been proposed in which the first incision by XPF-ERCC1 is followed by exonuclease activity of SNM1A beyond the ICL leading to unhooking (Amunugama *et al.*, 2018, Wang *et al.*, 2011). Finally, XPF-ERCC1 could perform both unhooking incisions, as suggested based on experiments with fork-like DNA templates and purified proteins (Fisher *et al.*, 2008, Hodskinson *et al.*, 2014, Kuraoka *et al.*, 2000). In fact, SLX4 dimerization could promote a similar model in which two XPF-ERCC1 complexes are recruited to each ICL to perform dual incisions. Although this might not be the most likely model due to the strict substrate specificity of XPF-ERCC1, a recent study has suggested a similar model where SLX4 dimerization acts to bridge two MUS81 molecules for controlled breakage of stalled replication intermediates

(Duda *et al.*, 2016).

The role of SLX4 in ICL repair includes, but is not necessarily limited to, unhooking incisions. Downstream events in the pathway include double strand break (DSB) repair via homologous recombination (HR). In cells, SLX4-SLX1 promotes homologous recombination by Holliday junction resolution at G2/M phase, when CDK1 and PLK1 activate MUS81-EME1 by phosphorylation. This induces binding to SLX4-SLX1-XPF-ERCC1, thereby forming an active HJ resolving enzyme (Wyatt *et al.*, 2017, Wyatt *et al.*, 2013). Our finding that the C-terminal half of SLX4 is not required for ICL repair, supported by data that MUS81 and SLX1 are dispensable for ICL repair, suggests that SLX4 plays no preferred role during HR in the FA pathway (Figure 2, Figure 3, (Klein Douwel *et al.*, 2014)).

Our observation that SLX4¹⁻⁸⁴⁰ is fully functional in ICL repair further suggests that SLX4 interaction with PLK1, TopBP1, and SUMOylated factors is dispensable for this process. Instead, SLX4 likely employs these factors for its roles in other genome maintenance pathways (Gritenaite *et al.*, 2014, Guervilly *et al.*, 2015, Ouyang *et al.*, 2015, West *et al.*, 2015, Yin *et al.*, 2016). Mutation of the three SUMO interaction motifs in SLX4 has led to variable effects on ICL sensitivity: in one study it had no effect (Ouyang *et al.*, 2015), while in two other studies it caused a very mild sensitivity to MMC (Gonzalez-Prieto *et al.*, 2015, Guervilly *et al.*, 2015). We show that the SIMs are not required for the repair of cisplatin interstrand crosslinks (Figure 3), however, they could play a role in other types of ICLs such as those induced by MMC.

The MLR domain of SLX4 has been shown to mediate the recruitment of XPF-ERCC1 to damage foci in cells and we previously demonstrated that it directly promotes the interaction with XPF-ERCC1 (Crossan *et al.*, 2011, Kim *et al.*, 2013, Klein Douwel *et al.*, 2017). Using MLR domain mutants we now show that the interaction between SLX4 and XPF-ERCC1 is crucial for ICL repair (Figure 4). In addition to preventing XPF-interaction, deletion of the MLR domain prevents efficient SLX4-recruitment to ICL sites. Since SLX4 is recruited to ICLs independently of XPF (Klein Douwel *et al.*, 2014), this indicates a novel function for the MLR domain in SLX4 localization. It is currently believed that recruitment of SLX4 to ICL damage sites is mediated by the UBZ domains (Kim *et al.*, 2011, Lachaud *et al.*, 2014), however, whether this is through a direct interaction, or mediated by another factor is currently unclear (Lachaud *et al.*, 2014, Yamamoto *et al.*, 2011). Our finding that an additional SLX4 domain is involved in ICL recruitment is important for further studies on how SLX4 is recruited to ICLs.

To examine the importance of the BTB domain of SLX4 in ICL repair we generated a C-terminal truncation lacking this domain based on an FA patient mutation. Notably, in the cells of this patient the mutant protein was not detected indicating that the absence of SLX4 protein is likely the cause of the FA phenotype (Kim *et al.*, 2011, Kim *et al.*, 2013). Overexpression of this patient mutant, consisting of the N-terminal 671 residues of SLX4 followed by 119 non-SLX4 residues, partially rescued MMC sensitivity. In addition, disruption of the SLX4 BTB domain in human cells has been shown to cause a very minor (Yin *et al.*, 2016) to mild sensitivity to ICL-inducing agents (Guervilly *et al.*, 2015, Kim *et al.*, 2013), suggesting that the BTB domain is not absolutely required for ICL repair. Consistent with this, we find that deletion of the BTB domain does not affect ICL repair in our system. The mild effect of BTB mutations in cells could be caused by reduced XPF interaction, and/or defective SLX4 dimerization as was demonstrated previously (Guervilly *et al.*, 2015). However, we and others have not observed a defect in XPF interaction in

BTB mutants (Figure 5C, Supplementary Figure S5I and (Kim *et al.*, 2013)). Although our previous work suggested that there is a transient interaction between XPF and the SLX4 BTB domain, this could also be mediated by another site on SLX4 (Klein Douwel *et al.*, 2017). Mutations in the BTB domain seem to have a greater effect on dimerization of the human SLX4 compared to the *Xenopus laevis* SLX4 (Guervilly *et al.*, 2015, Yin *et al.*, 2016). However, we find that *x*SLX4 lacking the BTB domain is still able to dimerize, albeit less efficient compared to wildtype. It is possible that an alternative dimerization site plays a more important role in *Xenopus laevis* SLX4 which could explain why the BTB mutants still support efficient ICL repair in our system.

Materials and methods

Xenopus egg extracts and DNA replication and repair assay

DNA replication assays and preparation of *Xenopus* egg extracts were performed as described previously (Tutter & Walter, 2006, Walter *et al.*, 1998). Preparation of plasmid with a site-specific cisplatin ICL (pICL), and ICL repair assays were performed as described (Enoiu *et al.*, 2012, Räschle *et al.*, 2008). Briefly, pICL was first incubated in a high-speed supernatant (HSS) of egg cytoplasm for 20 minutes, which promotes the assembly of prereplication complexes on the DNA. Addition of two volumes nucleoplasmic egg extract (NPE), which also contained ^{32}P - α -dCTP, triggers a single round of DNA replication. Aliquots of replication reactions (5 μL) were stopped at various times with nine volumes Stop II solution (0.5% SDS, 10 mM EDTA, 50 mM Tris pH 7.5). Sample were incubated with RNase (0.13 $\mu\text{g}/\mu\text{L}$) for 30 minutes at 37°C followed by proteinase K (0.5 $\mu\text{g}/\mu\text{L}$) overnight (O/N) at RT. DNA was extracted using phenol/chloroform, ethanol-precipitated in the presence of glycogen (30 mg/mL) and resuspended in 5 μL 10 mM Tris pH 7.5. ICL repair was analyzed by digesting 1 μL extracted DNA with HincII, or HincII and SapI, separation on a 0.8% native agarose gel, and quantification using autoradiography. Repair efficiency was calculated as described (Knipscheer *et al.*, 2012). As repair kinetics and absolute efficiency is dependent on the egg extract preparation and depletion conditions, we always use a positive and negative control condition in each experiment using the same extract.

Antibodies and immunodepletions

Antibodies against *x*XPF and *x*ERCC1 were previously described (Klein Douwel *et al.*, 2014). An antibody against *x*SLX4 that was previously described (Klein Douwel *et al.*, 2014) was used for detection by western blot. An additional SLX4 antibody was raised against residues 275-509 of *x*SLX4. The antigen was overexpressed in bacteria, purified by his-tag affinity purification and denaturing PAGE, and used for immunization of rabbits (PRF&L, Canadensis, USA). This antibody was used for immunodepletions and immunoprecipitations of SLX4. The antibody against SLX1 was raised against residues 93-282 of *x*SLX1 and generated similar to the *x*SLX4 antibody. Specificity of the antiserum was confirmed using western blot (Supplemental Figure S2F). The anti-FLAG M2 antibody was purchased from Sigma and anti-His antibody from Westburg. To deplete egg extracts of SLX4, one volume protein A sepharose Fast Flow (PAS) (GE Healthcare) was bound to 2.5 volumes α -SLX4 serum or pre-immune serum and washed extensively: twice with PBS, once with ELB (10 mM HEPES-KOH pH 7.7, 50 mM KCl, 2.5 mM MgCl_2 , and 250

mM Sucrose), twice with ELB + 0.5 M NaCl, and twice with ELB. One volume antibody-bound PAS mixture was then mixed with 5.0 or 6.5 volumes NPE or HSS, respectively, incubated for 20 minutes at room temperature (RT), after which the extract was harvested. This procedure was repeated twice for NPE and once for HSS. To deplete egg extracts of SLX1, one volume PAS was bound to 3.5 volumes α -SLX1 serum or pre-immune serum and washed as previously described. One volume antibody-bound PAS mixture was mixed with 4.5 volumes NPE or HSS, incubated for 20 minutes at RT, after which the extract was harvested. This procedure was repeated twice for NPE and once for HSS. After the last depletion round, extracts were collected and immediately used for DNA replication assays. The mock, SLX1, or SLX4 depleted HSS was diluted 2x prior to addition to NPE to reduce protein levels further.

Recombinant protein expression and purification

Xenopus laevis SLX4 containing an N-terminal FLAG-, or his-tag, and a C-terminal Strep-tag, was cloned into pDONR201 (Life Technologies). *Xenopus laevis* SLX1 containing a C-terminal FLAG-tag was also cloned into pDONR201. Point mutations for SLX4^{SBD*}, SLX4^{MLR*}, and SLX4^{BTB*} mutants were introduced in pDONR-FLAG-strep-SLX4 using QuikChange site-directed mutagenesis (Agilent Technologies). Similarly, a stop codon was cloned at position 559 in pDONR-FLAG-strep-SLX4 for the generation of the SLX4¹⁻⁵⁵⁸ mutant, which consequently lacks the C-terminal Strep-tag. The MLR domain was deleted by PCR amplification of flanking regions that were ligated by the introduction of a short linker containing a KpnI restriction site. An in-gene reverse primer was used to clone SLX4⁸⁴⁰ in pDONR201, this deletion mutant does not contain a C-terminal Strep-tag to maximize resemblance to mini-SLX4 (Hodkinson *et al.*, 2014). Baculoviruses were produced using the BaculoDirect system following manufacturer's protocol (Life Technologies). Proteins were expressed in suspension cultures of Sf9 insect cells by infection with xSLX4 viruses for 65 h. Cells from 150 mL culture were collected by centrifugation, resuspended in 6 mL lysis buffer (50 mM Tris pH 8.0, 250 mM NaCl, 0.1% NP-40, 5% glycerol, 0.4 mM PMSF, 1 tablet/10 mL Complete Mini EDTA-free Protease Inhibitor Cocktail (Roche)), and lysed by sonication. The soluble fraction obtained after centrifugation (20,000 \times g for 20 minutes at 4°C) was incubated for 1 hour at 4°C with 250 μ L anti-FLAG M2 affinity gel (Sigma) that was pre-washed with lysis buffer. After incubation, the beads were washed with 40 mL wash buffer I (50 mM Tris pH 8.0, 250 mM NaCl, 0.1% NP-40, 5% glycerol, 0.4 mM PMSF) and subsequently with 30 mL wash buffer II (20 mM Tris pH 8.0, 200 mM NaCl, 0.1% NP-40, 5% glycerol, 0.1 mM PMSF, 10 μ g/mL aprotinin/leupeptin). The xSLX4 protein was eluted in wash buffer II containing 100 μ g/mL 3 \times FLAG peptide (Sigma). The protein was aliquoted, flash frozen, and stored at -80°C. Expression and purification of xSLX4 mutant proteins were identical to the wild-type protein. Proteins analyzed by circular dichroism (CD) were separately expressed and purified to avoid the presence of chloride ions in the buffers. (NH₄)₂SO₄ was used instead of NaCl and Tris buffers were adjusted with phosphoric acid instead of HCl. Expression and purification of xSLX4-xSLX1 protein complexes were similar to xSLX4 proteins, with only minor deviations listed here. Proteins were expressed by co-infection with xSLX4 and xSLX1 viruses. Lysis buffer and wash I buffer contained 1 mM PMSF; wash II buffer contained 40 mM Tris pH 8.0, 0.08% NP-40, 4% glycerol, and 1 mM PMSF. The xXPF-hsERCC1 complex was prepared as previously described (Klein Douwel *et al.*, 2014).

Immunoprecipitations

Immunoprecipitations (IPs) were performed in cell lysates from Sf9 cells expressing recombinant proteins, or from *Xenopus* egg extracts. For IPs from insect cell lysates, proteins were individually expressed in adherent Sf9 insect cell cultures by infection with x/SLX1 or x/SLX4 (or x/SLX4 mutants) viruses for 65 h. Cells were collected, resuspended in 550 μ L lysis buffer (50 mM Tris pH 8.0, 300 mM NaCl, 1% Triton, 4 mM EDTA, 10 μ g/mL aprotinin/leupeptin), and lysed by sonication. After centrifugation (20,000 \times g for 20 minutes at 4°C) the soluble fractions were collected. The x/SLX1 soluble fraction (250 μ L) was mixed with the x/SLX4 (or x/SLX4 mutants) soluble fraction (250 μ L) and incubated for 1 hour at 4°C to allow protein binding. Five volumes PAS were mixed with one volume α -SLX4 or α -SLX1 sera, incubated at 4°C for 1 hour, and washed with lysis buffer. Antibody-bound PAS (8 μ L) was added to 200 μ L of the soluble fraction mixtures followed by a 30-minute incubation at 4°C. The beads were washed using 2 mL lysis buffer, taken up in 30 μ L 2 \times SDS sample buffer, and incubated for 4 minutes at 95°C. Proteins were separated by SDS-PAGE and visualized by western blot using indicated antibodies.

For IPs from *Xenopus* egg extract, x/SLX4 (or x/SLX4 mutants) was added to HSS at a concentration of 5 ng/ μ L. To each 10 μ L extract, 55 μ L IP buffer (1 \times ELB salts, 0.25 M sucrose, 75 mM NaCl, 2 mM EDTA, 10 μ g/mL aprotinin/leupeptin, 0.1% NP-40) and 10 μ L pre-washed FLAG M2 beads (Sigma-Aldrich) were added. Beads were incubated for 60 minutes at 4°C and subsequently washed using 2.5 mL IP buffer. Beads were taken up in 30 μ L 2 \times SDS sample buffer and incubated for 4 minutes at 95°C. Proteins were separated by SDS-PAGE and visualized by western blot using the indicated antibodies.

Proteins were expressed in adherent cultures of Sf9 insect cells in 6-well plates by co-infection with His-x/SLX4 and FLAG-x/SLX4 (or FLAG-x/SLX4 mutants) viruses for 65 h. Cells were resuspended in medium and collected by centrifugation, resuspended in 250 μ L lysis buffer (50 mM Tris pH 8.0, 300 mM NaCl, 1% Triton, 4 mM EDTA, 10 μ g/mL aprotinin/leupeptin), and lysed by sonication. After centrifugation (20,000 \times g for 20 minutes at 4°C), 200 μ L soluble fraction was incubated for 30 minutes at 4°C with 8 μ L FLAG M2 beads (Sigma-Aldrich) that were pre-washed with lysis buffer. When benzonase treatment was included in the experiment the fractions were split in two, 0.25 μ L benzonase (Sigma-Aldrich) or buffer was added and incubation was continued for another 30 minutes. After incubation, the beads were washed using 2 mL lysis buffer. Beads were taken up in 30 μ L 2 \times SDS sample buffer and incubated for 5 minutes at 95°C. Proteins were separated by SDS-PAGE and visualized by western blot using respective antibodies.

Chromatin immunoprecipitation

Chromatin immunoprecipitation (ChIP) was performed as described previously (Pacek *et al.*, 2006). Briefly, reaction samples were crosslinked with formaldehyde, sonicated to yield DNA fragments of roughly 100-500 bp, and immunoprecipitated with the indicated antibodies. Protein-DNA crosslinks were reversed and DNA was phenol/chloroform-extracted for analysis by quantitative real-time PCR with the following primers: pICL (5'-AGCCAGATTTTCTCCTCTC-3' and 5'-CATGCATTGGTTCTGCACTT-3') and pQuant (5'-TACAAATGTACGGCCAGCAA-3' and 5'-GAGTATGAGGAAGCGGTGA-3'). pQuant was analyzed to determine non-specific localization to undamaged DNA. The values from pQuant primers were subtracted from the values for pICL primers to establish

the specific recruitment to ICL sites.

Circular dichroism

Far-UV circular dichroism (CD) experiments were performed on a J-810 spectropolarimeter (Jasco) using a quartz glass cuvette with an optical pathlength of 1 mm at room temperature. Experimental parameters included a wavelength increment of 2 nm and SLX4 concentrations ranging from 55-137 ng/ μ L as determined by Coomassie staining. In some cases the protein was recovered after analysis, diluted 2.5 times with 5M GuHCl or demineralized water and measured again. The resulting spectra are buffer- and concentration-corrected averages of 4 scans in the range of 200-250 nm (native) or 212-250 nm (denatured). The reported mean residue ellipticity (MRE) values were obtained using the molecular mass, total number of amino acids and protein concentration of each SLX4 preparation.

Funding

This work was supported by the Netherlands organization for Scientific Research (VIDI 700.10.421 to P.K.) and a project grant from the Dutch Cancer Society (KWF HUBR 2015-7736 to P.K.).

Acknowledgements

We thank Koichi Sato and Alice Bolner for critical reading of the manuscript and Eefjan Breukink (Utrecht University) for help with the circular dichroism experiments. We thank Julie Schouten for technical assistance, Daisy Klein Douwel for helpful discussions, the Hubrecht animal caretakers for animal support, and the other members of the Knipscheer laboratory for feedback.

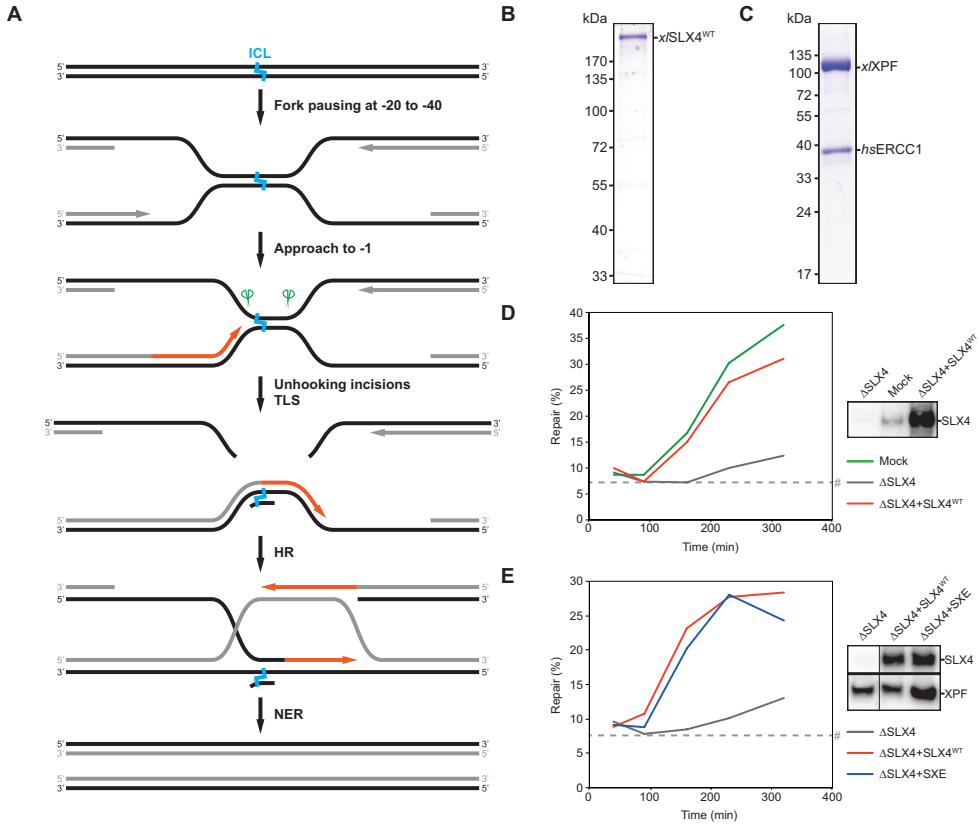
References

- Akkari YM, Bateman RL, Reifsteck CA, Olson SB & Grompe M (2000) DNA replication is required To elicit cellular responses to psoralen-induced DNA interstrand cross-links. *Molecular and cellular biology* 20: 8283-9
- Amunugama R, Willcox S, Wu RA, Abdullah UB, El-Sagheer AH, Brown T, McHugh PJ, Griffith JD & Walter JC (2018) Replication Fork Reversal during DNA Interstrand Crosslink Repair Requires CMG Unloading. *Cell reports* 23: 3419-3428
- Andersen SL, Bergstralh DT, Kohl KP, LaRocque JR, Moore CB & Sekelsky J (2009) Drosophila MUS312 and the vertebrate ortholog BTBD12 interact with DNA structure-specific endonucleases in DNA repair and recombination. *Molecular cell* 35: 128-35
- Bogliolo M, Schuster B, Stoepker C, Derkunt B, Su Y, Raams A, Trujillo JP, Minguillon J, Ramirez MJ, Pujol R, Casado JA, Banos R, Rio P, Knies K, Zuniga S, Benitez J, Bueren JA, Jaspers NG, Scharer OD, de Winter JP et al. (2013) Mutations in ERCC4, encoding the DNA-repair endonuclease XPF, cause Fanconi anemia. *American journal of human genetics* 92: 800-6
- Budzowska M, Graham TG, Sobeck A, Waga S & Walter JC (2015) Regulation of the Rev1-pol zeta complex during bypass of a DNA interstrand crosslink. *The EMBO journal* 34: 1971-85
- Castor D, Nair N, Declais AC, Lachaud C, Toth R, Macartney TJ, Lilley DM, Arthur JS & Rouse J (2013) Cooperative control of holliday junction resolution and DNA repair by the SLX1 and MUS81-EME1 nucleases. *Molecular cell* 52: 221-33
- Cheng G, Shi Y, Sturla SJ, Jalas JR, McIntee EJ, Villalta PW, Wang M & Hecht SS (2003) Reactions of formaldehyde plus acetaldehyde with deoxyguanosine and DNA: formation of cyclic deoxyguanosine adducts and formaldehyde crosslinks. *Chem Res Toxicol* 16: 145-52
- Crossan GP & Patel KJ (2012) The Fanconi anaemia pathway orchestrates incisions at sites of crosslinked DNA. *The Journal of pathology* 226: 326-37
- Crossan GP, van der Weyden L, Rosado IV, Langevin F, Gaillard PH, McIntyre RE, Sanger Mouse Genetics P, Gallagher F, Kettunen MI, Lewis DY, Brindle K, Arends MJ, Adams DJ & Patel KJ (2011) Disruption of mouse Slx4, a regulator of structure-specific nucleases, phenocopies Fanconi anemia. *Nature genetics* 43: 147-52
- Cybulski KE & Howlett NG (2011) FANCP/SLX4: a Swiss army knife of DNA interstrand crosslink repair. *Cell Cycle* 10: 1757-63
- Deans AJ & West SC (2011) DNA interstrand crosslink repair and cancer. *Nat Rev Cancer* 11: 467-80
- Duda H, Arter M, Gloggnitzer J, Teloni F, Wild P, Blanco MG, Altmeyer M & Matos J (2016) A Mechanism for Controlled Breakage of Under-replicated Chromosomes during Mitosis. *Dev Cell* 39: 740-755
- Enoiu M, Jiricny J & Scharer OD (2012) Repair of cisplatin-induced DNA interstrand crosslinks by a replication-independent pathway involving transcription-coupled repair and translesion synthesis. *Nucleic acids research* 40: 8953-64
- Fekairi S, Scaglione S, Chahwan C, Taylor ER, Tissier A, Coulon S, Dong MQ, Ruse C, Yates JR, 3rd, Russell P, Fuchs RP, McGowan CH & Gaillard PH (2009) Human SLX4 is a Holliday junction resolvase subunit that binds multiple DNA repair/recombination endonucleases. *Cell* 138: 78-89
- Fisher LA, Bessho M & Bessho T (2008) Processing of a psoralen DNA interstrand cross-link by XPF-ERCC1 complex in vitro. *The Journal of biological chemistry* 283: 1275-81
- Fu YV, Yardimci H, Long DT, Ho TV, Guainazzi A, Bermudez VP, Hurwitz J, van Oijen A, Scharer OD & Walter JC (2011) Selective bypass of a lagging strand roadblock by the eukaryotic replicative DNA helicase. *Cell* 146: 931-41
- Garaycochea JI, Crossan GP, Langevin F, Daly M, Arends MJ & Patel KJ (2012) Genotoxic consequences of endogenous aldehydes on mouse haematopoietic stem cell function. *Nature* 489: 571-5
- Gaur V, Wyatt HD, Komorowska W, Szczepanowski RH, de Sanctis D, Gorecka KM, West SC & Nowotny M (2015) Structural and Mechanistic Analysis of the Slx1-Slx4 Endonuclease. *Cell reports* 10: 1467-1476
- Gonzalez-Prieto R, Cuijpers SA, Luijsterburg MS, van Attikum H & Vertegaal AC (2015) SUMOylation and PARylation cooperate to recruit and stabilize SLX4 at DNA damage sites. *EMBO reports* 16: 512-9
- Gritenaite D, Princz LN, Szakal B, Bantele SC, Wendeler L, Schilbach S, Habermann BH, Matos J, Lisby M, Branzei D & Pfander B (2014) A cell cycle-regulated Slx4-Dpb11 complex promotes the resolution of DNA repair intermediates linked to stalled replication. *Genes & development* 28: 1604-19
- Guervilly JH, Takedachi A, Naim V, Scaglione S, Chawhan C, Lovera Y, Despras E, Kuraoka I, Kannouche P, Rosselli F & Gaillard PH (2015) The SLX4 complex is a SUMO E3 ligase that impacts on replication stress outcome and genome stability. *Molecular cell* 57: 123-37
- Hashimoto K, Wada K, Matsumoto K & Moriya M (2015) Physical interaction between SLX4 (FANCP) and XPF (FANCD1) proteins and biological consequences of interaction-defective missense mutations. *DNA repair* 35: 48-54
- Hira A, Yabe H, Yoshida K, Okuno Y, Shiraishi Y, Chiba K, Tanaka H, Miyano S, Nakamura J, Kojima S, Ogawa S, Matsuo K, Takata M & Yabe M (2013) Variant ALDH2 is associated with accelerated progression of bone marrow failure in Japanese Fanconi anemia patients. *Blood* 122: 3206-9
- Hodskinson MR, Silhan J, Crossan GP, Garaycochea

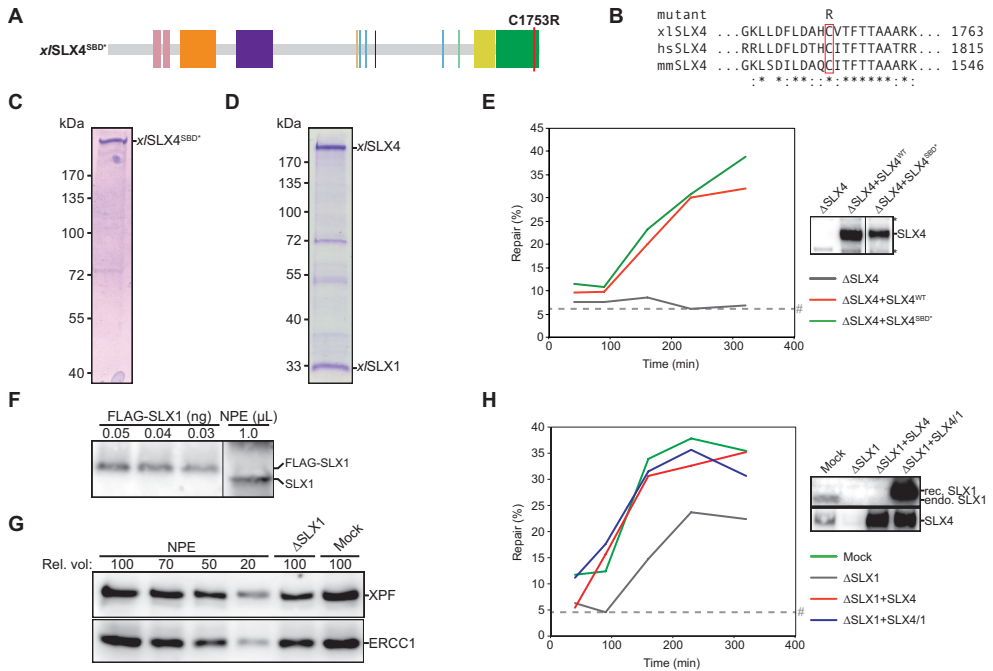
- Jl, Mukherjee S, Johnson CM, Scharer OD & Patel KJ (2014) Mouse SLX4 is a tumor suppressor that stimulates the activity of the nuclease XPF-ERCC1 in DNA crosslink repair. *Molecular cell* 54: 472-84
- Hoogenboom WS, Klein Douwel D & Knipscheer P (2017) *Xenopus* egg extract: A powerful tool to study genome maintenance mechanisms. *Dev Biol* 428: 300-309
- Huang J, Liu S, Bellani MA, Thazhathveetil AK, Ling C, de Winter JP, Wang Y, Wang W & Seidman MM (2013) The DNA translocase FANCM/MHF promotes replication traverse of DNA interstrand crosslinks. *Molecular cell* 52: 434-46
- Kashiyama K, Nakazawa Y, Pilz DT, Guo C, Shimada M, Sasaki K, Fawcett H, Wing JF, Lewin SO, Carr L, Li TS, Yoshiura K, Utani A, Hirano A, Yamashita S, Greenblatt D, Nardo T, Stefanini M, McGibbon D, Sarkany R *et al.* (2013) Malfunction of nuclease ERCC1-XPF results in diverse clinical manifestations and causes Cockayne syndrome, xeroderma pigmentosum, and Fanconi anemia. *American journal of human genetics* 92: 807-19
- Kim Y (2014) Nuclease delivery: versatile functions of SLX4/FANCP in genome maintenance. *Molecules and cells* 37: 569-74
- Kim Y, Lach FP, Desetty R, Hanenberg H, Auerbach AD & Smogorzewska A (2011) Mutations of the SLX4 gene in Fanconi anemia. *Nature genetics* 43: 142-6
- Kim Y, Spitz GS, Veturi U, Lach FP, Auerbach AD & Smogorzewska A (2013) Regulation of multiple DNA repair pathways by the Fanconi anemia protein SLX4. *Blood* 121: 54-63
- Klein Douwel D, Boonen RA, Long DT, Szybowska AA, Räschle M, Walter JC & Knipscheer P (2014) XPF-ERCC1 acts in Unhooking DNA interstrand crosslinks in cooperation with FANCD2 and FANCP/SLX4. *Molecular cell* 54: 460-71
- Klein Douwel D, Hoogenboom WS, Boonen RA & Knipscheer P (2017) Recruitment and positioning determine the specific role of the XPF-ERCC1 endonuclease in interstrand crosslink repair. *The EMBO journal* 36: 2034-2046
- Knipscheer P, Räschle M, Scharer OD & Walter JC (2012) Replication-coupled DNA interstrand cross-link repair in *Xenopus* egg extracts. *Methods Mol Biol* 920: 221-43
- Knipscheer P, Räschle M, Smogorzewska A, Enoiu M, Ho TV, Scharer OD, Elledge SJ & Walter JC (2009) The Fanconi anemia pathway promotes replication-dependent DNA interstrand cross-link repair. *Science* 326: 1698-701
- Kottemann MC & Smogorzewska A (2013) Fanconi anaemia and the repair of Watson and Crick DNA crosslinks. *Nature* 493: 356-63
- Kuraoka I, Kobertz WR, Ariza RR, Biggerstaff M, Essigmann JM & Wood RD (2000) Repair of an interstrand DNA cross-link initiated by ERCC1-XPF repair/recombination nuclease. *The Journal of biological chemistry* 275: 26632-6
- Lachaud C, Castor D, Hain K, Munoz I, Wilson J, MacArtney TJ, Schindler D & Rouse J (2014) Distinct functional roles for the two SLX4 ubiquitin-binding UBZ domains mutated in Fanconi anemia. *Journal of cell science* 127: 2811-7
- Langevin F, Crossan GP, Rosado IV, Arends MJ & Patel KJ (2011) Fancd2 counteracts the toxic effects of naturally produced aldehydes in mice. *Nature* 475: 53-8
- Long DT, Joukov V, Budzowska M & Walter JC (2014) BRCA1 promotes unloading of the CMG helicase from a stalled DNA replication fork. *Molecular cell* 56: 174-85
- Long DT, Räschle M, Joukov V & Walter JC (2011) Mechanism of RAD51-dependent DNA interstrand cross-link repair. *Science* 333: 84-7
- Munoz IM, Hain K, Declais AC, Gardiner M, Toh GW, Sanchez-Pulido L, Heuckmann JM, Toth R, Macartney T, Eppink B, Kanaar R, Ponting CP, Lilley DM & Rouse J (2009) Coordination of structure-specific nucleases by human SLX4/BTBD12 is required for DNA repair. *Molecular cell* 35: 116-27
- Ouyang J, Garner E, Hallet A, Nguyen HD, Rickman KA, Gill G, Smogorzewska A & Zou L (2015) Noncovalent interactions with SUMO and ubiquitin orchestrate distinct functions of the SLX4 complex in genome maintenance. *Molecular cell* 57: 108-22
- Pacek M, Tutter AV, Kubota Y, Takisawa H & Walter JC (2006) Localization of MCM2-7, Cdc45, and GINS to the site of DNA unwinding during eukaryotic DNA replication. *Molecular cell* 21: 581-7
- Perez-Torrado R, Yamada D & Defossez PA (2006) Born to bind: the BTB protein-protein interaction domain. *Bioessays* 28: 1194-202
- Räschle M, Knipscheer P, Enoiu M, Angelov T, Sun J, Griffith JD, Ellenberger TE, Scharer OD & Walter JC (2008) Mechanism of replication-coupled DNA interstrand crosslink repair. *Cell* 134: 969-80
- Ridpath JR, Nakamura A, Tano K, Luke AM, Sonoda E, Arakawa H, Buerstedde JM, Gillespie DA, Sale JE, Yamazoe M, Bishop DK, Takata M, Takeda S, Watanabe M, Swenberg JA & Nakamura J (2007) Cells deficient in the FANCD2/BRCA pathway are hypersensitive to plasma levels of formaldehyde. *Cancer Res* 67: 11117-22
- Rosado IV, Langevin F, Crossan GP, Takata M & Patel KJ (2011) Formaldehyde catabolism is essential in cells deficient for the Fanconi anemia DNA-repair pathway. *Nature structural & molecular biology* 18: 1432-4
- Sarbajna S, Davies D & West SC (2014) Roles of SLX1-SLX4, MUS81-EME1, and GEN1 in avoiding genome instability and mitotic catastrophe. *Genes & development* 28: 1124-36
- Semlow DR, Zhang J, Budzowska M, Drohat AC & Walter JC (2016) Replication-Dependent Unhooking of DNA Interstrand Cross-Links by the NEIL3 Glycosylase. *Cell* 167: 498-511 e14
- Sengerova B, Wang AT & McHugh PJ (2011)

- Orchestrating the nucleases involved in DNA interstrand cross-link (ICL) repair. *Cell Cycle* 10: 3999-4008
- Svendsen JM, Smogorzewska A, Sowa ME, O'Connell BC, Gygi SP, Elledge SJ & Harper JW (2009) Mammalian BTBD12/SLX4 assembles a Holliday junction resolvase and is required for DNA repair. *Cell* 138: 63-77
- Tutter AV & Walter JC (2006) Chromosomal DNA replication in a soluble cell-free system derived from *Xenopus* eggs. *Methods Mol Biol* 322: 121-37
- Voulgaridou G-P, Anastopoulos I, Franco R, Panayiotidis MI & Pappa A (2011) DNA damage induced by endogenous aldehydes: Current state of knowledge. *Mutation Research/Fundamental and Molecular Mechanisms of Mutagenesis* 711: 13-27
- Walden H & Deans AJ (2014) The Fanconi anemia DNA repair pathway: structural and functional insights into a complex disorder. *Annual review of biophysics* 43: 257-78
- Walter J, Sun L & Newport J (1998) Regulated chromosomal DNA replication in the absence of a nucleus. *Molecular cell* 1: 519-29
- Wang AT, Sengerova B, Cattell E, Inagawa T, Hartley JM, Kiakos K, Burgess-Brown NA, Swift LP, Enzlin JH, Schofield CJ, Gileadi O, Hartley JA & McHugh PJ (2011) Human SNM1A and XPF-ERCC1 collaborate to initiate DNA interstrand cross-link repair. *Genes & development* 25: 1859-70
- Wang M, McIntee EJ, Cheng G, Shi Y, Villalta PW & Hecht SS (2000) Identification of DNA adducts of acetaldehyde. *Chem Res Toxicol* 13: 1149-57
- West SC, Blanco MG, Chan YW, Matos J, Sarbajna S & Wyatt HD (2015) Resolution of Recombination Intermediates: Mechanisms and Regulation. *Cold Spring Harbor symposia on quantitative biology* 80: 103-9
- West SC & Chan YW (2017) Genome Instability as a Consequence of Defects in the Resolution of Recombination Intermediates. *Cold Spring Harbor symposia on quantitative biology* 82: 207-212
- Williams HL, Gottesman ME & Gautier J (2013) The differences between ICL repair during and outside of S phase. *Trends in biochemical sciences* 38: 386-93
- Wilson JS, Tejera AM, Castor D, Toth R, Blasco MA & Rouse J (2013) Localization-dependent and -independent roles of SLX4 in regulating telomeres. *Cell reports* 4: 853-60
- Wyatt HD, Laister RC, Martin SR, Arrowsmith CH & West SC (2017) The SMX DNA Repair Tri-nuclease. *Molecular cell* 65: 848-860 e11
- Wyatt HD, Sarbajna S, Matos J & West SC (2013) Coordinated actions of SLX1-SLX4 and MUS81-EME1 for Holliday junction resolution in human cells. *Molecular cell* 52: 234-47
- Wyatt HD & West SC (2014) Holliday junction resolvases. *Cold Spring Harb Perspect Biol* 6: a023192
- Yamamoto KN, Kobayashi S, Tsuda M, Kurumizaka H, Takata M, Kono K, Jiricny J, Takeda S & Hirota K (2011) Involvement of SLX4 in interstrand cross-link repair is regulated by the Fanconi anemia pathway. *Proceedings of the National Academy of Sciences of the United States of America* 108: 6492-6
- Yildiz O, Majumder S, Kramer B & Sekelsky JJ (2002) *Drosophila* MUS312 interacts with the nucleotide excision repair endonuclease MEI-9 to generate meiotic crossovers. *Molecular cell* 10: 1503-9
- Yin J, Wan B, Sarkar J, Horvath K, Wu J, Chen Y, Cheng G, Wan K, Chin P, Lei M & Liu Y (2016) Dimerization of SLX4 contributes to functioning of the SLX4-nuclease complex. *Nucleic acids research* 44: 4871-80
- Zhang J, Dewar JM, Budzowska M, Motnenko A, Cohn MA & Walter JC (2015) DNA interstrand cross-link repair requires replication-fork convergence. *Nature structural & molecular biology* 22: 242-7
- Zhang J & Walter JC (2014) Mechanism and regulation of incisions during DNA interstrand cross-link repair. *DNA repair* 19: 135-42

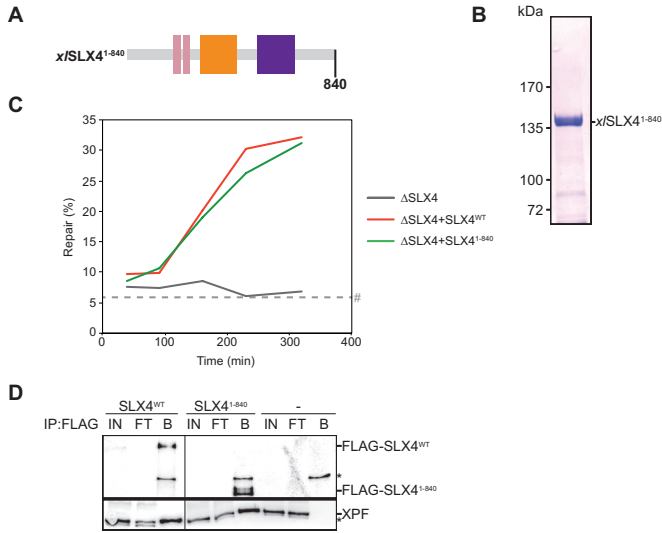
Supplemental Figures



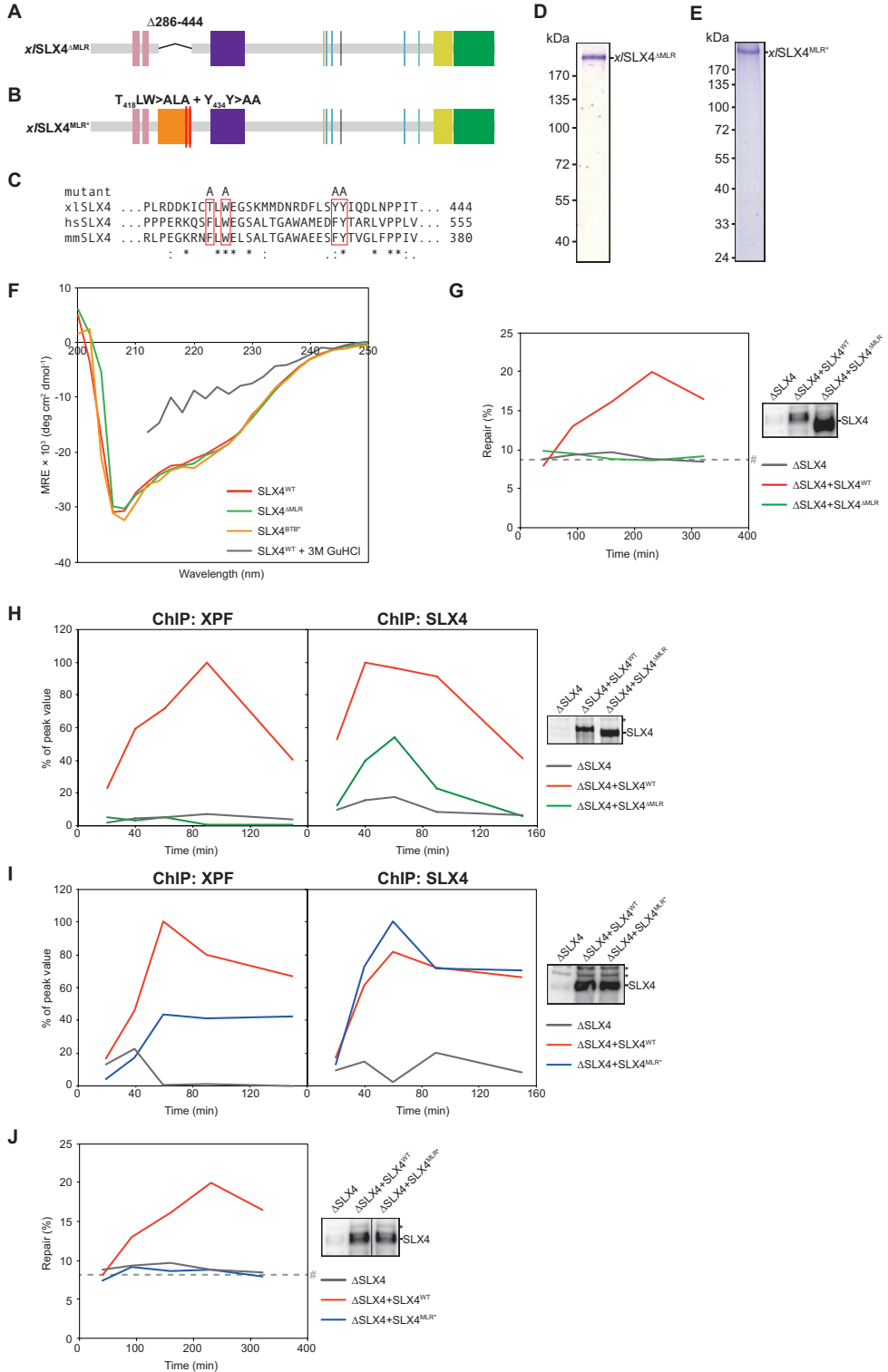
Supplemental Figure S1: Addition of SLX4 to SLX4-depleted extract rescues ICL repair. Related to Figure 1. A) Schematic representation of replication-dependent ICL repair in *Xenopus* egg extract. B) Recombinant x/SLX4^{WT}, containing an N-terminal FLAG-tag and a C-terminal Strep-tag, was expressed in Sf9 insect cells and isolated via affinity purification using anti-FLAG M2 affinity gel (Sigma). Purity and concentration were determined using Coomassie blue staining of samples on SDS-PAGE. C) Recombinant FLAG-x/XPF-His-hsERCC1 complex was isolated via affinity purification using NiNTA resin and anti-FLAG M2 affinity gel (Sigma). Purity and concentration were determined using Coomassie blue staining of samples on SDS-PAGE. D) Mock-depleted (Mock), SLX4-depleted (Δ SLX4), and SLX4-depleted NPE complemented with wild-type SLX4 (Δ SLX4+SLX4^{WT}) were analyzed by western blot using α -SLX4 antibody (right panel). These extracts, with SLX4-depleted HSS, were used to replicate pICL. Repair efficiency was calculated and plotted (left panel). Independent duplicate experiment related to Figure 1D. E) SLX4-depleted (Δ SLX4), and SLX4-depleted NPE complemented with wild-type SLX4 (Δ SLX4+SLX4^{WT}) or wild-type SLX4 and XPF-ERCC1 (Δ SLX4+SXE) were analyzed by western blot using α -SLX4 (upper right panel) or α -XPF antibodies (lower right panel). These extracts, with SLX4-depleted HSS, were used to replicate pICL. Repair efficiency was calculated and plotted (left panel). Line within blot indicates position where irrelevant lanes were removed. Independent duplicate experiment related to Figure 1E. #, SapI fragments from contaminating uncrosslinked plasmid present in varying degrees in different pICL preparations.



Supplemental Figure S2: SLX1 is not required for ICL repair. Related to Figure 2. A) Schematic illustration of the *x/SLX4^{SBD*}* mutant protein. The C1753R mutation is indicated by a red line. B) Fragment of a sequence alignment between *Xenopus laevis* (*x/SLX4*), human (*hsSLX4*), and mouse (*mmSLX4*) by Clustal Omega. The red box in the alignment indicates the residue in the wild-type proteins that are mutated in *SLX4^{SBD*}*, the R above the red box indicates the substitution to an arginine residue. (*), conserved residue; (:), conservative residue, (.), semi-conservative residue. C) Recombinant *x/SLX4^{SBD*}*, containing an N-terminal FLAG-tag and a C-terminal Strep-tag, was expressed in Sf9 insect cells and isolated via affinity purification using anti-FLAG M2 affinity gel (Sigma). Purity and concentration were determined using Coomassie blue staining of samples on SDS-PAGE. D) Recombinant *x/SLX4*, containing an N-terminal FLAG-tag and a C-terminal Strep-tag, and recombinant *x/SLX1*, containing an N-terminal FLAG-tag, were co-expressed in Sf9 cells and isolated via affinity purification using anti-FLAG M2 affinity gel (Sigma). Purity and concentration were determined using Coomassie blue staining of samples on SDS-PAGE. E) SLX4-depleted (Δ SLX4), and SLX4-depleted NPE complemented with wild-type SLX4 (Δ SLX4+SLX4^{WT}) or mutant SLX4 (Δ SLX4+SLX4^{SBD*}) were analyzed by western blot using α -SLX4 antibody (right panel). These extracts, with SLX4-depleted HSS, were used to replicate piCL. Repair efficiency was calculated and plotted (left panel). Line within blot indicates position where irrelevant lanes were removed. Independent duplicate experiment related to Figure 2B. F) NPE was analyzed by western blot using α -SLX1 antibody alongside a dilution series of purified *x/SLX4*-*x/SLX1* protein. Line within blot indicates position where irrelevant lanes were removed. G) Mock- and SLX1-depleted NPE were analyzed by western blot using α -XPF (upper panel) and α -ERCC1 antibodies (lower panel). A dilution series of undepleted extract was loaded on the same blots to determine the degree of depletion. A relative volume of 100 corresponds to 0.4 μ L NPE. H) Mock-depleted (Mock), SLX1-depleted (Δ SLX1), and SLX1-depleted NPE complemented with wild-type SLX4 (Δ SLX1+SLX4^{WT}) or wild-type SLX4-SLX1 complex (Δ SLX1+SLX4/1) were analyzed by western blot using α -SLX1 (upper right panel) and α -SLX4 antibodies (lower right panel). These extracts, with SLX1-depleted HSS, were used to replicate piCL. Repair efficiency was calculated and plotted (left panel). Independent duplicate experiment related to Figure 2F. *, background band. #, SapI fragments from contaminating uncrosslinked plasmid present in varying degrees in different piCL preparations.

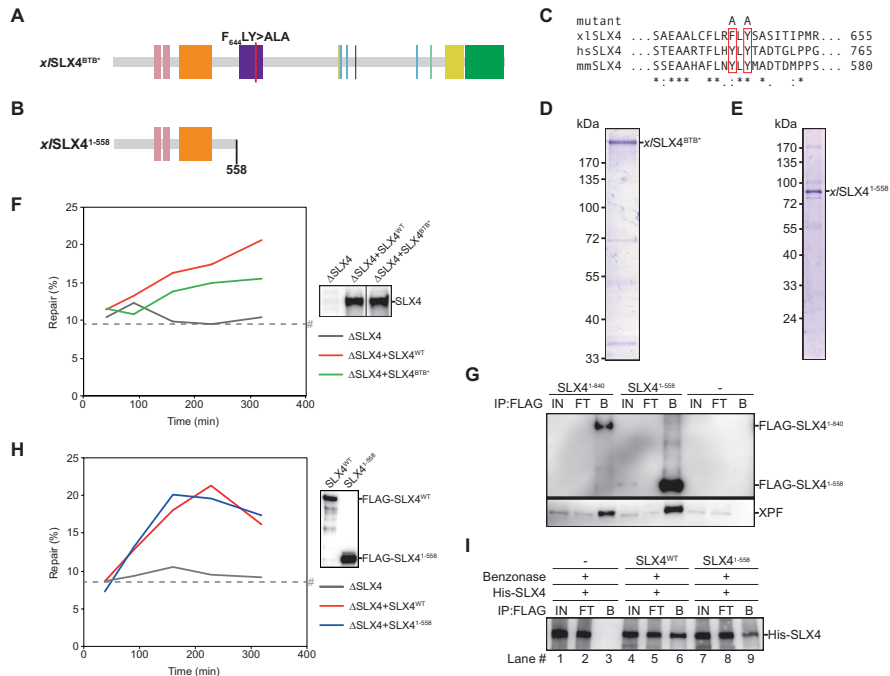


Supplemental Figure S3: The C-terminal half of SLX4 is dispensable for ICL repair. Related to Figure 3. A) Schematic illustration of the $x/SLX4^{\Delta C}$ mutant protein. This protein is truncated at residue 840. B) Recombinant $x/SLX4^{\Delta C}$, containing an N-terminal FLAG-tag, was expressed in Sf9 insect cells and isolated via affinity purification using anti-FLAG M2 affinity gel (Sigma). Purity and concentration were determined using Coomassie blue staining of samples on SDS-PAGE. C) SLX4-depleted ($\Delta SLX4$), and SLX4-depleted NPE complemented with wild-type SLX4 ($\Delta SLX4+SLX4^{WT}$) or mutant SLX4 ($\Delta SLX4+SLX4^{\Delta C}$), were used with SLX4-depleted HSS to replicate pICL. Repair efficiency was calculated and plotted. Independent duplicate experiment related to Figure 3C. D) Purified wild-type SLX4 ($SLX4^{WT}$), mutant SLX4 ($SLX4^{\Delta C}$) or buffer (-) were added to HSS. After incubation, recombinant SLX4 was immunoprecipitated using anti-FLAG M2 affinity gel (Sigma). The input (IN), flow-through (FT), and bound fractions (B) were analyzed by western blot using α -FLAG (upper panel) and α -XPF antibodies (lower panel). Line within blot indicates position where irrelevant lanes were removed. *, background band. #, SapI fragments from contaminating uncrosslinked plasmid present in varying degrees in different pICL preparations.



Supplemental Figure S4: The MLR domain is essential for ICL repair by binding XPF and contributes to SLX4 recruitment to ICLs. Related to Figure 4.

A) Schematic illustration of the $xSLX4^{AMLR}$ mutant protein. In this protein, residues 286-444 of $xSLX4$, representing the MLR domain, are replaced by a short linker (TGSGTGST), indicated by the black line. B) Schematic illustration of the $xSLX4^{MLR^*}$ mutant protein. In this protein, residues Thr418, Trp420, Tyr434, and Tyr435 are mutated to alanines, indicated by two red lines. C) Fragment of a sequence alignment between *Xenopus laevis* ($xSLX4$), human ($hsSLX4$), and mouse ($mmSLX4$) by Clustal Omega. The red boxes in the alignment indicate the residues in the wild-type proteins that are mutated in $SLX4^{MLR^*}$, the A's above the red boxes indicate the substitutions to alanine residues. (*), conserved residue; (:), conservative residue, (.), semi-conservative residue. D) Recombinant $xSLX4^{AMLR}$, containing an N-terminal FLAG-tag and a C-terminal Strep-tag, was expressed in Sf9 insect cells and isolated via affinity purification using anti-FLAG M2 affinity gel (Sigma). Purity and concentration were determined using Coomassie blue staining of samples on SDS-PAGE. E) As in (D), but for recombinant $xSLX4^{MLR^*}$. F) The structural integrity of $xSLX4^{AMLR}$ and $xSLX4^{BTB^*}$ was assessed by circular dichroism (CD). The spectra of purified wild-type ($SLX4^{WT}$) or mutant $SLX4$ ($SLX4^{MUT}$) were obtained by subtraction of the spectrum for buffer without $SLX4$ protein. The measurements were repeated after addition of 3M guanidine hydrochloride (GuHCl) to denature the protein (only $SLX4^{WT}$ shown here). The spectra are shown as mean residue ellipticity (MRE). G) $SLX4$ -depleted ($\Delta SLX4$), and $SLX4$ -depleted NPE complemented with wild-type $SLX4$ ($\Delta SLX4+SLX4^{WT}$) or mutant $SLX4$ ($\Delta SLX4+SLX4^{AMLR}$) were analyzed by western blot using α - $SLX4$ antibody (right panel). These extracts, with $SLX4$ -depleted HSS, were used to replicate pICL. Repair efficiency was calculated and plotted (left panel). Independent duplicate experiment related to Figure 4C. H) $SLX4$ -depleted ($\Delta SLX4$), and $SLX4$ -depleted NPE complemented with wild-type $SLX4$ ($\Delta SLX4+SLX4^{WT}$) or mutant $SLX4$ ($\Delta SLX4+SLX4^{AMLR}$) were analyzed by western blot using α - $SLX4$ antibody (right panel). These extracts, with $SLX4$ -depleted HSS, were used to replicate pICL. Samples were taken at various times and immunoprecipitated with α -XPF (left panel) or α - $SLX4$ antibodies (middle panel). Co-precipitated DNA was isolated and analyzed by quantitative PCR using the pICL or pQuant primers. Recovery values of pQuant were subtracted from pICL recovery values. The resulting data were plotted as the percentage of peak value with the highest value within one experiment set to 100%. Independent duplicate experiment related to Figure 4D. I) As in (H) but using the $xSLX4^{MLR^*}$ mutant protein. Independent duplicate experiment related to Figure 4F. J) As in (G) but using the $xSLX4^{MLR^*}$ mutant protein. Line within blot indicates position where irrelevant lanes were removed. Independent duplicate experiment related to Figure 4G. *, background band. #, SapI fragments from contaminating uncrosslinked plasmid present in varying degrees in different pICL preparations.



Supplemental Figure S5. The BTB domain contributes to SLX4-dimerization but is not crucial for ICL repair. Related to Figure 5. A) Schematic illustration of the *xSLX4*^{BTB} mutant protein. In this protein, residues Phe644 and Tyr646 are mutated to alanines, indicated by a red line. B) Schematic illustration of the *xSLX4*¹⁻⁵⁵⁸ mutant protein. This protein is truncated at residue 558. C) Fragment of a sequence alignment between *Xenopus laevis* (*xSLX4*), human (*hsSLX4*), and mouse (*mmSLX4*) by Clustal Omega. The red box in the alignment indicates the residues in the wild-type proteins that are mutated in *SLX4*^{BTB}, the A's above the red boxes indicate the substitutions to alanine residues. (*), conserved residue; (:), conservative residue, (.), semi-conservative residue. D) Recombinant *xSLX4*^{BTB}, containing an N-terminal FLAG-tag and a C-terminal Strep-tag, was expressed in Sf9 insect cells and isolated via affinity purification using FLAG-beads. Purity and concentration were determined using Coomassie blue staining of samples on SDS-PAGE. E) As in (D) but for recombinant *xSLX4*¹⁻⁵⁵⁸. F) *SLX4*-depleted (Δ *SLX4*), and *SLX4*-depleted NPE complemented with wild-type *SLX4* (Δ *SLX4*+*SLX4*^{WT}) or mutant *SLX4* (Δ *SLX4*+*SLX4*^{BTB}) were analyzed by western blot using α -*SLX4* antibody (right panel). These extracts, with *SLX4*-depleted HSS, were used to replicate pICL. Repair efficiency was calculated and plotted (left panel). Line within blot indicates position where irrelevant lanes were removed. Independent duplicate experiment related to Figure 5D. G) Purified *xSLX4*^{AC} and *xSLX4*¹⁻⁵⁵⁸ mutant proteins or buffer (-) were added to HSS. After incubation, recombinant *SLX4* was immunoprecipitated using anti-FLAG M2 affinity gel (Sigma). The input (IN), flow-through (FT), and bound fractions (B) were analyzed by western blot using α -FLAG (upper panel) and α -XPF antibodies (lower panel). Line within blot indicates position where irrelevant lanes were removed. H) *SLX4*-depleted (Δ *SLX4*), and *SLX4*-depleted NPE complemented with wild-type *SLX4* (Δ *SLX4*+*SLX4*^{WT}) or mutant *SLX4* (Δ *SLX4*+*SLX4*¹⁻⁵⁵⁸) were used with *SLX4*-depleted HSS to replicate pICL. Repair efficiency was calculated and plotted (left panel). Protein dilutions of wild-type *SLX4* (*SLX4*^{WT}) and mutant *SLX4* (*SLX4*¹⁻⁵⁵⁸) were analyzed by western blot using α -FLAG antibody to ensure equivalent protein concentrations (right panel). Independent duplicate experiment related to Figure 5F. I) Wild-type (*SLX4*^{WT}) or mutant *SLX4* (*SLX4*¹⁻⁵⁵⁸) containing an N-terminal FLAG-tag, were co-expressed with wild-type *SLX4* containing an N-terminal His-tag and a C-terminal Strep-tag (*His-SLX4*) in Sf9 insect cells. Cells were lysed and FLAG-tagged *SLX4* was immunoprecipitated using anti-FLAG M2 affinity gel (Sigma). To examine the contribution of DNA to *SLX4*-dimerization the cell lysates were split during the immunoprecipitation step and treated with benzonase (Sigma). The input (IN), flow-through (FT), and bound fractions (B) were analyzed by western blot using α -FLAG and α -His antibodies. #, SapI fragments from contaminating uncrosslinked plasmid present in varying degrees in different pICL preparations.



Chapter 5

Two domains mediate SLX4/ FANCP recruitment to DNA interstrand crosslinks

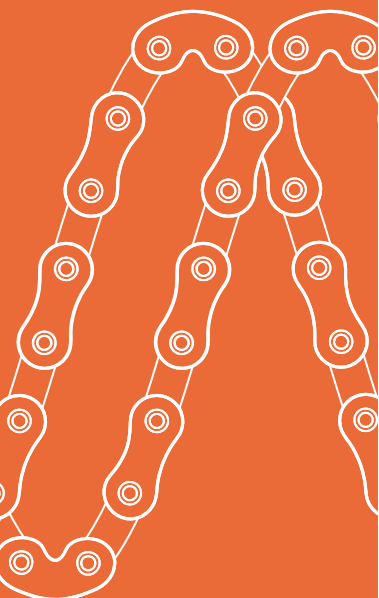
Wouter Hoogenboom¹, Rick A.C.M. Boonen^{1,†}, Connor
Arkinson², Helen Walden², and Puck Knipscheer^{1,*}

¹) Oncode Institute, Hubrecht Institute–KNAW and University Medical
Center Utrecht, Utrecht, The Netherlands

²) Institute of Molecular Cell and Systems Biology, University of Glasgow,
Glasgow, UK

[†]) Present address: Department of Human Genetics, Leiden University
Medical Center, Leiden, The Netherlands

*Corresponding author. Email: p.knipscheer@hubrecht.eu



Abstract

Biallelic mutations in any of the 22 FA genes cause Fanconi anemia (FA), a genetic disorder that is associated with the inability to repair toxic DNA lesions known as DNA interstrand crosslinks (ICLs). A crucial role in ICL repair is assigned to the scaffold protein SLX4/FANCP, that recruits the endonuclease XPF-ERCC1 and facilitates ICL-unhooking in response to FA pathway activation. Nevertheless, how SLX4 is recruited to the site of damage, and how monoubiquitylation of the FANCI-FANCD2 complex promotes this, is not known. Using the *Xenopus* egg extract ICL repair system we show that two domains of SLX4 are important for its localization to ICLs: an N-terminal ubiquitin interaction (UBZ) domain mutated in FA patients, and a previously uncharacterized more C-terminal domain. Mutation of either domain reduces SLX4 recruitment to the ICL and strongly inhibits ICL repair. Although it has been speculated that SLX4 directly binds to ubiquitylated FANCD2 through its UBZ domain we find no evidence for this. Moreover, we show that full length SLX4 interacts with ubiquitin chains rather than monoubiquitin and speculate that an additional, polyubiquitylated, factor is required to recruit SLX4 to ICL sites. In our efforts to identify this factor we demonstrate a repair- and UBZ-mediated interaction of SLX4 with the helicase RTEL1. However, although RTEL1 immunodepletion reduces ICL repair it does not affect SLX4 recruitment. Our data supports a model in which SLX4 is recruited to ICLs by a currently unknown, polyubiquitylated factor, and that this is mediated by two different domains of SLX4.

Introduction

Fanconi anemia (FA) is a genetically heterogeneous disorder characterized by developmental defects, bone marrow failure, cancer predisposition and a cellular inability to repair DNA interstrand crosslinks (ICLs) (Kottemann & Smogorzewska, 2013, Walden & Deans, 2014). Biallelic mutations in any of the currently 22 identified FA genes cause this disorder, which is illustrative of the complexity that comes with the repair of ICLs. ICLs, induced by certain chemotherapeutics or by endogenously formed metabolic by-products such as reactive aldehydes (Garaycochea *et al.*, 2012, Langevin *et al.*, 2011, Rosado *et al.*, 2011), are exceptionally toxic. They form covalent 'road blocks' that prevent DNA replication and transcription and their repair in S-phase is coupled to DNA replication (Supplemental Figure S1A) (Räschle *et al.*, 2008).

We and others have used the *Xenopus laevis* egg extract system to construct a step-by-step model for replication-dependent ICL repair (Räschle *et al.*, 2008). Repair is initiated when replication forks are stalled on both sides of an ICL (Zhang *et al.*, 2015) (Figure S1A). Next, the replicative helicase complex CDC-45, MCM2-7, and GINS (CMG) is unloaded, which is mediated by the ubiquitin E3 ligase TRAF-interacting protein (TRAIP) and the p97 ATPase (Fullbright *et al.*, 2016, Wu *et al.*, 2019). This allows one leading strand to 'approach' the ICL to 1 nt from the crosslink, which is essential for nucleolytic incisions that unhook the ICL (Fu *et al.*, 2011, Long *et al.*, 2014). The substrate for ICL unhooking could be the X-shaped structure generated by the two converged forks, or may be generated by fork reversal of one of the forks (Amunugama *et al.*, 2018). Unhooking incisions require the action of the structure specific endonuclease XPF-ERCC1 and the scaffold protein SLX4. The strand containing the unhooked adduct is replicated with the help of translesion synthesis (TLS) polymerases, providing the template for homology directed repair of the other, incised strand (Budzowska *et al.*, 2015, Long *et al.*, 2011).

An alternative replication-dependent pathway exists for the repair of a subset of ICLs, which includes psoralen/UV and abasic site ICLs. This pathway is also mediated by TRAIP that initially creates short ubiquitin chains on CMG that are directly bound by the NEIL3 DNA glycosylase (Wu *et al.*, 2019). NEIL3 catalyzes cleavage of the *N*-glycosyl bond between the sugar and the base of either one of the crosslinked nucleotides, allowing repair without the need for CMG unloading and unhooking backbone incisions (Semlow *et al.*, 2016). However, in contrast to mutations in FA genes, mutations in the NEIL3 gene are not associated with a severe phenotype.

ICL unhooking is a defining step in the FA pathway and requires the action of several FA factors. In response to ICL damage detection, the FA core complex monoubiquitylates the FANCI-FANCD2 (ID2) complex, which marks FA pathway activation and ensures stable ID2 binding DNA near the crosslink (Klein Douwel *et al.*, 2014, Knipscheer *et al.*, 2009). This promotes the recruitment of SLX4(FANCP) bound to the structure specific endonuclease XPF(FANCP)-ERCC1 that mediates ICL unhooking (Klein Douwel *et al.*, 2014). How SLX4 is recruited to ICLs and whether this is through direct interaction with FANCD2-Ub is currently unclear.

SLX4 has a versatile function in genome maintenance by not only acting in ICL repair but also in Holliday junction resolution, telomere maintenance, and replication stress response (Guervilly & Gaillard, 2018). It does not have any catalytical domains but is thought to act as a scaffold that interacts with many factors including the three structure specific endonucleases XPF-ERCC1, MUS81-EME1 and SLX1. We previously used *Xenopus*

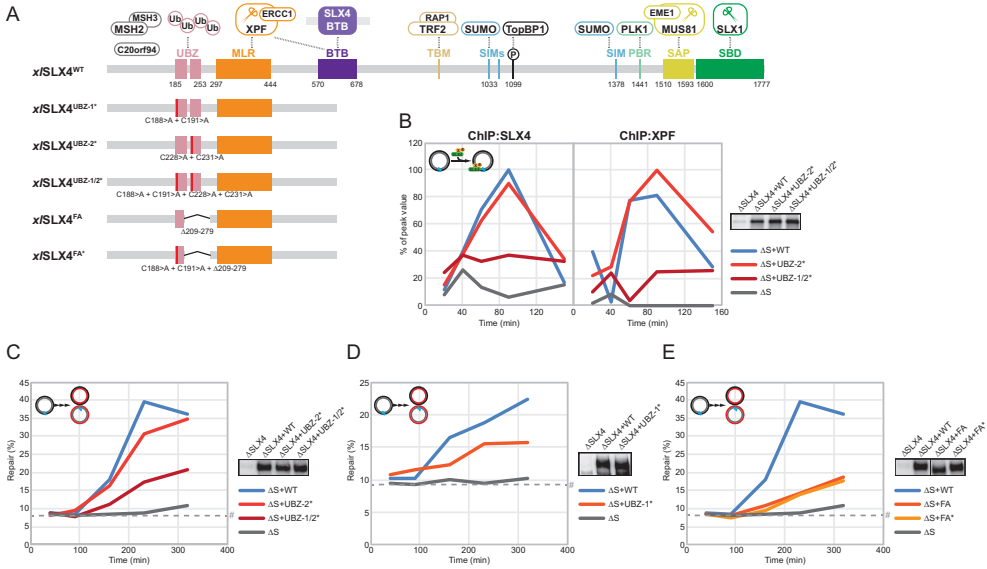


Figure 1: Mutations in UBZ-1, but not UBZ-2, impair ICL repair and SLX4 recruitment. A) Schematic representations of the x/SLX4 wild type and mutant proteins. For the mutants, only the N-terminal region containing the mutations is shown, full length proteins were purified. The mutated residues are indicated. B) SLX4-depleted (Δ SLX4), and SLX4-depleted NPE supplemented with wild-type SLX4 (Δ SLX4+WT) or mutant SLX4 (Δ SLX4+MUT) were analyzed by western blot using α -SLX4 antibody (right panel). These extracts, with SLX4-depleted HSS, were used to replicate pICL. Samples were taken at various times and immunoprecipitated with α -SLX4 (left panel) or α -XPF (middle panel) antibodies. Co-precipitated DNA was isolated and analysed by quantitative PCR using the pICL or pQuant primers. Recovery values of pQuant were subtracted from pICL recovery values. The resulting data were plotted as the percentage of peak value with the highest value within one experiment set to 100%. C) SLX4-depleted (SLX4), and SLX4-depleted NPE supplemented with wild-type SLX4 (Δ SLX4+WT) or mutant SLX4 (Δ SLX4+MUT) were analyzed by western blot using α -SLX4 antibody (right panel). These extracts, with SLX4-depleted HSS, were used to replicate pICL. Repair efficiency at various times was calculated and plotted (left panel). D) As in (C) but using the x/SLX4^{UBZ-1*} mutant protein. E) As in (C) but using the x/SLX4^{FA} and x/SLX4^{FA*} mutant proteins. Line within blot indicates position where irrelevant lanes were removed. #, SapI fragments from contaminating uncrosslinked plasmid present in varying degrees in different pICL preparations. See also Supplemental Figure S2.

egg extracts to study its role in the FA pathway and established that the N-terminal region, which contains the binding site for XPF-ERCC1 but not MUS81-EME1 or SLX1, is sufficient for ICL repair (Hoogenboom *et al.*, 2018). This region also includes two ubiquitin-binding zinc-finger (UBZ) domains (Fekairi *et al.*, 2009) and deletion of the second and part of the first UBZ domains causes Fanconi anemia (Kim *et al.*, 2011, Stoepker *et al.*, 2011). In addition, mainly the first UBZ domain is associated with SLX4 recruitment to damage foci and K63-poly-ubiquitin chain binding (Kim *et al.*, 2011, Lachaud *et al.*, 2014, Yamamoto *et al.*, 2011). Since FANCD2 ubiquitylation was shown to be required for SLX4 recruitment to ICL repair sites and to mitomycin C foci (Klein Douwel *et al.*, 2014, Yamamoto *et al.*, 2011), a model has been suggested in which SLX4 directly interacts with FANCD2-Ub through its UBZ domains. However, another report has shown that FANCD2 ubiquitylation is dispensable for the recruitment of SLX4 to psoralen/UV induced damage stripes (Lachaud *et al.*, 2014). Therefore, it remains unclear how activation of the FA pathway by ID2 ubiquitylation is linked to SLX4 recruitment.

Here, we use the *Xenopus* egg extract system to investigate the mechanism of SLX4 recruitment to ICLs during repair. We find that mutations in the UBZ domains, in particular in UBZ-1, strongly reduce recruitment of SLX4 to a cisplatin ICL. Consequently, mutations in UBZ-1 as well the FA-causing mutation in the UBZ domains, impair efficient ICL repair. Moreover, we identify an additional region in SLX4 that is important for ICL recruitment and repair. We find no evidence for a direct interaction between SLX4 and monoubiquitylated FANCD2 and speculate that SLX4 is recruited via an unknown polyubiquitylated factor. One potential factor could be RTEL1, however, we find that RTEL1 is not important for recruitment of SLX4 to ICLs. These results provide insights into how SLX4 is recruited to ICLs during repair and bring us closer to understanding how FA pathway activation leads to SLX4-dependent unhooking incisions.

Results

The UBZ-1 domain is important for SLX4 recruitment and ICL repair

During ICL repair by the FA pathway, SLX4 recruits XPF-ERCC1 to ICL sites which is essential for ICL unhooking (Klein Douwel *et al.*, 2014). However, how SLX4 is recruited to the site of damage is unclear. A previous report has shown that the first of two N-terminal UBZ domains is important for SLX4 recruitment to psoralen/UV induced damages stripes (Lachaud *et al.*, 2014). We used the *Xenopus* egg extract-based ICL repair system to investigate the recruitment of SLX4 specifically to the site of damage. To this end, we replicate a plasmid with a site-specific cisplatin ICL (pICL) in egg extract and perform chromatin immunoprecipitations (ChIP) with SLX4 or XPF antibodies followed by quantitative PCR with ICL-site specific primers (Supplemental Figure S1B). Using this method, we previously demonstrated that depletion of SLX4 impaired recruitment of SLX4 and XPF, while addition of recombinant wild-type SLX4 restored recruitment of both proteins (Hoogenboom *et al.*, 2018). To study the role of the UBZ region, we generated full-length mutant SLX4 proteins with point mutations in critical cysteine residues in one or both UBZ domains (x/SLX4^{UBZ-1*}, x/SLX4^{UBZ-2*}, x/SLX4^{UBZ-1/2*}; Figure 1A and Supplemental Figure S2A). To examine recruitment of these mutants to the ICL we performed the ChIP assay on pICL replicated in SLX4-depleted extract supplemented with the wild type or mutant SLX4 proteins. Addition of SLX4^{UBZ-2*} restored localization of SLX4 and XPF to ICL sites with similar efficiency as SLX4^{WT}. In contrast, a strong decrease in SLX4 and XPF recruitment was observed when SLX4^{UBZ-1/2*} was added to SLX4-depleted extract (Figure 1B and Supplemental Figure S2B). This indicates that efficient recruitment of SLX4 to ICLs is strongly dependent on the UBZ-1 domain.

We next asked whether these UBZ mutations affect ICL repair. In the *Xenopus* egg extract system, ICL repair can be directly monitored by measuring the regeneration of a SapI recognition site that is initially blocked by the crosslink (Supplemental Figure S1C). ICL repair was efficiently restored by addition of SLX4^{WT} or SLX4^{UBZ-2*} to SLX4-depleted extract, but much less efficiently by SLX4^{UBZ-1/2*} (Figure 1C, Supplemental Figure S2C and D). Consistent with an important role of the UBZ-1 domain, addition of SLX4^{UBZ-1*} to SLX4-depleted extract did not efficiently rescue ICL repair (Figure 1D and Supplemental Figure S2D).

A deletion in SLX4, removing all of the second and part of the first UBZ domains, causes Fanconi anemia (Kim *et al.*, 2011, Stoepker *et al.*, 2011). To investigate the defect of this mutant protein in ICL repair we generated full length x/SLX4 harboring the equivalent

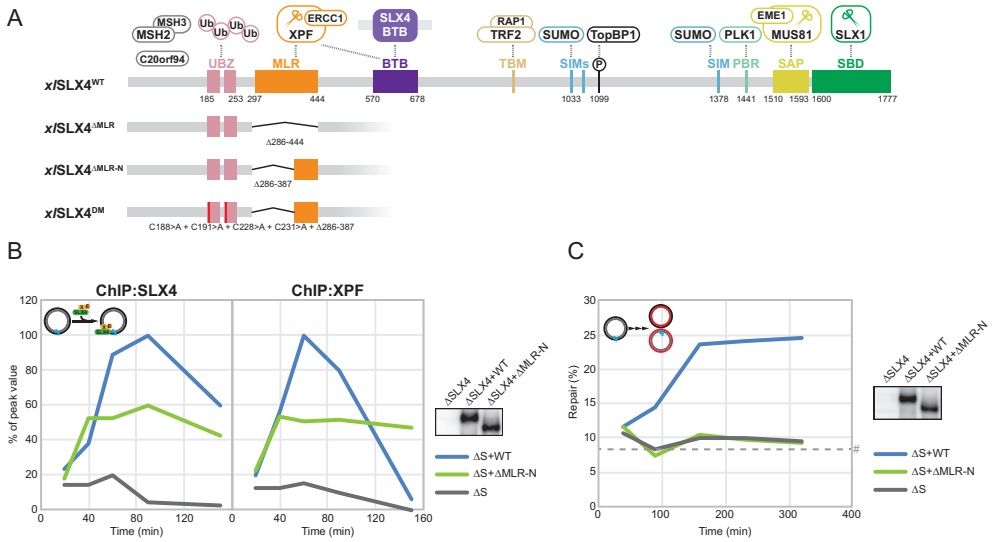


Figure 2: The MLR-N region is crucial for ICL repair and contributes to SLX4 recruitment. A) Schematic representations of the *x*/SLX4 wild type and mutant proteins. For the mutants, only the N-terminal region containing the mutations is shown, full length proteins were purified. The mutated residues are indicated. B) SLX4-depleted (Δ SLX4), and SLX4-depleted NPE supplemented with wild-type SLX4 (Δ SLX4+WT) or mutant SLX4 (Δ SLX4+ Δ MLR-N) were analyzed by western blot using α -SLX4 antibody (right panel). These extracts, with SLX4-depleted HSS, were used to replicate pICL. Samples were taken at various times and immunoprecipitated with α -SLX4 (left panel) or α -XPF (middle panel) antibodies. Co-precipitated DNA was isolated and analysed by quantitative PCR using the pICL or pQuant primers. Recovery values of pQuant were subtracted from pICL recovery values. The resulting data were plotted as the percentage of peak value with the highest value within one experiment set to 100%. C) SLX4-depleted (Δ SLX4), and SLX4-depleted NPE supplemented with wild-type SLX4 (Δ SLX4+WT) or mutant SLX4 (Δ SLX4+ Δ MLR-N) were analyzed by western blot using α -SLX4 antibody (right panel). These extracts, with SLX4-depleted HSS, were used to replicate pICL. Repair efficiency at various times was calculated and plotted (left panel). #, SapI fragments from contaminating uncrosslinked plasmid present in varying degrees in different pICL preparations. See also Supplemental Figure S3.

deletion (*x*/SLX4^{FA}; Figure 1A and Supplemental Figure S2A). Similar to SLX4^{UBZ-1*}, addition of SLX4^{FA} to SLX4-depleted extract did not efficiently restore ICL repair (Figure 1E and Supplemental Figure S2E). In the SLX4^{FA} deletion mutant, only one of the four metal coordinating residues is removed from UBZ-1. To examine whether this could result in residual function of this UBZ domain we additionally mutated the first two metal coordinating cysteines creating the *x*/SLX4^{FA*} mutant (Figure 1A and Supplemental Figure S2A). However, addition of this SLX4^{FA*} mutant caused no, or only a minor reduction in ICL repair compared to the SLX4^{FA} mutant, indicating that the UBZ-1 domain is not functional in the original FA mutant (Figure 1E and Supplemental Figure S2E). These data also show that functional deletion of both UBZ-domains does not fully block ICL repair in our system, indicating they are not absolutely required for repair.

Collectively, our results demonstrate that particularly the UBZ-1 domain of SLX4 is important for SLX4 recruitment and for its function in ICL repair. In addition, we find that an FA-causing deletion in the UBZ region compromises SLX4 function in ICL repair, most likely by affecting the function of UBZ-1.

The MLR domain is important for SLX4 recruitment and crucial for ICL repair

We previously demonstrated that the MLR domain of SLX4 not only mediates the interaction with XPF but is also important for recruitment of SLX4 to ICL sites (Hoogenboom *et al.*, 2018). To further investigate the SLX4 recruitment function of the MLR domain we aimed to isolate this from its role in XPF-binding. To this end, we generated a mutant protein with a smaller deletion that does not include the XPF-binding region (Δ SLX4^{AMLR-N}, Figure 2A and Supplemental Figure S3A) (Hashimoto *et al.* 2015). We replicated pICL in SLX4-depleted extract supplemented with wildtype or mutant SLX4 and used ChIP to assess recruitment of SLX4 to ICL sites. We found that recruitment of the SLX4^{AMLR-N} mutant to the ICL was reduced by about half compared to SLX4^{WT} (Figure 2B and Supplemental Figure S3B, left panels), suggesting a role for this region in recruitment of SLX4. Localization of XPF was similarly impaired (Figure 2B and Supplemental Figure S3B, middle panels) indicating that XPF-binding was unaffected by this mutation which was confirmed by pull down experiments (Supplemental Figure S3C).

While mutations in the UBZ or MLR domains reduce the recruitment of SLX4 to ICL sites, they did not completely prevent it. To test whether mutation of both domains would completely prevent SLX4 recruitment, we generated a double mutant (DM) with mutations in UBZ-1/2 and a deletion of MLR-N (Δ SLX4^{DM}; Figure 2A and Supplemental Figure S3A). As expected, XPF-binding was not affected by these mutations (Supplemental Figure S3D). We used ChIP to measure recruitment of this mutant to ICL sites and found that it was still partially recruited (Supplement Figure S3E). This result indicates that, in addition to the MLR and UBZ domains, other domains of SLX4 play a role in recruitment.

Finally, we tested the effect of the Δ MLR-N mutation on ICL repair. Addition of SLX4^{AMLR-N} to SLX4-depleted extracts completely failed to restore repair (Figure 2C and Supplemental Figure S3F). This is not likely caused by structural defects resulting from the mutation because it still interacted with XPF and ubiquitin efficiently (Supplemental Figure S3C) and we previously showed that the Δ MLR mutant has a similar overall structure compared to the wild type protein (Hoogenboom *et al.* 2018). We conclude that the MLR-N domain plays a role in SLX4 recruitment and is crucial for ICL repair. This indicates that even though the Δ MLR-N mutant is partially recruited, it still does not support ICL repair, suggesting the MLR-N region may have additional roles such as positioning of XPF-ERCC1 or interaction with another factor.

Not FANCD2, but a polyubiquitylated factor recruits SLX4 through UBZ-1

Activation of FANCD2 through monoubiquitylation by the FA core complex is required for SLX4-XPF-ERCC1-mediated unhooking incisions (Klein Douwel *et al.*, 2014, Knipscheer *et al.*, 2009). However, it is debated whether FANCD2 is directly involved in recruitment of SLX4. Previous reports have suggested that SLX4 can localize to psoralen/UV-induced damage stripes independent of FANCD2 or its monoubiquitylation (Lachaud *et al.*, 2014, Svendsen *et al.*, 2009). On the other hand, SLX4 recruitment to mitomycin-C (MMC) induced foci in chicken DT40 cells or to the ICL locus of pICL in *Xenopus* egg extracts is shown to depend on FANCD2 and its monoubiquitylation (Klein Douwel *et al.*, 2014, Yamamoto *et al.*, 2011). Although wild-type SLX4, but not a UBZ-deletion mutant, co-precipitated monoubiquitylated FANCD2 in MMC-treated DT40 cells, a direct interaction between SLX4 and FANCD2 has not been demonstrated (Yamamoto *et al.*, 2011). To

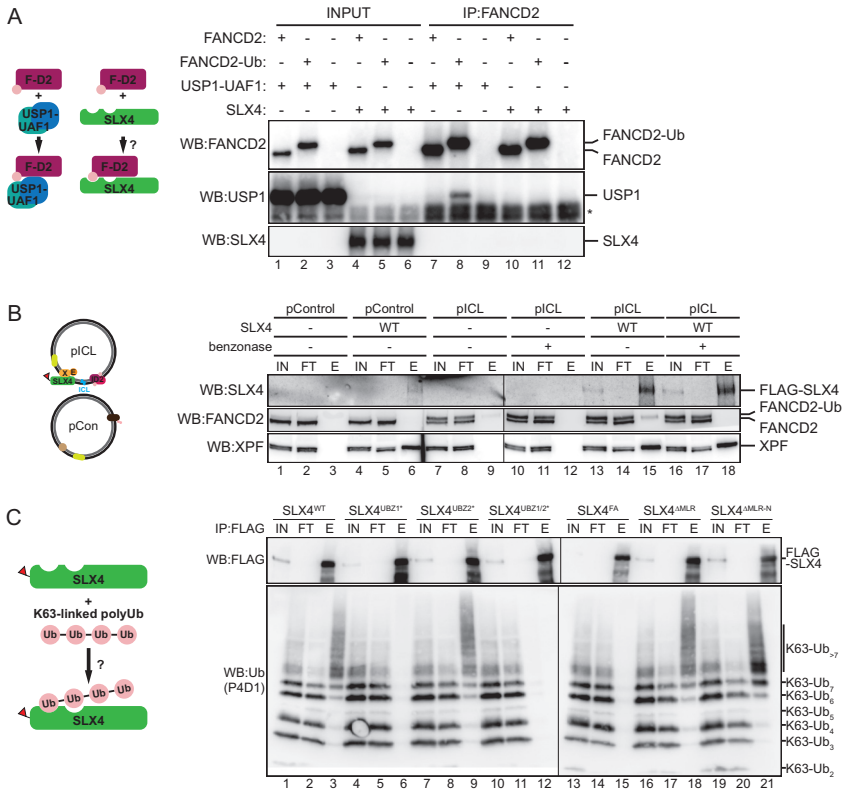


Figure 3: SLX4 does not directly bind FANCD2-Ub, but can bind K63-linked ubiquitin chains. A) Purified FANCD2 or monoubiquitylated FANCD2 (FANCD2-Ub) was bound to α -FANCD2 conjugated Dynabeads™ Protein A (ThermoFisher). Purified wild-type *x*SLX4 or *hs*USP1 Δ 1 Δ 2 C905-*hs*UAF1 (USP1-UAF1) was added to the beads and beads were incubated. After washing beads were resuspended in sample buffer. The input and FANCD2-IP fractions were analyzed by western blot using α -FANCD2 (upper panel), α -USP1 (middle panel) and α -SLX4 antibodies (lower panel). B) Purified FLAG-tagged wild-type SLX4 (WT) or buffer (-) was added to *Xenopus* egg extract that was used to replicate a plasmid with a site-specific cisplatin ICL (pICL) or an undamaged plasmid with the same sequence (pControl). After 60 minutes replication was stopped and FLAG-SLX4 was immunoprecipitated with FLAG-M2 resin (Sigma-Aldrich) supplemented with benzonase or buffer. After 90 minutes of incubation FLAG-SLX4 was eluted with 3 \times FLAG peptide. The input (IN), flow-through (FT), and eluted fractions (E) were analyzed by western blot using α -SLX4 (upper panel), α -FANCD2 (middle panel), and α -XPF (lower panel) antibodies. Line within blot indicates position where irrelevant lanes were removed. C) Purified FLAG-tagged wild type (SLX4^{WT}) and mutant SLX4 (SLX4^{MUT}) constructs were incubated with K63-linked polyubiquitin chains (Boston Biochem) and immunoprecipitated with FLAG-M2 resin (Sigma-Aldrich). FLAG-SLX4 was eluted with 3 \times FLAG peptide. The input (IN), flow-through (FT), and eluted fractions (E) were analyzed by western blot using α -FLAG (upper panel) and α -ubiquitin (P4D1) antibodies (lower panel). Line within blot indicates position where irrelevant lanes were removed. *, background band. See also Supplemental Figure S4.

examine this interaction, we sought a biochemical approach using purified components. We first purified monoubiquitylated *x*FANCD2 (*x*FANCD2-Ub) as was recently described (Chaugule *et al.*, 2019). We pre-incubated α -FANCD2-conjugated Dynabeads Protein A (ThermoFisher) with either *x*FANCD2 or *x*FANCD2-Ub, and added wild-type *x*SLX4 (Supplemental Figure S4A), or buffer. After further incubation the beads were washed and the bound proteins were analyzed by western blot. We observed no co-precipitation

of SLX4 with FANCD2 or FANCD2-Ub (Figure 3A, lanes 10 and 11). To confirm that our experimental conditions allow the detection of low-affinity interactions we examined the interaction of the *hsUSP1-UAF1* complex with FANCD2 and FANCD2-Ub. As previously reported, we found that *hsUSP1-UAF1* co-precipitated with FANCD2-Ub (Figure 3A, lane 8) (Arkinson *et al.*, 2018). This strongly suggests that there is no direct interaction between SLX4 and monoubiquitylated FANCD2.

However, it is possible that in the context of ICL repair additional factors or (structural) modifications promote the interaction between SLX4 and FANCD2-Ub. To explore this possibility, we used *Xenopus* egg extracts to replicate pICL or a control plasmid (pCon) in the presence of recombinant FLAG-tagged wild type SLX4. At 60 minutes of replication, when SLX4 recruitment reaches its maximum (Klein Douwel *et al.*, 2014), we stopped the reaction, immunoprecipitated recombinant SLX4 using anti-FLAG M2 affinity gel (Sigma-Aldrich), and analyzed the samples by western blot. Consistent with IP experiments in non-replicating extracts (Supplemental Figure S3C and D) (Hoogenboom *et al.*, 2018), XPF was pulled down efficiently with SLX4 in all conditions (Figure 3B, lane 6, 15 and 18). In contrast, unmodified FANCD2 was not precipitated in any of the conditions, while the monoubiquitylated form of FANCD2 precipitated only when pICL was replicated (Figure 3B, compare lanes 6 and 15). Yet, since SLX4 is recruited to the ICL during repair, SLX4 immunoprecipitation will also precipitate the crosslinked plasmid. To examine whether FANCD2-Ub co-precipitated through interaction with pICL, or is in a direct complex with SLX4, we added benzonase to the immunoprecipitation. We found that co-precipitation of monoubiquitylated FANCD2 with SLX4 was lost when the samples were treated with benzonase, indicating that the interaction with SLX4 was not direct but mediated by DNA (Figure 3B, compare lanes 15 and 18). Collectively, although SLX4 and FANCD2-Ub likely function in close proximity at ICL sites, we find no indication for a direct interaction.

If there is no direct interaction between SLX4 and FANCD2-Ub, another mechanism is responsible for the UBZ-mediated recruitment of SLX4 to ICL sites. Previous experiments with fragments of the *hsSLX4* UBZ region have indicated that SLX4 has affinity for long polyubiquitin chains linked through lysine-63 (K63) of ubiquitin (Kim *et al.*, 2011, Lachaud *et al.*, 2014). Since these interactions may be influenced by other regions of the protein, we performed similar experiments using full-length *xSLX4*. We incubated recombinant FLAG-tagged wild-type (SLX4^{WT}) and mutant (SLX4^{MUT}) proteins with K63-linked ubiquitin chains of varying length (Boston Biochem) and pulled down SLX4 using anti-FLAG M2 affinity gel (Sigma-Aldrich). We found that full-length SLX4 co-precipitated long (≥ 6 subunits) K63-linked polyubiquitin chains, while mutations in UBZ-1, but not UBZ-2, disrupted this interaction (Figure 3C, lanes 3, 6, 9 and 12), which is consistent with the data previously obtained with SLX4 fragments (Kim *et al.*, 2011, Lachaud *et al.*, 2014). However, these fragments did not allow the examination of the FA-causing deletion in the UBZ region. We found that SLX4^{FA} mutant inhibited co-precipitation of K63-linked polyubiquitin (Figure 3C, lane 15) similar to UBZ-1 mutants. In contrast, deletion of the MLR domain did not affect SLX4 affinity for K63-linked polyubiquitin chains (Figure 3C, lanes 18 and 21).

Consistent with an affinity for long chains, SLX4^{WT} did not co-precipitate monoubiquitin (Supplemental Figure S4B). To examine the specificity for K63 chains we incubated wild type and mutant SLX4 with K48-linked polyubiquitin chains. In contrast to what was previously observed with the protein fragments, we found that SLX4 interacts with K48-linked ubiquitin chains in a UBZ-1 dependent fashion (Supplementary Figure

S4C) (Kim *et al.*, 2011, Lachaud *et al.*, 2014). Interestingly, while the interaction with K63-linked ubiquitin chains was not affected by mutations in UBZ-2, interaction of SLX4^{UBZ-2*} with K48-linked ubiquitin chains was reduced compared to wild type. This could indicate difference in interaction of SLX4 with the K48 and K63 ubiquitin chains.

Collectively, these results indicate that there is most likely no direct interaction between SLX4 and FANCD2-Ub but that SLX4 is recruited to the ICL via K63-, or K48-linked ubiquitin chains attached to a currently unknown factor. The interaction with this factor is important for ICL repair and is lost when UBZ-1 is disrupted and in the FA-associated SLX4 UBZ mutant.

RTEL1 is not responsible for recruitment of SLX4

To further understand the mechanism of SLX4 recruitment it is important to identify the polyubiquitylated factor that forms a UBZ-1-dependent interaction with SLX4. Regulator of telomere length 1 (RTEL1) is an essential DNA helicase that acts in telomere processes such as T-loop disassembly and telomeric G4 DNA unwinding (Vannier *et al.*, 2012) but also functions in controlling HR and promoting genome-wide DNA replication (Uringa *et al.*, 2011, Vannier *et al.*, 2013). RTEL1 recruitment to telomeres depends on TRF2 (Sarek *et al.*, 2015), which is also important for the telomere function of SLX4 (Guervilly & Gaillard, 2018), yet they perform profoundly distinct roles in telomere maintenance (Margalef *et al.*, 2018). Interestingly, RTEL1 is found to be enriched at psoralen-ICL DNA in a replication-dependent manner (Räschle *et al.*, 2015) and cellular deficiency leads to sensitivity to the crosslinking agent MMC (Speckmann *et al.*, 2017, Uringa *et al.*, 2012), suggesting a role in ICL repair. Moreover, recent work in egg extracts revealed a role for RTEL1 in processing DNA-protein crosslinks (DPCs) by facilitating CMG bypass (Sparks *et al.*, 2019). Based on this, and on the fact that RTEL1 was found to be ubiquitylated (Udeshi *et al.*, 2013), we considered that RTEL1 may act in SLX4 recruitment. Therefore, we investigated the presence of RTEL1 in FLAG-SLX4 pulldown samples during replication of pICL or pCon. Indeed, RTEL1 co-precipitated with wild-type SLX4, and this interaction was enhanced in the presence of the ICL-containing plasmid compared to the control (Figure 4A, compare lanes 6 and 15). Co-precipitation of RTEL1 was resistant to benzonase treatment, indicating that it is not mediated by DNA (Figure 4A, compare lanes 15 and 18). Moreover, RTEL1 co-precipitation was reduced to non-damage background level when SLX4^{UBZ-1/2*} was used instead of SLX4^{WT} (Figure 4A, compare lanes 6, 15, and 21), indicating that the damaged-induced interaction is UBZ-mediated.

Considering a possible function for RTEL1 in recruiting SLX4 to ICL sites, we explored its role in ICL repair. To this end, we replicated pICL in a Mock- and RTEL1-depleted extract and determined ICL repair. Compared to mock-depleted extract, ICL repair in RTEL1-depleted extract was moderately impaired (Figure 4B). Addition of recombinant x/RTEL1 to RTEL1-depleted extract did not restore ICL repair (Figure 4B), possibly because a large excess of recombinant protein is required for full rescue as previously shown for DPC bypass (Sparks *et al.*, 2019). Similar to DPC bypass, addition of a catalytic mutant of RTEL1 (RTEL1^{K48R}) to RTEL1-depleted extract further reduced ICL repair efficiency (Figure 4B) indicating that this mutant may act as a dominant negative. These results suggest a possible function for RTEL1 in ICL repair.

If RTEL1 exerts its role in ICL repair by recruiting SLX4 to ICL sites, we would expect to see a reduction in SLX4 recruitment during repair in RTEL1-depleted extracts.

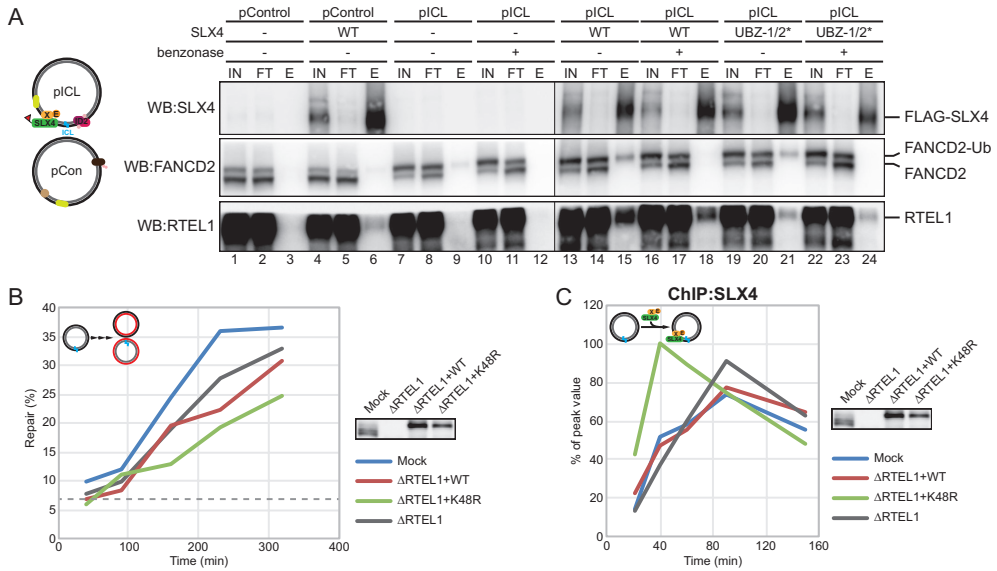


Figure 4: SLX4 recruitment to ICL sites does not depend on RTEL1. A) Purified FLAG-tagged wild-type (WT), mutant (UBZ-1/2*) SLX4 or buffer (-) was added to *Xenopus* egg extract that was used to replicate a plasmid with a site-specific cisplatin ICL (pICL) or an undamaged plasmid with the same sequence (pControl). After 60 minutes replication was stopped and FLAG-SLX4 was immunoprecipitated with FLAG-M2 resin (Sigma-Aldrich) supplemented with benzonase or buffer. After 90 minutes of incubation FLAG-SLX4 was eluted with 3× FLAG peptide. The input (IN), flow-through (FT), and eluted fractions (E) were analyzed by western blot using α -SLX4 (upper panel), α -FANCD2 (middle panel), and α -RTEL1 antibodies (lower panel). Line within blot indicates position where irrelevant lanes were removed. B) Mock-depleted (Mock), RTEL1-depleted (Δ RTEL1), and RTEL1-depleted NPE supplemented with wild-type (Δ RTEL1+WT) or mutant (Δ RTEL1+K48R) were analysed by western blot using α -RTEL1 antibody (right panel). These extracts, with Mock-depleted or RTEL1-depleted HSS extract, were used to replicate pICL. Repair efficiency was calculated and plotted (left panel). A higher than endogenous concentration of recombinant RTEL1 was required for complete rescue (Wu *et al.* 2019), likely due to partial loss of function of the recombinant protein during purification. C) Mock-depleted (Mock), RTEL1-depleted (Δ RTEL1), and RTEL1-depleted NPE supplemented with wild-type (Δ RTEL1+WT) or mutant (Δ RTEL1+K48R) were analysed by western blot using α -RTEL1 antibody (right panel). These extracts, with Mock-depleted or RTEL1-depleted HSS extract, were used to replicate pICL. Samples were taken at various times and immunoprecipitated with α -SLX4 (left panel) antibodies. Co-precipitated DNA was isolated and analysed by quantitative PCR using the pICL or pQuant primers. Recovery values of pQuant were subtracted from pICL recovery values. The resulting data were plotted as the percentage of peak value with the highest value within one experiment set to 100%. #, SapI fragments from contaminating uncrosslinked plasmid present in varying degrees in different pICL preparations.

However, RTEL1 depletion did not reduce SLX4 recruitment to ICL sites compared to mock-depletion measured by ChIP, and neither did addition of the dominant negative mutant RTEL1 (Figure 4C). This suggests that RTEL1 is not important for SLX4 recruitment to ICLs. Further research is required to determine the role of RTEL1 in ICL repair and to identify the factor that mediates SLX4 recruitment to ICL sites.

Discussion

SLX4/FANCP plays an essential role in the FA pathway by facilitating XPF(FANCP)-ERCC1-dependent incisions that initiate ICL unhooking, but how SLX4 is recruited to ICLs

is unclear. We used *Xenopus* egg extracts and mutational analysis of full-length proteins to explore the mechanism of SLX4 recruitment at a molecular level. Mutations in the UBZ-1 and MLR domains of SLX4 impair but not completely block SLX4 recruitment, suggesting that recruitment is complex and involves two, or possibly more, interaction sites. SLX4 recruitment is not mediated by a direct interaction with monoubiquitylated FANCD2, instead our results suggest that SLX4 recruitment is mediated by an unknown polyubiquitylated factor. Although our results identify the helicase RTEL1 as a damage- and UBZ-dependent interactor of SLX4, they rule out RTEL1 as an essential factor for SLX4 recruitment.

Consistent with a study that uses trimethyl-psoralen (TMP) and UV irradiation to induce ICLs in cells (Lachaud *et al.*, 2014), our work shows that the UBZ-1 domain of SLX4, but not the UBZ-2 domain, is important for SLX4 recruitment and ICL repair. However, UBZ-1 mutants do not completely block SLX4 recruitment and repair, suggesting that SLX4 could perform some function without this domain (Figure 1). This could indicate that SLX4 recruitment can be achieved by more than one mechanism, such as one involving the MLR domain. However, SLX4-deficient cells expressing UBZ-mutants of SLX4 are as sensitive to MMC as SLX4-deficient cells (Kim *et al.*, 2011, Kim *et al.*, 2013, Lachaud *et al.*, 2014, Stoepker *et al.*, 2011), which indicates that cells are very sensitive to reduced ICL repair activity.

In contrast, deletion of a conserved region in the MLR domain completely abrogated ICL repair (Figure 2). Since this mutation had only a modest impact on SLX4 recruitment, we assume that the repair defect does not originate from reduced recruitment efficiency alone. Based on the fact that the XPF interaction site on SLX4 is in close proximity, we hypothesize that this deletion, while not affecting the affinity for XPF, may disturb proper positioning of XPF-ERCC1 onto the DNA substrate. It is not clear why deletion of MLR-N affects SLX4 recruitment to the ICL. Since it does not affect the interaction with ubiquitin chains it could mediate a ubiquitin-independent interaction with a factor involved in SLX4 recruitment. Whether this is the same factor involved in the UBZ-1 interaction remains to be determined. Alternatively, deletion of the MLR-N domain could also affect the SLX4 tertiary structure and thereby cause steric hindrance with the polyubiquitylated factor interacting with the UBZ-1 domain.

Based on our data, and in contrast to some previously reported views, SLX4 is not directly recruited to ICLs by ubiquitylated FANCD2. We find no interaction between recombinant SLX4 and FANCD2-Ub, while a repair-dependent interaction in extracts is mediated by DNA (Figure 3). In addition, the preferred interaction of full length SLX4 with ubiquitin chains over monoubiquitin makes an interaction with monoubiquitylated FANCD2 less likely. Although our previous results have demonstrated that SLX4 recruitment is dependent on FANCD2 and its monoubiquitylation (Klein Douwel *et al.*, 2014), we propose this must be mediated by an additional factor.

While the results of our ubiquitin-binding assays were similar to previous reports (Kim *et al.*, 2011, Lachaud *et al.*, 2014), an important difference is that we observed a robust affinity of SLX4 for K48-linked polyubiquitin chains. This discrepancy likely results from the use of full-length SLX4 compared to isolated UBZ domains. Consistently, inefficient but detectable binding of K48-linked chains was observed by Kim *et al.* (2011), whereas Lachaud *et al.* (2014) used shorter fragments that did not bind K48-linked polyubiquitin. However, we cannot exclude the possibility of a difference in ubiquitin chain-binding

between human and *Xenopus* SLX4.

It is striking that one UBZ domain preferably interacts with ubiquitin chains of at least five K48- or six K63-linked subunits (Figure 3C, Supplemental Figure S4B) (Lachaud *et al.*, 2014). Although crystal structures of di-ubiquitin chains binding to one ubiquitin binding domain have been solved, structural data of longer ubiquitin chains binding to one ubiquitin binding domain is lacking (Dikic *et al.*, 2009, Hofmann, 2009). Several UBZ family proteins are reported to bind monoubiquitin and ubiquitin chains of various types, albeit through distinct binding modes (Crosetto *et al.*, 2008, Iha *et al.*, 2008, Toma *et al.*, 2015). Ubiquitin-binding by murine TAXBP1 is remarkably similar to SLX4, as it contains tandem UBZ domains of which one does not bind ubiquitin, while the other facilitates binding to monoubiquitin as well as K48- and K63-linked ubiquitin chains of 3 or more subunits (Iha *et al.*, 2008). A structural approach would be required to elucidate the binding mode of long ubiquitin chains with a UBZ domain. As K48-linked ubiquitin chains have a more closed conformation compared to the extended conformation of K63-linked chains (Varadan *et al.*, 2004, Varadan *et al.*, 2002), our finding that SLX4 binds both linkage types could be important for the structural basis of long chain ubiquitin binding.

In order to understand how SLX4 is recruited to ICL sites, it is imperative to identify the polyubiquitylated factor that binds SLX4's UBZ-1 domain. Our pulldown experiments in the context of ICL repair have identified a potential novel interactor of SLX4, the helicase RTEL1. Although RTEL1 can travel with the replication fork via a PCNA-interaction peptide (PIP) box (Vannier *et al.*, 2013), our findings suggest that it is enriched at ICL-containing DNA, which is consistent with previous findings (Räschle *et al.*, 2015). Its benzonase-resistant and UBZ-dependent interaction with SLX4 suggested it to be a promising candidate for recruiting SLX4 to ICLs. However, efficient recruitment of SLX4 in the absence of RTEL1 does not favor this hypothesis. Alternatively, SLX4 may promote recruitment of RTEL1 to ICL sites in a UBZ-dependent manner. Although a definitive role requires complementation of repair by addition of recombinant protein, immunodepletion of RTEL1 slightly affected ICL repair in *Xenopus* egg extracts; it would be interesting to determine how RTEL1 contributes to ICL repair and whether this has a connection with SLX4.

A recent report showed that when forks converge and CMGs are stalled on either side of a cisplatin ICL, TRAIPI ubiquitylates CMG subunits leading to p97-dependent unloading of the CMG from the DNA (Wu *et al.*, 2019). An interesting hypothesis could be that this polyubiquitylated CMG is involved in SLX4 recruitment to ICL sites. Although this may seem unlikely since polyubiquitylated CMG is unloaded before the substrate of incisions is generated (Amunugama *et al.*, 2018), there could be a handover mechanism to retain SLX4 at the ICL site. If this hypothesis is true, TRAIPI depletion would prevent SLX4 recruitment, and preventing CMG unloading using p97 ATPase inhibitor could result in prolonged recruitment of SLX4. These experiments are currently ongoing in our laboratory.

While the mechanism by which monoubiquitylated FANCD2 promotes ICL unhooking is still elusive, our findings provide novel details in the requirements for SLX4 recruitment to ICLs and its connection to FANCD2-Ub. We expect that identification of the polyubiquitylated ligand will help to further understand how SLX4 is recruited and how both the UBZ-1 and MLR domains are involved in this.

Acknowledgements

We thank J. Sparks and J.C. Walter for the *x*/RTEL1 purified proteins and the *x*/RTEL1 antibody. We also thank the Hubrecht animal caretakers for animal support and the other members of the Knipscheer laboratory for feedback.

Materials and Methods

Xenopus egg extracts and DNA replication and repair assay

DNA replication assays and preparation of *Xenopus* egg extracts were performed as described previously (Tutter & Walter, 2006, Walter *et al.*, 1998). Preparation of plasmid with a site-specific cisplatin ICL (pICL), and ICL repair assays were performed as described (Enoiu *et al.*, 2012, Räschle *et al.*, 2008). Briefly, pICL was first incubated in a high-speed supernatant (HSS) of egg cytoplasm for 20 minutes, which promotes the assembly of prereplication complexes on the DNA. Addition of two volumes nucleoplasmic egg extract (NPE), which also contained ^{32}P - α -dCTP, triggers a single round of DNA replication. Aliquots of replication reactions (5 μL) were stopped at various times with nine volumes Stop II solution (0.5% SDS, 10 mM EDTA, 50 mM Tris pH 7.5). Sample were incubated with RNase (0.13 $\mu\text{g}/\mu\text{L}$) for 30 minutes at 37°C followed by proteinase K (0.5 $\mu\text{g}/\mu\text{L}$) overnight (O/N) at RT. DNA was extracted using phenol/chloroform, ethanol-precipitated in the presence of glycogen (30 mg/mL) and resuspended in 5 μL 10 mM Tris pH 7.5. ICL repair was analyzed by digesting 1 μL extracted DNA with HincII, or HincII and SapI, separation on a 0.8% native agarose gel, and quantification using autoradiography. Repair efficiency was calculated as described (Knipscheer *et al.*, 2012). As repair kinetics and absolute efficiency is dependent on the egg extract preparation and depletion conditions, we always use a positive and negative control condition in each experiment using the same extract.

Antibodies and immunodepletions

Antibodies against *x*/FANCD2, *x*/XPF, *x*/SLX4, and *x*/RTEL1 have been previously described (Hoogenboom *et al.*, 2018, Klein Douwel *et al.*, 2014, Räschle *et al.*, 2008, Sparks *et al.*, 2019). The anti-FLAG M2 antibody was purchased from Sigma, the USP1 antibody (A301-699A) from Bethyl Laboratories, the ubiquitin antibody (P4D1) from Santa Cruz, and the ubiquitin antibody (FK2) from Enzo Life Sciences. To deplete egg extracts of SLX4, one volume Dynabeads Protein A (ThermoFisher) was washed three times with 5 volumes 100 mM phosphate buffer, pH 8.0, supplemented with 0.25 mg/mL BSA, bound to 0.5 volumes α -SLX4 serum, then washed four times with 5 volumes 100 mM phosphate buffer, pH 8.0, and three times with 5 volumes ELB (10 mM HEPES-KOH pH 7.7, 50 mM KCl, 2.5 mM MgCl_2 , and 250 mM Sucrose). One volume antibody-bound Dynabeads Protein A mixture was then aspirated and mixed with 1.5 volumes NPE or HSS and incubated for 30 minutes at room temperature (RT), after which the extract was harvested. This procedure was repeated once for NPE. After the last depletion round, extracts were collected and immediately used for DNA replication assays. To deplete egg extracts of RTEL1, one volume Dynabeads Protein A (ThermoFisher) was bound to 0.5 volumes α -RTEL1 serum or protein A sepharose (PAS) purified rabbit IgG (mock depletion) and washed as previously described. The mock, RTEL1, or SLX4 depleted HSS was diluted 2x prior to addition to NPE to reduce protein levels further.

Recombinant protein expression and purification

Xenopus laevis SLX4 containing an N-terminal FLAG-, or his-tag, and a C-terminal Strep-tag, was cloned into pDONR201 (Life Technologies). Point mutations for $x/SLX4^{UBZ-1^*}$, $x/SLX4^{UBZ-2^*}$, and $x/SLX4^{UBZ-1/2^*}$ mutants were introduced in pDONR-FLAG-strep-SLX4 using QuikChange site-directed mutagenesis (Agilent Technologies). The MLR domain, MLR-N, and residues 209-279 ($x/SLX4^{FA}$) were deleted by PCR amplification of flanking regions that were ligated by the introduction of a short linker containing a KpnI restriction site. To obtain the $x/SLX4^{FA^*}$ and $x/SLX4^{DM}$ mutants, mutations were introduced using QuikChange site-directed mutagenesis (Agilent Technologies) in constructs for the generation of $x/SLX4^{FA}$ and $x/SLX4^{\Delta MLR-N}$ mutants, respectively. Baculoviruses were produced using the BaculoDirect system following manufacturer's protocol (Life Technologies). Proteins were expressed in suspension cultures of Sf9 insect cells by infection with $x/SLX4$ viruses for 65 h. Cells from 150 mL culture were collected by centrifugation, resuspended in 6 mL lysis buffer (50 mM Tris pH 8.0, 250 mM NaCl, 0.1% NP-40, 5% glycerol, 0.4 mM PMSF, 1 tablet/10 mL Complete Mini EDTA-free Protease Inhibitor Cocktail (Roche)), and lysed by sonication. The soluble fraction obtained after centrifugation ($20,000 \times g$ for 20 minutes at $4^\circ C$) was incubated for 1 hour at $4^\circ C$ with 250 μL anti-FLAG M2 affinity gel (Sigma-Aldrich) that was pre-washed with lysis buffer. After incubation, the beads were washed with 40 mL wash buffer I (50 mM Tris pH 8.0, 250 mM NaCl, 0.1% NP-40, 5% glycerol, 0.4 mM PMSF) and subsequently with 30 mL wash buffer II (20 mM Tris pH 8.0, 200 mM NaCl, 0.1% NP-40, 5% glycerol, 0.1 mM PMSF, 10 $\mu g/mL$ aprotinin/leupeptin). The $x/SLX4$ protein was eluted in wash buffer II containing 100 $\mu g/mL$ 3 \times FLAG peptide (Sigma-Aldrich). The protein was aliquoted, flash frozen, and stored at $-80^\circ C$. Expression and purification of $x/SLX4$ mutant proteins were identical to the wild-type protein.

Expression and purification of $x/FANCD2$ and K562-ubiquitin conjugated $x/FANCD2$ (FANCD2-Ub), both containing a C-terminal 6 \times His-HA tag, was performed as described (Chaugule *et al.*, 2019). Expression and purification of $hsUSP1^{\Delta 1\Delta 2 C905}$ and $hsUAF1$ containing a C-terminal Strep-His tag was performed as described (Arkinson *et al.*, 2018). *Xenopus laevis* RTEL1 and mutant $x/RTEL1^{K48R}$ were expressed and purified as previously described (Sparks *et al.*, 2019). Human recombinant monoubiquitin, K48-linked polyubiquitin, and K63-linked polyubiquitin were purchased from Boston Biochem.

Chromatin immunoprecipitation

Chromatin immunoprecipitation (ChIP) was performed as described previously (Pacek *et al.*, 2006). Briefly, reaction samples were crosslinked with formaldehyde, sonicated to yield DNA fragments of roughly 100-500 bp, and immunoprecipitated with the indicated antibodies. Protein-DNA crosslinks were reversed and DNA was phenol/chloroform-extracted for analysis by quantitative real-time PCR with the following primers: pICL (5'-AGCCAGATTTTCTCCTCTC-3' and 5'-CATGCATTGGTTCTGCACTT-3') and pQuant (5'-TACAAATGTACGCCAGCAA-3' and 5'-GAGTATGAGGGAAGCGGTGA-3'). pQuant was analyzed to determine non-specific localization to undamaged DNA. The values from pQuant primers were subtracted from the values for pICL primers to establish the specific recruitment to ICL sites.

Immunoprecipitations

Immunoprecipitations (IPs) were performed *in vitro* using recombinant proteins or from *Xenopus* egg extracts, in absence or in presence of DNA replication. For IPs from *Xenopus* egg extract in the absence of DNA replication, SLX4 (or SLX4 mutants) was added to HSS at a concentration of 5 ng/ μ L. To each 10 μ L extract, 55 μ L extract-IP buffer (1 \times ELB salts, 0.25 M sucrose, 75 mM NaCl, 2 mM EDTA, 10 μ g/mL aproptin/leupeptin, 0.1% NP-40) and 10 μ L pre-washed anti-FLAG M2 affinity gel (Sigma-Aldrich) were added. Beads were incubated for 60 minutes at 4°C and subsequently washed using 2.5 mL extract-IP buffer. Beads were taken up in 30 μ L 2 \times SDS sample buffer and incubated for 4 minutes at 95°C. Proteins were separated by SDS-PAGE and visualized by western blot using the indicated antibodies.

For IPs in the presence of DNA replication, we added recombinant FLAG-tagged wild type or mutant SLX4 to *Xenopus* egg extracts which we used to replicate pICL or an undamaged plasmid with the same sequence (pCon). After 60 minutes, to each 23.5 μ L extract replication mix, 65 μ L extract-IP buffer, 10 μ L pre-washed anti-FLAG M2 affinity gel (Sigma-Aldrich) and (when indicated) 0.2 μ L benzonase (Sigma-Aldrich) were added. Beads were incubated for 90 minutes at 4°C and subsequently washed using 2.0 mL extract-IP buffer. FLAG-SLX4 was eluted by addition of 50 μ L extract-IP buffer containing 100 μ g/mL 3 \times FLAG peptide (Sigma-Aldrich), separated from beads by centrifugation through a home-made column containing a NITEX membrane, added to 12.5 μ L 5 \times SDS sample buffer, and incubated for 4 minutes at 95°C. Proteins were separated by SDS-PAGE and visualized by western blot using the indicated antibodies.

For FANCD2 IPs 0.5 volumes α -FANCD2 serum was bound to 1 volume of Dynabeads Protein A (ThermoFisher). Beads were resuspended in FANCD2-IP buffer (50 mM Tris, pH 7.5, 120 mM NaCl, 5% glycerol, 1 mM DTT, 0.01% Triton-X, 100 μ g/mL BSA). 1 μ g α -FANCD2 or α -FANCD2-Ub was added to 10 μ L beads and incubated for 1 hour at 4°C. Beads were washed with 180 μ L FANCD2-IP buffer before addition of 1 μ g *hsUSP1* ^{Δ 1 Δ 2^{C905}}-UAF1 or 1 μ g wild type α -SLX4. Beads were incubated for 1 hour at 4°C, washed with 120 μ L FANCD2-IP buffer, resuspended in 30 μ L 1 \times SDS sample buffer, and incubated for 2 minutes at 95°C. Proteins were separated by SDS-PAGE and visualized by western blot using the indicated antibodies.

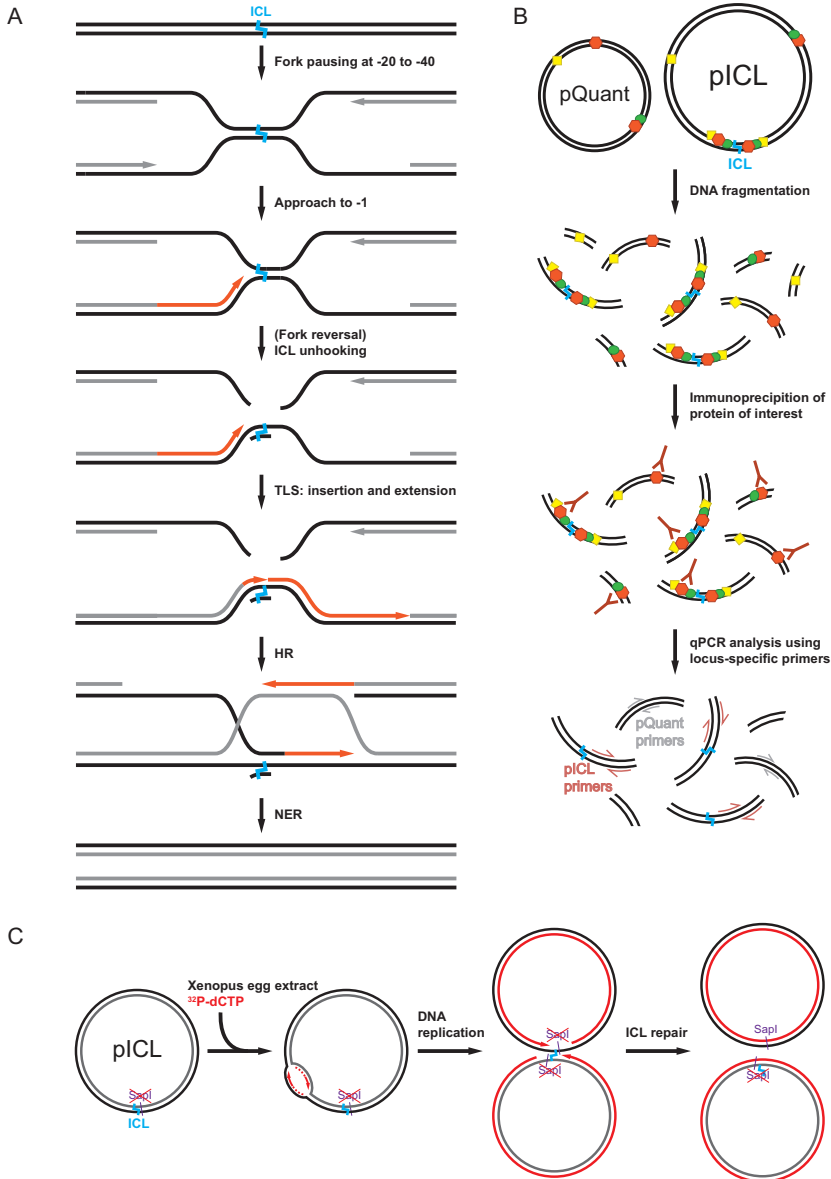
For ubiquitin IPs, we added 1 μ g ubiquitin (K63-linked poly(2-7)ubiquitin, K48-linked poly(2-7)ubiquitin, or monoubiquitin), 1 μ g wild type or mutant SLX4, and 5 μ L pre-washed anti-FLAG M2 affinity gel (Sigma-Aldrich) to 50 μ L ubiquitin-IP buffer (50 mM Tris, pH 8.0, 25 mM NaCl, 0.1% Triton-X, 10% glycerol, 200 μ g/mL BSA, 10 μ g/mL aproptin/leupeptin). Beads were incubated for 3 hours at 4°C and subsequently washed using 1.2 mL ubiquitin-IP buffer. FLAG-SLX4 was eluted by addition of 20 μ L buffer containing 5 μ g/ μ L 3 \times FLAG peptide (Sigma-Aldrich), separated from beads by centrifugation through a home-made column containing a NITEX membrane, added to 12.5 μ L 5 \times SDS sample buffer, and incubated for 4 minutes at 95°C. Proteins were separated by SDS-PAGE and visualized by western blot using the indicated antibodies.

References

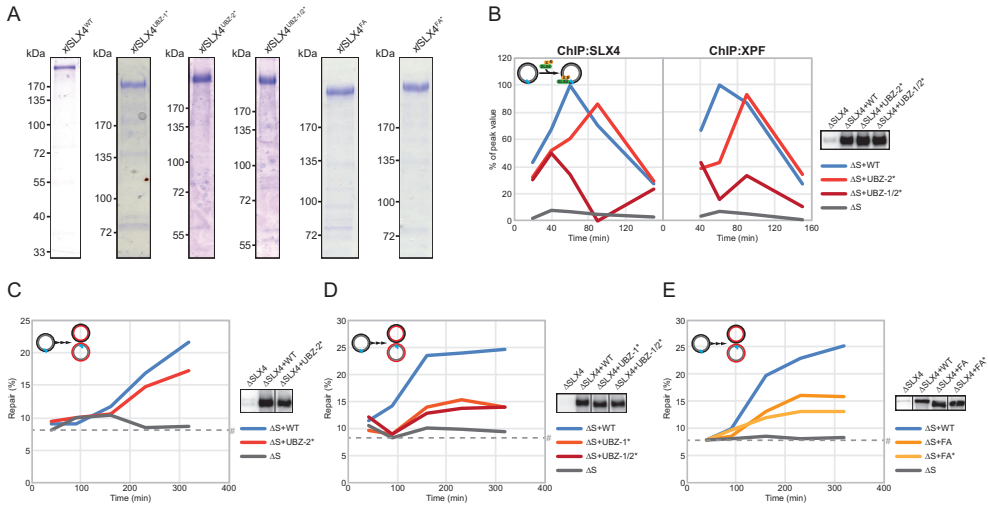
- Amunugama R, Willcox S, Wu RA, Abdullah UB, El-Sagheer AH, Brown T, McHugh PJ, Griffith JD & Walter JC (2018) Replication Fork Reversal during DNA Interstrand Crosslink Repair Requires CMG Unloading. *Cell reports* 23: 3419-3428
- Arkinson C, Chaugule VK, Toth R & Walden H (2018) Specificity for deubiquitination of monoubiquitinated FANCD2 is driven by the N-terminus of USP1. *Life Sci Alliance* 1: e201800162
- Budzowska M, Graham TG, Sobeck A, Waga S & Walter JC (2015) Regulation of the Rev1-pol zeta complex during bypass of a DNA interstrand crosslink. *The EMBO journal* 34: 1971-85
- Chaugule VK, Arkinson C, Toth R & Walden H (2019) Enzymatic preparation of monoubiquitinated FANCD2 and FANCI proteins. *Methods Enzymol* 618: 73-104
- Crosetto N, Bienko M, Hibbert RG, Perica T, Ambrogio C, Kensche T, Hofmann K, Sixma TK & Dikic I (2008) Human Wrn1p is localized in replication factories in a ubiquitin-binding zinc finger-dependent manner. *The Journal of biological chemistry* 283: 35173-85
- Dikic I, Wakatsuki S & Walters KJ (2009) Ubiquitin-binding domains - from structures to functions. *Nat Rev Mol Cell Biol* 10: 659-71
- Enoiu M, Jiricny J & Scharer OD (2012) Repair of cisplatin-induced DNA interstrand crosslinks by a replication-independent pathway involving transcription-coupled repair and translesion synthesis. *Nucleic acids research* 40: 8953-64
- Fekairi S, Scaglione S, Chahwan C, Taylor ER, Tissier A, Coulon S, Dong MQ, Ruse C, Yates JR, 3rd, Russell P, Fuchs RP, McGowan CH & Gaillard PH (2009) Human SLX4 is a Holliday junction resolvase subunit that binds multiple DNA repair/recombination endonucleases. *Cell* 138: 78-89
- Fu YV, Yardimci H, Long DT, Ho TV, Guainazzi A, Bermudez VP, Hurwitz J, van Oijen A, Scharer OD & Walter JC (2011) Selective bypass of a lagging strand roadblock by the eukaryotic replicative DNA helicase. *Cell* 146: 931-41
- Fullbright G, Rycenga HB, Gruber JD & Long DT (2016) p97 Promotes a Conserved Mechanism of Helicase Unloading during DNA Cross-Link Repair. *Molecular and cellular biology* 36: 2983-2994
- Garaycoechea JI, Crossan GP, Langevin F, Daly M, Arends MJ & Patel KJ (2012) Genotoxic consequences of endogenous aldehydes on mouse haematopoietic stem cell function. *Nature* 489: 571-5
- Guervilly JH & Gaillard PH (2018) SLX4: multitasking to maintain genome stability. *Crit Rev Biochem Mol Biol* 53: 475-514
- Hofmann K (2009) Ubiquitin-binding domains and their role in the DNA damage response. *DNA repair* 8: 544-56
- Hoogenboom WS, Boonen R & Knipscheer P (2018) The role of SLX4 and its associated nucleases in DNA interstrand crosslink repair. *Nucleic acids research*
- Iha H, Peloponese JM, Verstrepen L, Zapart G, Ikeda F, Smith CD, Starost MF, Yedavalli V, Heyninck K, Dikic I, Beyaert R & Jeang KT (2008) Inflammatory cardiac valvulitis in TAX1BP1-deficient mice through selective NF-kappaB activation. *The EMBO journal* 27: 629-41
- Kim Y, Lach FP, Desetty R, Hanenberg H, Auerbach AD & Smogorzewska A (2011) Mutations of the SLX4 gene in Fanconi anemia. *Nature genetics* 43: 142-6
- Kim Y, Spitz GS, Veturi U, Lach FP, Auerbach AD & Smogorzewska A (2013) Regulation of multiple DNA repair pathways by the Fanconi anemia protein SLX4. *Blood* 121: 54-63
- Klein Douwel D, Boonen RA, Long DT, Szybowska AA, Räschle M, Walter JC & Knipscheer P (2014) XPF-ERCC1 acts in Unhooking DNA interstrand crosslinks in cooperation with FANCD2 and FANCP/SLX4. *Molecular cell* 54: 460-71
- Knipscheer P, Räschle M, Scharer OD & Walter JC (2012) Replication-coupled DNA interstrand crosslink repair in *Xenopus* egg extracts. *Methods Mol Biol* 920: 221-43
- Knipscheer P, Räschle M, Smogorzewska A, Enoiu M, Ho TV, Scharer OD, Elledge SJ & Walter JC (2009) The Fanconi anemia pathway promotes replication-dependent DNA interstrand crosslink repair. *Science* 326: 1698-701
- Kottemann MC & Smogorzewska A (2013) Fanconi anaemia and the repair of Watson and Crick DNA crosslinks. *Nature* 493: 356-63
- Lachaud C, Castor D, Hain K, Munoz I, Wilson J, MacArtney TJ, Schindler D & Rouse J (2014) Distinct functional roles for the two SLX4 ubiquitin-binding UBZ domains mutated in Fanconi anemia. *Journal of cell science* 127: 2811-7
- Langevin F, Crossan GP, Rosado IV, Arends MJ & Patel KJ (2011) Fancd2 counteracts the toxic effects of naturally produced aldehydes in mice. *Nature* 475: 53-8
- Long DT, Joukov V, Budzowska M & Walter JC (2014) BRCA1 promotes unloading of the CMG helicase from a stalled DNA replication fork. *Molecular cell* 56: 174-85
- Long DT, Räschle M, Joukov V & Walter JC (2011) Mechanism of RAD51-dependent DNA interstrand crosslink repair. *Science* 333: 84-7
- Margalef P, Kotsantis P, Borel V, Bellelli R, Panier S & Boulton SJ (2018) Stabilization of Reversed Replication Forks by Telomerase Drives Telomere Catastrophe. *Cell* 172: 439-453 e14
- Pacek M, Tutter AV, Kubota Y, Takisawa H & Walter JC (2006) Localization of MCM2-7, Cdc45, and GINS to the site of DNA unwinding during eukaryotic DNA replication. *Molecular cell* 21: 581-7
- Räschle M, Knipscheer P, Enoiu M, Angelov T, Sun J, Griffith JD, Ellenberger TE, Scharer OD & Walter

- JC (2008) Mechanism of replication-coupled DNA interstrand crosslink repair. *Cell* 134: 969-80
- Räschle M, Smeenk G, Hansen RK, Temu T, Oka Y, Hein MY, Nagaraj N, Long DT, Walter JC, Hofmann K, Storchova Z, Cox J, Bekker-Jensen S, Mailand N & Mann M (2015) DNA repair. Proteomics reveals dynamic assembly of repair complexes during bypass of DNA cross-links. *Science* 348: 1253671
- Rosado IV, Langevin F, Crossan GP, Takata M & Patel KJ (2011) Formaldehyde catabolism is essential in cells deficient for the Fanconi anemia DNA-repair pathway. *Nature structural & molecular biology* 18: 1432-4
- Sarek G, Vannier JB, Panier S, Petrini JHJ & Boulton SJ (2015) TRF2 recruits RTEL1 to telomeres in S phase to promote t-loop unwinding. *Molecular cell* 57: 622-635
- Semlow DR, Zhang J, Budzowska M, Drohat AC & Walter JC (2016) Replication-Dependent Unhooking of DNA Interstrand Cross-Links by the NEIL3 Glycosylase. *Cell* 167: 498-511 e14
- Sparks JL, Chistol G, Gao AO, Räschle M, Larsen NB, Mann M, Duxin JP & Walter JC (2019) The CMG Helicase Bypasses DNA-Protein Cross-Links to Facilitate Their Repair. *Cell* 176: 167-181 e21
- Speckmann C, Sahoo SS, Rizzi M, Hirabayashi S, Karow A, Serwas NK, Hoernberg M, Damatova N, Schindler D, Vannier JB, Boulton SJ, Pannicke U, Gohring G, Thomay K, Verdu-Amoros JJ, Hauch H, Woessmann W, Escherich G, Laack E, Rindle L *et al.* (2017) Clinical and Molecular Heterogeneity of RTEL1 Deficiency. *Frontiers in immunology* 8: 449
- Stoepker C, Hain K, Schuster B, Hilhorst-Hofstee Y, Roomans MA, Steltenpool J, Oostra AB, Eirich K, Korthof ET, Nieuwint AW, Jaspers NG, Bettecken T, Joenje H, Schindler D, Rouse J & de Winter JP (2011) SLX4, a coordinator of structure-specific endonucleases, is mutated in a new Fanconi anemia subtype. *Nature genetics* 43: 138-41
- Svendsen JM, Smogorzewska A, Sowa ME, O'Connell BC, Gygi SP, Elledge SJ & Harper JW (2009) Mammalian BTBD12/SLX4 assembles a Holliday junction resolvase and is required for DNA repair. *Cell* 138: 63-77
- Toma A, Takahashi TS, Sato Y, Yamagata A, Goto-Ito S, Nakada S, Fukuto A, Horikoshi Y, Tashiro S & Fukai S (2015) Structural basis for ubiquitin recognition by ubiquitin-binding zinc finger of FAAP20. *PLoS one* 10: e0120887
- Tutter AV & Walter JC (2006) Chromosomal DNA replication in a soluble cell-free system derived from *Xenopus* eggs. *Methods Mol Biol* 322: 121-37
- Udeshi ND, Mertins P, Svinkina T & Carr SA (2013) Large-scale identification of ubiquitination sites by mass spectrometry. *Nat Protoc* 8: 1950-60
- Uringa EJ, Lisaingo K, Pickett HA, Brind'Amour J, Rohde JH, Zelensky A, Essers J & Lansdorp PM (2012) RTEL1 contributes to DNA replication and repair and telomere maintenance. *Mol Biol Cell* 23: 2782-92
- Uringa EJ, Youds JL, Lisaingo K, Lansdorp PM & Boulton SJ (2011) RTEL1: an essential helicase for telomere maintenance and the regulation of homologous recombination. *Nucleic acids research* 39: 1647-55
- Vannier JB, Pavicic-Kaltenbrunner V, Petalcorin MI, Ding H & Boulton SJ (2012) RTEL1 dismantles T loops and counteracts telomeric G4-DNA to maintain telomere integrity. *Cell* 149: 795-806
- Vannier JB, Sandhu S, Petalcorin MI, Wu X, Nabi Z, Ding H & Boulton SJ (2013) RTEL1 is a replisome-associated helicase that promotes telomere and genome-wide replication. *Science* 342: 239-42
- Varadan R, Assfalg M, Haririnia A, Raasi S, Pickart C & Fushman D (2004) Solution conformation of Lys63-linked di-ubiquitin chain provides clues to functional diversity of polyubiquitin signaling. *The Journal of biological chemistry* 279: 7055-63
- Varadan R, Walker O, Pickart C & Fushman D (2002) Structural Properties of Polyubiquitin Chains in Solution. *Journal of molecular biology* 324: 637-647
- Walden H & Deans AJ (2014) The Fanconi anemia DNA repair pathway: structural and functional insights into a complex disorder. *Annual review of biophysics* 43: 257-78
- Walter J, Sun L & Newport J (1998) Regulated chromosomal DNA replication in the absence of a nucleus. *Molecular cell* 1: 519-29
- Wu RA, Semlow DR, Kamimae-Lanning AN, Kochenova OV, Chistol G, Hodskinson MR, Amunugama R, Sparks JL, Wang M, Deng L, Mimoso CA, Low E, Patel KJ & Walter JC (2019) TRAIIP is a master regulator of DNA interstrand crosslink repair. *Nature*
- Yamamoto KN, Kobayashi S, Tsuda M, Kurumizaka H, Takata M, Kono K, Jiricny J, Takeda S & Hirota K (2011) Involvement of SLX4 in interstrand cross-link repair is regulated by the Fanconi anemia pathway. *Proceedings of the National Academy of Sciences of the United States of America* 108: 6492-6
- Zhang J, Dewar JM, Budzowska M, Motnenko A, Cohn MA & Walter JC (2015) DNA interstrand cross-link repair requires replication-fork convergence. *Nature structural & molecular biology* 22: 242-7

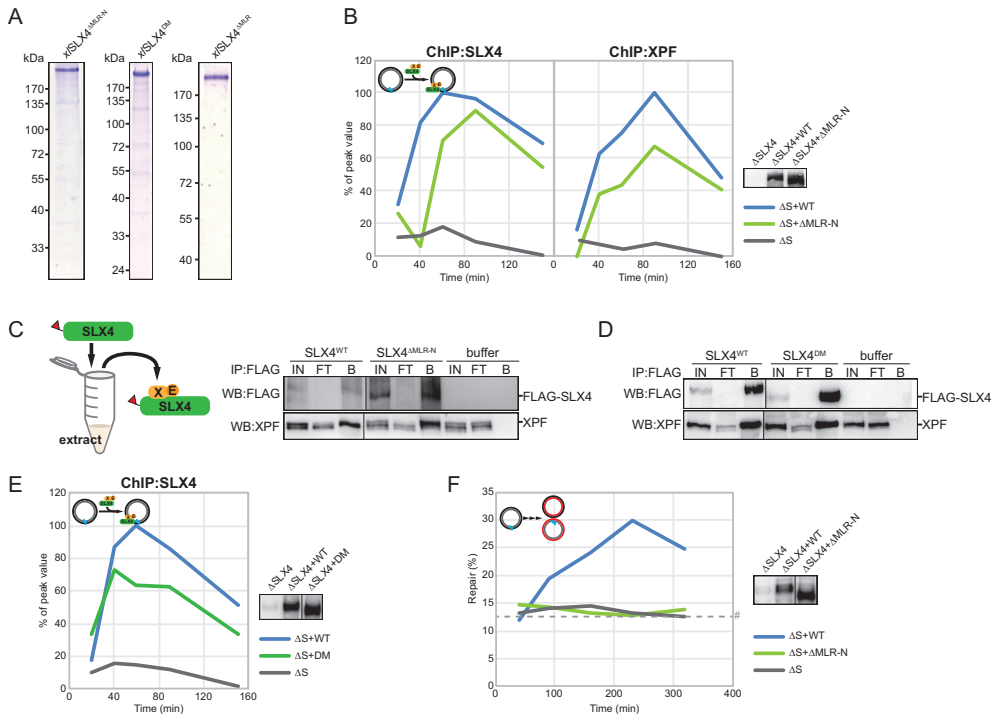
Supplemental Figures

**Supplemental Figure S1: Schematic representations of FA pathway, and ChIP and Repair assays.**

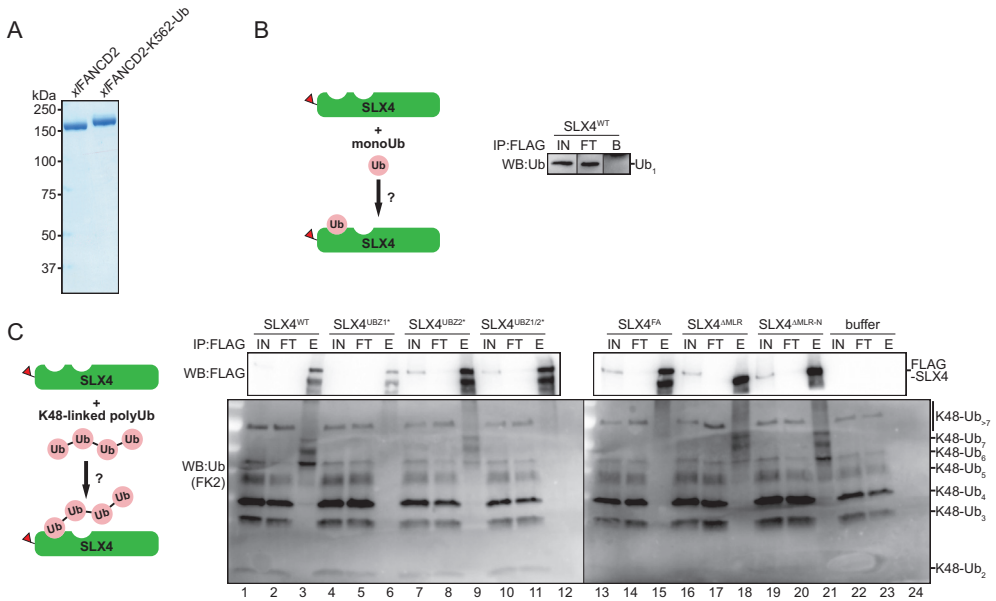
A) Schematic representation of replication-dependent ICL repair by the FA pathways in *Xenopus* egg extracts. See text for details. B) Repair intermediates of pICL and an undamaged smaller plasmid (pQuant) and bound proteins are crosslinked with formaldehyde at various time points. The DNA is fragmented by sonication and fragments containing the protein of interest are immunoprecipitated with specific antibodies. The DNA is purified by phenol-chloroform extraction and the recovery of the pICL locus or a control locus on pQuant is analyzed using qPCR and locus-specific primers. C) Schematic representation of Repair experiments in *Xenopus* egg extracts. The SapI site that is blocked by the ICL becomes available on one of the replicated molecules after full repair via homologous recombination using the sister molecule. The sister molecule retains the unhooked ICL that is not efficiently removed in *Xenopus* egg extracts (Raschle *et al.*, 2008).



Supplemental Figure S2: Mutations in UBZ-1, but not UBZ-2, impair ICL repair and SLX4 recruitment. A) Coomassie images of the purified wild type (*x/SLX4^{WT}*) and mutant (*x/SLX4^{MUT}*) mutant proteins used in this figure. B) SLX4-depleted (Δ SLX4), and SLX4-depleted NPE supplemented with wild-type SLX4 (Δ SLX4+WT) or mutant SLX4 (Δ SLX4+MUT) were analyzed by western blot using α -SLX4 antibody (right panel). These extracts, with SLX4-depleted HSS, were used to replicate pICL. Samples were taken at various times and immunoprecipitated with α -SLX4 (left panel) or α -XPF (middle panel) antibodies. Co-precipitated DNA was isolated and analysed by quantitative PCR using the pICL or pQuant primers. Recovery values of pQuant were subtracted from pICL recovery values. The resulting data were plotted as the percentage of peak value with the highest value within one experiment set to 100%. Independent duplicate experiment related to Figure 1B. C) SLX4-depleted (Δ SLX4), and SLX4-depleted NPE supplemented with wild-type SLX4 (Δ SLX4+WT) or mutant SLX4 (Δ SLX4+UBZ-2*) were analyzed by western blot using α -SLX4 antibody (right panel). These extracts, with SLX4-depleted HSS, were used to replicate pICL. Repair efficiency was calculated and plotted (left panel). Line within blot indicates position where irrelevant lanes were removed. Independent duplicate experiment related to Figure 1C. D) As in (C) but using the *x/SLX4^{UBZ-1*}* and *x/SLX4^{UBZ-1/2*}* mutant proteins. Line within blot indicates position where irrelevant lanes were removed. Independent duplicate experiment related to Figure 1C and D. E) As in (C) but using the *x/SLX4^{FA}* and *x/SLX4^{FA*}* mutant proteins. Line within blot indicates position where irrelevant lanes were removed. Independent duplicate experiment related to Figure 1E. #, SapI fragments from contaminating uncrosslinked plasmid present in varying degrees in different pICL preparations.



Supplemental Figure S3: The MLR-N region is crucial for ICL repair and contributes to SLX4 recruitment. A) Coomassie images of the purified mutant (x /SLX4^{MUT}) mutant proteins used in this figure. B) SLX4-depleted (Δ SLX4), and SLX4-depleted NPE supplemented with wild-type SLX4 (Δ SLX4+WT) or mutant SLX4 (Δ SLX4+ Δ MLR-N) were analyzed by western blot using α -SLX4 antibody (right panel). These extracts, with SLX4-depleted HSS, were used to replicate pICL. Samples were taken at various times and immunoprecipitated with α -SLX4 (left panel) or α -XPF (middle panel) antibodies. Co-precipitated DNA was isolated and analysed by quantitative PCR using the pICL or pQuant primers. Recovery values of pQuant were subtracted from pICL recovery values. The resulting data were plotted as the percentage of peak value with the highest value within one experiment set to 100%. Independent duplicate experiment related to Figure 2B. C) Purified wild type (SLX4^{WT}), mutant SLX4 (SLX4 ^{Δ MLR-N}) or buffer were added to HSS. After incubation, recombinant SLX4 protein was immunoprecipitated with anti-FLAG M2 affinity gel (Sigma-Aldrich). The input (IN), flow-through (FT), and bound fractions (B) were analyzed by western blot using α -FLAG (upper panel) and α -XPF antibodies (lower panel). Line within blot indicates position where irrelevant lanes were removed. D) As in (C) but using the x /SLX4^{DM} mutant protein. Line within blot indicates position where irrelevant lanes were removed. E) As in (B) but using the x /SLX4^{DM} mutant protein. Line within blot indicates position where irrelevant lanes were removed. F) SLX4-depleted (Δ SLX4), and SLX4-depleted NPE supplemented with wild-type SLX4 (Δ SLX4+WT) or mutant SLX4 (Δ SLX4+ Δ MLR-N) were analyzed by western blot using α -SLX4 antibody (right panel). These extracts, with SLX4-depleted HSS, were used to replicate pICL. Repair efficiency was calculated and plotted (left panel). Line within blot indicates position where irrelevant lanes were removed. Independent duplicate experiment related to Figure 2C. #, SapI fragments from contaminating uncrosslinked plasmid present in varying degrees in different pICL preparations.



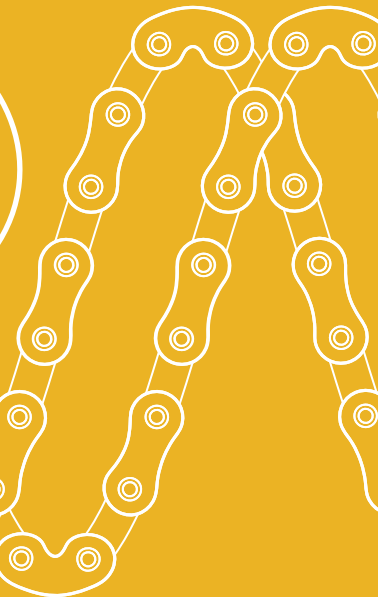
Supplemental Figure S4: SLX4 binds K48-linked polyubiquitin chains but not monoubiquitin. A) Coomassie image of purified xFANCD2 and xFANCD2-K562-Ub proteins. B) Purified FLAG-tagged wild type (SLX4^{WT}) was incubated with monoubiquitin (Boston Biochem) and immunoprecipitated with FLAG-M2 resin (Sigma-Aldrich). FLAG-SLX4 was eluted with 3× FLAG peptide. The input (IN), flow-through (FT), and eluted fractions (E) were analyzed by western blot using α -ubiquitin (P4D1) antibodies. Line within blot indicates position where irrelevant lanes were removed. C) Purified FLAG-tagged wild type (SLX4^{WT}) and mutant SLX4 (SLX4^{MUT}) constructs were incubated with K48-linked polyubiquitin chains (Boston Biochem) and immunoprecipitated with FLAG-M2 resin (Sigma-Aldrich). FLAG-SLX4 was eluted with 3× FLAG peptide. The input (IN), flow-through (FT), and eluted fractions (E) were analyzed by western blot using α -FLAG (upper panel) and α -ubiquitin (FK2) antibodies (lower panel). Line within blot indicates position where irrelevant lanes were removed.

Chapter 6

General discussion

Wouter S. Hoogenboom and Puck Knipscheer

Oncode Institute, Hubrecht Institute–KNAW and University Medical Center
Utrecht, Utrecht, The Netherlands



Introduction

Among various types of DNA damage, one particularly toxic DNA lesion is the DNA interstrand crosslink (ICL). ICLs covalently attach both strands of the double helix, thereby preventing separation of the strands that is required for several important cellular processes. The toxic effects of ICL inducing agents are widely exploited in cancer chemotherapeutic drugs, as fast-dividing tumour cells are particularly sensitive to ICL damage. Repair of ICL damage strongly relies on the replication-dependent Fanconi anemia (FA) pathway, a complex mechanism that involves tightly regulated nucleolytic incisions, translesion synthesis (TLS), homologous recombination (HR), and nucleotide excision repair (NER). Although the involvement of many factors in this pathway has been demonstrated, the exact role of each of these factors in ICL repair remains poorly understood. The mechanism by which nucleolytic incisions unhook the ICL from one of the strands, in particular the roles of the scaffold protein SLX4 and the structure specific endonuclease (SSE) XPF-ERCC1 during this step, is the main subject of this thesis. In this chapter I will address and discuss the major findings of my research and speculate how future experiments could complement these findings.

How can substrate specificity of XPF-ERCC1 be exploited for anti-cancer therapies?

XPF-ERCC1 functions in several genome maintenance pathways, and plays essential roles in nucleotide excision repair (NER) and in the FA pathway for ICL repair. High expression of ERCC1 is associated with poor responses to chemotherapy in several cancer types (Gavande *et al.*, 2016, Gentile *et al.*, 2018, McNeil *et al.*, 2015). Consistently, downregulation of XPF-ERCC1 by RNA interference resulted in increased efficacy of cisplatin cytotoxicity in various cancer cells (Arora *et al.*, 2010). Targeting XPF-ERCC1 to enhance cancer therapy could be more specific and efficient when the function is targeted that is specifically responsible for resistance to ICL inducing agents, or it could be exploited in novel treatments based on synthetic lethal interactions with other DNA repair pathways (Guainazzi & Scharer, 2010). To achieve that, a better understanding of how XPF-ERCC1 contributes to ICL repair is vital.

In **chapter 3** we identified several mutations in XPF that specifically affect the function of XPF-ERCC1 in ICL repair, while NER function was unaffected. Two of these 'separation of function' mutations reside in the nuclease domain of XPF and could interfere with recognition of DNA structures that are specific to ICL unhooking. However, the development of specific inhibitors that exploit the nuclease domain is challenging, as the structure of the DNA substrate is not known and there is a risk that other nucleases are targeted as well due to shared mechanistic activities (McNeil *et al.*, 2015).

Specific inhibition of XPF-ERCC1 could also be achieved by targeting protein-protein interactions that are specific for ICL repair. We show in **chapter 3 and 4** that XPF-ERCC1 interaction with SLX4 is crucial for ICL repair, as mutations that disrupt this interaction abrogate ICL repair. We established this using the L219R mutation in XPF, as well as by introducing mutations in the C-terminal end of the MLR domain in SLX4. We propose that the regions where these residues reside constitute a major binding interface that could be targeted to inhibit ICL repair. In addition, our results identify a region in XPF (residues 312-315) that is not essential for binding to SLX4, but could mediate an interaction to

properly position XPF on the DNA substrate. This interaction does not involve the BTB domain of SLX4, as a truncated protein lacking this domain was functional in ICL repair. We have not examined other regions in SLX4 that could facilitate this minor interaction with XPF-ERCC1. In addition to SLX4, XPF-ERCC1 was shown to have affinity for the FA core component FANCG. A yeast two-hybrid study demonstrated that this is mediated by the central domain of ERCC1 and several tetratricopeptide repeats (TPRs) of FANCG (Wang & Lambert, 2010). Although it is unknown whether this interaction is important for ICL repair, it is likely to be specific, and targeting this interaction may inhibit the ICL repair function of XPF-ERCC1. However, recruitment of XPF-ERCC1 to ICLs is completely blocked by depletion of SLX4, indicating that the interaction between FANCG and ERCC1 may not be crucial for ICL repair.

To develop targets for these interactions it is important to have detailed knowledge about how they are formed. Various methods could be employed to achieve this. Ultimately, crystal structures of the binding interfaces would be extremely useful, while obtaining those could benefit from preliminary studies that map the interactions to defined regions. We purified full-length and truncated proteins of XPF-ERCC1 and SLX4, which could be used for chemical crosslinking followed by fractionation and mass spectrometry (MS) analysis to identify interaction regions (Leitner *et al.*, 2010, Trakselis *et al.*, 2005). To find a minor interaction site between SLX4 and residues 312-315 of XPF, various fragments of SLX4's N-terminal region could be tested in a size exclusion chromatography, similar to what was done with the BTB domain in chapter 3. An interaction could then be validated by repeating the experiment with the mutant of XPF.

What is the mechanism of ICL unhooking?

The Fanconi anemia pathway promotes ICL repair in part through incisions that unhook the ICL from one of the strands (Räschle *et al.*, 2008). Identifying the required nuclease(s) that induce these incisions is of great importance for our understanding of the ICL repair mechanism. Previous work in *Xenopus* egg extracts demonstrated that XPF-ERCC1 is required for unhooking incisions during ICL repair, while FAN1 and MUS81-EME1 are dispensable (Klein Douwel *et al.*, 2014). Another SSE, SLX1, has been suggested to be the second nuclease, based on its substrate specificity and association with SLX4. In **chapter 4** we demonstrate that SLX1 is not required for ICL repair by depleting it from extract. However, this does not rule out a redundant role with another nuclease. To explore this possibility, similar experiments could be conducted involving depletion of two proteins, such as FAN1 and SLX1 that have similar substrate specificity.

In an alternative model, XPF-ERCC1 may perform incisions on either side of the crosslink, despite a preference for 5' flap structures and perhaps stimulated by SLX4, as is demonstrated to be possible using *in vitro* reconstitution studies (Das *et al.*, 2017, Fisher *et al.*, 2008, Hodskinson *et al.*, 2014, Kuraoka *et al.*, 2000). This model would explain why incisions on either side fail in absence of XPF-ERCC1 (Klein Douwel *et al.*, 2014). SLX4 could also play a role in this mechanism by forming homodimers through its BTB domain, essentially positioning two XPF-ERCC1 heterodimers on the DNA flanking the ICL. Although results shown in **chapter 4** demonstrate that reduced dimerization of SLX4 does not affect ICL repair, full disruption of SLX4 dimer formation is needed to exclude this mode of action. Alternatively, since this model likely involves two molecules of SLX4 and XPF-ERCC1 at one ICL, an approach that is sufficiently reliable for a quantitative

determination of the unhooking machinery at an ICL could be informative. The largely synchronous ICL repair in *Xenopus* egg extracts and recent advances in the technology of MS could be well enough to perform such analyses (Smits *et al.*, 2013, Urban, 2016).

A different model that was recently proposed involves replication fork reversal to create a DNA structure around the ICL that facilitates unhooking. This study, that is based on the examination of ICL repair intermediates generated in *Xenopus* egg extracts using electron microscopy (EM), demonstrated that after unloading of the replicative helicase (CMG), but prior to unhooking incisions one replication fork undergoes reversal (Amunugama *et al.*, 2018). This results in the formation of a DNA structure that resembles a single stalled replication fork. Reconstitution experiments have shown that XPF-ERCC1, aided by RPA, can make an incision on the duplex DNA region next to the ICL in a similar structure (Abdullah *et al.*, 2017). This incision may be used by the exonuclease SNM1A as an entry point for 5' to 3' digestion past the ICL (Amunugama *et al.*, 2018), consistent with ICL unhooking being dependent on an initial incision by XPF-ERCC1 but does not include the action of a second endonuclease. However, the proposed model is speculative and requires validation. Only a subset of the plasmid molecules in the reaction undergo fork reversal, and evidence that reversal is essential for ICL unhooking or repair is lacking. The authors note that fork reversal could be a non-productive repair intermediate, so identifying and inhibiting the motor protein that promotes reversal at these structures would help to determine the importance of their finding. Additionally, blocking the exonuclease reaction could result in single incision products that can be biochemically visualized. However, it is not unlikely that SNM1A works redundantly with other factors in this step, such as FAN1 and SNM1B, which would complicate the outcome of this experiment (Allerston *et al.*, 2015, Cattell *et al.*, 2010).

In conclusion, there is still a lot to be learnt about how ICL unhooking is achieved. Identification of the required set of nucleases and the DNA structure that they act on would be a big step forward but has proven to be an ongoing challenge.

What is the role of SLX4 dimerization in ICL repair?

Two studies recently demonstrated that the BTB domain is important for the formation of SLX4 homodimers, and that dimerization-disrupting mutations have a slight impact on cellular sensitivity to ICL-inducing agents (Guervilly *et al.*, 2015, Yin *et al.*, 2016). We envision two mechanisms by which SLX4 dimerization could contribute to ICL. First, a dimer of SLX4 could enable simultaneous recruitment and possibly positioning of two XPF-ERCC1 molecules, allowing rapid unhooking of the ICL (discussed in the previous paragraph). Second, a dimer of SLX4 could be required to properly bind polyubiquitin chains required for efficient recruitment (discussed below).

Our work presented in **chapter 4** demonstrates that the BTB domain is dispensable for ICL repair. However, we find that deletion of BTB does not completely abrogate SLX4 dimer formation, indicating that an unknown region could contribute to ICL repair by interaction with another SLX4 molecule. Identification of this region is needed to establish whether and how dimerization could be important for ICL repair. Similar to finding SLX4-XPF interaction sites, chemical crosslinking followed by MS could help to identify how dimers are formed in absence of the BTB domain. In addition, further elucidation of the mechanisms for ICL unhooking or SLX4 recruitment could indicate the importance of SLX4

dimerization.

What is the substrate of UBZ-1?

Previous work in *Xenopus* egg extracts has shown that SLX4 recruitment to ICLs depends on monoubiquitylation of FANCD2 (Klein Douwel et al. 2014). However, the mechanism of SLX4 recruitment remains unclear. A ubiquitin-mediated mechanism was proposed when a deletion in the UBZ region of SLX4 was shown to be causative of FA (Kim et al., 2011).

In **chapter 5** we examined the effect of mutations in the UBZ region and our results indicate that an interaction mediated by UBZ-1 is crucial for ICL repair, although the nature of this interaction is unknown. Using *in vitro* pulldown assays we demonstrated that full-length SLX4 failed to interact with monoubiquitin and short (<5 subunits) polyubiquitin chains, whereas longer chains linked via the lysine residues at positions 48 and 63 of ubiquitin (K48- and K63-linked polyubiquitin) were readily pulled down. This is striking because ubiquitin binding domains (UBDs) of the zinc-finger (UBZ) type are not normally associated with binding chains longer than diubiquitin (Hofmann, 2009, Suzuki et al., 2016, Toma et al., 2015). Mutation of UBZ-2 only slightly affected pulldown of K48-linked chains, indicating that UBZ-1 is largely responsible for the ubiquitin binding specificity. It would be interesting to see if future crystal structures could reveal how this interaction is mediated by a single UBD. Alternatively, it is conceivable that dimerization of SLX4 contributes to this interaction by utilizing two UBZ-1 domains to bind one polyubiquitin chain. Our own data is not in favour of this mode of interaction, as we show in **chapter 4** that a reduction of dimerization does not lead to reduced recruitment of SLX4. However, complete disruption of dimerization is necessary to rule this option out.

It is currently unknown what the identity is of the factor whose ubiquitin chain is recognized by UBZ-1, while identification of this factor is crucial for understanding SLX4 recruitment. Our work in **chapter 5** suggests that this factor contains a long (>4 subunits) polyubiquitin chain of K48- or K63-linkage, although we cannot exclude other linkage types. K63-linked chains primarily act as non-proteolytic signals in intracellular pathways, including DNA damage tolerance (Pickart & Fushman, 2004), and are therefore a likely candidate for recruitment of SLX4. Long, free K63-linked polyubiquitin chains are even capable of independently binding DNA to recruit repair factors (Liu et al., 2018). In contrast, K48-linked chains of 4 or more subunits are easily recognized by the proteasome, targeting substrates for degradation (Li & Ye, 2008). However, examples of non-proteolytic function of K48-linked chains exist, including one that activates the p97 ATPase (Ye, 2006), which is responsible for CMG unloading during ICL repair (Fullbright et al., 2016). Collectively, there is currently no ubiquitin linkage type that could be excluded for recruitment of SLX4.

We considered that, in addition to the ubiquitin-UBZ interaction, interaction between other regions of the two proteins could enhance the affinity. Therefore, despite the lack of affinity between SLX4 and monoubiquitin, we examined the interaction between SLX4 and monoubiquitylated FANCD2 (FANCD2-Ub). However, our work presented in **chapter 5** indicates that SLX4 and FANCD2-Ub do not interact directly but only form a DNA-mediated interaction.

Several approaches could help to identify the ubiquitylated substrate of UBZ-1. During replication in *Xenopus* egg extracts in the presence of wild type or mutant SLX4, immunoprecipitations of recombinant SLX4 could be analysed by MS to search for

differentially co-precipitation of ubiquitylated proteins. Analysis of ubiquitylated factors by MS is well established (Na & Peng, 2012). Another approach is to test whether SLX4 recruitment is inhibited by depletion of specific E2 or E3 ubiquitin ligases from extract. Identification of the responsible ubiquitin ligase(s) could help to find the substrate of UBZ-1 from a list of known targets. However, this approach is not very straightforward, since there are many such ligases that can even be used in different combinations to achieve specific modifications (Suryadinata *et al.*, 2014). However, several factors could be worth examining, such as NEDD4 that is specific for K63-linked ubiquitin, and RNF8 that is already involved in ICL repair (Medvar *et al.*, 2016, Yan *et al.*, 2012).

What is the link between FANCD2 ubiquitylation and for SLX4 recruitment?

It remains elusive how monoubiquitylation of FANCD2 leads to recruitment of SLX4 and subsequent ICL unhooking. Previous work in our lab combined with results presented in **chapter 5** indicate that FANCD2-Ub promotes recruitment of SLX4 through another mechanism than a direct interaction (Klein Douwel *et al.*, 2014). Crystal structures have shown that the ligation sites for ubiquitin in FANCD2 and FANCI are embedded in the heterodimer structure (Joo *et al.*, 2011), while monoubiquitylation is speculated to help retain association with DNA (Lopez-Martinez *et al.*, 2016). It is therefore conceivable that this monoubiquitin is not involved in any protein interactions but rather essential to confer a structural change in the ID2 heterodimer which locks it onto DNA. The function of monoubiquitylated FANCD2 at ICL sites is currently poorly understood. Previous work in our own lab has demonstrated that after localization to an ICL, multiple FANCD2-Ub molecules are loaded on the plasmid and spread to either side of the ICL (Klein Douwel *et al.*, 2014). The function of this 'spreading' is currently unclear but further characterization of this feature could help to understand the role of FANCD2 monoubiquitylation and its link to SLX4 recruitment.

As discussed before, a UBZ-1 mediated interaction with an unidentified ubiquitin chain is important for recruitment of SLX4. However, work presented in **chapter 5** demonstrates that mutation of the UBZ region does not completely abrogate SLX4 recruitment and ICL repair. Although our results suggested that the MLR-N region could mediate a ubiquitin-independent mechanism of recruitment, we observed no decrease in recruitment when both regions were mutated. We suggest that deletion of MLR-N could affect UBZ-1 interaction with its ubiquitylated substrate, or prevent a necessary secondary interaction. However, this does not explain why ICL repair is completely abrogated in absence of this region. Identification of the substrate of UBZ-1 will likely allow us to investigate how the MLR domain is involved in SLX4 recruitment and ICL repair. In addition, residual recruitment of the double mutant suggests that SLX4 recruitment can be achieved through an MLR-N and UBZ-independent mechanism. Further characterization of the N-terminal region required for ICL repair could provide answers as to what this mechanism could be.

What is the role of SLX4 in ICL repair?

Our results presented in **chapter 3 and 4** show that SLX4 is required to bring, and possibly position, XPF-ERCC1 at ICL sites, and that interactions mediated by the C-terminal half of

SLX4 are not required for ICL repair. This indicates that the sole purpose of SLX4 in ICL repair is to facilitate one or both incisions by XPF-ERCC1, however that is not necessarily the case. Although the short truncated SLX4 mutant encompasses less than a third of the full-length protein, it contains several regions that are poorly characterized. As discussed earlier, we expect to find currently unidentified regions that contribute to XPF-ERCC1 interaction, dimer formation, and recruitment. In addition, this region is shown to bind the MSH2/MSH3 mismatch repair complex and the uncharacterized protein C20orf94, also known as SLX4 interacting protein (SLX4IP or SIP) (Svendsen *et al.*, 2009). Deletion of SIP is a common alteration in childhood acute lymphoblastic leukemia, although any functional details are lacking (Meissner *et al.*, 2014). The functional roles of these factors or their relation with SLX4 remains to be determined.

To investigate this, a first approach would be to examine the function using *Xenopus* egg extracts immunodepleted of MSH2 or SIP. If this results in completely or partially defective repair, it would be interesting to find if a direct interaction with SLX4 is essential for their function. It is possible that one or both proteins interact with SLX4 through the N-terminal end of SLX4, which could be tested with the generation of a short truncation. Alternatively, precise mapping of the interaction sites could be achieved by crystal structures, or MS analysis of chemically crosslinked purified proteins.

If these interactions appear to be dispensable for ICL repair, it would be interesting to try to generate a 'minimal SLX4 protein' that functions in ICL repair but lacks any unnecessary sites. Proper recruitment and positioning of XPF may be all that is required from SLX4 during ICL repair. However, we currently have insufficient understanding of the role of SLX4 in ICL repair to conduct such experiments.

Concluding remarks

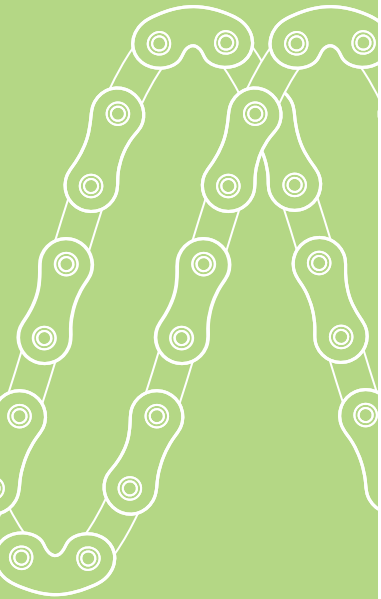
The *Xenopus* egg extract system has played a vital role in our current understanding of the FA pathway. This system fully recapitulates the replication-dependent repair of ICLs, while giving the researcher the unique advantage of having complete control over the DNA lesion that is introduced. SLX4 functions in several genome maintenance pathways; by using *Xenopus* egg extracts I could be confident that I was examining functions specific to ICL repair. I have used this model system to expand our understanding of how SLX4 facilitates XPF-ERCC1 mediated unhooking of the ICL. Cancer therapies often exploit the toxic effects of ICL damage, while cancer cells are known to develop resistance by upregulation of DNA repair factors such as XPF-ERCC1. Detailed knowledge of how repair factors restore ICL damage is therefore useful for the development of improved cancer therapies and to fight resistance to existing treatments. Furthermore, understanding how defects in the function of Fanconi anemia proteins lead to the disease may help to improve treatment and/or the prediction of disease progression in the future.

References

- Abdullah UB, McGouran JF, Brolihan S, Ptchelkine D, El-Sagheer AH, Brown T & McHugh PJ (2017) RPA activates the XPF-ERCC1 endonuclease to initiate processing of DNA interstrand crosslinks. *The EMBO journal* 36: 2047-2060
- Allerston CK, Lee SY, Newman JA, Schofield CJ, McHugh PJ & Gileadi O (2015) The structures of the SNM1A and SNM1B/Apollo nuclease domains reveal a potential basis for their distinct DNA processing activities. *Nucleic acids research* 43: 11047-60
- Amunugama R, Willcox S, Wu RA, Abdullah UB, El-Sagheer AH, Brown T, McHugh PJ, Griffith JD & Walter JC (2018) Replication Fork Reversal during DNA Interstrand Crosslink Repair Requires CMG Unloading. *Cell reports* 23: 3419-3428
- Arora S, Kothandapani A, Tillison K, Kalman-Maltese V & Patrick SM (2010) Downregulation of XPF-ERCC1 enhances cisplatin efficacy in cancer cells. *DNA repair* 9: 745-53
- Cattell E, Sengerova B & McHugh PJ (2010) The SNM1/Pso2 family of ICL repair nucleases: from yeast to man. *Environmental and molecular mutagenesis* 51: 635-45
- Das D, Faridounnia M, Kovacic L, Kaptein R, Boelens R & Folkers GE (2017) Single-stranded DNA Binding by the Helix-Hairpin-Helix Domain of XPF Protein Contributes to the Substrate Specificity of the ERCC1-XPF Protein Complex. *The Journal of biological chemistry* 292: 2842-2853
- Fisher LA, Bessho M & Bessho T (2008) Processing of a psoralen DNA interstrand cross-link by XPF-ERCC1 complex in vitro. *The Journal of biological chemistry* 283: 1275-81
- Fullbright G, Rycenga HB, Gruber JD & Long DT (2016) p97 Promotes a Conserved Mechanism of Helicase Unloading during DNA Cross-Link Repair. *Molecular and cellular biology* 36: 2983-2994
- Gavande NS, VanderVere-Carozza PS, Hinshaw HD, Jalal SI, Sears CR, Pawelczak KS & Turchi JJ (2016) DNA repair targeted therapy: The past or future of cancer treatment? *Pharmacology & therapeutics* 160: 65-83
- Gentile F, Barakat KH & Tuszyński JA (2018) Computational Characterization of Small Molecules Binding to the Human XPF Active Site and Virtual Screening to Identify Potential New DNA Repair Inhibitors Targeting the ERCC1-XPF Endonuclease. *Int J Mol Sci* 19
- Guainazzi A & Schärer OD (2010) Using synthetic DNA interstrand crosslinks to elucidate repair pathways and identify new therapeutic targets for cancer chemotherapy. *Cell Mol Life Sci* 67: 3683-97
- Guervilly JH, Takedachi A, Naim V, Scaglione S, Chawhan C, Lovera Y, Despras E, Kuraoka I, Kannouche P, Rosselli F & Gaillard PH (2015) The SLX4 complex is a SUMO E3 ligase that impacts on replication stress outcome and genome stability. *Molecular cell* 57: 123-37
- Hodskinson MR, Silhan J, Crossan GP, Garaycochea JJ, Mukherjee S, Johnson CM, Schärer OD & Patel KJ (2014) Mouse SLX4 is a tumor suppressor that stimulates the activity of the nuclease XPF-ERCC1 in DNA crosslink repair. *Molecular cell* 54: 472-84
- Hofmann K (2009) Ubiquitin-binding domains and their role in the DNA damage response. *DNA repair* 8: 544-56
- Joo W, Xu G, Persky NS, Smogorzewska A, Rudge DG, Buzovetsky O, Elledge SJ & Pavletich NP (2011) Structure of the FANCI-FANCD2 complex: insights into the Fanconi anemia DNA repair pathway. *Science* 333: 312-6
- Kim Y, Lach FP, Desetty R, Hanenberg H, Auerbach AD & Smogorzewska A (2011) Mutations of the SLX4 gene in Fanconi anemia. *Nature genetics* 43: 142-6
- Klein Douwel D, Boonen RA, Long DT, Szypowska AA, Räschele M, Walter JC & Knipscheer P (2014) XPF-ERCC1 acts in Unhooking DNA interstrand crosslinks in cooperation with FANCD2 and FANCP/SLX4. *Molecular cell* 54: 460-71
- Kuraoka I, Kobertz WR, Ariza RR, Biggerstaff M, Essigmann JM & Wood RD (2000) Repair of an interstrand DNA cross-link initiated by ERCC1-XPF repair/recombination nuclease. *The Journal of biological chemistry* 275: 26632-6
- Leitner A, Walzthoeni T, Kahraman A, Herzog F, Rinner O, Beck M & Aebersold R (2010) Probing native protein structures by chemical cross-linking, mass spectrometry, and bioinformatics. *Mol Cell Proteomics* 9: 1634-49
- Li W & Ye Y (2008) Polyubiquitin chains: functions, structures, and mechanisms. *Cell Mol Life Sci* 65: 2397-406
- Liu P, Gan W, Su S, Hauenstein AV, Fu TM, Brasher B, Schwerdtfeger C, Liang AC, Xu M & Wei W (2018) K63-linked polyubiquitin chains bind to DNA to facilitate DNA damage repair. *Science signaling* 11
- Lopez-Martinez D, Liang CC & Cohn MA (2016) Cellular response to DNA interstrand crosslinks: the Fanconi anemia pathway. *Cell Mol Life Sci* 73: 3097-114
- McNeil EM, Astell KR, Ritchie AM, Shave S, Houston DR, Bakrania P, Jones HM, Khurana P, Wallace C, Chapman T, Wear MA, Walkinshaw MD, Saxty B & Melton DW (2015) Inhibition of the ERCC1-XPF structure-specific endonuclease to overcome cancer chemoresistance. *DNA repair* 31: 19-28
- Medvar B, Raghuram V, Pisitkun T, Sarkar A & Knepper MA (2016) Comprehensive database of human E3 ubiquitin ligases: application to aquaporin-2 regulation. *Physiol Genomics* 48: 502-12
- Meissner B, Bartram T, Eckert C, Trka J, Panzer-Grumayer R, Hermanova I, Ellinghaus E, Franke A, Moricke A, Schrauder A, Teigler-Schlegel A, Dorge P, von Stackelberg A, Basso G, Bartram CR, Kirschner-Schwabe R, Bornhauser B, Bourquin JP,

- Cazzaniga G, Hauer J *et al.* (2014) Frequent and sex-biased deletion of SLX4IP by illegitimate V(D) J-mediated recombination in childhood acute lymphoblastic leukemia. *Human molecular genetics* 23: 590-601
- Na CH & Peng J (2012) Analysis of ubiquitinated proteome by quantitative mass spectrometry. *Methods Mol Biol* 893: 417-29
- Pickart CM & Fushman D (2004) Polyubiquitin chains: polymeric protein signals. *Curr Opin Chem Biol* 8: 610-6
- Räschle M, Knipscheer P, Enoiu M, Angelov T, Sun J, Griffith JD, Ellenberger TE, Schärer OD & Walter JC (2008) Mechanism of replication-coupled DNA interstrand crosslink repair. *Cell* 134: 969-80
- Smits AH, Jansen PW, Poser I, Hyman AA & Vermeulen M (2013) Stoichiometry of chromatin-associated protein complexes revealed by label-free quantitative mass spectrometry-based proteomics. *Nucleic acids research* 41: e28
- Suryadinata R, Roesley SN, Yang G & Sarcevic B (2014) Mechanisms of generating polyubiquitin chains of different topology. *Cells* 3: 674-89
- Suzuki N, Rohaim A, Kato R, Dikic I, Wakatsuki S & Kawasaki M (2016) A novel mode of ubiquitin recognition by the ubiquitin-binding zinc finger domain of WRNIP1. *FEBS J* 283: 2004-17
- Svendsen JM, Smogorzewska A, Sowa ME, O'Connell BC, Gygi SP, Elledge SJ & Harper JW (2009) Mammalian BTBD12/SLX4 assembles a Holliday junction resolvase and is required for DNA repair. *Cell* 138: 63-77
- Toma A, Takahashi TS, Sato Y, Yamagata A, Goto-Ito S, Nakada S, Fukuto A, Horikoshi Y, Tashiro S & Fukai S (2015) Structural basis for ubiquitin recognition by ubiquitin-binding zinc finger of FAAP20. *PLoS one* 10: e0120887
- Trakselis MA, Alley SC & Ishmael FT (2005) Identification and mapping of protein-protein interactions by a combination of cross-linking, cleavage, and proteomics. *Bioconjug Chem* 16: 741-50
- Urban PL (2016) Quantitative mass spectrometry: an overview. *Philos Trans A Math Phys Eng Sci* 374
- Wang C & Lambert MW (2010) The Fanconi anemia protein, FANCG, binds to the ERCC1-XPF endonuclease via its tetratricopeptide repeats and the central domain of ERCC1. *Biochemistry* 49: 5560-9
- Yan Z, Guo R, Paramasivam M, Shen W, Ling C, Fox D, 3rd, Wang Y, Oostra AB, Kuehl J, Lee DY, Takata M, Hoatlin ME, Schindler D, Joenje H, de Winter JP, Li L, Seidman MM & Wang W (2012) A ubiquitin-binding protein, FAAP20, links RNF8-mediated ubiquitination to the Fanconi anemia DNA repair network. *Molecular cell* 47: 61-75
- Ye Y (2006) Diverse functions with a common regulator: ubiquitin takes command of an AAA ATPase. *J Struct Biol* 156: 29-40
- Yin J, Wan B, Sarkar J, Horvath K, Wu J, Chen Y, Cheng G, Wan K, Chin P, Lei M & Liu Y (2016) Dimerization of SLX4 contributes to functioning of the SLX4-nuclease complex. *Nucleic acids research* 44: 4871-80

Addendum



Nederlandstalige samenvatting

Vrijwel iedere cel in ons lichaam bevat alle erfelijke informatie die we hebben gekregen van onze ouders. Dit is verdeeld over 46 chromosomen die elk weer bestaan uit twee lange strengen DNA. Deze strengen zijn om elkaar heen gewikkeld en vormen zo de dubbele helix die kenmerkend is voor DNA. DNA kan informatie dragen doordat een bepaalde volgorde of 'sequentie' wordt gevormd door 4 verschillende bouwstenen of 'nucleotiden': adenine, thymine, guanine en cytosine, afgekort A, T, C en G. Elke nucleotide vormt een paar met de tegenovergestelde nucleotide in de andere DNA-streng. Van essentieel belang is dat er maar twee paren – AT en GC – mogelijk zijn; hierdoor kan de sequentie van de ene streng worden bepaald door het aflezen van de andere, 'complementaire' streng. Op dit principe berust het kopiëren of 'repliceren' van DNA: de strengen worden uit elkaar gehaald en elke oude streng vormt een sjabloon voor de aanmaak van een nieuwe streng. Dit gebeurt voorafgaand aan een celdeling, waarna iedere nieuwe cel volgens een strak gereguleerd proces precies één kopie van elk chromosoom meekrijgt.

Verdeeld over ons DNA zitten vele duizenden 'genen' die, middels de sequentie van nucleotiden, elk een code bevatten voor de aanmaak van een eiwit. Het is van belang dat deze code behouden blijft; een verandering of 'mutatie' kan betekenen dat een eiwit niet meer werkt. Dit ligt ten grondslag aan genetische ziekten zoals kanker en taaislijmziekte. Mutaties kunnen worden overgedragen aan het nageslacht of kunnen ontstaan tijdens het leven wanneer een fout wordt gemaakt tijdens de DNA-replicatie. Mutaties kunnen ook gevormd worden als gevolg van schade aan het DNA. DNA-schade manifesteert zich in vele verschillende vormen, bijvoorbeeld wanneer een deel van een nucleotide mist, één of beide strengen gebroken zijn, of een chemische stof aan het DNA gebonden is. Er zijn vele oorzaken van DNA-schade, zoals uv-licht, straling en sigarettenrook, maar ook bepaalde stoffen die ontstaan bij de verwerking van voedsel kunnen ons DNA beschadigen. Naar schatting krijgt elke cel in ons lichaam dagelijks te maken met tienduizenden beschadigingen van het DNA, die moeten verwijderd worden om te voorkomen dat ze leiden tot mutaties of zelfs tot celdood.

Gelukkig beschikken onze cellen over geavanceerde mechanismen voor DNA-reparatie die onder normale omstandigheden de meeste schades kunnen opruimen. Gespecialiseerde eiwitten herkennen een specifieke DNA-beschadiging en geven een signaal aan de rest van de cel dat ervoor zorgt dat processen die de situatie erger kunnen maken worden gestaakt, terwijl reparatie-eiwitten worden verzameld. Soms zijn dit tientallen verschillende eiwitten die de reparatie uitvoeren volgens strak gereguleerde processen bestaande uit meerdere stappen. In **hoofdstuk 1** worden enkele van de belangrijkste reparatiesystemen kort besproken. Kennis van de verschillende typen DNA-schade en -reparatiesystemen helpt bij het begrijpen van het ontstaan en de reparatie van andere typen schade. Dat geldt ook voor het type schade dat centraal staat in dit proefschrift: de *interstrand crosslink* ofwel ICL.

ICLs kunnen veroorzaakt of 'geïnduceerd' worden door verschillende reactieve moleculen die met het DNA reageren en zo aan het DNA gebonden raken. Om een ICL te vormen moet een molecuul beschikken over twee reactieve groepen waardoor het twee verschillende plekken in het DNA met elkaar kan verbinden. Deze plekken kunnen in dezelfde DNA streng zitten, we spreken dan over een *intrastrand crosslink*. Het is echter pas echt gevaarlijk als het reactieve molecuul de complementaire strengen met elkaar verbindt. De zo ontstane ICL voorkomt dan dat de twee strengen op die plek van elkaar



los kunnen komen, wat noodzakelijk is om DNA af te lezen of de repliceren. Dit heeft gevolgen voor de cel, bijvoorbeeld wanneer het heeft besloten tot celdeling over te gaan maar de replicatie van het DNA door aanwezigheid van de ICL niet voltooid kan worden. De cel kan dan besluiten om zichzelf op te offeren. Dit is ook een manier om de groei van kankercellen te bestrijden, daarom worden ICL-inducerende stoffen gebruikt in chemotherapie. Helaas zijn deze middelen niet altijd effectief en ontwikkelen tumoren soms resistentie tegen deze middelen, bijvoorbeeld door de productie van reparatie-eiwitten op te schroeven. Met gedetailleerde kennis over de reparatie van ICLs kunnen we mogelijk nieuwe en verbeterde strategieën ontwikkelen om kanker te behandelen.

Het is lang onduidelijk geweest waardoor ICLs gewoonlijk ontstaan en hoe cellen ICLs repareren. Veel kennis hierover is opgedaan door het bestuderen van patiënten met Fanconi anemie (vaak afgekort tot FA), een zeldzame genetische ziekte dat onder meer geassocieerd is met beenmergfalen en een verhoogde kans op kanker. Door deze patiënten te bestuderen is gebleken dat de cellen van deze patiënten niet in staat om ICLs te repareren als gevolg van een mutatie in een gen dat codeert voor een eiwit dat betrokken is bij de reparatie. Op het moment zijn er 22 van dergelijke 'FA-eiwitten' geïdentificeerd die allemaal een essentiële functie hebben in hetzelfde reparatie-systeem. Dit reparatie-systeem wordt aangeduid als het 'FA pathway' en wordt beschouwd als het belangrijkste mechanisme voor het verwijderen van ICLs. In **hoofdstuk 1** wordt het moleculaire mechanisme van dit proces beschreven zover dat momenteel bekend is. In het kort werkt het als volgt. De aanwezigheid van de ICL wordt opgemerkt wanneer DNA-replicatie vastloopt omdat de twee DNA-strengen aan elkaar vast zitten. Essentieel voor de reparatie is het loskoppelen van de strengen, wat gebeurt door in één van de twee strengen te knippen. Hiervoor zijn in ieder geval het eiwit SLX4 en het eiwitcomplex XPF-ERCC1, noodzakelijk. SLX4 en XPF zijn FA-eiwitten, wat betekent dat een defect in deze eiwitten Fanconi anemie veroorzaakt. SLX4 en XPF staan daarom ook bekend als respectievelijk FANCP en FANCP en zijn een belangrijk onderwerp van dit proefschrift. In de volgende stappen wordt de DNA-replicatie van de ongeknijpte streng voltooid door speciale reparatie-eiwitten, en de breuk in de geknijpte streng wordt weer hersteld door andere reparatie-eiwitten. Hoewel het reparatieproces globaal bekend is, zijn veel details onduidelijk. Voor dit proefschrift is met name onderzocht hoe SLX4 en XPF-ERCC1 op moleculair niveau zorgen voor het loskoppelen van een DNA-streng in het proces van ICL-reparatie.

Om te onderzoeken wat het precieze mechanisme is van DNA-reparatie, is een geschikt modelsysteem nodig. In het geval van ICLs is dat niet eenvoudig om twee voorname redenen. De eerste is dat ICL-inducerende stoffen niet erg efficiënt zijn in het aanbrengen van dit type DNA-schade; ze veroorzaken veel andere typen achtergrondschade die de onderzoeksresultaten sterk kunnen beïnvloeden. De tweede reden heeft te maken met het feit dat de reparatie voor een groot deel afhankelijk is van DNA-replicatie, wat erg complex is en moeilijk na te bootsen. Beide problemen worden aangepakt in een uniek systeem op basis van extracten van kikkereitjes, welke ook is gebruikt voor de onderzoeken die zijn beschreven in dit proefschrift. Onbevruichte "oocytten" van de kikkersoort *Xenopus laevis*, ook wel Afrikaanse klauwkikker genoemd, zitten boordevol eiwitten die gespecialiseerd zijn in DNA-replicatie en verwante processen zoals DNA-schadeherstel. Van de eitjes worden in verschillende stappen eiwit-extracten gemaakt en hiermee zijn we in staat zijn om stukjes DNA te repliceren zonder dat daarvoor een cel nodig is. In het laboratorium kunnen we het DNA vervolgens zo aanpassen dat er op ieder stukje DNA één ICL aanwezig

is. Wanneer we dit DNA vervolgens aan de extracten toevoegen wordt het niet alleen gerepliceerd, maar wordt ook de ICL verwijderd. Dit proces is nauwkeurig te volgen en te controleren, en veel kennis van het mechanisme van ICL-herstel is dan ook afkomstig van studies met deze ei-extracten. Hoewel we hiermee in feite bestuderen hoe kikkercellen ICLs repareren, is gebleken dat dit sterk overeenkomt met de manier waarop ICLs worden gerepareerd in cellen van mensen. Deze extracten zijn ook gebruikt om andere cellulaire processen te bestuderen; in **hoofdstuk 2** is beschreven hoe onderzoeken met deze extracten hebben bijgedragen aan de kennis van verscheidene processen die gericht zijn op onderhoud van de erfelijke informatie, het DNA, in onze cellen.

In **hoofdstuk 3** staat het eiwitcomplex XPF-ERCC1 centraal. In dit complex zorgt ERCC1 voor stabiliteit, terwijl XPF de activiteit bezit om specifieke DNA-structuren te knippen. Dit doet XPF-ERCC1 niet alleen tijdens de reparatie van ICLs, maar ook bij het verwijderen van schade dat is veroorzaakt door uv-straling. Dit reparatie-proces wordt aangeduid met NER, wat staat voor *nucleotide excision repair*, en net als bij ICL-reparatie wordt het onvermogen om dit proces te voltooien geassocieerd met een zeldzame genetische ziekte. Opmerkelijk is dat bepaalde mutaties in het gen voor XPF patiënten gevoelig maken voor ICLs en niet voor uv-schade, en voor andere mutaties het omgekeerde geldt. Dit kan duiden op verschillende werkwijzen van XPF-ERCC1 in de twee DNA-reparatie processen. Door gebruik te maken van het *Xenopus* ei-extract systeem hebben we deze processen onafhankelijk van elkaar kunnen bestuderen. Hiervoor zijn mutaties in het XPF-eiwit aangebracht die overeenkomen met de mutaties van patiënten. In het extract vervangen we het normale eiwit met het gemuteerde eiwit, waarna we het verloop van het reparatie-proces volgen. Zodoende laten we onder andere zien dat één mutatie de interactie met het eiwit SLX4 onmogelijk maakt en dat dat essentieel is voor de reparatie van ICLs, maar niet voor NER. Deze bevindingen helpen ons te begrijpen hoe XPF-ERCC1 en SLX4 te werk gaan tijdens het proces van ICL-schadeherstel. Daarnaast kan het bijdragen aan de ontwikkeling van stoffen die specifiek de functie van XPF-ERCC1 in ICL-reparatie remmen. Dit is nuttig omdat kankercellen in sommige gevallen weerstand opbouwen tegen chemotherapeutische stoffen door de productie van XPF-ERCC1 op te voeren. Dergelijke 'remmers' zouden kankercellen gevoeliger kunnen maken voor therapie terwijl bijwerkingen beperkt blijven.

Wat de rol van SLX4 is in het proces van ICL-reparatie wordt onderzocht in **hoofdstuk 4**. SLX4 heeft naast een rol in ICL-reparatie ook functies in verschillende andere DNA-gerelateerde processen. Een opvallende eigenschap van SLX4 is dat het vele andere eiwitten aan zich kan binden waaronder 3 verschillende 'nucleasen', eiwitten die in DNA kunnen knippen, waarvan het eiwitcomplex XPF-ERCC1 er één is. We vermoeden dat SLX4 het loskoppelen van de ICL bevordert door XPF-ERCC1 naar de ICL toe te brengen, maar mogelijk brengt het tegelijkertijd een tweede nuclease mee die aan de andere zijde van de ICL knipt. Dit hebben we getest met het *Xenopus* ei-extract systeem in combinatie met mutant-eiwitten van SLX4 die wel XPF-ERCC1 kunnen binden maar niet de andere twee nucleasen. Deze mutanten blijken volledig in staat om ICL-reparatie voltooien, terwijl mutaties die de binding met XPF-ERCC1 verstoren ICL-reparatie onmogelijk maken. Dit toont aan dat de rol van SLX4 in ieder geval is om XPF-ERCC1 naar de ICL te brengen en correct te positioneren. Hiermee is de precieze manier waarop het loskoppelen gebeurt echter nog niet opgehelderd. Zo bestaat de mogelijkheid dat XPF-ERCC1 aan beide kanten van de ICL knipt, of dat een nog onbekende nuclease betrokken is bij deze stap in het proces. Verder onderzoek moet uitwijzen welke methode door cellen wordt toegepast,

of dat er wellicht reserve-opties zijn zodat reparatie bij uitval van één methode toch door kan gaan.

SLX4 zorgt er dus voor dat XPF-ERCC1 naar de ICL gebracht wordt en daar in het DNA knipt. Maar hoe wordt SLX4 dan gerekruteerd naar de ICL? Over die vraag gaat het in **hoofdstuk 5**. Een specifiek gedeelte van SLX4, bestaande uit twee zogenoemde UBZ-domeinen, heeft hier mogelijk mee te maken. Sommige Fanconi anemie patiënten hebben een mutatie in deze UBZ-domeinen, wat aangeeft dat de domeinen essentieel zijn voor ICL-reparatie. In dit hoofdstuk wordt weer gebruik gemaakt van de extracten en mutant eiwitten van SLX4. We laten zien dat het eerste van de twee UBZ-domeinen belangrijk is voor ICL-reparatie en het rekruteren van SLX4 naar de plek van de schade waar het zijn werk kan doen. Om te begrijpen hoe dit in zijn werk gaat, is het van belang om te weten welk eiwit door het eerste UBZ-domein wordt gebonden. Hiervoor onderzoeken we twee kandidaat-eiwitten. De eerste, FANCD2, is wel belangrijk voor rekrutering van SLX4 maar vormt geen directe binding terwijl de tweede, RTEL1, wel aan SLX4 bindt maar geen grote rol speelt in de rekrutering van SLX4. Hoewel we dus een stapje dichterbij zijn, is het mechanisme dat SLX4 gebruikt om naar ICLs te gaan nog erg onduidelijk.

In **hoofdstuk 6** worden de bevindingen van de voorgaande hoofdstukken bediscussieerd en door middel van de actuele beschikbare literatuur in een bredere context geplaatst. Zo wordt nagegaan in hoeverre de onderzoeksvragen die voorafgingen aan de experimenten zijn beantwoord. Er wordt gespeculeerd welke experimenten en technieken mogelijk kunnen bijdragen aan het vinden van de antwoorden en wat een eventuele bevinding van een toekomstig onderzoek betekent voor onze kijk op het proces. Tot slot wordt kort ingegaan op de vraag hoe de onderzoeken die zijn beschreven in dit proefschrift kunnen bijdragen aan het verbeteren van therapieën voor de behandeling van kanker.



Curriculum Vitae

Wouter Simon Hoogenboom was born on March 3rd 1987 in Lutong, Malaysia, and raised in Woerden, The Netherlands where he received his Atheneum diploma from the Minkema College in 2005. He then moved to Brisbane, Australia to follow introduction courses on Biomedical Sciences at the Griffith University and for travelling. In the summer of 2006 he came back to The Netherlands and moved to Leiden where he stayed during his bachelor in Life Science & Technology, in a joint program between Leiden University and Delft University of Technology. After finishing his bachelor degree, he continued with his master Life Science Research & Development in Leiden which he finished in 2013.

Wouter's first hands-on experience with proteins and DNA was during a short bachelor internship at the Leiden Institute of Chemistry in the group of Dr. Remus T. Dame where he studied how high order oligomerization of the bacterial protein H-NS contributes to the compaction of DNA in *E. coli*. He performed his first master's internship at the Leiden University Medical Center where he worked in the group of Dr. Mariet C.W. Feltkamp to characterize the small T antigen of the trichodysplasia spinulosa polyomavirus. During his second master's internship at the Institute of Biology Leiden in the group of Prof. Dr. Gilles P. van Wezel he studied the involvement of the genes SGR_6890 and SGR_6891 on the production of the regulatory substance A-factor in the soil bacterium *Streptomyces griseus*.

In November 2013, Wouter started his PhD at the Hubrecht Institute in the group of Dr. Puck Knipscheer on "The Molecular Mechanisms of DNA Interstrand Crosslink Repair". The work he developed on that subject is presented in this thesis.



Publications

Klein Douwel D, **Hoogenboom WS**, Boonen RACM and Knipscheer P. Recruitment and positioning determine the specific role of the XPF-ERCC1 endonuclease in interstrand crosslink repair. *The EMBO Journal* 2017, July 14, 36 (14): 2034-2046

Hoogenboom WS[#], Klein Douwel D[#] and Knipscheer P. *Xenopus* egg extract: A powerful tool to study genome maintenance mechanisms. *Developmental Biology* 2017, August 15, 428 (2): 300-309

Hoogenboom WS, Boonen R and Knipscheer P. The role of SLX4 and its associated nucleases in DNA interstrand crosslink repair. *Nucleic Acids Research* 2019, March 18, 47 (5): 2377-2388

Hoogenboom WS, Boonen RACM, Arkinson C, Walden H, and Knipscheer P. Two domains mediate SLX4/FANCP recruitment to DNA interstrand crosslinks. *Manuscript in preparation*

[#]) Co-first author

Dankwoord / Acknowledgements

A lot has happened since I started my PhD six years ago. The Hubrecht Institute has doubled in size, some 'generations' of PhD students and Postdocs passed by, and I transformed from a heavy fraternity student to a family guy and cycling enthusiast, just to name a few. I've had an amazing time during this period, for which I have a number of people to thank.

Als eerste natuurlijk **Puck**, de reden dat ik überhaupt naar het Hubrecht ben gekomen. Wat heb ik het enorm getroffen met jou als PI! Wanneer anderen zouden klagen over hun PI's kon ik me daar simpelweg geen voorstelling van maken, want ik heb alleen prettige ervaringen in dat opzicht. Je bent altijd bereid om me te helpen, je hebt me nooit onder druk gezet en altijd vrijgelaten om mijn projecten aan te pakken zoals mij dat zelf uitkomt. Deze prettige werkomstandigheden zal ik nog vaak gaan missen! Ik denk ook graag terug aan leuke borrels, uitjes, en meetings zoals die in Atlanta. Tot slot wil ik je bedanken voor jouw bereidheid om me nog even onderdeel van het lab te laten zijn, waardoor ik meer tijd heb om me op de volgende stap in mijn carrière te richten. Bedankt!

Ik wil hierbij ook de leden van mijn lees-/promotiecommissie bedanken, zonder wie geen promotieplechtigheid mogelijk zou zijn. **Eva van Rooij, Geert Kops, Alain de Bruin, Marcel Tijsterman** en **Hannes Lans**, bedankt voor jullie tijd en moeite en ik kijk erg uit naar onze gedachtenwisseling op 17 december. Ook dank aan mijn promotor en voornaamgenoot **Wouter de Laet**, voor je hulp op de officiële momenten, gesprekken bij de koffieautomaat en vertrouwen in het verloop van mijn PhD. **Litha Schipper**, bedankt voor alle advies en voor het in goede banen leiden van de goedkeuringen van het manuscript, inclusief updates vanaf je vakantieadres.

Eveneens van essentieel belang zijn mijn paranimfen Bas en Dave. **Bas**, al sinds het moment dat ik begon aan mijn PhD en jij nog student was zijn we maatjes, al voelt het wel alsof ik je de laatste jaren steeds meer in de steek heb gelaten. Zonder me te willen verschuilen achter excuses: wacht maar tot jouw 'vrije' dagen in het teken staan van een rennende peuter. Hoewel dat voor jou misschien niet zal gelden, gezien je schier eindeloze energie voor een 'biertje, terrasje, zonnetje, gewoon heerlijk'. Je Brabantse opgewektheid is aanstekelijk en de zeldzame borrels zonder jou zijn dan ook gewoon toch iets minder leuk. Ik hoop van harte dat het voor jou ook niet lang meer zal duren voor je mag afronden! **Dave**, jij bent als het ware mijn anker voor die studententijd waaraan ik zoveel te danken heb. Jouw uitgesproken toewijding aan Leiden en volharding over de wens dat ieder van ons jaar weer terugkomt op het 'nest' is voor mij voldoende reden om Leiden nooit helemaal los te laten. Een gedenkwaardig moment was toen ik Leiden voor Utrecht verruilde en ik van jou een sleutelbos van jouw huis kreeg. Deze heb ik altijd bij me, je weet immers nooit wanneer je weer in Leiden terecht komt en de wetenschap dat ik bij jou altijd welkom ben, is goud waard. Wellicht komt jouw droom uit en is het in de nabije toekomst niet meer nodig. Onvergetelijk is ook jouw rol tijdens mijn bruiloft, ten koste van je voet. Je rol als paranimf is vooral ceremonieel dus je kunt alles heel houden deze keer!

Naturally, I need to thank everyone in the Knipscheer group for listening to endless lab meetings about SLX4. You have all been very helpful scientifically and quite simply great company during our many hours in the lab, the office, during lunch and at 'borrels'. **Merlijn**, jij bent van onschatbare waarde voor de groep, niet alleen vanwege een paar plasmiden (thanks voor alle pCL!) maar vooral ook vanwege het feit dat je verder meedenkt en nieuwe technieken opzet. Ik maak graag grapjes ten koste van jou maar zie dat vooral als iets goeds; dat doe ik alleen bij mensen die ik zeer waardeer! **Alice**, I admire

how you managed to stay in control of the intense aldehyde project while also doing well on other levels such as supervising students, your various committees and learning Dutch. It was also amazing to be part of your wedding during our stay in Sicily! **Koichi**, you must be the most efficient lab 'machine' I'll ever get to meet. Not only are your experiments always perfectly executed, you also manage to cramp a lot of them in an amazing short timeframe. Apart from that you are fun to have around and when you are not performing biochemistry-art it usually means that you are travelling and meeting friends. You are an example to us all (though perhaps not a very realistic one)! **Roxanne**, jij bent altijd heel relaxed en goed gehumeurd, wat prettig is voor de sfeer in het lab. Daarnaast komen jouw projecten nu lekker van de grond, dus je zou zomaar eens in no-time klaar kunnen zijn. En als dat niet zo is... houd vol! **Aiko**, ik dacht dat ik zelf goed georganiseerd was totdat ik jouw Excel-sheet van de kikkertanks zag, vol kleurtjes en handige drop-down menuutjes. Dit is echt next-level! Een lab met rommelige en ongeïnteresseerde gebruikers (elk lab dus) kan een dergelijke organisatie goed gebruiken. Ik hoop dat je nog lang blijft plakken! **Jamie**, you've only just started when I write this but already you fit in exceptionally well. I expect great things from you, just don't stab yourself when making extracts!

Some people who left the Knipscheer group before me have had a huge impact on my time here. **Daisy**, ik heb ontzettend veel aan jou te danken, misschien het meeste nog wel nadat je klaar was met je promotie. Immers, mijn derde hoofdstuk is voor het overgrote deel jouw werk en tijdens het schrijven van mijn manuscript heb ik te allen tijde jouw proefschrift bij de hand gehad als mijn inspiratie me even in de steek liet ("hmm, hoe deed Daisy dat dan?"). Natuurlijk staan de herinneringen van toen je hier nog rondliep me ook helder bij. Onze projecten waren nauw verbonden dus we hadden veel met elkaar te maken, en met jou erbij was een ChIP-plaat pipetteren niet saai meer! **Rick**, voor jou geldt ook dat ik heel veel aan je te danken heb, zie de auteurslijsten van mijn wetenschappelijke hoofdstukken waarin jij steevast vermeld staat. Het meeste van mijn werk is een doorontwikkeling geweest van jouw experimenten. Ik heb ook veel om je gelachen, in het lab wanneer je Daisy verraste met platte vragen, tijdens de meeting in Egmond aan Zee (waar ook **Kim** bij was), dat leuk was totdat we bij vertrek de rekening moesten betalen, en tijdens jouw afscheidsdiner met onze eigen biertap. Succes met de laatste loodjes in Leiden! **Nerea**, I still miss your presence in the office and lab to this day, your positive attitude was really catching! I hope you like München, I'm not worried that you'll feel lonesome because you're super easy-going and an example on how to be both hard working and social to everyone. Good luck there! **Anna** and **Pau**, although it's been awhile we did spend a lot of time together and that was always a treat, thank you! My students **Julie** and **Nandhini**, thank you so much for your work and dedication to the lab!

Our group meetings were recently joined by the people of the Mattioli group, which has been a great decision as the 'fresh set of eyes' really helps to improve the quality of our science. **Francesca**, you are always highly interested in our work and providing us with great suggestions, thank you! You have some exciting work going on in your own lab, I wish you all the best with that! **Clément**, **Bruna**, **Jan**, you are fantastic neighbours and very talented scientists, I hope our labs will continue to collaborate closely and that your promising projects will work out well!

De volgende personen hebben een algemene rol in het Hubrecht maar zijn voor ons werk van levensbelang. **John**, net als voor elk ander lab heb jij op alle vlakken veel voor ons betekend, waaronder strak onderhoud van alle apparaten en twee verhuizingen,

en we konden regelmatig praten over onze gedeelde passie: fietsen. Dank! **Huub**, dankzij jou kunnen we intensief gebruik maken van radioactief materiaal wat voor vrijwel elk experiment in ons lab noodzakelijk is. In sommige periodes maakten we elke week vroeg in de ochtend een praatje, maar aangezien schrijven niet in het RA-lab hoeft is dat helaas alweer even geleden. Dankjewel! Dank ook aan de **dierverzorgers**, zonder wie wij geen extracten kunnen maken.

A special thanks goes to everyone in the Creighton group, who promptly collected us every day at 12.00h exact to take us downstairs for lunch. **Caroline**, we hebben het altijd over sport kunnen hebben, eerst hockey en later wielrennen, en ook een paar mooie activiteiten gedaan zoals de Vikingrun en rondjes fietsen met Jochem. Maar het leukste werd het eigenlijk wanneer jij even geen sport hoefde te doen en je gewoon ongestoord kon borrelen, want dat kun je ook heel goed! Dank je voor alle leuke momenten, ik kijk alvast uit naar jouw verdediging en heel veel succes daarna in Boston! **Ilia**, I'll miss your slightly cynical view on things, it feels very natural to just make jokes about all our complaints which makes dealing with them a lot easier. I hope your 'new' lab will prove to be an inspiring environment for you, good luck! **Maartje**, jij was een perfect voorbeeld van hoe je het maximale uit een PhD haalt, geheel volgens het 'work hard, play hard' principe. Je zit al een tijdje in Philadelphia, ik ga ervan uit dat je ook daar maximaal presteert! **Sander**, jij had een moedige keuze gemaakt om je PhD te stoppen voor een positie met meer impact. Tijdens je tijd hier hebben we veel gelachen, gevoetbald, geborrel, gepraat over computers en fietsen, en meer. Succes verder! **Menno**, dank voor je scherpe opmerkingen tijdens lunch, enkele mooie borrels en twee memorabele afscheidsdiners. Veel succes in Rotterdam!

Thanks to everyone else at the Hubrecht Institute (and some UMC/PMC) who contributed to lots of fun during borrels, BBQs, LSDs, Christmas dinners, centennial celebrations, pub quizzes, etc., including but not limited to: the PV 2015 (**Kim, Annabel, Sander, Joep, Bas, Euclides**, and **Daniël**), it was a joy to work with you while organising fun activities, our Bavarian suits have set a bar!), the Futsal team (including **Pieterjan, Javi, Saman, Axel, Geert, AJ Hale, Enric, Guy, Mauro**, it was tough but fun!), the board game gang (including **Wim, Margit, Annabel, Caro, Bas**), and other 'unspecified' great people (including and in random order: **Lenno, Kadi, Sasja, Corina, Chloé, Brian, Bas M., Ive, Tim, Suzanne, Stijn, Deepak, Sanne, Bram, Jimmy, Marta, Timo, Ator, Kay, Lennart, Banafsheh, Ana, Kim L., Ajit, Lorenzo, Hesther, Charlotte, AK, Niels, Carien, Rob, Anna, Erik, Panagiota, Tim K., Susanne, Abel, Van Rheenen Girls**, and many others).

Op sportief vlak moet ik het leukste hockeyteam van Utrecht – **Heren 6 'hockeyles' van MMHC Voordaan** – danken voor de mooie jaren dat ik jullie verdediging heb mogen versterken! Nooit gescoord, wel veel lol gehad. Bedankt! Veel dank ook aan het Da Vinci-peloton (**Strand, Hugo, Rik, Geert, Dekker, Vincent, Jaap, Simon, Rogier, Rob, Floor, Carel, Pim, Tim, Chris, Teun, Bond, Munt, Loef, Niels-Jan, Wynand, Bob**): door jullie ben ik begonnen met wielrennen, wat een prachtige sport! Vanaf de eerste keer dat ik mee kon naar de Pyreneeën heb ik nooit meer een fietsvakantie willen missen. Onthoud: goed ontbijten want je weet nooit wanneer je weer te eten krijgt!

Dank ook aan de volgende personen. **Thomas** en **Juriaan**, die mijn fantastische getuigen waren tijdens mijn bruiloft en natuurlijk vrienden om trots op te zijn. De 'senatoren' (**Jap, Mad, Strand, Mars, Sop, Vin, Kamp**), dank voor jullie ongekende interesse in de kikkers. **Chris** en **Lisette** voor de gezellige bezoeken en diners, de laatste tijd stevast met

kids erbij die fijn samen spelen. **Glenn** en **Judith**, voor het uit de brand helpen wanneer wij niet voor sluitingstijd bij de opvang konden zijn en natuurlijk ook de vele afspraakjes in Lent. Mijn schoonfamilie aka 'de Wallages' (**Philip, Anjo, Bas, Dagmar, Hans, Mandy** en **Woody**), bij wie ik terecht kan wanneer mijn eigen familie in het buitenland zit. Altijd leuk op vakantie of in het Uilennest, en met jullie erbij heb ik even geen omkijken naar Marit. Heel bijzonder is natuurlijk dat **Anjo** elke week vanuit Alphen a/d Rijn komt rijden om de tuin te onderhouden, vooral omdat ze ook de zorg over Marit op zich neemt zodat wij onbezorgd kunnen werken. Ontzettend veel dank daarvoor!

Natuurlijk ook dank aan de 'Hoogenboom familie' voor alle steun en vertrouwen de afgelopen jaren. Ik maak graag grapjes over het feit dat jullie me in de steek laten in Nederland maar dat voelt echt niet zo, mede omdat we met videobellen toch goed contact kunnen houden. **Papa** en **mama** (of tegenwoordig vaak **opa** en **oma**) jullie staan altijd voor me klaar, ook al zijn jullie aan de andere kant van de wereld. Ik kan jullie alles toevertrouwen en doe dat dan ook regelmatig! Dat ik zo veel aan jullie te danken heb is iets dat ik me pas kort realiseer. **Maarten, Lonneke, Julotte** en **Thoas**, hoe jullie het hele circus draaiende houden is mij een raadsel en een voorbeeld van hoe het ook kan! Volgens mij hebben jullie het super naar je zin in Seattle en wij kijken erg uit naar ons bezoek daar. Stiekem hopen we wel dat jullie ooit nog eens terugkomen...! **Lieke**, jij staat ook altijd voor ons klaar, of het nou is als tante Lieke of wanneer ik een fietstochtje in Limburg heb. Eventjes waren wij de achterblijvers in Nederland totdat ook jij ons verliet! Gelukkig is Londen niet zo ver en kunnen we dus vrij gemakkelijk 'even langs'. Niet verder verhuizen dus, oké?

Marit, wat ben ik blij dat jij nu deel uitmaakt van onze familie! Ik heb dit proefschrift aan jou opgedragen omdat je mij net als dit proefschrift ontzettend trots maakt. Alles kan tegen zitten: experimenten, het verkeer, maar als jij bij thuiskomst zwaaiend achter het raam staat, ben ik dat allemaal zo weer vergeten. Je doet het zo goed, je bent lief tegen iedereen en hard bezig om een goed maar pittig karakter te ontwikkelen. Ik geniet van onze dagen samen en zal er ook in de toekomst altijd voor je zijn!

Jacqueline, het is klaar! Als er iemand heeft uitgekeken naar het einde van mijn PhD, dan ben jij het wel. Hoe vaak ik wel niet moest uitleggen dat ik dat zelf niet helemaal in de hand heb! Maar een beetje pushen hielp wel dus misschien was ik zonder jou nog steeds niet aan het schrijven begonnen. De laatste tijd ging het dan weer over het dankwoord. Dat zal een beetje tegenvallen want je weet alles al! Ik heb heel veel aan je te danken omdat ik altijd zorgeloos mijn werk heb kunnen doen, de laatste tijd stevast met een bordje eten en een blije dochter bij thuiskomst. Ik ben trots op je, we hebben veel lol, we zijn het over veruit de meeste dingen eens en hebben alles helemaal onder controle. Ik kijk uit naar onze toekomst samen!

